



Università  
Ca'Foscari  
Venezia

Corso di Dottorato di ricerca  
in Scienze Ambientali  
ciclo XXIX

Tesi di Ricerca

***Assessment of air pollutants  
contribution of harbour activities in  
Venice and Brindisi areas***

SSD: GEO/12

**Coordinatore del Dottorato**  
ch. prof. Gabriele Capodaglio

**Supervisore**  
ch. prof. Andrea Gambaro  
dott. Antonio Donateo

**Dottorando**  
Eva Merico Matricola 956093

Shipping could be considered a relatively clean form of transport, being the most energy efficient transportation mode (in terms of emission rate per tonne-kilometre) compared to rail, aviation and car transport (IMO, 2009). On the other hand, if its global coverage and expected growth in next decades are considered, shipping could influence air quality, especially in coastal areas, but also at long distances from the emitting source (Eyring et al., 2010). Annual emissions from oceangoing ships are estimated to be 1.2-1.6 Tg of particulate matter (PM), 4.7-6.5 Tg of sulphur oxides (SO<sub>x</sub> as S) and 5-6.9 of nitrogen oxides (NO<sub>x</sub> as N) (Healy et al., 2009).

Shipping emissions has been demonstrated having potential climate effects. However, the nature of the contribution to climate change is complicated since that the cooling effect could reverse to the warming one from short to long-term because of slow removal of CO<sub>2</sub> and the reduction of SO<sub>2</sub> emissions (Fuglestedt et al., 2009).

Maritime emissions have been left unregulated for too long, so that their share in global emissions has grown dramatically with respect to other transport sectors. If the trend is not inverted, by 2020 shipping emissions will likely exceed the EU emissions from land-based sources (EEA, 2013). At the growth rate of 30%-45% by 2020 (Buhaug, 2008), shipping will be the largest single emitter sector in Europe in the next future. In addition, to assess environmental impacts related to shipping is a challenging task because different spatial and temporal scales involved.

Although in-port releases from vessels represent a small fraction of global maritime emissions, their effects on human health and climate of surrounding areas could be detrimental. To estimate shipping contribution within harbour is complicated, depending on many factors (i.e. engine load, fuel type, ship category, operational mode).

Furthermore, the weaker emission standards applicable to ship engines and poor management practices in harbours increase shipping environmental impacts in coastal areas and in large city-ports. Harbours may be considered as traffic congestion points and therefore air pollution local hot-spot. Oppositely, across oceans shipping emissions are not evenly spread but concentrated along the main international routes.

Relatively little is known about ship emissions in ports. In fact, existing studies evaluating air pollution from shipping on coastal areas are scarce and not homogeneous, being based on different methodological approaches. In most cases, studies are focused on one port and use dispersion models, experimental results, receptor models based on identification of chemical tracers.

Recently, some projects at European level were funded to evaluate contribution of ships and harbour activities to atmospheric pollutants with different tools. Specifically, APICE (Common Mediterranean strategy and local practical Actions for the mitigation of Port, Industries and Cities Emissions) and CAIMANs (Cruise and passenger ships Air quality Impact Mitigation ActionNs) projects, involving five Mediterranean port-cities (Barcelona, Genoa, Marseille, Thessaloniki, Venice), focused on impact of cruise ship traffic and proposed future mitigation scenarios by using modelling simulations. CESAPO (Contribution of Emission Sources on the Air quality of the Port-cities in Greece and Italy) project contributed to estimate shipping contribution to air quality in some Adriatic harbours (Brindisi in Italy and Patras in Greece). Another project was POSEIDON (Pollution monitoring of ship emissions: an integrated approach for harbours of the Adriatic basin, MED 2007-2013) in which four port-cities were studied (Brindisi and Venice in Italy, Patras in Greece, and Rijeka in Croatia) introducing a common state-of-the-art methodology based on emission inventories, numerical modeling and experimental data taken at both high and low temporal resolutions.

This work was done within the framework of the POSEIDON project focusing on the two Italian port-cities of Brindisi and Venice, along the Adriatic coastline. Specifically the impact of shipping to several atmospheric pollutants will be evaluated and compared among the two port-cities. In addition, inter-annual trends of specific impacts and, consequently, the efficiency of mitigation strategies applied at local, national, and international levels will be discussed.

This thesis, after a general introduction on maritime transport sector (Chapter 1), is structured as:

- a brief description of the study areas and measurement sites with instrumental set-up implemented (Chapter 2);

- methodologies used in data processing for quantifying impact of shipping to PM and gaseous pollutants (Chapter 3);
- presentation and discussion of the results obtained in Brindisi and Venice, as well as comparison of impacts and analysis of trends (Chapter 4).

Main conclusions and perspectives will be provided at the end of the work.

**TABLE OF CONTENTS****Chapter 1. Introduction**

1.1 Study context	3
1.1.1 Global nature of shipping	6
1.1.2 Study approaches	8
1.2 Shipping sector statistics worldwide	9
1.2.1 European statistics	13
1.2.2 Focus on the Mediterranean area	16
1.3 Environmental impacts	20
1.3.1 Climate change	21
1.3.2 Effects on human health	25
1.3.3 Social and economic issues	27
1.4 The EU policy	29
1.4.1 The Adriatic-Ionian macro-region	32
1.5. Emissions reduction efforts	36
1.5.1 Technical and operational measures	37
1.5.2 Fuel and power type-based operations	40
1.5.3 Cold ironing	42
1.6 International and national legislation	47
1.6.1 IMO regulations	47
1.6.2 EU legislation	52
1.6.3 Other initiatives	54

**Chapter 2. Measurements**

2.1 Area description	56
2.1.1 Brindisi	56
2.1.2 Venice	63
2.2 Sampling sites	71
2.3 Aerosol characterisation	74
2.3.1 Gravimetric determination	75
2.3.2 Optical photometer	77
2.3.3 Condensation Particle Counter	79

2.3.4 Optical Particle Counter	81
2.4 Gaseous pollutants	83
2.4.1 Gas analysers	84
2.4.2 DOAS system	86
2.5 Ships and vehicular traffic	89
<b>Chapter 3. Methods to estimate shipping contribution to air pollution</b>	
3.1 Source Apportionment approach	93
3.2 High resolution measurement approach	97
3.3 Emission inventories approach	103
3.4 Modelling approach	111
3.5 Remote sensing approach	115
<b>Chapter 4. Results and discussion</b>	
4.1 Results in Brindisi	120
4.1.1 Meteorological conditions	120
4.1.2 Gaseous and particulate matter concentration	123
4.1.3 Patterns of ship traffic and concentrations	131
4.1.4 Primary contribution to pollutants of ship traffic	138
4.1.5 Particle size distribution	144
4.1.6 Aging of the plume	150
4.2 Results in Venice	154
4.2.1 Meteorological conditions	154
4.2.2 Particulate matter concentrations and ship traffic	160
4.2.3 Primary contribution to pollutants of ship traffic	167
4.3 Inter-annual trends in impacts	167
4.4 Comparison of emission inventories data	171
4.5 Modelling results over all the Adriatic/Ionian area	176
<b>Conclusions and perspectives</b>	181
<b>References</b>	185
<b>Web links</b>	210
<b>Scientific outputs</b>	211
<b>Acknowledgements</b>	212

## 1.1 Study context

Maritime transport has been a great player of economic development around the world since centuries because it promotes trade and contacts between several Countries. Nowadays transport by ships represents over 90% of global trade (IMO, 2011) and similar percentage stands also in Europe (Eurostat, 2014). For example, in 2005, less than 5% of full load containers transported between China and Europe moved by land-based modes (Farahmand-Razavi, 2008), confirming the important role of shipping compared to other transport sectors.

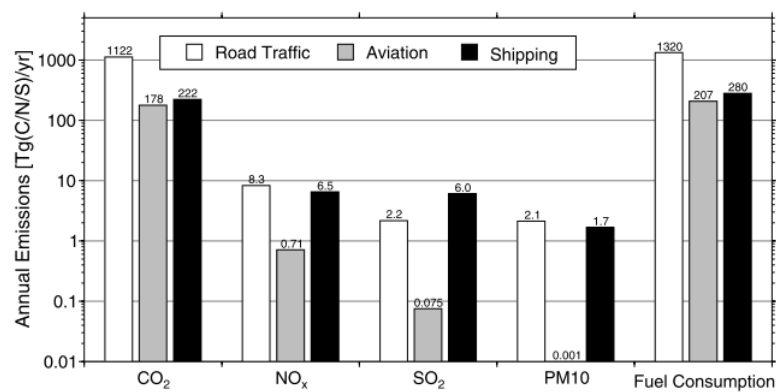


Figure 1.1. Estimates of annual emissions (in Tg) of CO<sub>2</sub> (C), NO<sub>x</sub> (N), SO<sub>2</sub> (S), and PM<sub>10</sub> as well as fuel consumption (in Mt) for the year 2000 (source: Eyring et al., 2005).

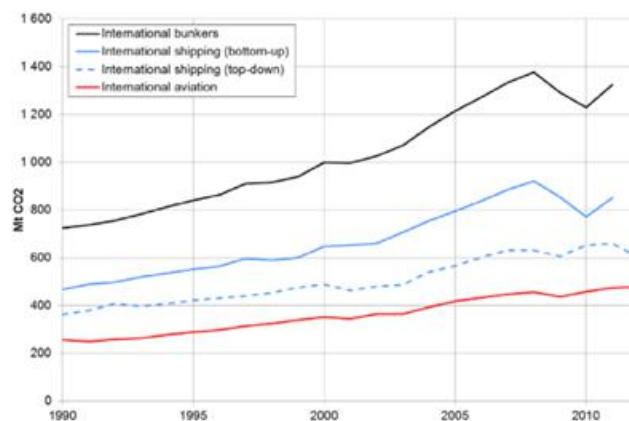


Figure 1.2. CO<sub>2</sub> emissions from international bunkers, period 1990-2012 (source: IEA, 2014; IMO, 2009, 2014; European Parliament, 2015).

Shipping is traditionally defined a relatively clean mode of transport, considering that, for example, typical ranges of CO<sub>2</sub> efficiencies of ships are 0-60 g/tonne-kilometre and 80-180 g/tonne-kilometre for road transport (IMO, 2009).

However, in absolute terms, marine sector is not a negligible emission source, especially for the main pollutants such as CO<sub>2</sub>, SO<sub>2</sub>, PM<sub>10</sub> and NO<sub>x</sub> and globally it is the first contributor of SO<sub>2</sub> (Fig. 1.1). Quantitatively, CO<sub>2</sub> emissions from shipping (interactive map available on <https://www.shipmap.org/>) were estimated approximately a fifth of those of road transport, NO<sub>x</sub> and particulate matter (PM) emissions are the same, and SO<sub>x</sub> emissions of shipping are substantially from 1.6 to 2.7 times higher than those of road transport (Feng et al., 2007). Aviation CO<sub>2</sub> emissions accounted from a quarter to an half of international shipping according to different approaches applied in the period 1990-2012 (Fig. 1.2).

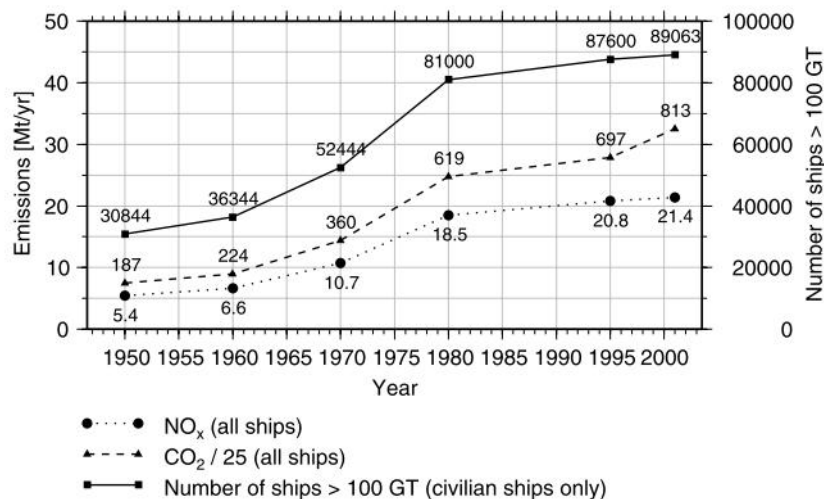


Figure 1.3. Number of ships (>100 GT) for the time period 1950-2001 (ISL, 1994; Lloyd's Register, 2002) as well as the estimated CO<sub>2</sub>, NO<sub>x</sub> and NO<sub>2</sub> emissions (in Tg).

Furthermore, in the last 50 years shipping grew, especially since 1980's and, consequently its related emissions (Fig. 1.3). The growth rate of global emissions was approximately estimated to a factor 4 over the period 1950-2001 (Eyring et al., 2005) and CO<sub>2</sub> releases will increase between 2 and 3 times up to 2050 (IMO, 2014). Recently the Intergovernmental Panel on Climate Change (IPCC) showed a range of possible future scenarios (Fig. 1.4), with shipping increasing by between 30% and 45% from 2007 to 2020, and by between 150% and 300% from 2007 to 2050 (IEA/OECD, 2009). According IMO projections, the strongest growth will be in container activity (from 65% to 95% by 2020 and 400% to 800% by 2050).



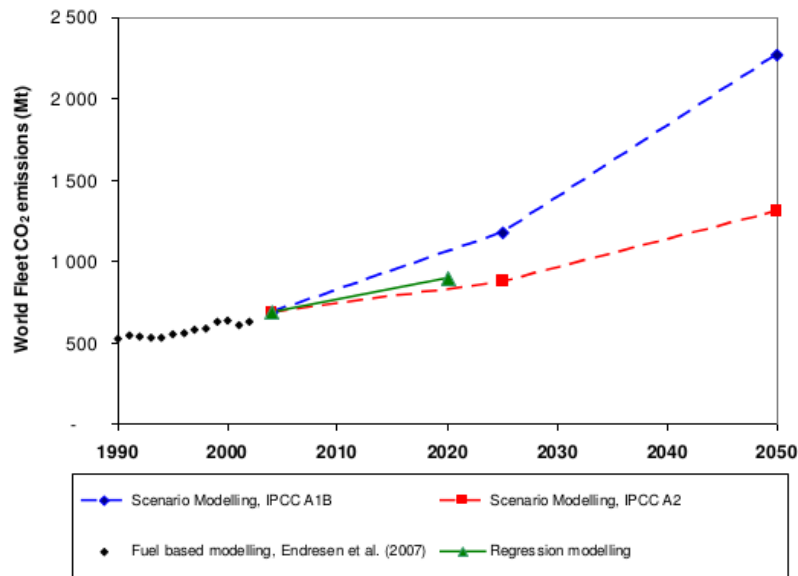


Figure 1.4. World fleet CO<sub>2</sub> emissions, based on IPCC scenarios (Eide et al., 2007) and extrapolation of trends (Endresen, 2008).

Taking in consideration that vessel emissions in Europe are expected to balance land-based sources by 2020 onwards (EEA, 2013) increasing pressure is put on industry and transportation modes, including shipping, to accomplish sustainable development. Transportation and industrial activities are responsible of 70% of black carbon (BC) emissions in Europe, North America and Asia (Bond et al., 2013).

In detail, exhaust emissions from a marine diesel engine are largely composed by carbon dioxide (CO<sub>2</sub>) and water vapour with smaller quantities of carbon monoxide (CO), sulphur oxides (SO<sub>x</sub>), nitrogen oxides (NO<sub>x</sub>), non-combusted hydrocarbons, particulate matter (PM), as well as transitional alkali earth metals (V, Ni, Ca, Fe) and their soluble or insoluble chemical forms (sulphides, sulphates and carbides). The exhaust gases are emitted into the atmosphere from the ship stacks and diluted through interaction with ambient air. During the dilution process in the ship plume the active chemical compounds are partly transformed and deposited on ground and on water surfaces. Furthermore, emissions of VOCs (Volatile Organic Compounds) are possible during oil transport and cargo handling (Endresen et al., 2003). However, the greatest attention in regulating is oriented essentially to PM<sub>10</sub>, PM<sub>2.5</sub>, SO<sub>x</sub> and NO<sub>x</sub> (see Section 1.6), although harmful effects related to the other

compounds (i.e. black carbon, CO<sub>2</sub>, nanoparticles) have been investigated lately (Eckhardt et al., 2013; Hallquist et al., 2013; Healy et al., 2009).

Unfortunately, only since few decades some impact aspects have been faced, being ship emissions and their atmospheric deposition defined as hazardous and polluting substances by the Marine Strategy Framework Directive 2008/56/EC of the European Parliament and of the Council (EC, 2008a).

In particular, the impact on health of coastal population is not still completely clear but involves millions of people who live near coasts and large harbours. For example, 23% of the world population density lives within 100 km from the shoreline (Nicholls and Small, 2012) while the European coastal population is around 40% (Collet and Engelbert, 2013).

For logistic and economic reasons, also important industrial centres are located along coasts, therefore in proximity of harbours and dense urban areas, exacerbating the local air quality. Not only ships moving in port contribute to local emissions but even when they are in “hotelling” mode (at berth) up to five times than during cruise in open sea (Deniz et al., 2010; Tzannatos, 2010). In these cases, emissions from harbour areas could be the dominant source of urban pollution.

### **1.1.1 Global nature of shipping**

Maritime transport, like aviation, has a global nature (<https://www.shipmap.org/>) with respect to other modes of transport (i.e. road and rail transport) and that poses a great problem in quantifying (and controlling) its magnitude, location and impacts (especially on climate forcing and human health).

It is not sufficient to improve inventory estimates or modelling calibration but it is essential to support policy makers in defining efficient control measures of emissions. Although motivation is stronger in regions directly affected by releases, policy actions should have an international application (Corbett, 2003).

However, some research issues need further improvements in order to better address mitigation strategies. For example, large-scale inventories are affected by great uncertainties, being based only on statistics on fuel used by internationally registered ships.

Another important issue is geographical allocation of shipping activity (and emissions) on the basis of ship location data provided nowadays by the Automated Identification System (AIS).

The introduction of this automatic reporting system enormously reduced uncertainty in ship activity data, improving inventory estimates based on time-dependent, high-resolution dynamic traffic patterns (Jalkanen et al., 2016). The current modelling approaches use AIS data, which reports on a global scale position of vessels larger than 300 tons in few seconds.

Instead, in previous works (Endresen et al., 2003; Wang et al., 2008; Corbett et al., 2007) other systems such as rescue and search services (AMVER-Automated Mutual-assistance Vessel Emergency Rescue System), voluntary weather reports (ICOADS), ship arrival/departure time were used but underestimated or neglected smaller vessel activity near coasts or in harbours.

Moreover, in-plume chemistry and dispersion of pollutants released by ships should be studied by chemical transport models, helping to understand long-range pollution transport. Several studies (Corbett et al., 1999; Eyring et al., 2010) put in evidence that shipping emissions may have a long-range dispersion also affecting climate (Bond et al., 2013).

Definitively, integration between geospatial and temporal conditions is necessary to sufficiently characterise ship emissions. A significant step in research should be to compare emission modelling to experimental measurements especially at coastal sites to determine the agreement between predicted  $\text{NO}_x$  and  $\text{SO}_x$  concentrations with direct observations (Jalkanen et al., 2016).

From the legislative point of view, some discussion topics are open. It should be considered that Countries of ship registry, ownership and operator significantly vary, complicating policy-making efforts and this issue is under discussion within the IMO. Two-thirds of the world's international maritime fleet is registered in Countries that have not defined GHG-reduction objectives (Fig. 1.5).

Further, de facto, global shared IMO requirements affect most ships, regardless of flag, but only in Countries which ratified the agreements, not being effective outside the areas of their jurisdiction.

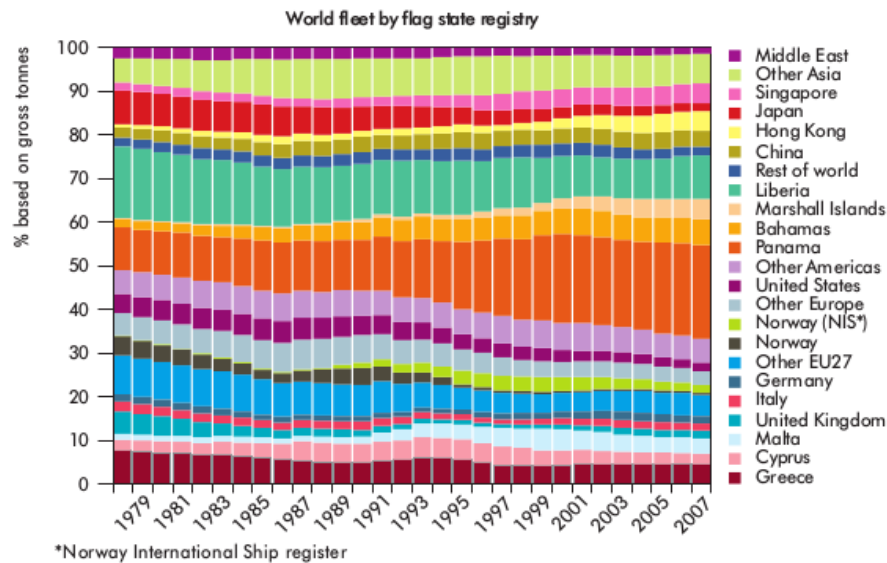


Figure 1.5. World fleet by flag, period 1978-2007 (source: IEA/OECD, 2009).

### 1.1.2 Study approaches

Although most of maritime emissions take place during cruising at open sea, the most directly noticeable part of emissions occurs in port areas. Until today, most studies addressed the global impacts of shipping, focusing on assessment of emission factors from ships to investigate climate and health impacts. However, the most recent scientific literature has demonstrated a growing interest in studying ship emissions in ports and proposing different options to reduce related impacts on air quality in harbour areas and surrounding coastal regions that are often very populated like in the Mediterranean region.

Available studies apply a variety of different methodologies and definitions so that the outputs are often difficult to be compared. This is essentially due to differences in methods used and input data. For example, a bottom-up approach is based on ship activity expressed as hours spent at cruising, manoeuvring and hotelling, with respect to a top-down approach which looks at specific fuel consumption. In addition, in most of cases, it is not easy to separate the effects of shipping, port operations, hinterland transport and industrial development on the port site.

Therefore, estimation outcomes may be site-dependent in the sense that differences are related to port size, industrialization rate, emission features of surrounding areas, ship types and port vessels (such as tugs) included, other activities within the port (port trucks, locomotives, cranes, cargo handling equipment) considered.

Because of this, today one of the main task is to characterise an anthropogenic source so variable in time and space with shared methodologies at larger scale to optimize risk assessment of the effects of maritime emissions (Blasco et al., 2014) and the effectiveness of mitigation strategies.

In this direction many projects, such as CESAPO (Contribution of Emission Sources on the Air quality of the Port-cities in Greece and Italy, <http://www.cesapo.upatras.gr>), APICE (Common Mediterranean strategy and local practical Actions for the mitigation of Port, Industries and Cities Emissions) and POSEIDON (Pollution monitoring of ship emissions: an integrated approach for harbours of the Adriatic basin, <http://www.medmaritimeprojects.eu/section/poseidon>) were conducted in the Mediterranean area to support decisions of policy-makers.

## 1.2 Shipping sector statistics worldwide

In order to get an overview of global shipping, several statistics from different agencies can be analysed. In general, seaborne transport replies to the global demand for food (such as grains, rice, meat, fish, sugar, and vegetables, vegetable oils, etc.), energy (in form of crude oil, refined petroleum products, coal and gas), raw materials (iron ore, minerals, cotton, wool, rubber) and finished products (Fig. 1.6). Other vessels provide services such as offshore activities, dredging, fishing, research and exploration, towing etc.

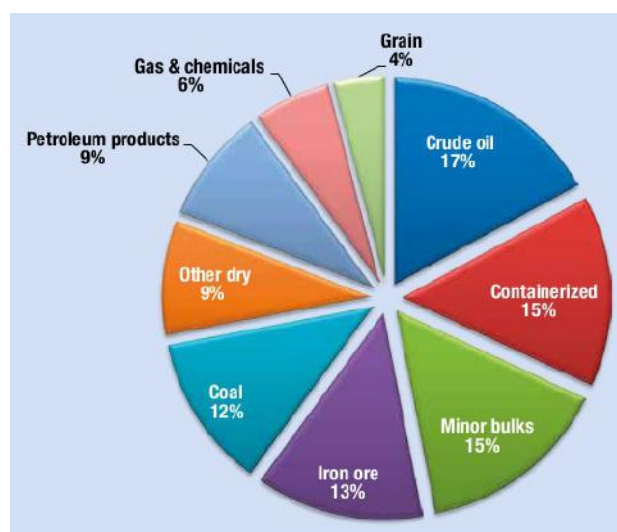


Figure 1.6. Composition of seaborne products in 2014 (source: UNCTAD, 2015).

Lloyd’s Register was chosen by IMO to manage the register of the world fleet, according to the IMO numbering scheme (introduced in 1987 but mandatory since 1996). The IMO Study 2009 clearly demonstrated the growth in world fleet of merchant vessels in numbers and ship sizes over the years. The 2007 world fleet comprised more than 100,000 ships (above 100 GT), of which just less than half are cargo ships (Fig. 1.7). In terms of GT, cargo ships accounted for 89% of total GT, followed by passenger ships (around 4%). Marked increase in ship size was observed for container ships, as also confirmed recently by IMO (IMO, 2016) and dry bulk (Fig. 1.8).

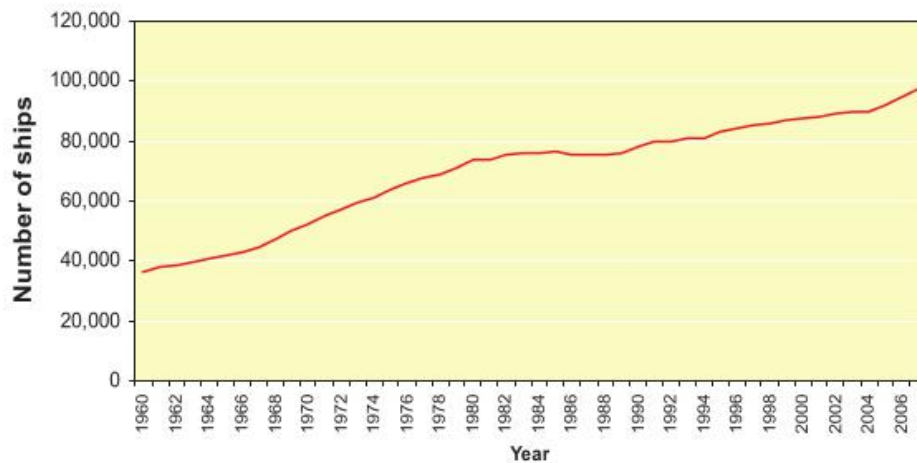


Figure 1.7. Growth in numbers of ships of the world fleet, period 1960-2007 (source: Lloyd’s Register – Fairplay).

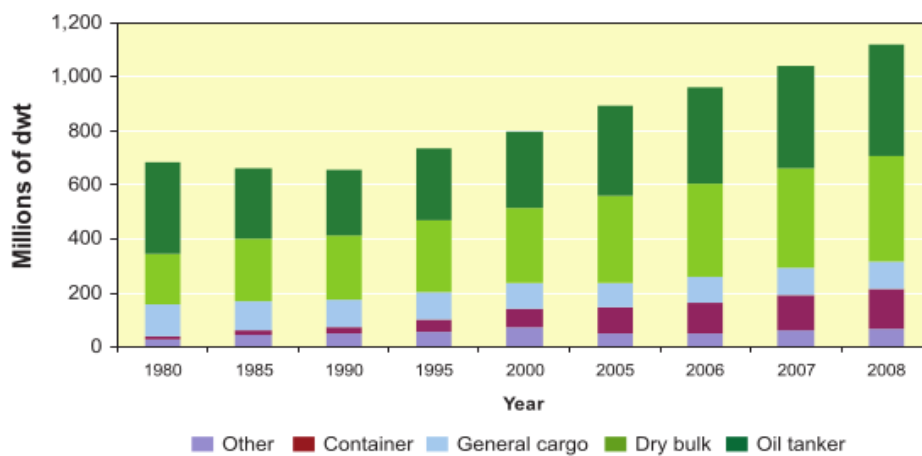
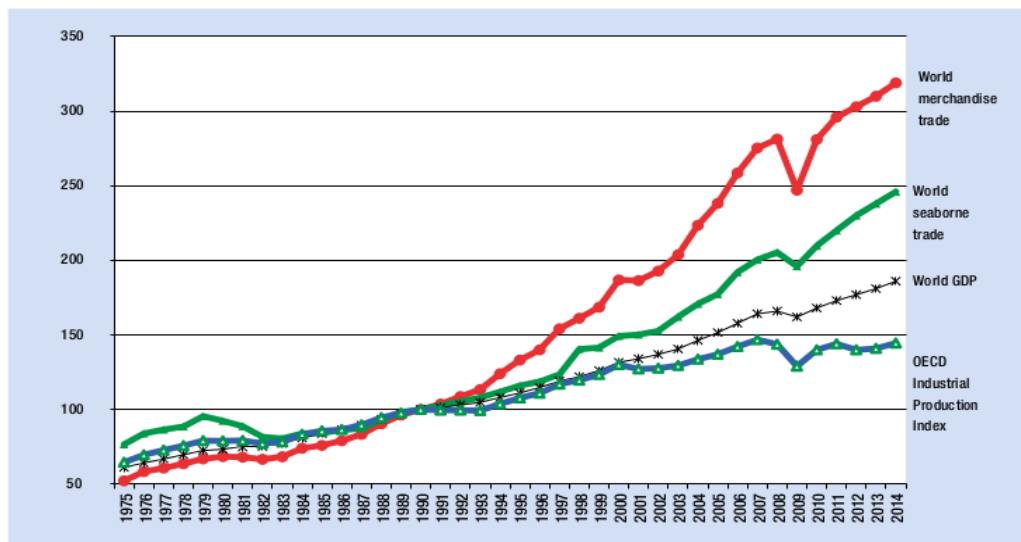


Figure 1.8. Growth in ship size (in millions of death weight tonnage - dwt) of the main vessel types, period 1980-2008 (source: UNCTAD, 2008).

Since that shipping is closely connected to trade sector, the economic growth is strongly dependent on merchant shipping. In the last 20 years international maritime activity has grown significantly, doubling in volumes of major categories of shipped goods (IEA/OECD, 2009). Clear evidence is the fact that world seaborne and merchandise trade have grown more quickly than world Gross Domestic Product (GDP). The total contribution of marine and shipping activities to global economy was calculated to be roughly US\$380 billion in freight rates deriving from the operation of ships (UNCTAD, 2006). Preliminary estimates indicate that global seaborne shipments have increased by 3.4% in 2014, as in 2013 (UNCTAD, 2015). In particular, world merchandise (containerized traffic) export drives overwhelmingly the whole maritime sector (Fig. 1.9).



Sources: UNCTAD secretariat, based on OECD Main Economic Indicators, June 2015; United Nations Department of Economic and Social Affairs, 2015; LINK Global Economic Outlook, June 2015; UNCTAD *Review of Maritime Transport*, various issues; WTO, appendix table A1a, World merchandise exports, production and gross domestic product, 1950–2012; WTO press release 739, 14 April 2015.

Figure 1.9. Growth in maritime trade, world trade and GDP (indexed), period 1994–2006.

In terms of regional distribution, according to the United Nations Conference on Trade And Development (UNCTAD) statistics, in 2014 Asia dominates as the main loading and unloading area, followed by the Americas, Europe, Oceania and Africa. The major shipping routes and trade patterns are prominent in the Northern hemisphere and along coastlines connecting the economic centres in Asia, Africa, Europe and the Americas crossing the Atlantic, Pacific and Indian Oceans (Fig. 1.10). On the other hand, the lowest density areas are the South Pacific. Finally, Tab.

1.1 shows the top-15 trading nations accounted for 65% of the world trade with a corresponding share in registration only of 19% in terms of GT.

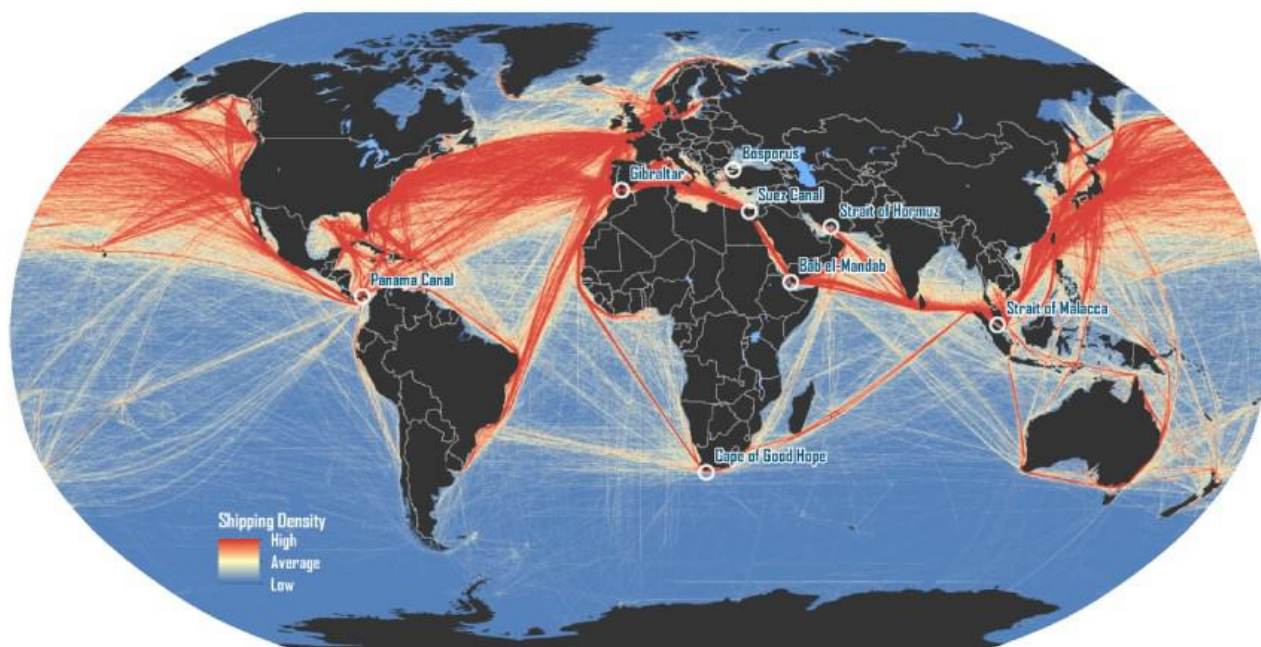


Figure 1.10. Map density of ship traffic worldwide (source: National Center for Ecological Analysis and Synthesis).

Table 1.1. Top-15 trading nations (source: UNCTAD, 2008).

Top trading nations	% share of world trade in terms of value	% of world fleet in terms of dwt	% of ownership of fleet in terms of dwt
United States of America	11.38	1.09	3.84
Germany	8.51	1.34	9.07
China	7.81	3.32	8.18
Japan	4.77	1.32	15.58
France	4.16	0.71	0.63
United Kingdom	3.76	0.42	2.5
Netherlands	3.72	0.56	0.83
Italy	3.55	1.19	1.71
Belgium	3.01	0.58	1.17
Canada	2.88	0.28	1.81
Republic of Korea	2.62	1.89	3.63
Hong Kong, China	2.56	5.3	3.22
Spain	2.18	0.25	0.43
Russian Federation	2.16	0.64	1.74
Mexico	2.04	0.14	n/a
<b>Total – top 15</b>	<b>65.11</b>	<b>19.03</b>	<b>54.34</b>
<b>Total – top 25</b>	<b>78.02</b>	<b>28.16</b>	<b>64.93</b>



### 1.2.1 European statistics

In 2015 European statistics demonstrated that in EU-28 territory road and maritime sectors were important drivers in freight and passenger transport. The two modes of transportation were comparable in absolute and relative terms (Tab. 1.2) in last years. In particular, freight transport of maritime and inland waterways slightly increased their share (+0.5%) from 2008 to 2013 (Fig. 1.11).

In March 2016, EUROSTAT has published data for 2014, regarding to maritime ports freight and passenger in European Union (EU), Iceland, Norway, Montenegro and Turkey.

Table 1.2. Freight transport (million tonne-kilometre) in the EU-28 (Air and maritime cover only intra-transport to/from the EU-28 countries). Own elaboration based on Eurostat, 2015.

	2008	2009	2010	2011	2012	2013
<b>Road</b>	<b>1,844,120</b>	<b>1,660,321</b>	<b>1,714,732</b>	<b>1,699,398</b>	<b>1,644,626</b>	<b>1,669,104</b>
Rail	442,763	363,540	393,531	422,096	406,852	406,710
Inland waterways	154,376	130,532	155,521	141,969	149,987	152,760
Air	2,385	2,227	2,313	2,283	2,265	2,243
<b>Maritime</b>	<b>1,163,916</b>	<b>1,062,372</b>	<b>1,117,777</b>	<b>1,133,154</b>	<b>1,113,126</b>	<b>1,088,606</b>
Total	3,607,560	3,218,992	3,383,874	3,398,900	3,316,857	3,319,423
% maritime	32.3	33.0	33.0	33.3	33.6	32.8
% maritime/road	63.1	64.0	65.2	66.7	67.7	65.2

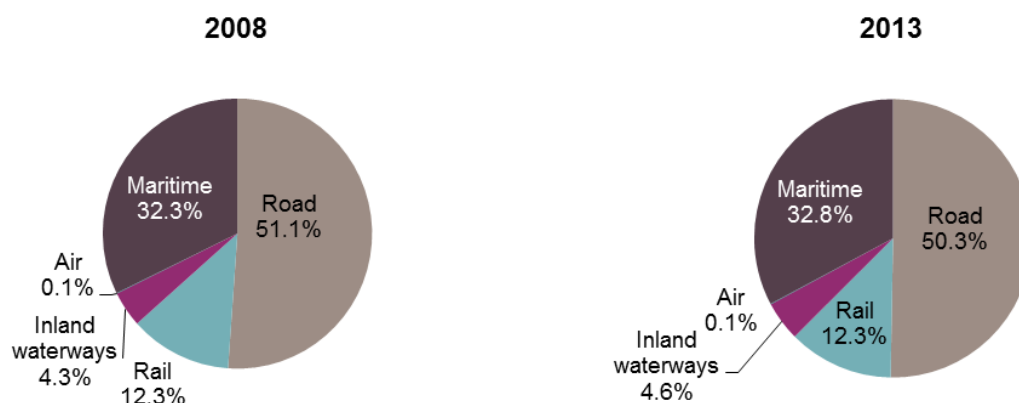


Figure 1.11. Freight transport (% of total tonne-kilometre) in the EU-28 (Air and maritime cover only intra-EU transport). Source: Eurostat, 2015.

In EU ports, the total GT weight of goods handled was estimated at close to 3.8 billion tons in 2014 with an increase of 2% from 2013. In parallel, also the number of passengers slightly increased 0.6% in 2013-2014 period. The leading maritime transport countries were Greece and Italy in 2014 (shared 37% of embarking and

disembarking passengers in EU) while the Netherlands was the EU's largest maritime freight transport country.

Focusing on seaborne passenger transport, the overall volume traffic (as number of passengers) remained stable to 210 million, with emerging Countries, like Malta (Fig. 1.12). Greece and Italy, facing to the Adriatic and Ionian Sea, object of this study, have 75 and 72 million passengers respectively, followed by Danish ports with 10% of the EU seaborne passengers (41 million passengers). These Member States (as well as Countries like Germany, Croatia and Portugal) are characterised by a high national maritime traffic, reflecting the dominant role of national ferry services in the European seaborne passenger transport (58%), oppositely to other Countries (such as Belgium, Denmark, Germany, France, Estonia, Ireland, Latvia, Lithuania, the Netherlands, Poland, Finland, Sweden, the United Kingdom, Spain).

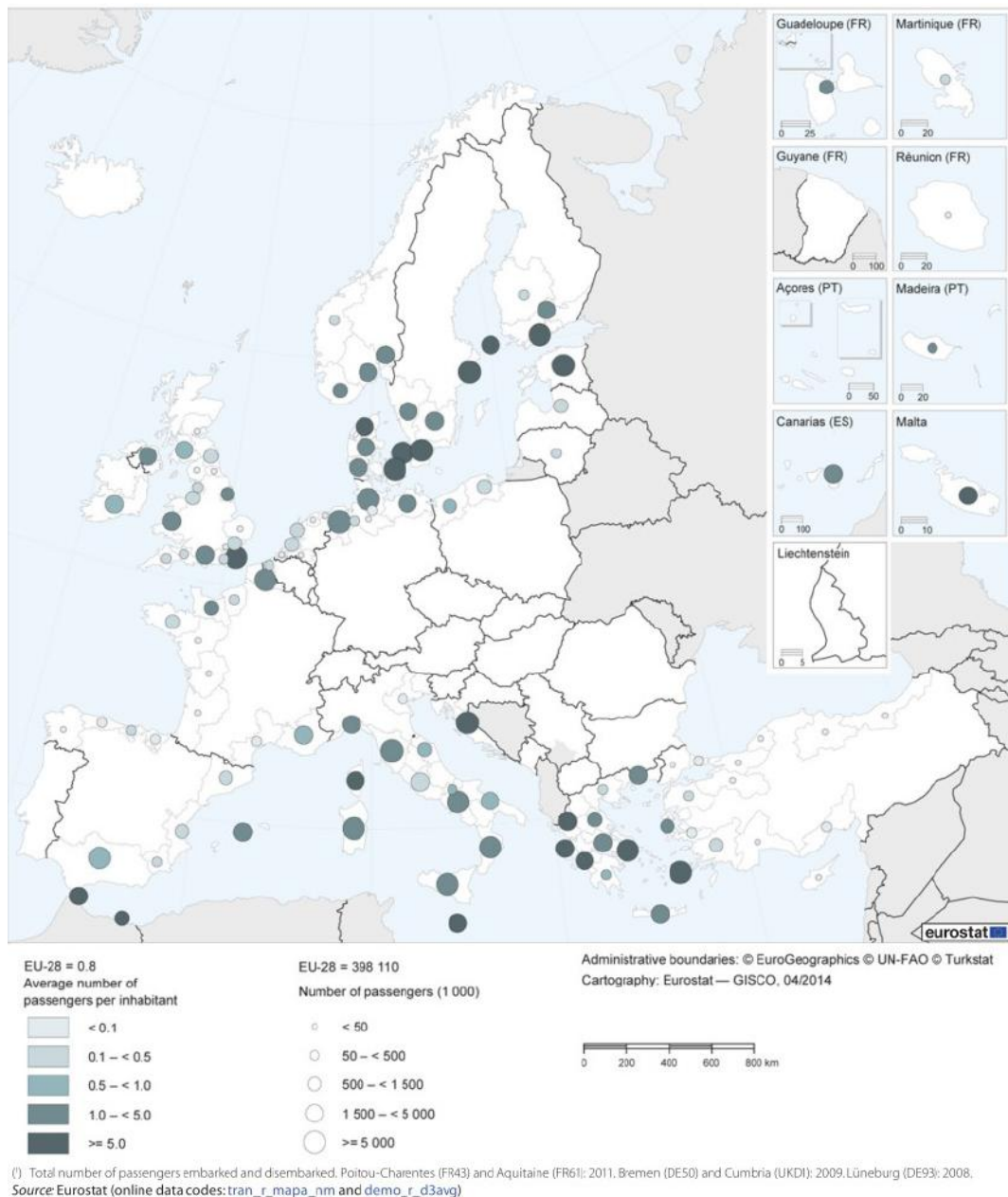


Figure 1.12. Number of maritime passengers per inhabitant and total number of passengers, by NUTS 2 regions, 2012 (source: Eurostat, 2014).

The highest Mediterranean cruise activity (as number of cruise ports) detected in 2010 was along Greek, Turkish and Croatian coasts, although the most frequent itinerary was in the Western Mediterranean (i.e. Savona, Sicily, Tunis, Balearic Islands and Barcelona).

Over 90% of all major cruise ports was located in Italy and Greece (35 ports each), followed by France, Spain, Croatia and Turkey (Marušić et al., 2012). Taking into account ship size, the majority of ports visited by the biggest ships (with a capacity

more than 3,000 passengers) were Italian and French (about 16% of total number of cruises in the Mediterranean Sea) while the remaining (with a capacity over 1,000 passengers) represented about 56%. In fact, the largest home-porting Country as well as the leading shipbuilder in cruise vessel in Europe is Italy (MedCruise, 2015).

### **1.2.2 Focus on the Mediterranean area**

The Mediterranean Basin - which stretches across 2 million km<sup>2</sup> and 34 countries, East from Portugal to Jordan, and South from Northern Italy to Cape Verde - is considered a “climatic hotspot”, being one of the most vulnerable (and threatened) worldwide ecosystems (for example, because of high levels of photochemical ozone formation, secondary aerosols). The enormous value is due to its rich biodiversity, unique economic and cultural importance.

Mediterranean coastal areas had experienced an exponential development in urbanization, major ports and related activities, with a detrimental effect on air quality (Im and Kanakidou, 2011).

One of the most significant large scale-pressure to the weak Mediterranean equilibrium is international maritime traffic. The Mediterranean Sea attracts 15% of the global shipping activity (by number of calls) and 10% by GT (Schinas and Bani, 2012), facilitated by the entrance of the Suez Canal and by many major harbours. Major shipping routes are concentrated across the Gibraltar Strait, the Suez Canal, the Dardanelles and the Bosphorus Strait, along the Adriatic Sea and Southern France (Fig. 1.13), with over 480 ports and terminals, most of which in Greece and Italy (LMIU, 2008).

However, a growing sector is constituted by cruise tourism which has been a relevant market in Europe (+162% in the 2002-2012 period) with the Mediterranean as the main destination for European passengers (UNWTO, 2010; Eurostat, 2015). Tourism in the Mediterranean Basin has been more focused towards the cultural and historical varieties of the destination itself compared to other locations labeled as “fun-sea” (Marušić et al., 2012). Projections for 2020 (ECC, 2012) predicted a growth in cruise traffic up to 10 million passengers.

The evolution of cruise sector in the Mediterranean area is illustrated in MedCruise annual reports. MedCruise is today one of the greatest and widest port associations

around the globe, with 74 port members, representing more than 100 ports in the Mediterranean region, including the Black Sea, the Red Sea and the Near Atlantic. For the Adriatic region, Venice and Brindisi joined to the Association.

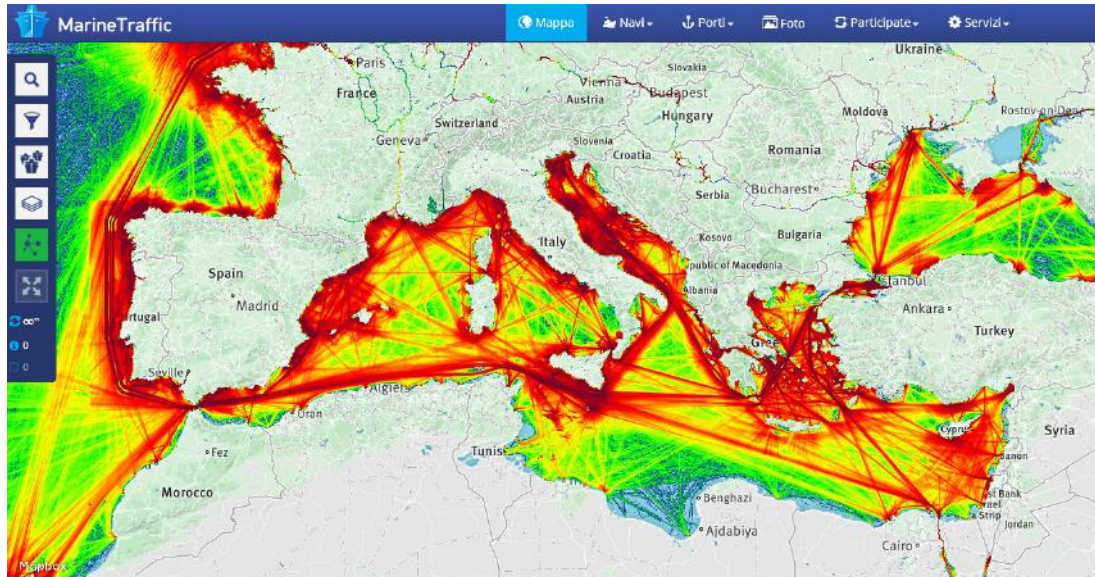


Figure 1.13. Traffic density map (all ships) in the Mediterranean Basin in 2015 (<http://www.marinetraffic.com/>), based on AIS (Automatic Identification System).

In total, 25,761,721 cruise passengers (including transits) were recorded in the MedCruise port region in 2014, with an increase of 4.8% in five years earlier. A relevant factor is represented by the changes in cruise seasonality last three years. Cruise traffic was not more concentrated in summertime but also in autumn (especially October) last years, obviously depending on the region.

The Adriatic and East Med were more trafficked in the period June-November, oppositely to the West Med, in which cruising was equally distributed throughout the year.

Ideally, four regions can represent the Mediterranean area: the Black Sea, the Adriatic, Eastern and Western Mediterranean. It is clear that the Western and Central (including the Adriatic and Eastern Mediterranean) areas play a driving role in cruise sector (Bartolomé et al., 2009), being the most attractive areas (Fig. 1.14). For purposes of this study, the Adriatic was the second “busy” cruise region, almost 18% of the total Mediterranean traffic.

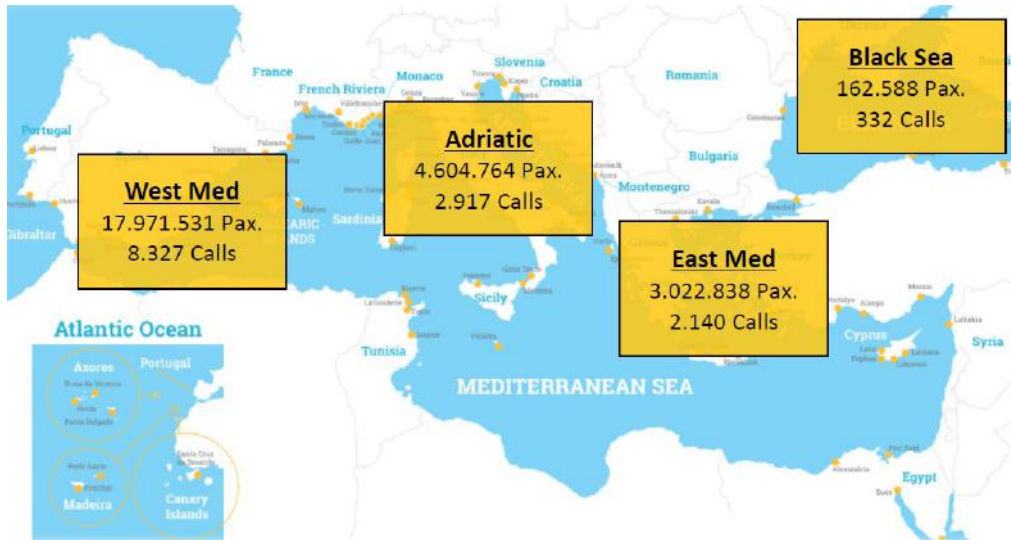


Figure 1.14. Cruise traffic (as number of passengers and ship calls) in MedCruise regions (source: MedCruise, 2015).

Also, an interesting result was that home-porting (embarking and disembarking) was the main activity in the Adriatic ports (Fig. 1.15), with an emerging share for the Black Sea (+15%). This is confirmed by the fact that Venice ranked as the first homeport in the Mediterranean for cruise passengers also in 2015 (1.686.606 passengers; source: Venice Port Authority), followed by Barcelona, Civitavecchia and Savona.

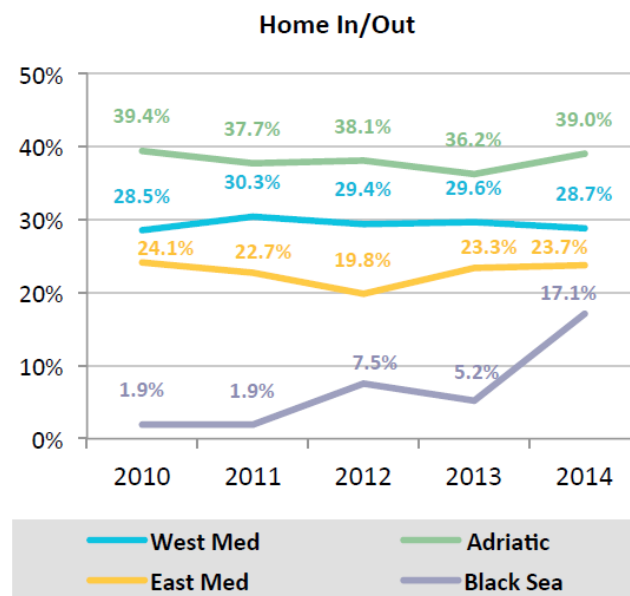


Figure 1.15. Trends in home-porting activity in MED regions, period 2010-2014 (source: MedCruise, 2015).

Definitively, Bari, Corfu and Piraeus (Atene harbour), as well as the Black Sea ports are emerging as transit locations, whereas the Turkish and Croatian harbours could be the major destinations in the next future. Croatia has becoming an emerging destination since the first decade of the 21<sup>st</sup> century, not only for cruises in the Adriatic Sea but also connecting the Greek Islands to Venice (Marušić et al., 2012). In fact, beyond Venice, Dubrovnik/Korcula is the second cruise location in the Adriatic Sea, followed by Corfu and Bari (Fig. 1.16).

Because of its strategic position, Italy is the principal Mediterranean Country which has the biggest share of all traffic, followed by Spain. For example, Italy hosted 52.2% and 26.5% of total passengers as home-ports. On long-term, French ports saw their cruise passenger numbers increasing by 33.7%, since 2010.

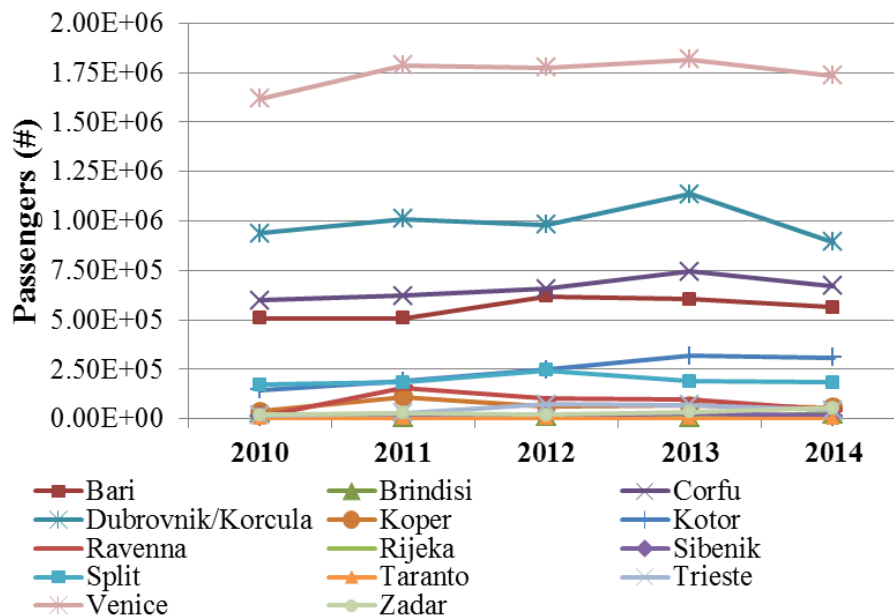


Figure 1.16. Trends in the Adriatic cruise ports, period 2010-2014 (data extracted from Medcruise, 2015).

Regarding maritime freight, approximately 30% of the world's container traffic (around 720 million tons) passes through the Mediterranean (Adamo and Garonna, 2009). Tankers are vessel types (just under 60%) which dominate intra-Mediterranean trade. "Internal" Mediterranean trade occurs among 95 ports, with a total global throughput of container trade estimated at 56 million TEU in 2013 (+5.5 with respect to 2012). Container volumes are expected to reach 171 million TEU by 2017, with the Western Mediterranean and Eastern areas as leaders, each expected to

account for 24% of the trade (Brett, 2014). Most of the major ports are developing new container handling infrastructure to compete for a share of this growing market. Also, Ro-Ro traffic between Mediterranean littoral States is expected to increase from approximately 14 million tons in 2012 to 16 million tons in 2020 (Graham, 2014). In particular, in the Short Sea Shipping (SSS) of goods (like Ro-Ro links) Italy is among the leaders, with ports of Trieste, Genoa, Augusta, Taranto, Venice and Gioia Tauro (REMPEC, 2008).

### 1.3 Environmental impacts

Despite recent efforts at international level, some environmental issues linked to marine transport need further knowledge and improvement. Much of the impacts are not included in legislation or are underestimated. Different temporal and spatial scales should be considered, distinguishing in-port impacts (from ships and associated activities) and open-sea impacts (cumulative effects of global traffic).

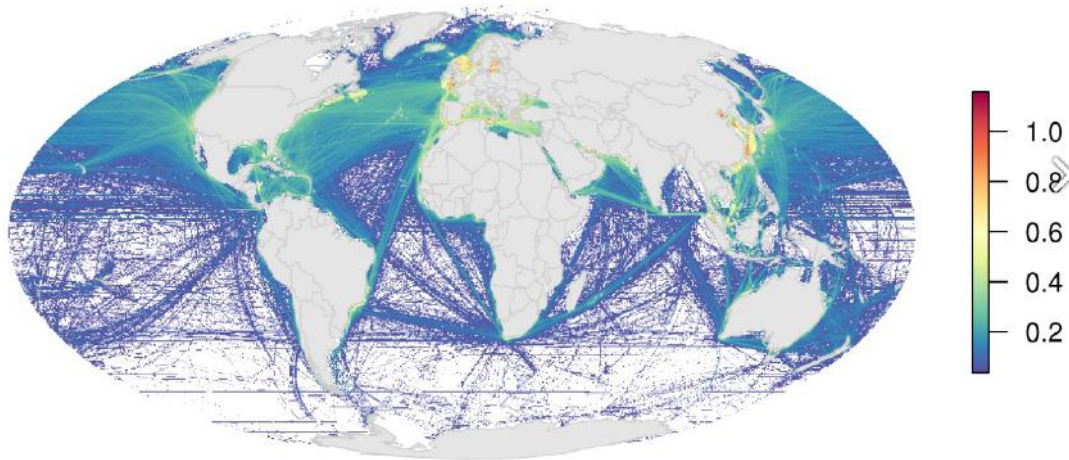


Figure 1.17. Cumulative global impact of shipping from the combination of nineteen individual stressors (source: National Center for Ecological Analysis and Synthesis).

It is evident how the global impact reflects the major shipping routes and it is higher along coastlines. The most influenced areas are the Mediterranean Basin, the North Sea and the China coasts (Fig. 1.17).

At local scale, in-port activities (arrival/departure of ships, vehicular traffic) may be a not-negligible source of pollution too (Fig. 1.18), involving all environmental matrices (air, water, soil). Generally, in a cost-benefits analysis, the main



environmental impact factors of ships are divided in those for which a monetary evaluation is possible (GHG, air emissions, discharges) and not (resources consumption and waste).

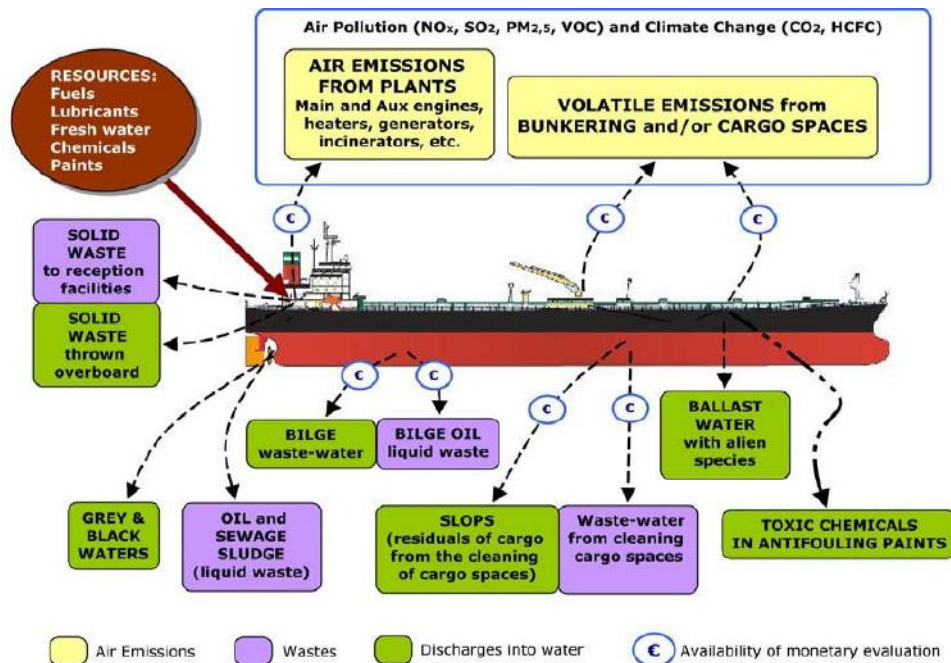


Figure 1.18. Main environmental impacts of shipping with eventual monetary evaluation (source: Maffii et al., 2007).

### 1.3.1 Climate change

Shipping, like other modes of transport (i.e. aviation), should be taken into consideration in international negotiations for its substantial contribution to climate change (IEA, 2009) and, even more important, because its emissions are not yet covered by the Kyoto Protocol.

The Fifth Assessment Report of the Intergovernmental Panel on Climate Change (IPCC) has recently stressed the urgency to avoid a global temperature increase of more than 2°C compared to preindustrial levels (IPCC, 2014) in order to allow no dramatic changes in climate system. This effort involves all sectors and, specifically, the transport sector since that demand in transport services rapidly grows, and consequently CO<sub>2</sub> emissions will continue to increase.

The White Paper, prepared by the European Commission in 2011, mentions:

“[...] a reduction of at least 60% of GHGs by 2050 with respect to 1990 is required from the transport sector [...]. By 2030, the goal for transport will be to reduce GHG emissions to around 20% below their 2008 level [...]”.

The potential impacts related to climate change could affect corridors above and beyond the ports acting as gateways. Climatic anomalies such as rising water levels, extreme weather events, coastal erosion, inundation have implications for shipping volumes and costs, cargo capacity, sailing and/or loading schedules, storage (UNCTAD, 2015).

In the light of that, the understanding to date on climate impact of shipping is essential. Actually, few studies discussed about the radiative forcing (RF) effect of this transport sector as whole. A study was carried out by the Center for International Climate and Environmental Research – Oslo (CICERO), within the EU project QUANTIFY - Quantifying the Climate Impact of Global and European Transport Systems, estimating how transportation will contribute to global warming in the future. This work was done analysing the differences among the transport subsectors (i.e. aviation, rail, road, shipping) in terms of magnitude of RF at different temporal scales. Results indicated that transport will have from a triple to quadruple larger “weight” in global emissions with respect to the current effect (Fuglestvedt et al., 2008). With particular reference to marine sector, the magnitude of shipping emissions and their impacts are emerging and relatively recent issues in scientific community.

The by-products of HFO and MDO combustion significantly influence air emissions. Emissions from ships influence both positively (warming) and negatively (cooling) RF (Fig. 1.20a) and may be distinct between CO<sub>2</sub> (the most significant GHG) and non-CO<sub>2</sub> emissions effect (of other pollutants such as O<sub>3</sub>, SO<sub>2</sub>, NO<sub>x</sub>).

In particular, CO<sub>2</sub>, tropospheric O<sub>3</sub> and soot (BC-Black Carbon) act as main global warming compounds while sulphate aerosols, NO<sub>x</sub> and organic aerosols as cooling ones. The aerosol indirect effect is due to the fact that aerosols ship-generated increase reflectivity and lifetime of clouds. In detail, the emitted SO<sub>2</sub> then oxidized to sulphate (SO<sub>4</sub><sup>2-</sup>) in the atmosphere, forms particles which, by scattering the solar radiation, determine a RF<sub>≈</sub>-31 W/m<sup>2</sup>. Furthermore, an indirect impact on climate is observed by forming cloud condensation nuclei from SO<sub>2</sub>, causing a RF<sub>≈</sub>-740 to -47

$\text{mW/m}^2$  (Eyring et al., 2010). The sunlight reflection (and therefore the cooling action) is also carried out by  $\text{NO}_x$  and organic matter.

However, according to the latest literature (Fuglestad and Berntsen, 2009), the net global effect of shipping is different at short and future temporal scales, shifting from cooling to warming in time (Fig. 1.20b), with the greatest uncertainty on the impact of  $\text{O}_3$  and BC estimates.

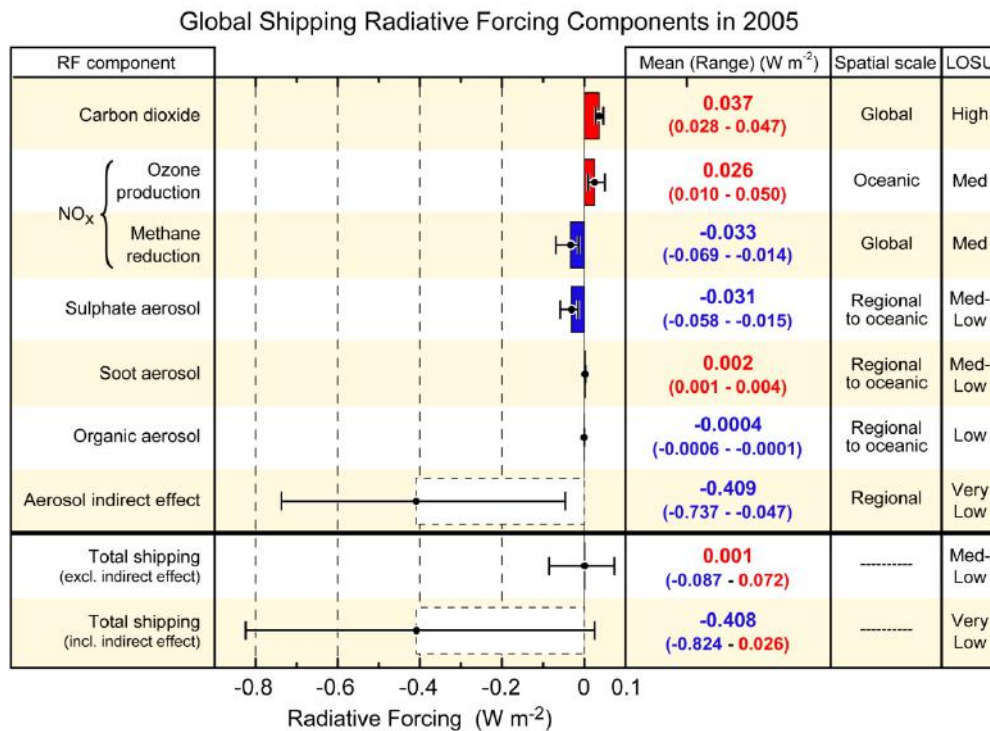


Figure 1.19. Global average annual mean RF ( $\text{W/m}^2$ ) of shipping, spatial scale and level of scientific understanding (LOSU) in 2005 (source: Eyring et al., 2010).

Presently, the net balance is negative with a RF around  $-0.4 \text{ W/m}^2$  in 2005 (Fig. 1.19), because of the compensation of the warming effect of  $\text{CO}_2$  by the double cooling effect of sulphate aerosols and reduction of methane lifetime by oxidation processes of  $\text{NO}_x$ . Actually, a more up-to-date estimate at such sectorial detail is not available in the last IPCC report (IPCC, 2014). Further, the great variability of RF values reported in literature, all results agree that today shipping has a net cooling contribution, in contrast to some estimates obtained with measurements from aircraft (Sausen et al., 2005).

It must be noted that studies of aerosol indirect effect have the widest uncertainty range (from 0 to  $0.7 \text{ W/m}^2$ ) due to the differences in modelling approaches in spatial scale, mechanisms, emission inventories used etc. For example, Lauer et al. (2007)

included contributions from several aerosol ( $\text{SO}_4$ ,  $\text{NO}_3$ ,  $\text{NH}_4$ , BC, organic matter) compared to other studies which considered only the indirect effect related to changes in  $\text{SO}_4$  (Eyring et al., 2010). Instead, Capaldo et al. (1999) applied a global model to estimate the indirect effect of sulphate particles ( $\text{RF} \approx -110 \text{ mW/m}^2$ ) derived from ships without detailed aerosol microphysics and aerosol-cloud interaction.

However, long term projections indicate that the reduction of  $\text{SO}_2$  (due to new regulations and technology improvements) in addition to the slow removal (hence accumulation) of  $\text{CO}_2$  is expected to turn to a positive RF by the mid or end of the century (Fuglestedt et al., 2009).

Approaches to solve problems with climate change could be implemented for  $\text{O}_3$  pollution lowering  $\text{NO}_x$  emissions in open sea and to cut sulphur oxides in coastal and in-port areas addressing the acidification problem (Endresen et al., 2003).

In the next future, the Arctic region could represent a dramatic proof of the economic (and environmental) impact in navigation of climate change. Smith and Stephenson (2013) simulations demonstrated, by midcentury, as climate-induced changes in sea ice concentration and thickness influenced technical feasibility of trans-Arctic ship navigation.

In fact, as the Arctic ice sheet melts, new routes along the Northern Sea, over the North Pole and the Northwest Passage could be accessible and shorter in distance. As consequence, navigability could extend in time and ship traffic rise in volume, leading to greater black carbon deposition on ice and snow surfaces. Having a significant warming effect (McConnell et al., 2007), the BC deposition would further accelerate snowmelt and sea ice loss, creating a vicious circle of negative impacts.

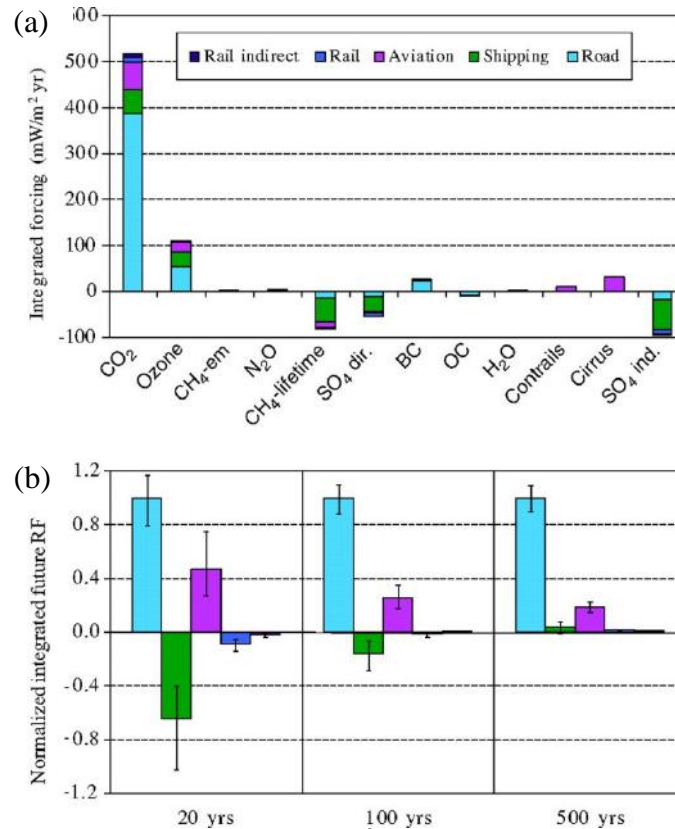


Figure 1.20. (a) Current global RF (mW/m<sup>2</sup> yr) due to 2000 transport emissions, by substance and transport subsector for a time horizon of one century; (b) future global mean RF per sector due to 2000 transport emissions, normalized to the values for road transport. Uncertainty ranges are given as one standard deviation (source: Fuglestvedt et al., 2008).

### 1.3.2 Effects on human health

In recent years, large research efforts have been made linking air pollution to negative health effects for exposed populations. Health effects densities along coasts have been demonstrated to be thousands of times greater than those seen in inland regions, accounting 60,000 deaths annually at a global scale to shipping-related PM emissions (Corbett et al., 2007). Data from the Los Angeles County Health Survey demonstrated that people living in close proximity to the Port of Los Angeles experienced higher rates (2.9%) of asthma, coronary heart disease and depression, compared to other communities in the urban area (Human Impact Partners, 2010). Additionally, data survey (Sharma et al., 2006) of the California Air Resources Board (CARB) attributed 3,700 premature deaths to ports.

At global scale epidemiological and toxicological studies are not available. In general, epidemiological studies on ships emissions are focused on particle mass but other metrics such as particle size makes particles more or less harmful. In fact, the

smaller the particle the higher the surface area and the toxicity. Hence, finer and irregular particles (i.e. those of BC), are more dangerous with respect to the spherical ones. Particles generated by marine diesel engines contain other compounds such as PAHs, vaporized heavy metals from lube oils, transition metals (Vanadium, Lead, Nickel) in fuels.

Soot particles are classified as human mutagen and carcinogenic agent by the International Agency for Research on Cancer (IARC) due to the fact that cause respiratory pathologies, as bronchitis, asthma, and in the worst cases, ischemic heart diseases and neurological problems (Slezakova et al., 2013; Rundell et al., 2007).

A comparison between particles emitted by IFO (Intermediate fuel oil) and MDO (Marine Diesel Oil) fueled ship engines showed that IFO particles are significantly more toxic because of higher transition metal content and aromatic compounds (Zimmermann et al., 2013; Sippula et al., 2014), although lower amount of EC. The addition of lubricant oils and additives increases the particle toxicity up to 10 times (Gualtieri et al., 2014).

Exposure to high levels of particulate matter finer than 2.5  $\mu\text{m}$  ( $\text{PM}_{2.5}$ ) is investigated in several surveys. Epidemiological studies (CARB, 2006; Winebrake et al., 2009; Davis et al., 1997; Pope et al., 2004; Nel et al., 2005; Kaiser et al., 2005; Ostro et al., 2004; Zanobetti et al., 2005) revealed a relatively consistent association between short-term  $\text{PM}_{2.5}$  exposure and mortality across several countries from South America to Western Europe. Estimates differences depending on inventories used accounted, for example, 83,500 and 76,700 premature cardiopulmonary and 7,100 and 7,000 lung cancer deaths annually for AMVER and ICOADS inventories, respectively (Winebrake et al., 2009). Also, a clear correlation between chronic exposure and mortality risk was found by toxicological studies in Netherlands (Brunekreef et al., 2009) and USA (Krewski et al., 2009).

Several studies (Corbett et al., 2007; USEPA, 2008; Viana et al., 2015; Jonson et al., 2015) highlighted that reductions of ship exhausts yield health benefits for coastal population. Some reduction measures are evaluated positive, technically viable and feasible, lowering exposure risk to ship-sourced air pollution. Bearing in mind that exposure risk is the product between exposure frequency and produced damage,

harbour personnel and people living along the most congested coastlines are subject to the highest risk.

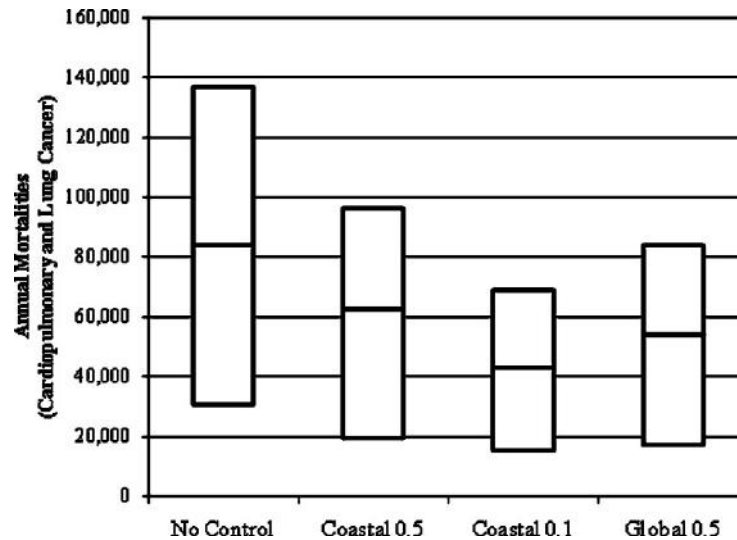


Figure 1.21. Mortality for four different emission control scenarios: no control, 0.5% S and 0.1% S limit on coastal areas, 0.5% S at global level, on the basis of the ICOADS dataset (source: Winebrake et al., 2009).

For example, designating an ECA (Emission Control Area – sea areas where stricter emissions standards are applied to minimize airborne emissions) in the Marmara Sea is illustrated to lead to environmental and health benefits (Viana et al., 2015). This is translated in the avoidance of 205, 460 and 390 hospital admissions annually from exposure to  $PM_{10}$ ,  $PM_{2.5}$  and  $SO_2$  respectively. In addition, 30 premature deaths annually due to exposure to  $PM_{2.5}$  could be prevented. Also, the analysis of different emission control scenarios (Winebrake et al., 2009) revealed that the application of more stringent sulphur limits (i.e. 0.1%S) in coastal areas could reduce total mortality for cardiopulmonary and lung cancer (Fig. 1.21).

### 1.3.3 Social and economic issues

Air degradation in port-cities presents large external costs to the local economy. Air pollution related to ships at berth in the port of Bergen (Norway) was estimated between 10 and 22 million euros (McArthur and Osland, 2011) while in Castells Sanabra et al. (2013) on 13 selected Spanish harbours valued the overall externalities in 206 million euros with an individual contribution of  $PM_{2.5}$ ,  $SO_2$  and  $NO_x$  was 95, 65 and 46 million euros respectively.

The economic impact of ship emissions for the port of Piraeus (Greece) demonstrated that annually the estimated externalities of in-port emissions were around 51 million euro (Tzannatos, 2010). The internalization of these costs is expected to lead to increase taxes from 1 (for cruise shipping) to 10% (for coastal passenger shipping). It is clear that emissions in harbour and surrounding areas contribute preponderantly, as opposed to those from cruise shipping, in terms of costs and relative impacts on health and environment.

A study requested by the European Parliament illustrated the external costs of air emissions from maritime transport in European seas in 2006 (Tab. 1.3). It is evident as the Mediterranean Sea pays the second highest price related to maritime transport especially for SO<sub>2</sub>, PM<sub>2.5</sub> and VOC. Also, SO<sub>2</sub> and NO<sub>x</sub> need more restrictions since that, together, represent about 83% of the total costs for Europe.

It must be noticed that these costs increase with a factor of 1 to 15 according to density surrounding population. The social costs for a ton of PM<sub>2.5</sub> and SO<sub>2</sub> can be 33,000 euros and 6,000 euros, respectively (Holland and Watkiss, 2002).

Table 1.3. External costs of air pollution from shipping in Europe in 2005 (source: CAFE, 2005).

Area	SO <sub>2</sub>	NO <sub>x</sub>	PM <sub>2.5</sub>	VOC (combustion)	Total per Sea	%
North Sea	9,230	8,504	3,795	131	21,660	47.7
Black Sea	533	391	198	6	1,127	2.5
<b>Mediterranean Sea</b>	<b>6,557</b>	<b>2,247</b>	<b>1,950</b>	<b>63</b>	<b>10,817</b>	<b>23.8</b>
Baltic Sea	2,115	1,915	733	18	4,780	10.5
NE Atlantic Sea	2,919	3,375	732	30	7,056	15.5
<b>Total per pollutant</b>	<b>21,355</b>	<b>16,431</b>	<b>7,407</b>	<b>247</b>	<b>45,441</b>	<b>100.0</b>
%	47.0	36.2	16.3	0.5	100.0	

The potential external cost benefit of Shore Side Electricity (SSE) has been evaluated in order to balance the infrastructure costs in some Northern Europe ports. Ballini and Bozzo (2015) provided a cost-benefit analysis of introducing cold-ironing technology at the new cruise ship pier in Copenhagen, Denmark. If 60% of cruise ships will use cold ironing technology, a health cost benefit of 2.8 million euro per year would be reached, balancing the capital cost in 12-13 years.



In EU ports the implementation of cold ironing is challenging. The total anticipated health benefits by using SSE were estimated to 2.94 billion euro for 2020, while the potential for reduction of carbon emissions reaches the 800,000 tons of CO<sub>2</sub> (Winkel et al., 2015).

#### 1.4 The EU policy

The European Parliament and the Council adopted the first guidelines in transport sector in 1996, enlarging priorities afterwards.

ESPO (European Sea Ports Organization) defined the top-10 of environmental priorities in its Environmental Review 2013 by examining the influence of factors such as the port size and geography.

Research sample consisted in 79 ports of 21 European Maritime States providing environmental data in a dedicated exercise through the EcoPorts website ([www.ecoport.com](http://www.ecoport.com)).

In line with the EU Air Quality policy and other initiatives to reduce shipping emissions and minimize health effects in coastal areas, air quality has increased in significance over time and currently is the top environmental priority by the European port sector as a whole (Tab. 1.4).

Table 1.4. Environmental priorities in European harbours, period 1996-2013 (ESPO, 2013).

	1996	2004	2009	2013
1	Port development (water)	Garbage/Port waste	Noise	Air quality
2	Water quality	Dredging: operations	Air quality	Garbage/Port waste
3	Dredging: disposal	Dredging: disposal	Garbage/Port waste	Energy consumption
4	Dredging: operations	Dust	Dredging: operations	Noise
5	Dust	Noise	Dredging: disposal	Ship waste
6	Port development (land)	Air quality	Relationship with local community	Relationship with local community
7	Contaminated land	Hazardous cargo	Energy consumption	Dredging: operations
8	Habitat loss/degradation	Bunkering	Dust	Dust
9	Traffic volume	Port development (land)	Port development (water)	Port development (land)
10	Industrial effluent	Ship discharge (bilge)	Port development (land)	Water quality

According to this ESPO study it is interesting to note that air quality priority is always high in ranking, independently of port size. Instead, geographical location plays a relevant influence on environmental priorities. All ports seem to face noise, air quality, energy consumption, as well as waste in environment management (ESPO, 2013).

A new legislative framework that came in force in January 2014 (EU Regulation n. 1315/2013) aimed to develop the Trans-European Transport Network (TEN-T). The great aim is to allow that travel time within the TEN-T network will be less than 30 minutes by 2050. In general, the main objectives will be: safer and less congested travel by an efficient multimodal transportation system, faster journeys and reduction of greenhouse gas emissions.

The infrastructure has a dual-layer structure which comprises a comprehensive (completed by 2050) and a core network (completed by 2030). This core network connects 94 European ports and 38 major airports with railways and roads, upgrades 15,000 km of railway line to high speed track. The core infrastructure is composed by nine main corridors in North-South and East-West directions (Fig. 1.22): Scandinavian-Mediterranean Corridor, North Sea-Baltic Corridor, North Sea-Mediterranean Corridor, Baltic-Adriatic Corridor, Orient/East-Med Corridor, Rhine-Alpine Corridor, Atlantic Corridor, Rhine-Danube Corridor, Mediterranean Corridor.

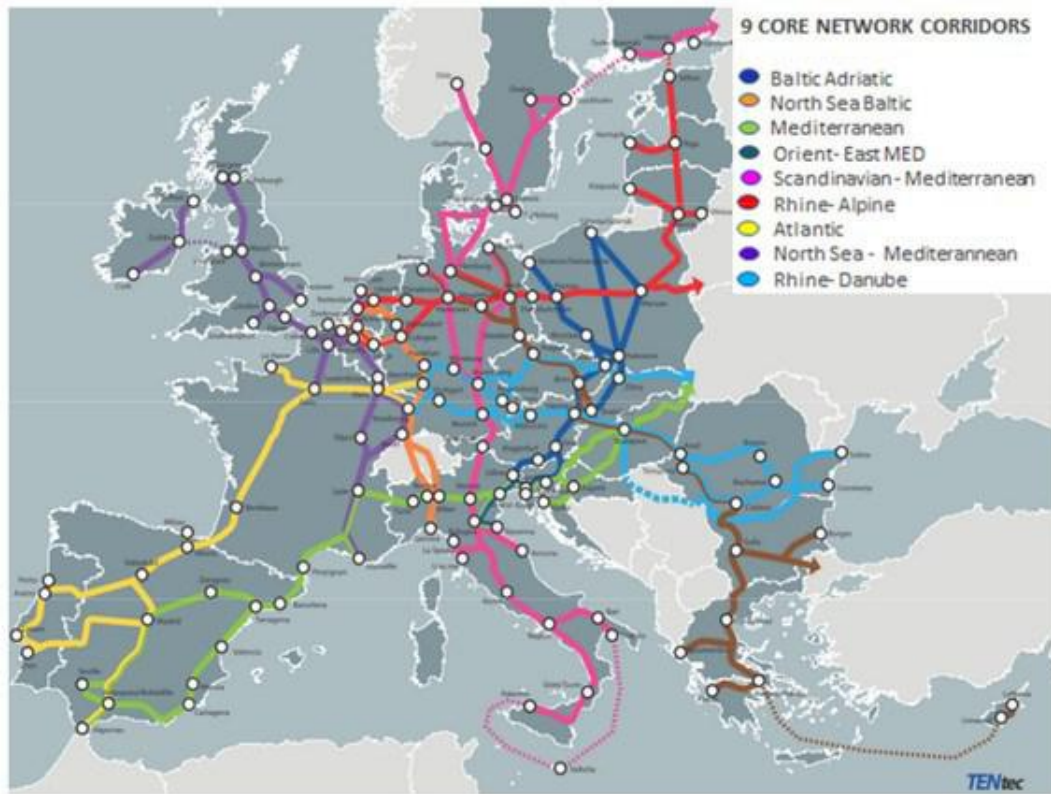


Figure 1.22. The TEN-T network.

Italy is crossed by four Core Network Corridors, involving some principal port-cities: the Baltic-Adriatic corridor includes Trieste, Venice, Ravenna and Capodistria; the Mediterranean corridor in Northern Italy (Po Valley) and the Scandinavian-Mediterranean corridor which passes through La Spezia, Livorno, Ancona, Bari, Taranto, Napoli and Palermo; the Rhine-Alpine corridor connects also the port of Genoa. According to the EU Regulation criteria, Italian has 14 core ports (i.e. Venice) as well as 9 comprehensive ports (included Brindisi) as reported in Fig. 1.23.

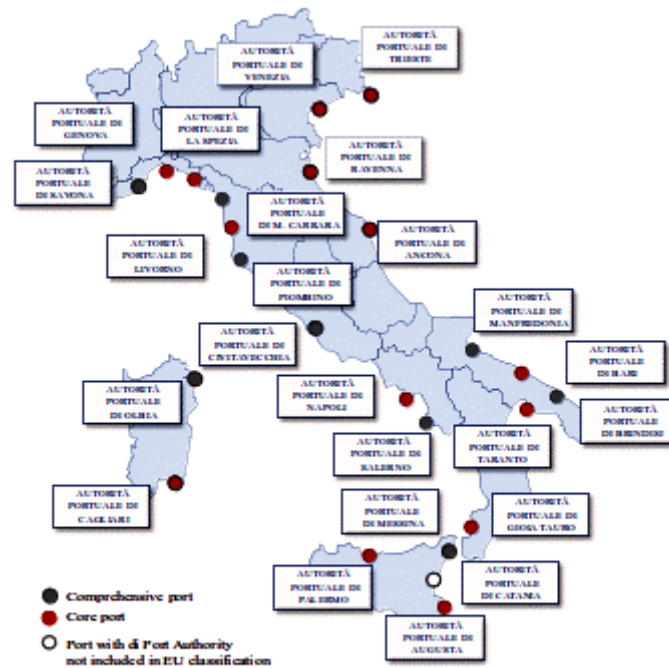


Figure 1.23. The Italian Core and Comprehensive ports (classified by EU).

In March 2011, the European Commission adopted the “White Paper - Roadmap to a Single European Transport Area- Towards a competitive and resource efficient transport system” (COM (2011) 144 final) which aims to create a unique, competitive transport system at European level with environmental, economic and social advantages. The main purposes of this comprehensive strategy is reduction of transport emissions by 2050, reaching a 60% overall. In particular, decreases should be up to 50% in aviation using low-carbon fuels, by 40 to 50% from shipping and by 80% from road transport adopting no more conventionally-fueled cars. Moreover, rail and waterborne networks for medium-distance connections will be encouraged, replacing road transport up to 50%.

#### 1.4.1 The Adriatic-Ionian macro-region

The Adriatic Sea is a semi-enclosed basin within the Mediterranean Sea, bordered by six coastal countries: Italy, Albania, Croatia, Slovenia and Montenegro, Bosnia and Herzegovina (Fig. 1.24). It is about 800 km long (distance from Venice to the Strait of Otranto) with a width of 85 nautical miles (nm) ( $\approx 160$  km), a maximum depth of 1,324 meters, and an area of 131,050 km<sup>2</sup> (1/20 of the Mediterranean Sea area). The

coastal area is represented almost totally by Croatian (~75%) and Italian coasts (~15%) and varies greatly in typology. Croatia has several large and small islands with twisty coastlines whilst Italian coasts are straight and relatively regular. Overall sea depths are not considerable in the Adriatic Sea, however, the southern part is far deeper than the northern part (Vrgoč et al., 2004). Maximum temperatures in the surface sea layer are reached in August with 24-25°C, and the minimum readings in winter (January-February) with 10 °C.

The prevailing winds in colder period are the bora, a strong northeast wind that blows from the nearby mountains into the sea, and a southeasterly wind named the scirocco. During warmer part of the year, sea and land breezes, as well as Etesians, are frequent, with or without an interval of a few days calm (Pandžić and Likso, 2005).

Because of its high biodiversity, historical and cultural value, easy accessibility, the Adriatic region is a very attractive and, consequently sensitive area. It is characterised by a slow nutrients exchange, pollutant inputs from the Po Valley area (Horvath et al., 1999). Furthermore, heavily urbanized agglomerates are located along coastal regions, concentrating industrial, tourism and harbour activities in restricted areas. Accordingly, environmental pressures act in a short time span, overcoming the carrying capacity of the host environment, without adequate infrastructures designed to process pollution of such magnitude and intensity (Klein, 2005).



Figure 1.24. Adriatic coastline length (in km) for facing Countries.

One of the most important environmental pressures is maritime traffic, rapidly grown in recent years in the Mediterranean (Carić et al., 2014). Intensive coastal tourism leads to sea pollution, especially due to the fact that waste waters aren't adequately treated and finally discharged directly into the sea. In fact, excluding accidental events, the "operational pollution" is the most dangerous, constant phenomenon of pollution at sea and nearby coastal regions caused by ships. Pollutants related to routine operations include oily ballast waters, washing residuals, fuel residuals, bilge waters.

The Adriatic and Black Seas markets are considered emerging markets in the Eastern Mediterranean because they will attract an increasing share of larger vessels (LMIU, 2008). For example, Adriatic ports are a natural gateway for Central and Eastern European traffic and are well placed take advantage of any hinterland infrastructure improvements to attract cargo currently routed via Northern European ports. Therefore, maritime traffic through the Strait of Otranto and into the Northern Adriatic is likely to increase (see Section 1.2.2).

Focusing on Italy, its fleet consists of around 14,000 fishing vessels, thirty oceanic vessels, 600 merchant vessels (FAO, Yearbook of fishery statistics).

The European Commission has launched the EU Strategy for the Adriatic and Ionian Region (EUSAIR) on 17 June 2014. The macro-regional initiative involves the Commission, together with the Adriatic-Ionian Region countries (four EU Member States-Croatia, Greece, Italy, Slovenia and four non-EU countries-Albania, Bosnia and Herzegovina, Montenegro, Serbia) and stakeholders in promoting EU integration. The four fundamental goals are: blue growth, energy and transport connectivity, environmental quality and sustainable tourism (Fig. 1.25). In particular, Italy and Serbia coordinate Pillar 2 "Connecting the region", encouraging a competitive regional intermodal port system, both for freight and passengers.

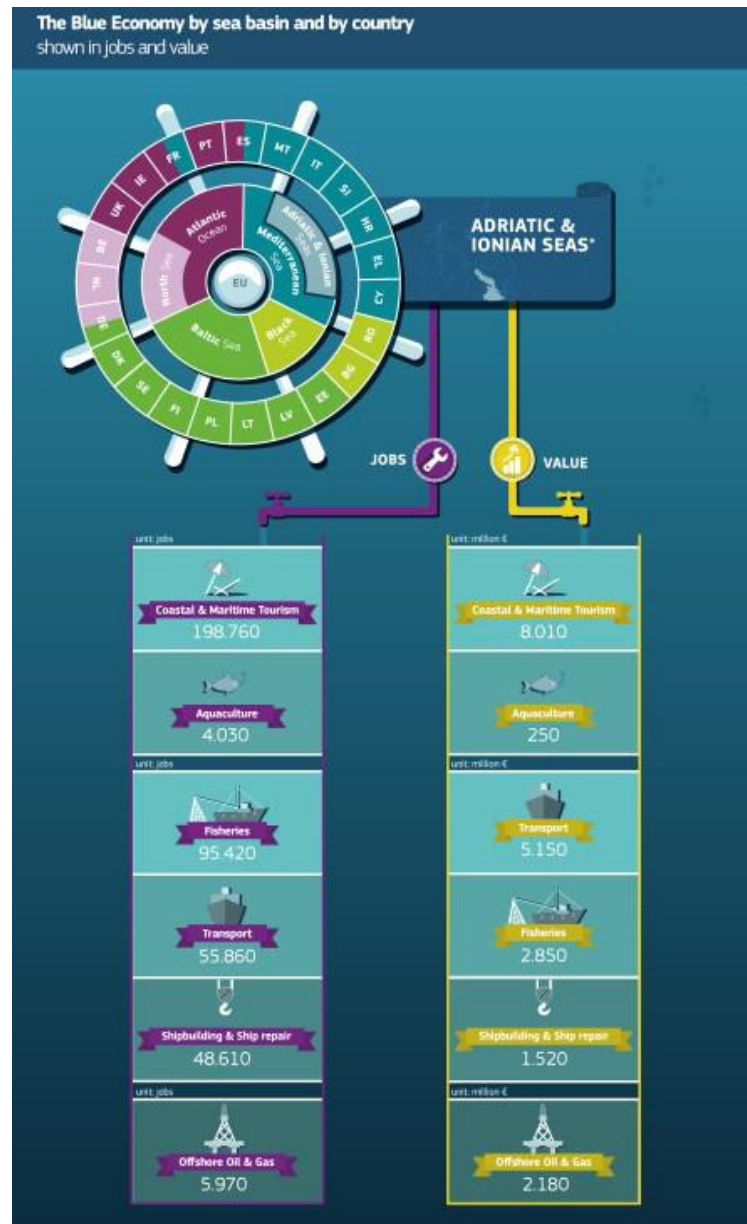


Figure 1.25. Blue growth in the Adriatic-Ionian Seas in terms of jobs and value. Source: [http://ec.europa.eu/maritimeaffairs/policy/blue\\_growth/infographics/#\\_Adriatic\\_and\\_Ionian\\_Seas](http://ec.europa.eu/maritimeaffairs/policy/blue_growth/infographics/#_Adriatic_and_Ionian_Seas).

In conclusion, the proposal of the designation of the Mediterranean Sea (therefore including the Adriatic-Ionian basin) as a (S)ECA is currently under discussion between the European Union, private and public stakeholders. In this perspective, studies, demonstrating the present impact of shipping on air quality, effective reduction of emissions and development of emission future scenarios in implementing a special area, are a fundamental support in the application procedure.

It must be noticed that the Mediterranean area also includes Asian and African States and few of them ratified the Annex VI of the MARPOL Convention, therefore a shared political strategy is required.

On the other hand, some cost-benefits analysis (Meech, 2008) reported the potential detrimental effects on Mediterranean ports compared to Atlantic coasts for some countries (i.e. France, Spain) because of lower freight costs and priced fuels. Moreover, the designation of an ECA could negatively affect cruise traffic (increase of 25% of low-sulphur fuel price) choosing other no-compliant routes.

### **1.5. Emissions reduction efforts**

Several technology-related strategies and operational measures have been proposed to curb emissions from the maritime transport sector. IMO regulations to restrict air pollution from ships act on three different points: ship design and building, efficiency improvement of existing ships and application of innovative green technologies (i.e. “cleaner” fuels). Some of them imply modifications of vessel design, engines and propulsion systems while other measures are based on optimization of working modes at sea and in port.

In this perspective, since 1 January 2013, the IMO made mandatory the EEDI (Energy Efficient Design Index) for new ships and the Ship Energy Efficiency Management Plan (SEEMP) for all ships with the adoption of amendments to MARPOL Annex VI (resolution MEPC.203 (62)).

The EEDI is a parameter specific for each ship category and expressed in grams of carbon dioxide (CO<sub>2</sub>) per ship’s capacity-mile and is calculated by a formula based on six technical factors (ship design architecture, main propulsion system, auxiliary energy systems, alternative propulsion system and energy recovery units, fuel type, routing and optimal operational procedures - SEEMP). To attain the required energy efficiency level, ship designers and builders can choose to apply among the most cost-efficient solutions. A progressive reduction of CO<sub>2</sub> emissions and of energy consumption compared with the 2008 baseline has been foreseen until 2025 and onwards, strengthened every five years in three steps: 0-10% for ships built within 01/01/2013 and 21/12/2019, 10-20% from 01/01/2020 to 31/12/2024 and 20-30% after 01/01/2025 (IMO, 2009; IMO, 2014).



In practice, the easiest method of limit emissions is to reduce fuel consumption as it also allows save money. This is the so-called ‘green-gold’ paradigm (McKinnon, 2010) and a useful parameter called Fuel Operational Consumption (FOC) that is the actual fuel consumption per travelled route is used. A variety of technical and operational measures to maximize the FOC index are available to the operators of ships (Fig. 1.26).

However, operational and maintenance-related measures are likely to be the major source of any efficiency results at short-medium term, whereas new fuels and power technology-related solutions will act after 2020 (IEA/OECD, 2008).

A comprehensive overview on measures that can be implemented relatively quickly, option’s likely payback period (ranging from to one year to more than 15 years) and class of vessels suitable to benefit from each approach, was provided in IEA/OED (2009).

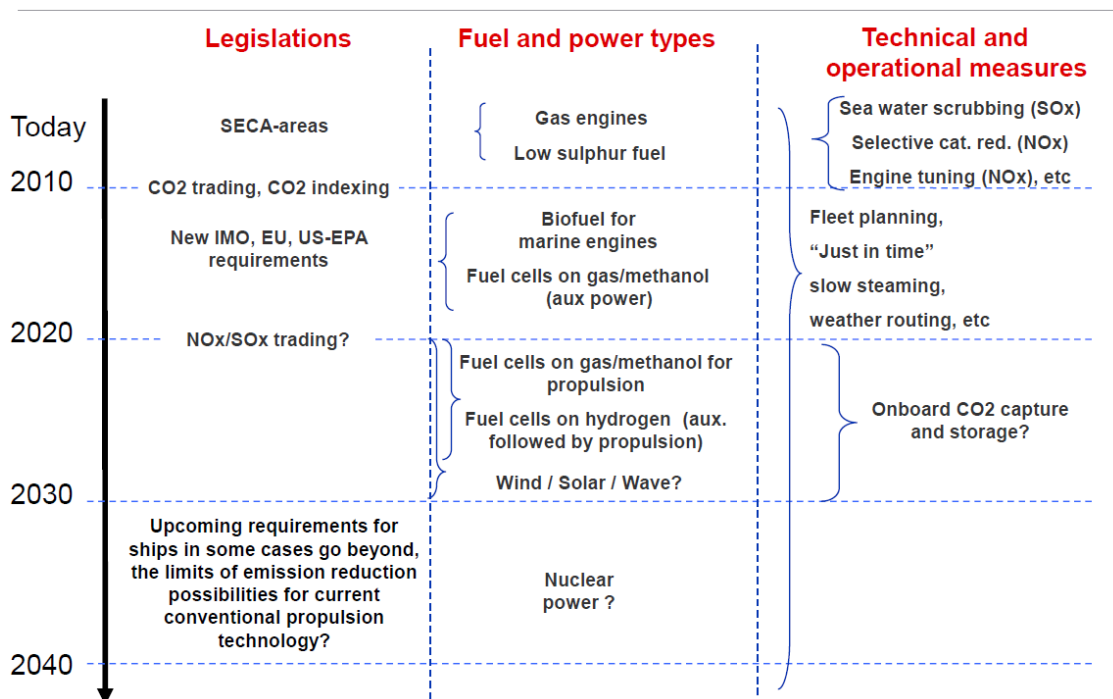


Figure 1.26. Current and future reduction measures in shipping emissions (source: Eide et al., 2007).

### 1.5.1 Technical and operational measures

Fuel savings related to the implementation of the SEEMP practices (mainly slow steaming) may cause PM reduction up to 40% (Di Natale and Carotenuto, 2015).

Nevertheless, in harbour areas emissions from manoeuvring and intense traffic (with higher emission factors than that at cruising mode) compensate the effect of low loads (EPA, 2000; IMO, 2009).

Rising fuel costs led to adopt slow steaming by the world's shipping community since 2007. Initially, marine operators were reluctant to fully adopt this solution since that when the engine (typically a two-stroke engine) operates at low load (below or even far below 60%) the system is not optimized at all.

This solution consists in slowing down ship speed, typically from 23 to 18 knots, in order to reduce fuel consumption (Fig. 1.27) more than 50% (MAN Diesel & Turbo, 2011). Theoretically, a 10% speed reduction involves a fuel saving of 15-19%, and 36-39% with a 20% speed reduction (ICCT, 2011).

Nevertheless, lowering velocity for long periods could cause some problems to engines, which are built to work continuously at a specific load and speed. Another disadvantage could be, an increase in delivery times (Lee, Lee, and Zhang, 2013), particularly in the container industry, and consequently reduced competitiveness of shipping versus other modes.

It is possible to act this option by minimizing time spent at berth by ships and optimizing loading/unloading activities in port.

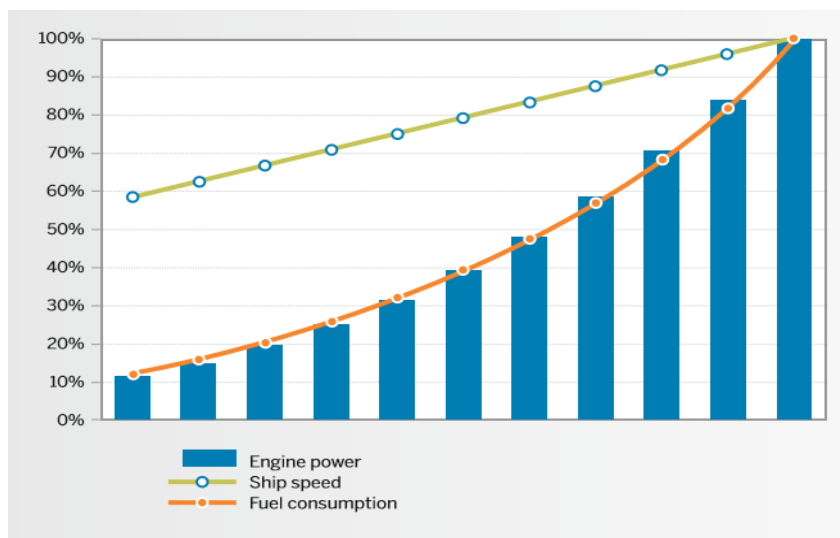


Figure 1.27. Relationship among ship speed, engine power and fuel consumption (source: <http://www.wartsila.com/docs/default-source/Service-catalogue-files/Engine-Services---2-stroke/slow-steaming-a-viable-long-term-option.pdf?sfvrsn=0>).

An optimal weather routing system that considers both weather conditions and route length allows save fuel and proportionally reducing exhaust gas emissions. This is a GIS-integrated system also allows navigate in safety conditions and could be improved by auto-piloting systems (ICCT, 2011). Wave height is one of the most important factors which influence the actual ship consumption. For example, a ship cruising at 25 knots velocity with 3 or 4 m of wave height needs from 22% to 33% more energy with respect to navigation in calm seas (Tsujimoto et al., 2013).

To drive down shipping emissions other strategies on voluntary basis are mainly used: application of scrubbers and filters, Selective Catalytic Reduction (SCR), and Humid Air Motor (HAM).

A scrubber is a packed tower on a ship in which exhaust gas is directed, and makes contact with seawater before pumped into. There  $\text{SO}_2$  comes into contact with seawater (fast reaction between the  $\text{SO}_2$  and calcium carbonate -  $\text{CaCO}_3$ ) to form  $\text{CO}_2$  and calcium sulphate (gypsum), a major constituent of ordinary seawater (Andreasen and Mayer, 2007). Two different device types exist: open-loop and closed-loop systems. In an open-loop system, the sludge is directly discharged into the sea without treatment, whereas into a closed-loop system the sewage can be filtered if required or stored in tanks. Actually, on-board conventional treatment use Venturi scrubbers to remove particles coarser than 500 nm (Di Natale and Carotenuto, 2015).

The use of retrofitting technologies (e.g. scrubbers) is efficient in removing PM and  $\text{SO}_2$  especially during hotelling and manoeuvring phases, and can be a more effective than the use of low-sulphur content of marine fuel (Cullinane K. and Cullinane S., 2013). The environmental benefits of scrubbers on new ships and retrofits are about 2.5 million euros per year (Cullinane and Bergqvist, 2014).

The removal of particles from marine diesel exhaust is related to its tri-modal size distribution but two main fractions can be considered: particles larger than 2  $\mu\text{m}$ , composed by ashes and sulphate particles, and particles in the range 0.1-2  $\mu\text{m}$  (Greenfield Gap), including the finest component (soot, finer ashes, sulphate particle, ultrafine-nanometric particles). Available exhaust gas cleaning systems are differentiated by physics and fluid dynamics of  $\text{PM}_{2.5}$  and  $\text{PM}_{<1}$ .

Table 1.5. Exhaust gas cleaning systems with relative PM reduction efficiencies and Technology Readiness Level (source: Di Natale and Carotenuto, 2015).

Exhaust gas cleaning systems			
Strategy	% PM reduction	% PM <sub>1</sub> reduction	TRL
Selective catalytic reduction	n.a.	Negligible	9
Wet scrubbers	<85	n.a.	9
Venturi scrubbers	>90	<50	9
Fabric filters	>90	>90	5
Diesel particulate filters	<95	<95	5-6
Diesel oxidation catalysts	<95	<95	5
Electrostatic precipitators	>90	60-80	5
Particle agglomerators	n.a.	90	4-5
Wet ESP	n.a.	n.a.	5
Wet electrostatic scrubbers	<85%	>90 in number	5
Heterogeneous condensation assisted scrubbers	n.a.	n.a.	3-4
Bubble towers	>90	>90	3-4

Briefly, particles larger than 5  $\mu\text{m}$  can be captured by cyclones, wet scrubbers and Venturi scrubbers, using centrifugal and inertial forces and directional interactions. PM<sub>2.5</sub> particles are retained by filtration and electrostatic precipitation. Electrostatic fields and filtration can be efficient in removing finer (and more harmful) particles (PM<sub>1</sub>), typical of diesel engines but some issue related to high-pressure drops, high costs, periodical regeneration limit their actual application.

New technologies are the Wet Electrostatic Precipitators (WESP), Wet Electrostatic Scrubbers (WES), Heterogeneous condensation assisted scrubbers (HCS) and Bubble Towers (BT). Laboratory experiments are using wet processes for submicrometric particle capture.

Each after-treatment technology is at a different development stage but the common ones are resumed in Tab. 1.5.

### 1.5.2 Fuel and power type-based operations

Other means to reduce SO<sub>2</sub> and PM emissions could be the use of alternative, low sulphur, liquid (as biodiesel) or synthetic fuels or power supply by renewable energy sources.

Renewable energy (wind, solar and wave energy) can be used either directly on board or generated on-shore (cold-ironing). In addition, nuclear energy is not considered a realistic option in the near future because of the cost, risk perception and regulatory challenges.

Environmental-friendly fuels may be a valid sustainable option and include methanol, biofuels, distillates. Biofuel option is actually limited because of costs, technology and processing issues. Present-day biofuels (often referred to as “first-

generation” biofuels) are produced from sugar, starch, vegetable oil, or animal fats. Many of these fuels can be used for ship diesels with minimum adaptation of the engine. Certain technical issues are necessary to avoid contamination with water, biological growth, engine deposits, and chemical instability. The “second generation” biofuels are derived from residual non-food crops, non-food parts of current crops (leaves, stems), and also industry waste. The “third generation” based on the use of algae is at an early stage of development.

Last years, it has been studied the potentialities of the use of LNG (Liquified Natural Gas) as alternative fuel to comply with ECA restrictions either for existing vessels and new ones (IMO, 2016). Natural gas demand is increasing, especially in OECD Americas and Europe, where experiences with natural gas technologies are improving and more and more ships are designed with dual-fuel propulsion (Thomson et al., 2015). Because of this, a transition to LNG could be justified there, especially in port areas. In the Mediterranean Sea, current and planned LNG import terminals are: La Spezia, Rovigo, Brindisi, Gioia Tauro, Livorno, Muggia, San Ferdinando, Taranto, Trieste, Vado Ligure in Italy, Fos (France), Barcelona, Cartagena and Valencia in Spain, Ereğli, Aliaga, Iskenderun in Turkey, Revithoussa (Greece), and Vassiliko (Cyprus).

Main advantages make LNG the most likely option in the short to medium future: low prices of natural gas compared to low-sulphur fuels since 2002 (IEA, 2012), newly build vessel can be powered continuously with gas or switch to gas at the occurrence (“dual-fuel engines”), availability of natural gas worldwide and a growing natural gas infrastructure (Fullenbaum, 2013). On the other hand, some drawbacks have to be considered: structural modification of harbours (with associated high investment costs), new safety and logistics practices for operators and harbour personnel. A substantial aspect is LNG storage tank(s) which reduce the cargo capacity, not being LNG stored as liquid fuel.

The different options, depending on ship type and tank size are: Truck to Ship transfer (TTS), Ship to Ship (STS), Shore Tank to Ship (TPS) as well as the use of standardized containers. TTS is often adopted for vessels with small tank capacities such as ferries, tugs and coastal vessels but the most efficient is considered to be STS (IMO, 2016).

From the environmental point of view, natural gas supply chain (extraction, processing, distribution, storage, combustion) implies important GHGs impacts, therefore negatively contributing to climate change.

However, at least in the near future the most viable option for ECA and in-port emission standards compliance by existing vessels seems to be the use of low-sulphur content fuels, indicating distillate fuels (mainly MGO/MDO), opposite to residual fuel (Heavy Fuel Oil – HFO). Distillate fuel is a light, refined product characterised by sulphur content of 0.5% (or less), lower than residual oils (around 2.5%). Also, other available diesel fuels are: LSMGO (Low-Sulphur Marine Gas Oil) (0.1%) and ULSMGO (Ultra Low Sulphur Marine Gas Oil), referred to as Ultra Low Sulfur Diesel (sulphur 0.0015% max) in the US and Auto Gas Oil (sulphur 0.001% max) in the EU. The use of low-sulphur content fuels may be adopted both outside and inside ECA or only when operating in ECA, switching from HFO. Commonly, the ocean going ships (and ships which spend a limited time inside the ECA) follow the second choice (due to the higher costs of distillate fuels), instead smaller vessels inside the ECA and the inland waterways (e.g. tugs, workboats, ferries and fishing vessels) with medium and high speed engines choose the first option (IMO, 2016). Cleaner fuels ensure compliance with SO<sub>x</sub> emissions requirements but improved engine technologies are necessary to meet restrictions for NO<sub>x</sub> in the ECA. A comparison between the alternatives (LNG, MGO and HFO) is reported in Tab. 1.6.

Table 1.6. Comparison among LNG, MGO and HFO (source: IMO, 2016).

Alternative	Environmental features compared to the traditional HFO alternative				Factors influencing viability compared to the traditional HFO alternative		
	SO <sub>x</sub>	NO <sub>x</sub>	PM	CO <sub>2</sub>	Cargo capacity	Capital Investments	Operating costs
LNG	++	++	++	+	Restricted	Very high	Low
MGO	+	-	-	-	Not restricted	Low	Very high
HFO/Scrubber	+	--	+	-	Slightly restricted	High	Medium <sup>a)</sup>

++ very good, + good, - bad, -- very bad

<sup>a)</sup> Fuel costs remain basically unchanged, a small increase (1% – 2%) can be expected.

Cost for scrubber maintenance and waste handling are yet unknown but may add to the total operating costs.

### 1.5.3 Cold ironing

Since hotelling represents almost 85% of total emissions, in-port mitigation actions assume a crucial role. In the perspective of “Green and Sustainable Ports” one of the emerging strategies is “cold ironing” (or Shore Connection, On Shore Power Supply,

Alternative Maritime Power Supply (AMP)), which is lately receiving much attention.

For several decades, it has been a practice in the military, and now is being campaigned and developing for the commercial shipping sector.

This technology involves the provision of the ships' electrical demands (for hotelling activities: emergency equipment, cooling/heating, lighting and any other equipment) while berthed from the port shore side supply, avoiding the need to run the onboard Auxiliary Engines (AE).

A shore-power system consists of three key components (Fig. 1.28): (a) shore-side electrical system and infrastructure; (b) cable management system; and (c) ship-side electrical system. The electrical power needed to keep ship activities at berth can be provided by various sources: port-city-own power grid, in-port power plants or even via renewable energy sources. However, in the latter case, the contribution in kW is not directly on ship supply and the capacity is small in comparison with the intensive consumption of cruise and container ships and the required power is intermittent and therefore not suitable for continuous power generations.

High voltage power requirements depend on vessel type at berth (source: TEFLES project):

- Container Ships 1-4 MWe
- Cruise Ships 7 MWe
- Reefers 2 MWe
- Ro-Ro 400 kWe -1 MWe
- Tankers 5-6 MWe
- Bulk/Cargo Ships 300 kWe-1 MWe.

The practice has been comprehensively implemented in all ports in Alaska and California (US) and is increasingly being adopted by ports in Europe (Arduino et al., 2011).

The European harbour of Gothenburg was the pioneering harbour in the sector and other EU ports are currently implementing OPS: Le Havre and Marseille (France), Civitavecchia (Italy), Valencia (Spain). Also in Venice a "high efficiency" cold-ironing system available only for mega-yachts was announced in 2010 with

renewable energy sources (photovoltaic panels and from biomass installed in 2011). Within the APICE project, future scenarios considered cold ironing able to lower NO<sub>x</sub> emissions of 6.5% and PM emissions of 3% with electricity supply from the near thermoelectric plant (with extra SO<sub>2</sub> produced). In Barcelona port, the electricity produced by a plant (with steam also) is transferred to the port through the city grid.

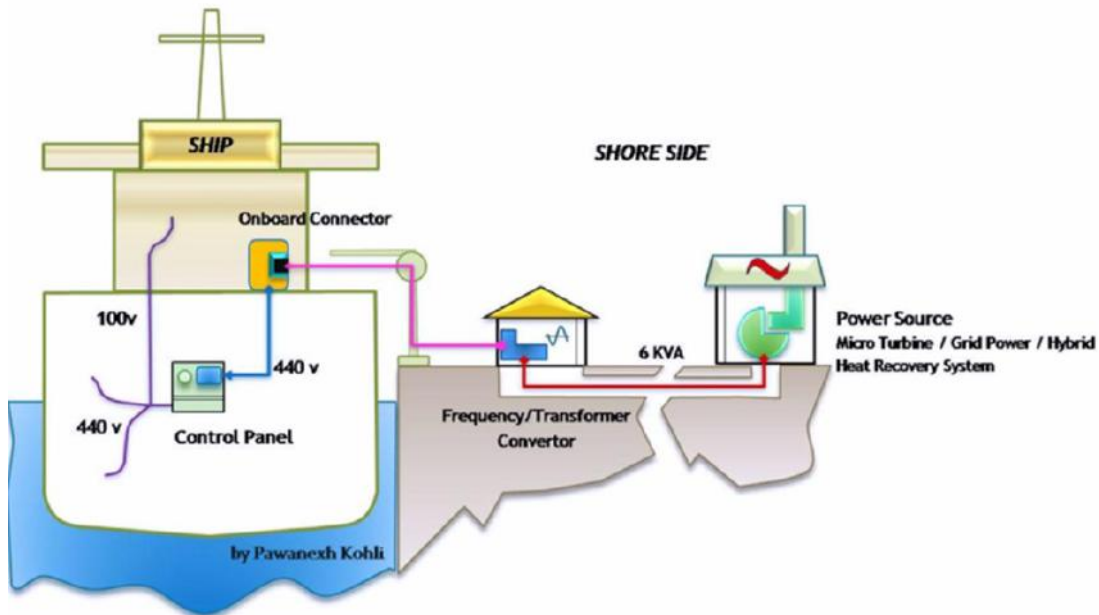


Figure 1.28. Schematic set-up for cold-ironing implementation.

From the regulatory perspective, currently, there are no international requirements that mandate or facilitate the use of OPS but implementation is encouraged in Europe and US.

In addition to the use of 0.1% sulphur by weight by ships at berth in European ports, the Directive 2005/33/EC allows OPS as an alternative to reduce in-port emissions.

Recently, the European Union approved the Directive 2014/94/EU that makes mandatory implementation of alternative infrastructure networks such as shore-side power technology by December 2025. In particular, shore power electricity will be “a priority in ports of the TEN-T Core Network, and in other ports, by 31 December 2025, unless there is no demand and the costs are disproportionate to the benefits, including environmental benefits” (Art. 4).



Moreover, EU recommends that installations should be particularly be placed in ports where air quality limit values are exceeded or where there are concern about the high levels of noise nuisance, especially in berths near residential areas.

To encourage OPS, under the revision of the Energy Tax Directive (2003/96), exemption from energy taxes for onshore power is now under discussion. Anticipating on this potential energy tax exemption, Sweden successfully requested to apply reduced tax rates to OPS from the European Commission.

In US, the California Air Resources Board (CARB) runs a subsidy program that supports investments for passenger ships and cargo ships (<http://www.arb.ca.gov/ports/shorepower/shorepower.htm>). In December 2007 the CARB approved a regulation ("Airborne Toxic Control Measure for Auxiliary Diesel Engines Operated on Ocean-Going Vessels At-Berth in a California Port" Regulation, commonly referred to as the At-Berth Regulation) to reduce emissions from diesel auxiliary engines on container ships, passenger ships, and refrigerated-cargo ships while berthed at a Californian port (defined as the Ports of Los Angeles, Long Beach, Oakland, San Diego, San Francisco, and Hueneme). Within the 24 nautical mile regulatory zone off the California coastline, 0.1% sulphur limit is in force for ocean-going vessels with respect to their main (propulsion) diesel engines, auxiliary diesel engines and auxiliary boilers when operating.

The regulation applies to operators of container ship and refrigerated-cargo ship fleets whose ships cumulatively make 25 or more visits annually to one of the specified ports and to operators of passenger ship fleets whose ships cumulatively make five or more visits annually to one of these ports. Fleets whose ships cumulatively make less than the specified minimum annual visits to a port are not affected by the regulation. The legislation provides vessel fleet operators visiting these ports two options to reduce at-berth emissions:

1. **reduced onboard power generation by auxiliary engines**, limiting engine use to three or five hours during a vessel visit for a specific percentage of a fleet's visits to a port;

2. **equivalent emissions reduction** by alternative control techniques that achieve equivalent emission reductions. Alternative options could be distributed

generation equipment such as natural gas-fueled engines or emission controls installed on the ships (e.g. particulate control traps, selective catalytic reduction units and alternative fuels) or at the pier (e.g. a bonnet emissions capture and treatment system).

In conclusion, cold ironing option could reduce greenhouse gases emissions and noise pollution, according to type of fuel burned, electricity generation onshore, ship size. Other regional factors are: grid characteristic, electricity price, port size and location. Calculated reduction of total shipping-related greenhouse gases were less than 0.5% (Frey, 2008) and 39% in yearly CO<sub>2</sub> maritime emissions (Winkel et al., 2016) but a large-scale application could be more effective (Hammingh et al., 2007). Therefore, deployment of short side electricity could be a sustainable choice, especially in ports in proximity of residential areas, with societal, economic and health benefits.

However, some obstacles to spread the technology are present: high costs of the infrastructure installation in port and beyond and retrofitting of appropriate power systems on ships as well as absence of safety procedures at international level. For example, the cost for building shoreside infrastructure at a berth can range from US\$170,000 to \$8 million in Europe ([www.ops.wpci.nl/costs/investments/](http://www.ops.wpci.nl/costs/investments/)), for electrical system on the sea side is approximately of 500,000 euros for a typical 2 MVA connection and \$1 million per ship for retrofit option (Winkel et al., 2016). Cost-benefits analysis of cold-ironing were carried out (Ballini et al., 2015; McArthur and Osland, 2013; Winkel et al., 2016). A proper analysis should consider the energy mix of the electricity supply (possibly with a high percentage of renewable energy) and the health benefits associated. The highest health benefits by using short side electricity in EU were estimated to 2.63 and 2.94 billion euros for 2010 and 2020, respectively, also outside the SECA (Sulphur Emission Control Area) zones, especially in the main ports of The Netherlands, Belgium, Germany, Italy and UK (Winkel et al., 2016). In Fig. 1.29 a positive health benefit is visualized as a negative number (in terms of the amount of money which is saved by using cold ironing), with the greatest positive effects on PM and SO<sub>2</sub> in 2020 projections.

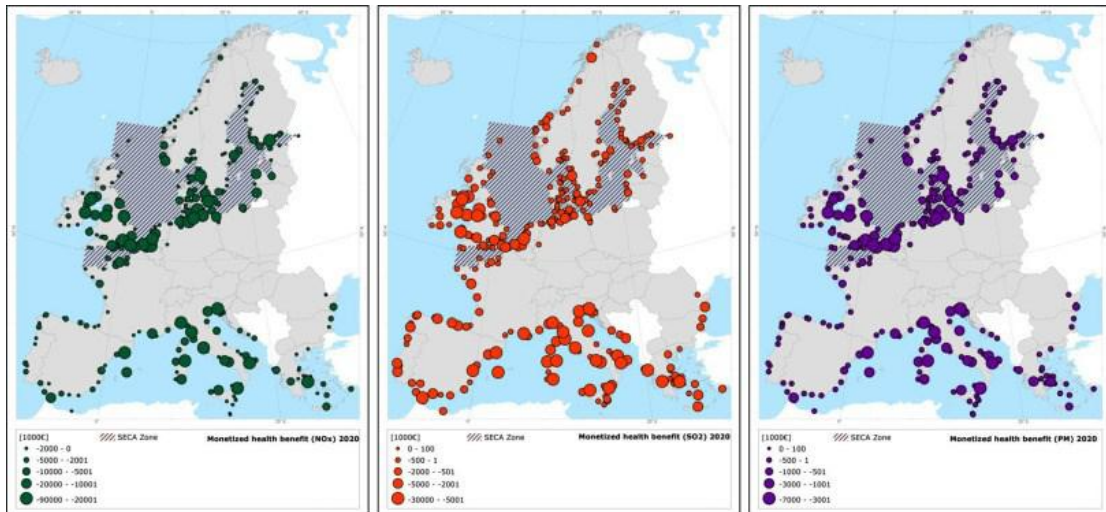


Figure 1.29. Monetized health benefits provisions for 2020 for  $\text{NO}_x$ ,  $\text{SO}_2$  and PM using cold-ironing (source: Winkel et al., 2016).

## 1.6 International and national legislation

Until the 1980's, shipping industry escaped attention due its international nature and fewer “perception” of its impacts on the population compared to other modes of transport (Cullinane and Bergqvist, 2014). Nowadays, the awareness of maritime transport “weight” is increasing, reinforcing the need to regulate levels of pollutants released and to improve reduction technologies (Miola and Ciuffo, 2010).

Various regulatory regimes are following through the years, especially in regulating  $\text{NO}_x$  and  $\text{SO}_x$  emission limits.

Nowadays, the shipping sector has to comply with a number of regulations at national and international level to prevent pollution to the atmosphere from vessels, especially for some pollutants which are of more concern in relating to maritime transport (such as  $\text{SO}_2$ ). However, some voluntary initiatives are applied at local level in addition to mandatory legislation.

### 1.6.1 IMO regulations

The International Maritime Organisation (IMO) is the United Nations agency dedicated to the safety and security of shipping as well as prevention of marine pollution within its member states.

IMO was formally born in 1948 by a convention signed during an international conference in Geneva with the original name Inter-Governmental Maritime Consultative Organisation (IMCO), then modified definitively in 1982.

On 2 October 1983 the IMO adopted the International Convention for the Prevention of Pollution from Ships (MARPOL - MARine POLLution) initially with Annexes I and II, then adding a new Protocol (Annex VI) in 1997. It has been reviewed and updated by amendments over the years.

It is named “MARPOL 73/78” (Fig. 1.30) because its origin from a combination of two treaties adopted in 1973 and 1978. Today this document is the main convention which aims to prevent marine pollution by ships from both accidental causes and routine operations at international scale. At the present form, it includes six technical Annexes, among which Annex I and II are compulsory.

In particular, the Annex VI, focused on air emissions, established:

1. a global limit of 4.5% of sulphur content fuel and a lower cap of 1.5% in SECAs;
2. limits on NO<sub>x</sub> emissions from diesel engines defined by a mandatory Technical Code;
3. prohibition of emissions of ozone depleting substances such as halons and chlorofluorocarbons (CFCs) on all ships and for hydro-chlorofluorocarbons (HCFCs) until 2020;
4. ban of emissions from incineration on board such as polychlorinated biphenyls (PCBs).

while Annexes III-VI are voluntary. Following the detailed list of the Annexes is reported.



- Annex I – Regulation for the Prevention of Pollution by Oil
- Annex II – Regulation for the Control of Pollution by Noxious Liquid Substances in Bulk
- Annex III – Prevention of Pollution by Harmful Substances Carried by Sea in Packaged Form
- Annex IV – Prevention of Pollution by Sewage from Ships
- Annex V – Prevention of Pollution by Garbage from Ships
- **Annex VI – Prevention of Air Pollution from Ships**

Figure 1.30. Cover of the MARPOL convention.

It is noted that specific limits for emissions of particle matter (PM) and Polycyclic Aromatic Hydrocarbons (PAHs) are not given in the MARPOL Annex VI regulations. However, more stringent emission standards are justified for ECAs because of intense vessel traffic patterns as well as the ecological, oceanographical sensitivity of the area to harmful pollution.

The Annex VI entered in force 19<sup>th</sup> May 2005, ratified by 75 States and revised in July 2005. The revision of the Annex VI was adopted in October 2008 and entered in force in July 2010 focusing on modification of Regulation 12, 13 and 14.

Regulation 13 strengthens NO<sub>x</sub> limits emissions for diesel engines installed before and after 2000 (Fig. 1.31). Although ship engines operate at high temperatures and pressures so having higher emissions (Corbett et al., 2007), the shipping sector has traditionally faced less stringent air emission regulations than other sectors of transport.

The current IMO limits for all engines constructed on or after 2011 are expressed by Tier II, while Tier III standard is for new engines built since 2016 entering in any NECAs (NO<sub>x</sub> Emission Control Areas). The latter standard reduces NO<sub>x</sub> emissions of 80% compared to Tier I limit. However, if a country proposes for an ECA, Tier III

will be applied only to ships build after the date of the adoption of the ECA designation by IMO. Finally, NO<sub>x</sub> emissions from older engines (constructed before 2011) have to meet the Tier I standard.

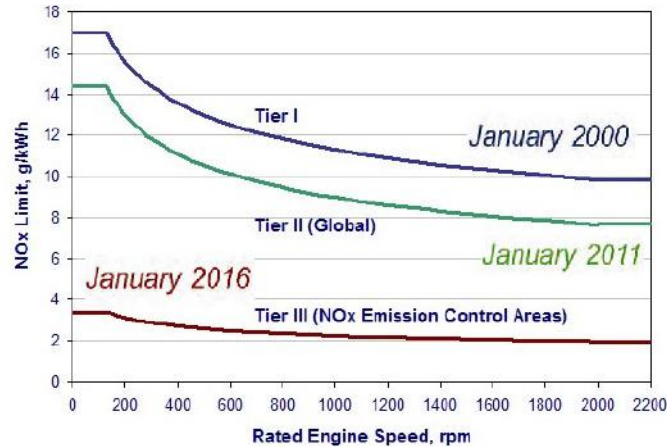


Figure 1.31. TIER I, II and III for NO<sub>x</sub> emissions (source: IMO, 2016).

The revised MARPOL substantially modified also Regulation 14 regarding SO<sub>x</sub> limit values and the means to comply. It is important to notice that introduced SO<sub>x</sub> limits cover also emissions of secondary PM.

The previous Regulation 14 set at 4.5% sulphur content fuel at general level and 1.5% inside ECAs.

Currently, the global sulphur cap is (from 1<sup>st</sup> January 2012) 35,000 ppm (3.5%) for bunker fuel, which will be progressively reduced to 5,000 ppm (0.5%) by 2020, subject to a feasibility review to be conducted by 2018. Inside ECAs, the sulphur limit is set at 10,000 ppm (1%), which has been further tightened to 1,000 ppm (0.1%) from 1<sup>st</sup> January 2015 (Tab. 1.7).

More stringent limit values are provided for ships at berth, that is 0.1% of sulphur in fuels since 2011. Similarly, inland navigation has the same restrictions being demonstrated a noticeable impact of ship exhausts on air quality near houses along waterways (van der Zee et al., 2012). Instead a limit of 1.5% is permitted to Ro-Pax ships prior to 2020, when the maximum value will be 0.5%, like all ships outside ECAs (Tab. 1.8).

Table 1.7. Evolution in IMO SO<sub>x</sub> limits in fuel oil for ocean-going vessels.

Outside ECAs	Inside ECAs
4.5% m/m prior to 1 January 2012	1.5% m/m prior to 1 July 2010
3.5% m/m on and after 1 January 2012	1.0% m/m on and after 1 July 2010
0.5% m/m on and after 1 January 2020*	0.1% m/m on and after 1 January 2015

\*depending on the outcome of a review, to be concluded by 2018, as to the availability of the required fuel oil, this date could be deferred to 1 January 2025.

Table 1.8. SO<sub>x</sub> limits for not open-sea navigation.

	2011	2012	2015	2020
Ships at berth	0.1%	0.1%	0.1%	0.1%
Inland waterways	0.1%	0.1%	0.1%	0.1%
Ro-Pax (outside SECAs)*	1.5%	1.5%	1.5%	0.5%

\*only in Member States' territorial seas as established by Directive 2005/33/EC.

There are currently four regions in the world designated as ECAs (Tab. 1.9):

- Baltic Sea Area;
- North Sea Area;
- North American Area;
- United States Caribbean Sea.

Table 1.9. Existing ECA areas with indication of adoption, entry into force and date of taking effect (source: [www.imo.org](http://www.imo.org)).

ECA	Adoption	Entry into force	Effect from
Baltic Sea	26/09/1997	19/05/2005	19/05/2006
North Sea	22/07/2005	22/11/2006	22/11/2007
North American	26/03/2010	01/08/2011	01/08/2012
US Caribbean Sea	26/07/2011	01/01/2013	01/01/2014

The European ECAs (Baltic and North Sea areas) only enforce the SOX (and indirectly PM) emissions limit while the others (North American and U.S. Caribbean Seas) regulate SOX, NOX and PM emissions (Fig. 1.32). Also, a wider discussion is open concerning the proposal of other ECAs such as China and the Mediterranean Sea (see Section 1.4).

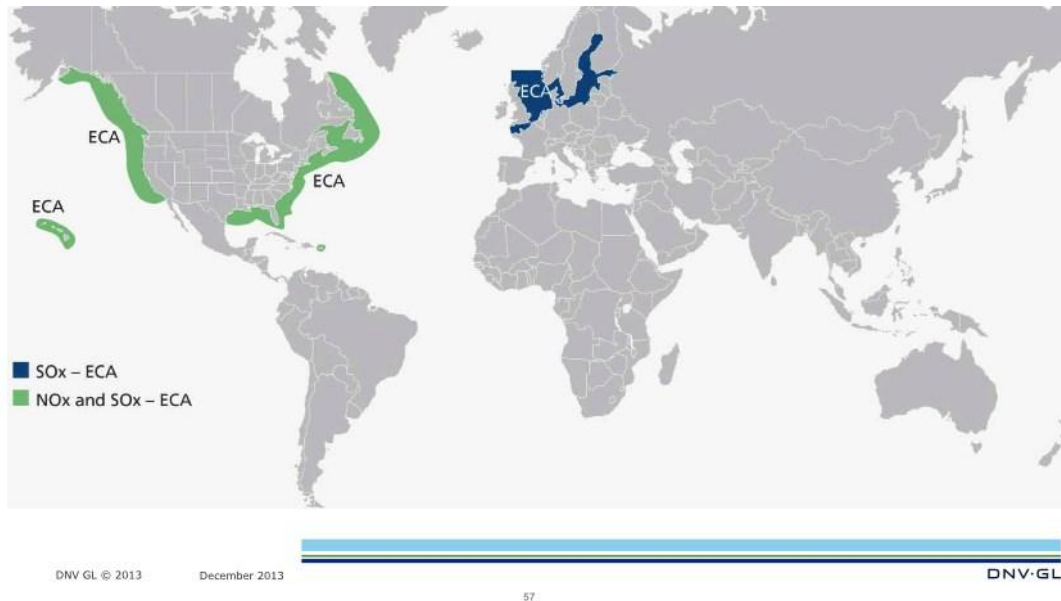


Figure 1.32. Geographical distribution of the ECAs in the world.

Finally, in the Regulation 18 of Annex VI other equivalent means by which levels of SO<sub>x</sub> and PM emission control could be achieved are mentioned. These may be methods termed primary (in which the formation of the pollutant is avoided) or secondary (in which the pollutant is formed but subsequently removed before its emission in atmosphere by gas exhausts).

### 1.6.2 EU legislation

In Europe efforts to curb maritime emissions started about twenty years ago, almost in correspondence of the MARPOL adoption at international level.

The Directive 99/32/EC of 26 April 1999 amended the previous Directive 93/12/EC and introduced limits on sulphur content in fuels, with some derogations for France, Portugal, Greece and Spain. It established:

1. limit for heavy fuel oil at 1.0% since 1 January 2003;



2. limit for marine gas oil at 0.2% after 1 January 2000, reduced to 0.1% since 1 January 2008.

The Directive 99/32/EC was amended by the subsequent Directive 2005/33/EC, at the same time of the introduction of the MARPOL Annex VI, which was largely followed in terms of sulphur content limits. In fact, the new values fixed were:

1. limit of 1.5% for marine fuels in SECAs and passenger ships operating to or from EU ports in Member States' territorial seas (excluding ships operating exclusively within the Greek territory until 1<sup>st</sup> January 2012);

2. 0.1% limit for inland waterway vessels and ships at berth in EU ports (for more than two hours) as from 1<sup>st</sup> January 2010.

This Directive excluded vessels at berth which switched off their engines using off-shore supply technology. Furthermore, other abatement technologies were approved provided that continuous emission monitoring and no impacts on ecosystems were allowed.

The Directive 2012/33/EU was perfectly in line with the MARPOL Annex VI making mandatory the IMO limits for ECAs and non-ECAs regions in Member States (see Tab. 1). However, alternative compliance methods, such as exhausts cleaning systems, are accepted. The adoption of the Directive 2012/33/EU by Member States was by 18th June 2014.

In conclusion, the general evolution in sulphur limits set by different authorities indicates drastic reductions in last years (Fig. 1.33). The EU rules are more restrictive compared to IMO regulations and are almost in agreement with the Californian legislation. However, only in European harbours emissions from ships at berth are regulated.

The effectiveness of the 2005/33/EC Directive in harbours from January 2010 was evaluated in some Mediterranean harbours. A significant reduction of SO<sub>2</sub> daily levels (66%) was recorded, with indirect positive effects on PM concentrations (Schembari et al., 2012). Beneficial effects in reducing SO<sub>2</sub> concentrations were evident also along the California coastline (Tao et al., 2013).

On the other hand, Mestl et al. (2013) highlighted the effective decrease in maximum sulphur concentrations rather than mean concentrations.

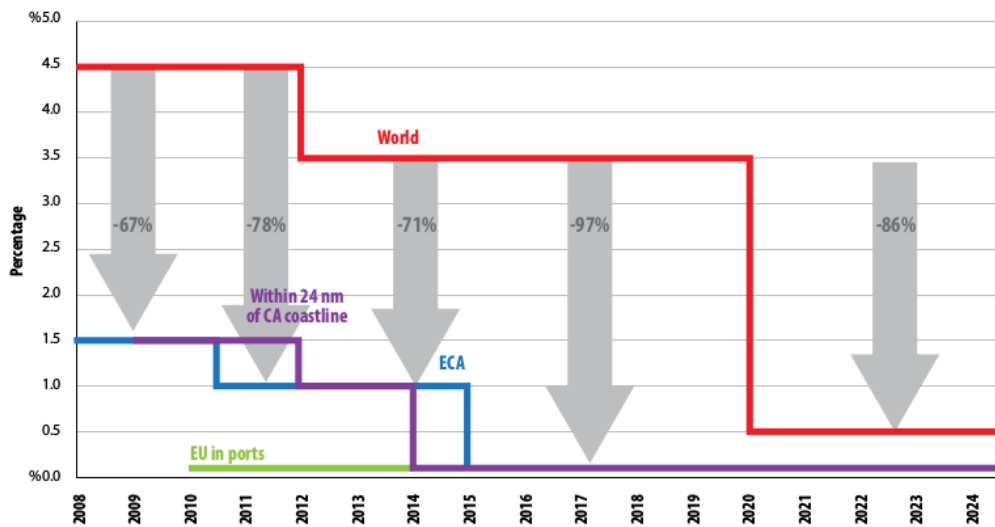


Figure 1.33. Fuel sulphur limits set by IMO, in force in EU ports and California waters.

Finally, the recent Directive 2014/94/EU promotes the deployment of alternative fuels infrastructures, indicating minimum requirements to implement them. In particular, cold-ironing is considered a valid way to reduce emissions from ships in port.

### 1.6.3 Other initiatives

In addition to existing regulations, others voluntary initiatives, both at local and global scale, may be taken in consideration to reduce in-port ship emissions.

At international level, voluntary fuel switch programs are applied in various ports and incentives are provided to shipping lines to use low sulphur fuel. For example, in Seattle harbour (US) the maximum sulphur content in fuel permitted is 0.5% in mass (ABC Fuels programme), in New York and Houston (US) are active the OGV Low sulphur program and the DERA Fuel Switch Program, respectively, with a 0.2% S limit. The EcoAction Program in Vancouver (Canada) and the Fair Winds Charter in Hong Kong (China) establishes a 0.5% S threshold whereas a higher value (1%) is permitted in Singapore (Green Port Program).

In Italy, a significant example is the voluntary agreement implemented in Venice in 2007 and reinforced in 2013, named “Venice Blue Flag”.

The Venice Blue Flag I was signed on 27<sup>th</sup> April 2007 between local authorities (Venice Municipality, Venice Port Authority, Harbour Master) and several cruise

companies (Fig. 1.34), who committed themselves to use cleaner fuels by more than three years (Tab. 1.10).

In following years, other cruise companies joined and in 2010 the Directive 2005/33/EC was adopted at national level lowering at 0.1% sulphur content in fuel when mooring.

Later in 2013, thanks to Venice Blue Flag II a “green zone” has been created in the Venice Lagoon, extending the maximum sulphur content allowed at 0.1% (lower than the European limit) as ships approach the Lido inlet.

Table 1.10. Venice Blue Flag I and II implementation (in parenthesis the tolerance margin is reported).

Year	Agreement	% S navigation	% S at berth
2007	Venice Blue Flag I	2.5% (+0.5%)	2.5% (+0.5%)
2008	Venice Blue Flag I	2.0% (+0.5%)	1.5% (+0.25%)
2009	Venice Blue Flag I	2.0%	1.5%
2013	Venice Blue Flag II	0.1%	0.1%

A cost-benefits analysis performed by ARPAV (Regional Environmental Protection Agency) and the local Port Authority evaluated the strong reduction of both SO<sub>x</sub> (-91%) and of PM (-46%) emissions as well as the marginal external costs related to Venice Blue Flags implementation with the highest saving costs per year for SO<sub>x</sub> and PM<sub>2.5</sub>.



Figure 1.34. Original parts of the Venice Blue Flag I.

## 2.1 Area description

Venice and Brindisi are two of the most important Italian port-cities located in Northern and Southern Italy, respectively, of the Adriatic Sea.

Although they are different for some aspects (i.e. size, economic vocation, history, climate), both towns are crucial hubs allowing important travel connections to and from Northern Europe (Venice) and the Mediterranean Sea (Brindisi). This is because of the high infrastructural development, consisting in the presence of international airports, harbours and large industrial areas (of national relevance). In particular, the harbour activities drive the local economy, especially encouraging tourism and trade sector according to the different vocation of each city.

### 2.1.1 Brindisi

Brindisi (13 m a.s.l.) is a town in Southeastern Italy (Apulia region). Probably, the town's name coming from the Greek *Brentesion* (*Βρεντήσιον*) which means "deer's head", invokes the particular shape of the natural bay in which is located the harbour area. Since ancient times, due to its position on the Italian Peninsula and its natural port on the Adriatic Sea, Brindisi has been known as the "Gateway to the East", being a strategic port for the Romans and for merchants of Venice. Even today its port is one of the major for trade with Greece and the Middle East.

The extension of the municipality is 332.98 km<sup>2</sup> with 88,667 inhabitants and therefore it has a housing density of 266 inhabitants/km<sup>2</sup> in 2015 (<http://demo.istat.it/>).

Brindisi faces the sea towards E. The meteorology is characterised by two prevalent wind directions: NW-NNW and SSE. However, a specific daily pattern in wind direction is not present. The highest wind velocities (see Section 2.2.1) are generally associated to the NW-NNW directions.

A typical Mediterranean climate characterises warm to hot (maximum mean temperature about 25°C in July), dry summers. Winters are mild (minimum temperature in January about 9-10°C) and wet (maximum rain over 70 mm, in October-November period and March) (Fig. 2.1).

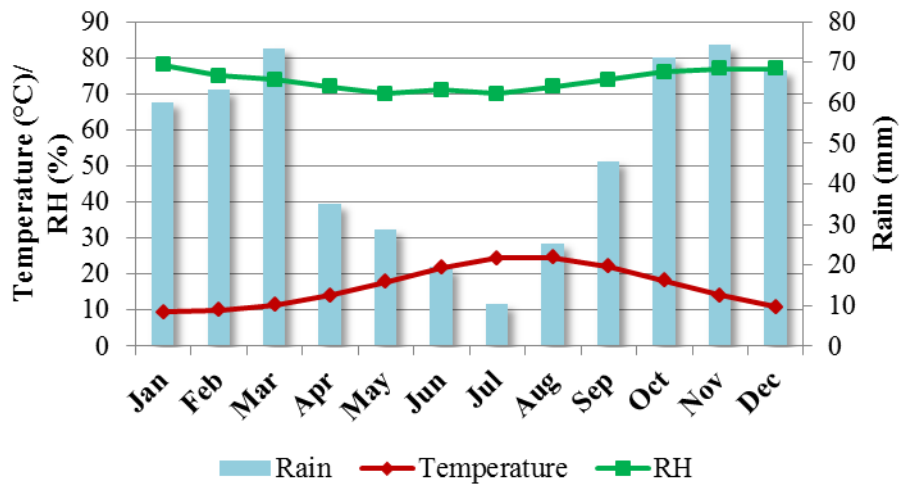


Figure 2.1. Climate diagram in Brindisi – averages in 1961-1990 period (source: own elaboration from <http://clima.meteoam.it/Clino61-90.php>).

Brindisi is included in the list of SIN (National Sites of Interest) for relevant and potentially dangerous pollution, according to the Italian Legislation (D.M. 471/99). This is because three thermo-electric power plants, a large industrial zone, and an international airport stand in the area (Fig. 2.2). At about 10 km SE of the urban area, the European largest coal-fired power plant (named “Federico II”) is located in Cerano (total capacity 2640 MW). The second coal (also using oil) power plant Edipower (1280 MW) is located at about 3 km ENE of the town, and the third one is the gas power plant of Enipower (1170 MW) situated inside the industrial area. The industrial area is characterised by the presence of an important petrochemical plant (production of polyethylene, PVC and other polymers), a pharmaceutical industry (Sanofi-Aventis), an industrial waste incinerator (Veolia-Servizi-Industriali), an industry for construction of airplanes components (Fiat Avio) and several artisan activities.



Figure 2.2. Main atmospheric pollution sources in the Brindisi area.

Infrastructural indicators calculated by Unioncamere as function of attraction capacity and accessibility of the infrastructure, showed that the province has a high infrastructural development, mainly due to the Brindisi municipality, both at regional and national level (Fig. 2.3). Bearing in mind that the indexes consider the effective catchment area (as number of passengers, international transport connections and trading), it is clear as the intense activity of the port and airport makes the area a crucial hub in transport sector in Apulia region and Southern Italy.

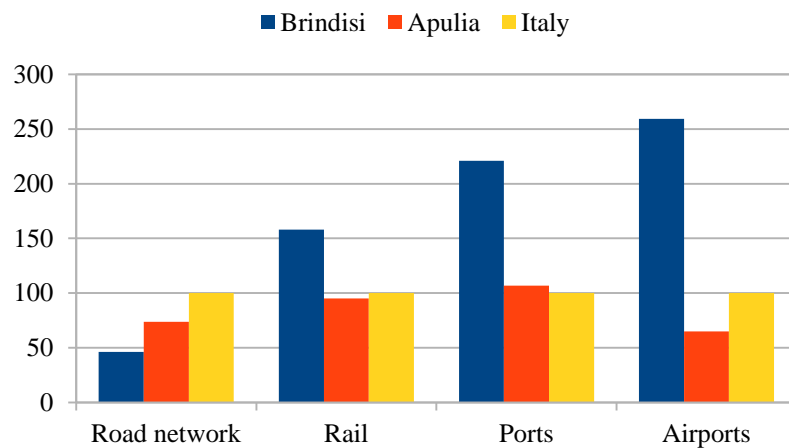


Figure 2.3. Infrastructural indicators for the Province of Brindisi and Apulia region, with respect to Italy (equal to 100) for year 2012 (source: C.C.I.A.A. Brindisi, 2014).

In opposition to a deficit road network, two significant transport infrastructures are present in the Municipality area: an international airport at 3 km NNE of the urban area and a medium-size harbour located E of the city.

The airport “Papola Casale” reached over 2,159,431 passengers in 2014, +8.5% compared to previous year (Fig. 2.4). The maximum passenger traffic flows were recorded in summertime, from June to August, with over one third of the yearly total traffic.

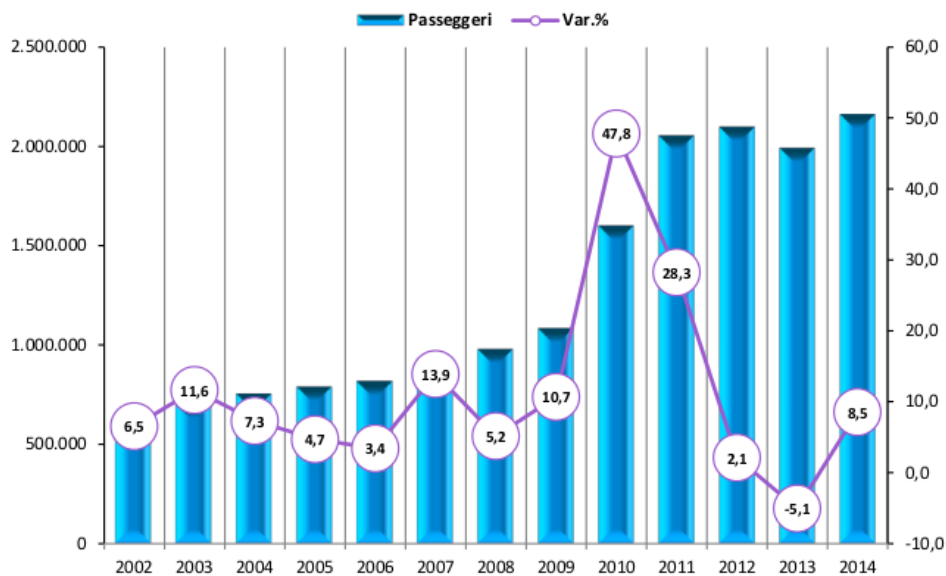


Figure 2.4. Passenger traffic and % variation in the Brindisi airport, period 2002-2014 (source: C.C.I.A.A. Brindisi, 2014).

The main commercial activities in Brindisi occur around the harbour area, which is the real economic heart of the city (Fig. 5). The port of Brindisi ( $40^{\circ}38'25''$  N  $17^{\circ}56'52''$  E) is a natural inlet (Fig. 2.6) ideally divided in three basins (Fig. 2.7).



Figure 2.5. Panoramic picture of the Brindisi harbour.





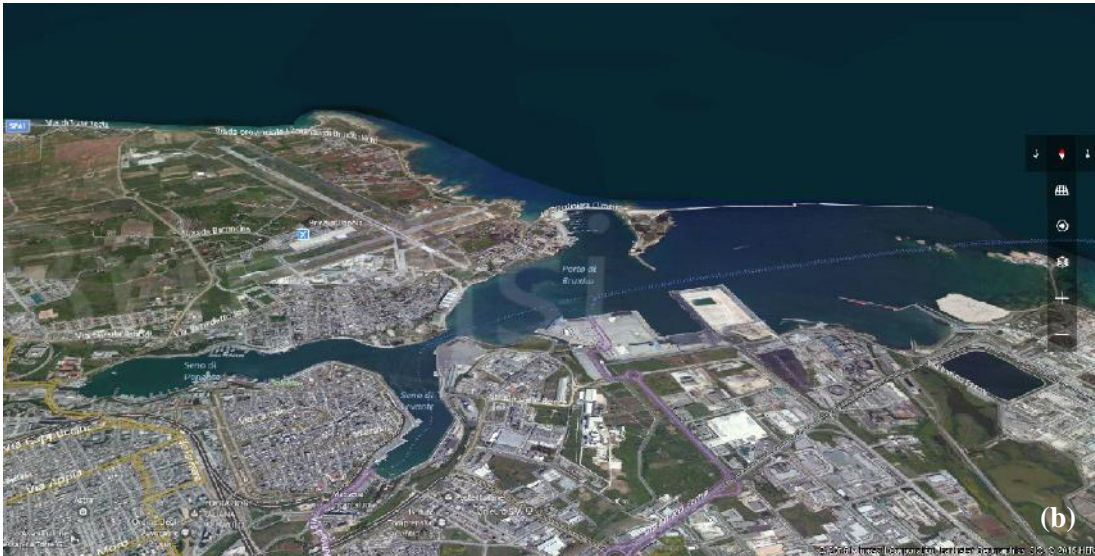


Figure 2.6. a) Satellite map of Brindisi (source: Google Earth) and b) 3D view of the harbour (source: Earthstar Geographics).

The internal harbour (727,000 m<sup>2</sup>, 2 km of docks) is divided in two arms: “Seno di Ponente” (North) and “Seno di Levante” (East). The first is 1.5 km length, 200 m width, partially dedicated to military ships. The branch “Seno di Levante” (1 km length, 200 m width) is available for mooring commercial ships to 10 docks.

The intermediate zone (1,200,000 m<sup>2</sup>, 3 km of docks) is connected to the internal harbour by “Canale Pigionati” and by “Seno Bocche di Puglia” to the external one.

The central harbour zone hosts commercial ships, thanks to Costa Morena docks (1,170 m) and 300,000 m<sup>2</sup> of quays. From Costa Morena Diga fuels are transported to the two thermoelectric plants located to the South and North of Brindisi.

The external zone (3,000,000 m<sup>2</sup>) is surrounded by “Isole Pedagne”, “Isola di Sant’Andrea”, “Diga di Punta Riso” and “Costa Morena” dock. It has industrial piers for coal ships, bulk carriers and small general cargo. Raw materials are handled for supplying the near industrial chemical pole.

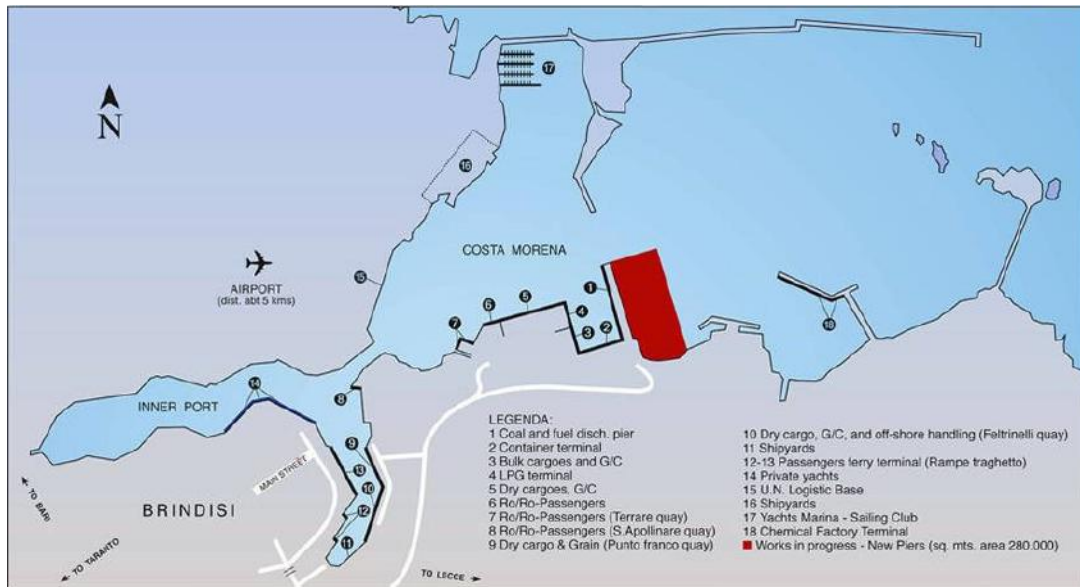


Figure 2.7. Site plan of the Brindisi harbour.

Trend analysis in 2009-2014 period shows that differentiating data by traffic type, cruise sector has obtained an emerging share (+463.36% in 2014 compared to 2013) in terms of passengers, opposite to ferry traffic (Fig. 2.8). This confirms that Brindisi aspires to be a new cruise destination (or transit port) in the Adriatic basin in the next future.

In 2014, the major passenger movements were increased for Greece (+3.13%) while decreasing for Albany (-6.37%). Similarly, bus, cars and trucks traffic diminished substantially for the same countries (source: Avvisatore Marittimo of Brindisi, 2014).

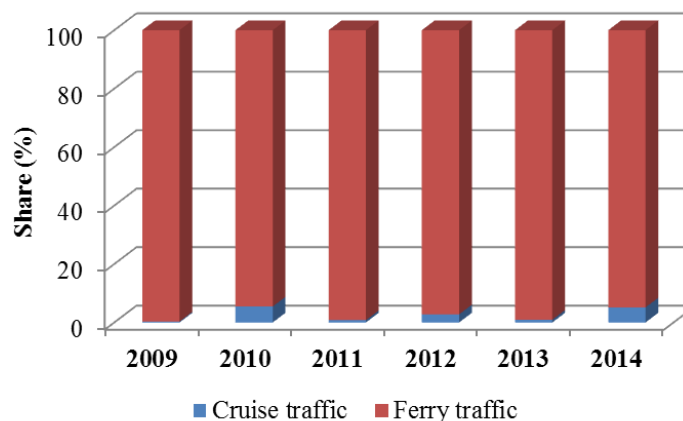


Figure 2.8. Volume traffic by type, period 2009-2014 (source: C.C.I.A.A. Brindisi 2014, based on data from the Avvisatore Marittimo of Brindisi).

Merchandise trade was relatively constant since 2005, except for the highest volume recorded in 2008 (Fig. 2.9). Solid bulk was the first product category carried by ferry and Ro-Ro (+0.10%), followed by liquid bulk and other goods.

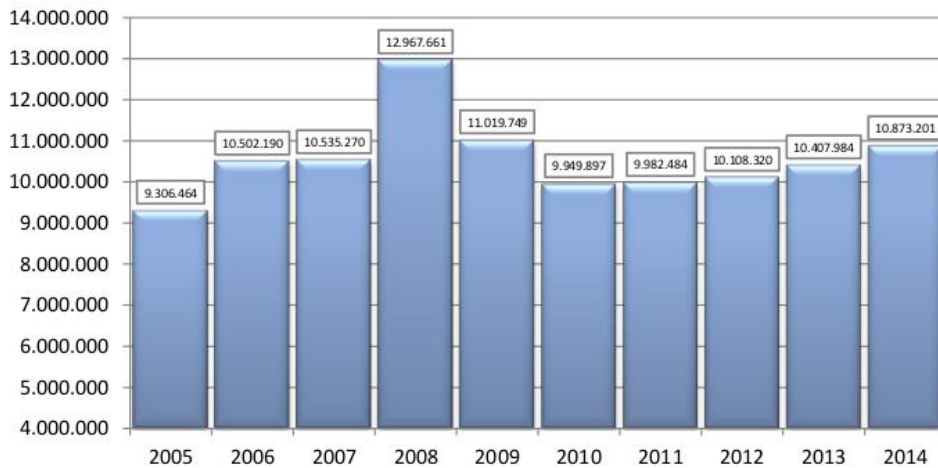


Figure 2.9. Goods movements in Brindisi, period 2005-2014 (source: C.C.I.A.A. Brindisi 2014, based on data from the Avvisatore Marittimo of Brindisi).

### 2.1.2 Venice

Venice is an Italian city in Northeastern Italy, capital of the Veneto region, located on more than 100 small islands separated by several (177) canals and linked by 409 bridges, in the marshy Venetian Lagoon. The Lagoon is a superficial basin, one of the most important wetland sites in the Mediterranean Sea.

Venice is famous around the world for its particular geographical conformation, history, architecture and artwork so the Lagoon and the historical part of the city are listed as a World Heritage Site (Fig. 2.10). Over the time, Venice has been known as the "La Dominante," "Serenissima," "Queen of the Adriatic", "City of Water," "City of Masks," "City of Bridges," "The Floating City," and "City of Canals". It was a very important centre of commerce (especially silk, grain, and spices) and art from the 13<sup>th</sup> century up to the 17<sup>th</sup> century.

Today, the region includes a metropolitan area and the famous historical islands as well as the town of Mestre. On average, estimated daily flux of tourists is from 40,000 to 60,000 (COSES, 2009). A relevant phenomenon is the persistent evacuation of local community from the historical centre and estuarine (Tab. 2.1)

towards the main land (Mestre) due to the competition of foreigners to buy homes in Venice.

Table 2.1. Inhabitants in Venice, period 2004-2014 (source: Venice Municipality, <http://www.comune.venezia.it>).

	2004	2005	2006	2007	2008	2009	2010	2011	2012	2013	2014
historical centre	63,353	62,296	61,611	60,755	60,311	59,942	59,621	58,991	58,215	56,683	56,311
estuarine	31,393	31,035	30,702	30,589	30,415	30,197	29,933	29,693	29,418	29,054	28,792
main land (Mestre)	176,505	176,449	176,621	177,649	179,372	180,662	181,330	181,905	181,494	179,149	179,476
<i>Municipality (total)</i>	271,251	269,780	268,934	268,993	270,098	270,801	270,884	270,589	269,127	264,886	264,579

The geographical position of Venice within the Po valley influences local climatology and, consequently, pollutant dispersion. The local air circulation is characterised by sea breezes, with winds coming from NE during night and from SE during morning. Therefore, this wind regime causes transport of pollutants toward the sea in nighttime hours and towards the hinterland in daytime.

Climate is typical of the Po Valley, with cool winters (minimum temperature in January around 3°C) and warm summers (maximum mean temperature in July around 24°C). Rains are spread relatively throughout the year with no evident seasonal pattern (Fig. 2.11).





Figure 2.10. a) 3D view of the Venice harbour (source: Earthstar Geographics, <http://www.es-geo.com/>) and b) satellite map of Venice (source: Google Earth, [https://www.google.com/intl/it\\_it/earth/](https://www.google.com/intl/it_it/earth/)).

The current economy is mainly based on tourism, services, trade and industrial exports. The glass and lace production in Murano and Burano islands, respectively, represent the local artisan, very well-regarded and exported all around the world. Moreover, shipbuilding is a developed industrial activity, done in the mainland (Mestre and Porto Marghera), with many industrial facilities.

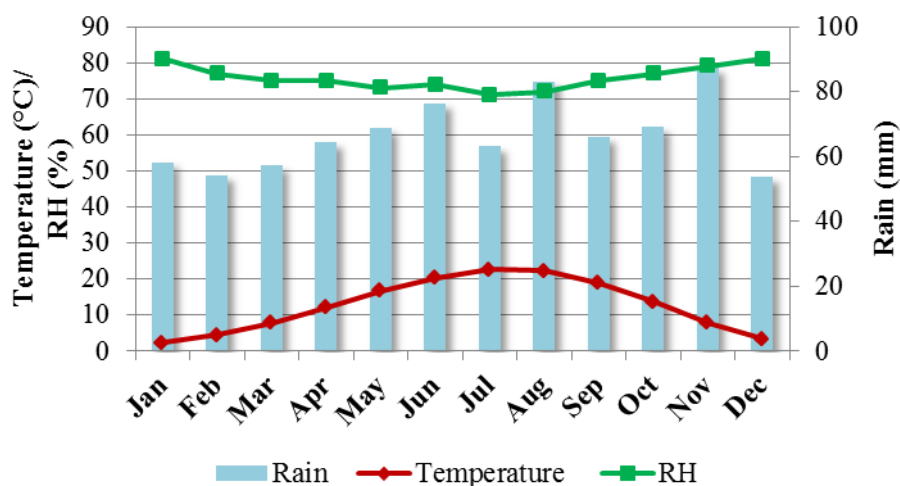


Figure 2.11. Climate diagram in Venice (own elaboration data from <http://clima.meteoam.it/Clino61-90.php>).

Venice is the Europe's largest urban car-free area, because transportation within the city (as in past) is only on water (with waterbuses and passenger ferries) or on foot. The entrance of the city is connected with land by road and rail, with parking facilities in Piazzale Roma and Tronchetto island. In the area there are two train stations (“St Lucia” in historic centre and one in Mestre) and the international airport “Marco Polo”, 8 km N from the islands, in the Tessera fraction. It is the fourth Italian airport and has a modern terminal opened in 2002 with the maximum passenger flow of 8,600,000 reached in 2011 (<http://www.veniceairport.net>).

The air quality of Venice is heavily influenced by industrial emissions from Porto Marghera, which is one of the Europe's largest coastal industrial zone (and the first in Italy). Its total area of 5,730 hectares is occupied by industrial and commercial activities at 70% and the rest is composed by railway lines, navigable canals, basins, roads and demanial areas. An important industrial harbour (for shipbuilding), petrochemical complex, metallurgical (iron, zinc) and chemical (production of sulphuric acid, synthetic resins) industries made Porto Marghera the first SIN site in Italy (Legge 426/98). A large investment will be direct to the reconversion of Porto Marghera with a new Container Terminal, which initially will host up to 1,400,000 TEUs yearly.

Tourism has been a major sector of Venetian economy since the 18<sup>th</sup> century and today is a major worldwide tourist destination so it can be overcrowded in particular periods of the year. In this picture, the harbour plays a fundamental role in local economic development.

The port of Venice is an excellent example in which modernity and history co-exist, being equipped with most modern facilities and welcoming visitors to the unique beauty of cultural heritage of Venice. It is a strategic gateway of the Adriatic Sea.



Figure 2.12. Entrance paths in Venice for different ship types.

The best facilities of the port are (Venice Passenger Terminal S.p.A., 2014):

- 290,000 m<sup>2</sup> of ground area of which 93,000 m<sup>2</sup> of walkable covered spaces;
- 3,431 m berth;
- 10 multifunctional passenger terminals equipped with boarding bridges;
- 5 car parks up to 2100 vehicles;
- easy and fast connections to the international airport, the railway station and motorway net.

On arrival, passenger ships enter the lagoon through the Lido inlet and navigate along the Giudecca channel, the deep water passage for tourist ships moving to and from the Venice cruise ship terminal (passenger port). Commercial ships follow a different route: oil terminal and industrial port (located in the hinterland) are reached crossing the Malamocco inlet. The Motorways of the Sea Port (MoS) is a new ferry (Ro-Ro, Ro-Pax) terminal in Fusina area, operational by 2014, with docks able to host four ships simultaneously (Fig. 2.12).

The analysis of passenger traffic indicates that cruise sector gives the strongest impulse, confirming in 2013 Venice as the first cruise homeport in the Mediterranean Sea with over 2,000,000 passengers (source: Venice Port Authority, <https://www.port.venice.it/it/crociere.html>). In 2012, only 11.4% of passengers were in transit in the city and 88.6% of them arriving and enjoying Venice from less than 6 hours to 72 hours (Venice Port Authority, 2013).

Recently, cruise sector has becoming a discussion topic, because of the phenomenon of the “ship gigantism”, that is the increasingly size of cruise ships crossing the historical centre, threatening the city's fragile equilibrium and safety. According a study requested by the Venice Port Authority, in 2012 medium ( $40,000 \leq GT \leq 100,000$ ) and large ( $>100,000$  GT) cruise ships increased their number approaches in the Venice harbour and, obviously passenger volume traffic compared to previous two years (Fig. 2.13).

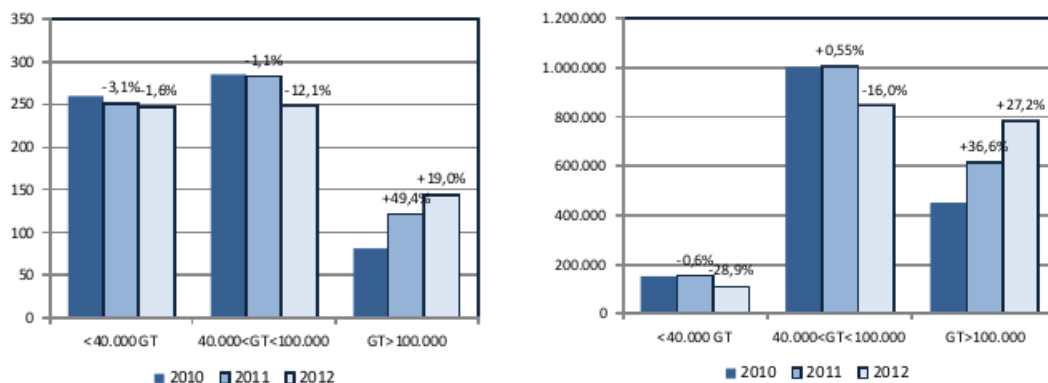


Figure 2.13. Number of approaches (left) and passengers (right) in the Venice harbour, period 2010-2012.

In 2015, a ban of the Italian Transport Ministry prohibits cruise ships larger than 40,000 GT to enter Venice's Giudecca Channel and St Mark's basin. A project under study consists in creating a new cruise terminal outside the Lagoon for the largest cruise ships. Figure 2.14 illustrates the total number of passengers of cruise ships, ferries and hydrofoils from 1997 to 2015 in the harbour of Venice. It is noticeable the increasing trend in annual traffic, especially in the last decade. Also, ferry and hydrofoil traffic allow connections with Greece (138,648 in 2013) and most Slovenian and Croatian destinations (Pula, Rovinj, Lošinj, Piran, Umag, Portoroz, Rabac) moving 92,984 passengers in 2013 (source: Venice Port Authority).



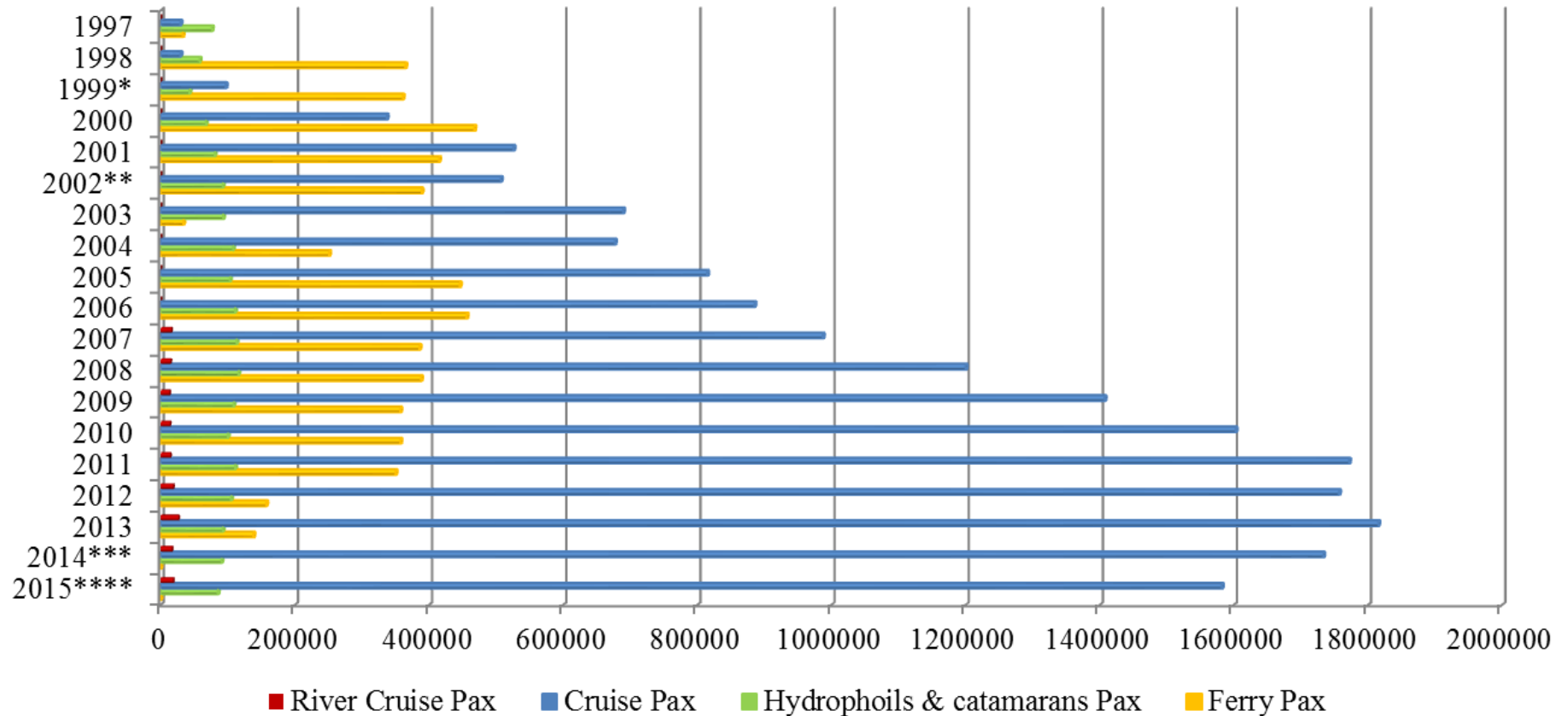


Figure 2.14. Trend in passenger traffic in Venice (adapted), period 1997-2015 with number of passengers (Pax) reported on x-axis. Adapted from Venice Terminal Passenger, [www.vtp.it](http://www.vtp.it). **Note:** \* In 1999 the cruise passenger traffic was badly influenced by the political events in the Balkans; \*\* in 2002 the cruise passenger traffic was badly influenced by 11th September political events; \*\*\* starting from January 1th 2014 ferry ships are not allowed to transit through San Marco and Giudecca Channels; \*\*\*\* starting from January 1th 2015 cruise lines have decided to deploy in Venice only ships up to 96,000-gross tons, until the new channel project will be approved.

Evaluating the commercial traffic, in total 22 million tons of goods are moved in 2014, with 6.9 million tons of liquid bulk, 7 million tons of dry bulk and 7.9 million tons of general cargo (source: Venice Port Authority statistics, <https://www.port.venice.it/en/the-port-in-figures.html>).

Over the time dry, liquid and general cargo reached the same share in 2014, with a slight predominance for general cargo and a significant reduction in liquid bulk compare to the previous years (Fig. 2.15).

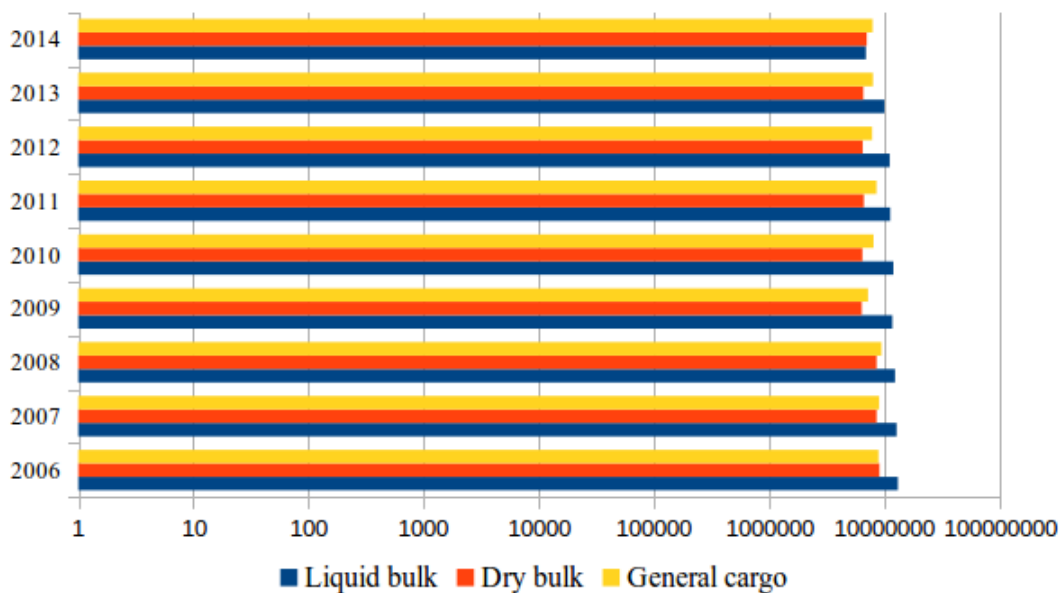


Figure 2.15. Trend in commercial traffic in Venice, period 2006-2014.

Many investments for the Port development have already allocated for the period 2016-2018. In particular, 258.8 million euro will be used to infrastructure-upgrading (i.e. restructuring of electrical, water and lighting systems, building of new quays). The port will be linked to the city centre by a city Gateway, a large area with many facilities. Finally, the Port Investment Plan 2008-2011 provided 870.5 million euro in total, including the creation of a new Container Terminal (in Porto Marghera), the MoS terminal and an off-shore terminal able to keep oil-tankers out of the Venice Lagoon.

## 2.2 Sampling sites

Different field campaigns were performed at sites representative of ship traffic in Venice and Brindisi areas. A summary of all campaigns and collected data is reported in Tab. 2.2.

In Venice a site at about 1 km S of the tourist harbour on the Sacca San Biagio island ( $45^{\circ} 25' 38.50''$  N –  $12^{\circ} 18' 33.86''$  E) was chosen. It is an uninhabited small island (minimizing so that the effect of extremely local sources), located at the end of the Giudecca Channel. Generally, navigating along this deep water passage tourist ships moved (under with their own power or towed) to and from the Venice cruise ship terminal, which was opposite to the sampling site (Fig. 2.16a). The sampling station was composed by an air-conditioned shelter hosting a personal computer, a vacuum system, and, only during the 2012 campaign, a Condensation Particle Counter. Next to the station, a telescopic mast was used to provide main micrometeorological parameters and an “outdoor box” contained an optical detector for  $PM_{2.5}$  measurements, a thermo-hygrometer and a pump (Fig. 2.16b).



Figure 2.16. Site position (a) and general instrumental setup (b) in Venice (set-up in 2012).

Table 2.2. Summary of measurements<sup>1</sup> available in Venice (green) and in Brindisi (orange).

	Period	PNC	PM <sub>2.5</sub>	PM <sub>1</sub>	PM <sub>10</sub>	Aerosol size distribution	O <sub>3</sub>	SO <sub>2</sub>	NO, NO <sub>2</sub> and NO <sub>x</sub>	Gaseous emissions (DOAS)	PAHs and PM <sub>2.5</sub> chemistry
2007	27 June-26 July; 28 August -26 September	x	✓	x	x	x	x	x	x	x	x
2009	22 July-1 September	x	✓	x	x	x	x	x	x	x	✓
2012	3 July-24 September	✓	✓	x	x	x	x	x	x	x	✓
	10 June-22 October	✓	✓	x	x	x	x	x	x	✓	✓
2014	24 June-15 October	✓	✓	✓	✓	✓	✓	✓	✓	✓	x

<sup>1</sup> Periods are referred only to PM and PNC sampling. DOAS and PAHs data were taken in specific days (not indicated here) within each campaign.

The sampling site in Brindisi was equipped with a Mobile Laboratory located inside harbour close (about 35 m) to the passenger terminal building ( $40^{\circ} 38' 43.32''$  N– $17^{\circ} 57' 36.39''$  E) and facing (about 50 m) the water and ferryboat docks (Fig. 2.17a). The van was equipped with instruments (placed both inside and on the roof) for high temporal resolution measurements of  $PM_{2.5}$  and particles number concentration (including ultrafine and nanoparticles) as well as a telescopic mast to collect micrometeorological data (Fig. 2.17b). However, in 2014 campaign, the measurements included also gaseous emissions (with a DOAS and different gas analysers) and aerosol characterisation in size distribution mode.

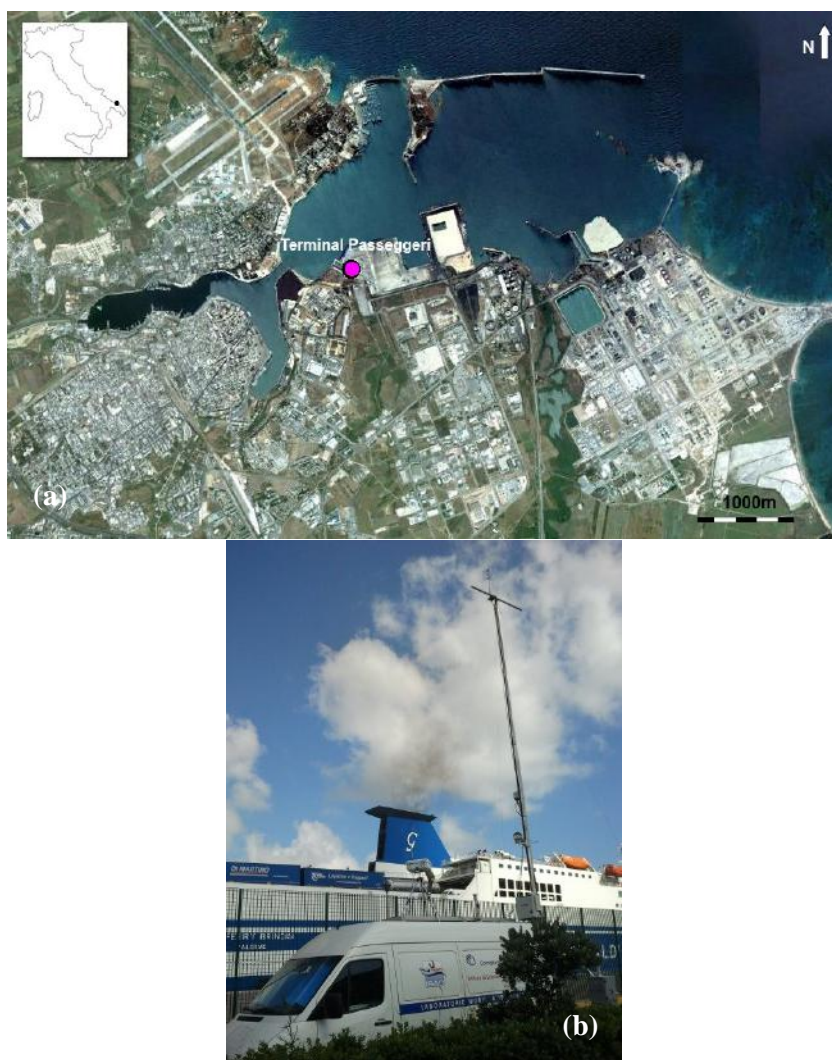


Figure 2.17. Site position (a) and instrumental setup (b) at the Terminal Passeggeri in Brindisi.

Venice campaigns were carried out for short periods (about 2 months) in three years: 2007, 2009 and 2012. Similarly, in Brindisi two campaigns were performed in 2012 and 2014 (Tab. 2.2). All measurements, both in Venice and Brindisi, were performed in summer periods allowing to collect data in a time interval which reflected maximum activity in the harbour areas (referring to passenger ships), and also at the beginning of autumn (since September) when a reduction of ship traffic was expected. Different instrumental setup and sampling strategies were applied but in general, instruments at high and low temporal resolution were run simultaneously as well as a micrometeorological station and a video camera to monitor ship movements (arrival, departure, passages, manoeuvring and hotelling).

The principal meteorological parameters (i.e. wind velocity, temperature, turbulence intensity and atmospheric stability) were provided by a micrometeorological station installed on a telescopic mast (Clark Mast SQT9/M) at 9.6 m above ground level (about 12 m a.s.l.) at Sacca San Biagio site, whereas it was at 10 m above ground level fixed at the van in Brindisi. At both measurement sites, a 3D ultrasonic anemometer (R3, Gill Instruments Ltd), placed on a horizontal bar at the top of the mast (Fig. 2.18), operating at 100 Hz in calibrated mode, measured wind characteristics and sonic temperature. At the same time, a slow-response Rotronic MP100A thermo-hygrometer (Campbell Scientific) provided relative humidity (RH) and air temperature data. All data from instruments were collected and digitized by the anemometer itself synchronously with wind components measurements.



Figure 2.18. Three-dimensional ultrasonic anemometer above the telescopic mast.

### 2.3 Aerosol characterisation

In each sampling site, particulate matter mass concentration was obtained at different temporal resolution, from daily samples and concentration data at 1Hz frequency. In

addition, for the 2014 campaign in Brindisi mass and number particle distribution was available for different size ranges.

### 2.3.1 Gravimetric determination

At both sites, PM<sub>2.5</sub> daily samples were collected on Teflon filters (Pall Corporation, diameter 47 mm) in Brindisi and on quartz filters (Sartorius, diameter 47 mm) in Venice. Samples were collected by using a sequential low-volume (2.3 m<sup>3</sup>/h) sampler installed only in the 2012 campaign in Venice (Fig. 2.19a) and in 2014 in Brindisi (Fig. 2.19b).

The gravimetric analysis was performed using a microbalance (Sartorius Cubis MSA6.6S, sensitivity 1 µg) for Brindisi samples and a Sartorius Competence CP64-0CE balance (precision 0.1 mg) for Venice samples, after stabilization (RH=50±5%; T=20±1°C) for 48 h in the same room in which the microbalance operated. The final uncertainty in measured concentration was evaluated combining the uncertainty in the weighing (2 standard deviations of the field blanks) with the uncertainty on the sampled volume.

Moreover, PM<sub>2.5</sub> daily concentrations were compared with the optically measured concentrations obtained by a fast-response optical photometer, described in the following.

After weighting procedure, PM<sub>2.5</sub> chemical characterisation was conducted on all filters collected. In Venice, chemical analysis of the samples consisted in anions (SO<sub>4</sub><sup>2-</sup>, NO<sub>3</sub><sup>-</sup>, NO<sub>2</sub><sup>-</sup>, Cl<sup>-</sup>, CHO<sub>2</sub><sup>-</sup>, and C<sub>2</sub>O<sub>4</sub><sup>2-</sup>) and total carbon determination. In particular, after an initial extraction from filters using an ultrasonic bath (30 minutes at 60°C) with ultrapure water (10 ml), anion concentration was obtained by Ionic Chromatography (761 Compact IC, Metrohm) technique. Further, total carbon concentration was determined by an Organic Carbon Analyser (TOC-5050A, Shimadzu).



Figure 2.19. Sequential low-volume samplers for  $PM_{2.5}$  sampling in (a) Venice (Sky Post PMHV – TCR Tecora) and (b) Brindisi (Zambelli Explorer Plus).

Instead, in Brindisi campaign determination of soluble ionic species ( $SO_4^{2-}$ ,  $NO_3^-$ ,  $NH_4^+$ ,  $Cl^-$ ,  $C_2O_4^{2-}$ ,  $Na^+$ ,  $K^+$ ,  $Mg^{2+}$ , and  $Ca^{2+}$ ) via High Performance Ion Chromatography (HPIC, Dionex DX-500 System) was performed as described in Cesari et al. (2014). In addition, the concentration of water-soluble organic carbon (WSOC) and of water-soluble inorganic carbon (WSIC) was measured in the same solutions used for HPIC, following the procedure used in Contini et al. (2014).

Quartz filters (Whatman Q-grade, diameter 47 mm) were collected during the 2012 campaign in an urban site at 1.3 km from the harbour measurement site for the analysis of total metal content. The acid digestion (solution of  $H_2O_2$ , HF and  $HNO_3$  and successive addition of  $H_3BO_3$ ) of the quartz filters were made with a MILESTONE MLS 1200 MEGA (FKV) microwave oven.  $PM_{2.5}$  samples were analysed via Graphite Furnace Atomic Absorption Spectroscopy (GF-AAS, Pinnacle System) for determination of trace elements (Ni, Cu, V, Mn, As, Pb, Cr, Sb) and by



Inductively Coupled Plasma Atomic Emission Spectroscopy (ICP-AES, Varian Liberty 110 spectrometer) for majority elements (Fe, Al, Zn and Ti).

Concentrations of the different chemical species were obtained with the removal of the average level present in the blank samples. Variability of blanks was used, together with analytical uncertainty, to obtain the final uncertainties in measured concentrations using the methodology discussed in Contini et al. (2012).

Finally, the results of chemical characterisation were used as input for source apportionment by using the statistical receptor model Positive Matrix Factorization (PMF), discussed elsewhere (Cesari et al., 2014).

### 2.3.2 Optical photometer

A fast-response optical detector pDR-1200 photometer (Personal Data logging Real time Aerosol Monitor, Thermo Electron Corporation) was used for measuring PM<sub>2.5</sub> concentrations at high resolution (1Hz). The instrument was housed in a box on a 1.5 m height tripod at Sacca San Biagio site (Fig. 2.21a) while in Brindisi site (Fig. 2.21b) it was fixed at the top of a tripod on the roof of the van (3 m height above ground).

The MIE pDR-1200 (Personal Data-logging Real-time Aerosol Monitor) is a high sensitivity nephelometric instrument (measurement range: 1  $\mu\text{g}/\text{m}^3$  - 400  $\text{mg}/\text{m}^3$ ) used for the measurement of the particle mass concentration. Instrument operation is based on infrared radiation (880 nm) scattered by particles. Concentration values are calculated by the radiation diffusion theory (Kerker, 1969) and factory calibrations, performed by gravimetric calibration with SAE Fine (ISO Fine) test dust (mmd = 2 to 3  $\mu\text{m}$ ,  $\sigma_g = 2.5$ , as aerosolized) (Chakrabarti et al., 2004). It is an ultra-compact (weight 0.5 kg), hand-held designed instrument. Instrument zeroing is accomplished by an inlet bulk filter cartridge. In addition, the instrument automatically checks agreement with its original factory calibration by checking its optical background during the zeroing sequence. It was verified that the stability of the zero (offset) varied by about 2-3  $\mu\text{m}/\text{m}^3$  in Venice (Contini et al., 2011) and about 5-6  $\mu\text{m}/\text{m}^3$  in Brindisi (Donateo et al., 2014) over a period of 3-4 weeks. This offset factor was checked once or twice per week and used to correct data in post-processing.

During all campaigns, the pDR-1200 was operated in active sampling mode (flow rate 4 L/min) and was equipped with a cyclone separator (model GK2.05) to select particle aerodynamic cut-off at 2.5  $\mu\text{m}$  at the specific flow-rate used (Fig. 2.20). A constant sampling flow throughout the entire campaign, periodically checked by the operators, was kept by a pump (Aquaria CF20E) in Venice, while a little pump Gardner-Denver was housed in the box for Brindisi campaign.

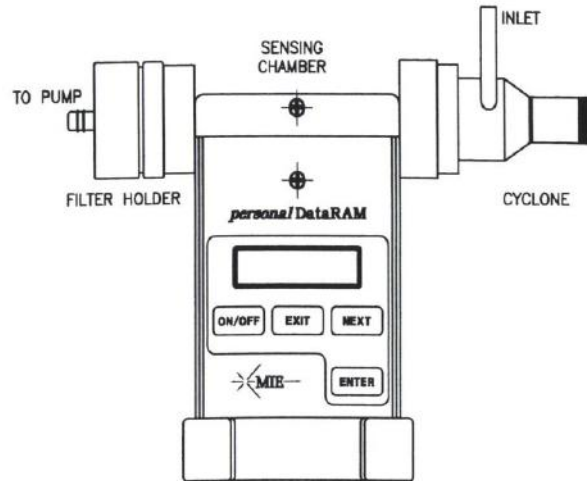


Figure 2.20. Schematization of the model pDR-1200 (source: Grimm Operator's manual).

Concentration measurements obtained by the pDR-1200 are demonstrated to be influenced by high humidity values ( $\text{RH} > 70\%$ ), because of the water vapour changes dimension, densities and optical properties of the particle (Sioutas et al., 2000; Chakrabarti et al., 2004) modifying their scattering and absorption coefficients and consequently the response of the optical instrument (Chakrabarti et al., 2004). Therefore, in order to take into account, the RH effect, the correction procedure developed in Donateo et al. (2006) was followed in cases with  $\text{RH} > 70\%$  (Eq. 2.1).

$$CF = \frac{C(\text{RH})}{C(\text{RH}=70)} =$$

$$4330.8282774 * \text{RH}^4 - 13628.3399181 * \text{RH}^3 + 16102.7519624 * \text{RH}^2 -$$

$$8456.2021129 * \text{RH} + 1664.7397809 \quad (\text{Eq. 2.1})$$

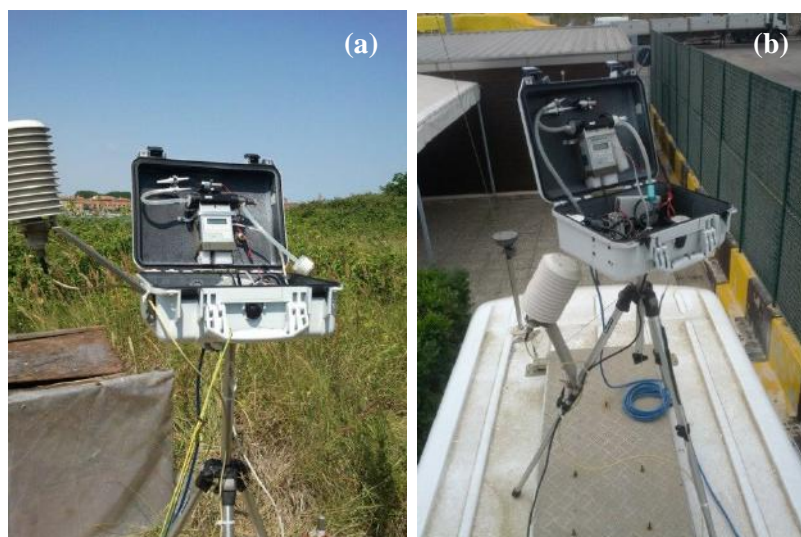


Figure 2.21. Fast-response optical detector pDR-1200 in the two sites: (a) Venice and (b) Brindisi.

### 2.3.3 Condensation Particle Counter

A Condensation Particle Counter (CPC) was used to measure total particles number concentration (PNC) at high resolution. Data were stored on the instrument SD card in Venice whereas a digital-to-analog converter interface was developed to connect CPC output with the inputs of the anemometer in Brindisi.

Generally, a CPC works on the so-called “condensation nucleus count mode” (Fig. 2.22). In practice, aerosol sample is led continuously through a heated ( $35^{\circ}$ ) saturator (C) in which alcohol (n-butanol) is vaporized and diffuses in the sample stream. Then, the mixture aerosol-butanol passes through a cooled ( $10^{\circ}$ ) condenser (E) where alcohol vapour being supersaturated starts to condense. Particles in the sample act as nuclei condensation and once condensation begins, they start to quickly grow in diameter into larger droplets so that they can be detected and counted. The detection is performed in the measuring cell (F) by a photo-diode (Q) integrating light scattering height pulses produced by each single particle passing the incident beam (emitted by a semiconductor laser).

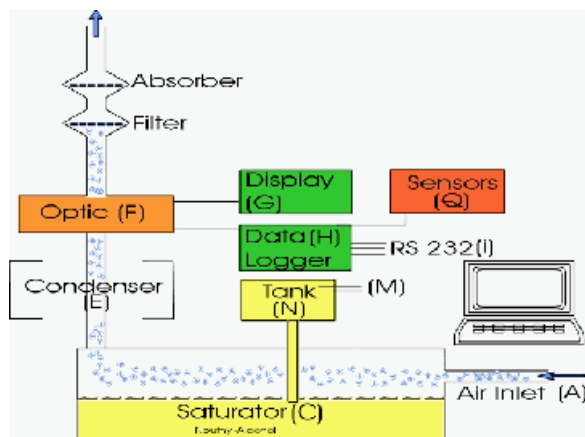


Figure 2.22. Measuring scheme of the CPC (source: Grimm User Manual).

The particle concentration can be determined by the CPC in the count range up to approximately  $10^7$  particles/L since this is the beginning of the coincidence level by scattered light.

In Venice, PNC measurements were performed only in 2012, using a CPC by TSI (model 3775) with a resolution time of 1 minute and recording data on SD card embedded with the instrument. In Brindisi, in both campaigns it was used a CPC by Grimm (model 5.403) with a resolution time of 1 s (frequency 1 Hz). The CPC was housed inside the air conditioned shelter at the Sacca San Biago site and in the Mobile Laboratory for the Brindisi campaign (Fig. 2.23). Aerosol was sampled through a plastic tube sampling (26 mm internal diameter) inlet with a stainless steel head outside at 2.5 m above the ground. A flow rate of 25 L/min in Venice and 30 L/min in Brindisi was kept by using a pump (Aquaria CF20E and Tecora Bravo H-plus, respectively). A portion of 1.5 L/min of the main flow was injected into the CPC using a 50 cm long conductive silicon tube (6 mm internal diameter). Sampled air went through a diffusion dryer to reduce water vapour concentration before the CPC. The same aerosol dryer (ATI model 250; 24 cm long and 2 cm internal diameter), designed and developed at ISAC-CNR laboratory, was used in Brindisi and Venice. Generally, the silica gel cartridges were replaced every two days after a periodical regeneration in an oven.

Briefly, a dryer system (Fig. 2.24) consists in a water trap at the inlet, removing coarse water droplets, before passing a removable silica gel cartridge. Here, the aerosol goes through the two concentric cylinders (an inner fine wire mesh screen

and an outer wire mesh screen) which form the cartridge. In the inner cylinder the water vapour diffuses into the silica gel trough the mesh screen.

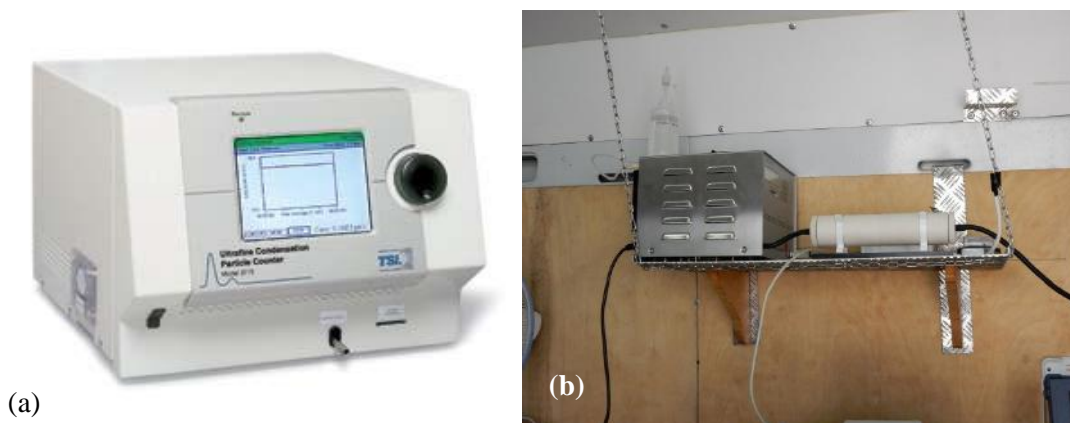


Figure 2.23. CPCs installed in (a) Venice and (b) Brindisi.

The penetration factor at the inlet of the CPC, as function of particle size, was calculated using the formulation reported in Hinds (1999). The total counting efficiency was calculated as the product between the penetration factor and the counting efficiency of the CPC obtained from Heim et al. (2004) for the Grimm model and from the constructor (TSI, 2007) for the TSI model. Results showed that the cut-off diameter (50% efficiency) was 5 nm in the configuration used in Venice and 9 nm for the other site. This means that CPC measured PNC in the range 5-3000 nm in Venice and 9-1000 nm in Brindisi (the latter are the upper limits of the CPC).

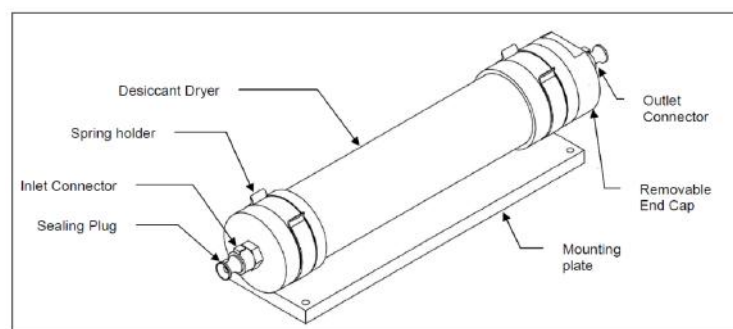


Figure 2.24. The diffusion dryer (source: ATI manual).

### 2.3.4 Optical Particle Counter

An OPC (Grimm 1.109, 31 channels) was added in the instrumental setup of the last campaign (2014) in Brindisi. It was located in an outdoor box (waterproof and

cooled) above the roof of the Mobile Laboratory (Fig. 2.25). Air was sampled at 1.2 L/min through a 50 cm long tube with a rain protection.



Figure 2.25. The OPC installed in Brindisi site in 2014.

The measuring principle relies on the light scattering of single particles detected by a receiver diode at  $90^\circ$  to the incident laser beam (Fig. 2.26). The sample air directly enters in the measuring cell where each particle crosses the incident beam (emitted at 655 nm by a semiconductor laser) originating a light scattering pulse. Counting the number of impulses and their intensity, the scattering light signals are classified into different (31) size channels. In this way, from particle size distribution in the range  $0.25\text{-}32\ \mu\text{m}$  (given as optical equivalent diameter) provides the basis for calculating also the size distribution in mass. Data output can be available in real-time (in intervals from 6 seconds up to 60 minutes) but in this work 1-minute averages were considered.

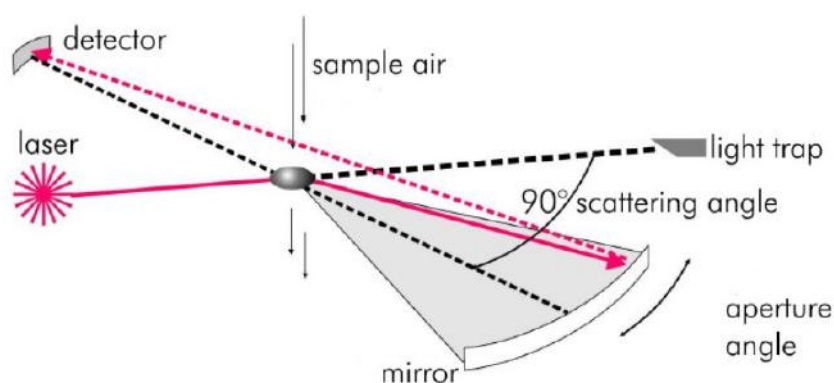


Figure 2.26. Measuring scheme of the OPC Grimm model 1.109 (source: Grimm Aerosol Manual).

By using the Grimm Windows software, the data can be displayed as particle concentration (in particles/L) or as mass concentration (in  $\mu\text{g}/\text{m}^3$ ) (Fig. 2.27). In addition, calculated particle surface area and occupational health respirable, thoracic and alveolic fractions are provided but they were not considered for the study purposes.

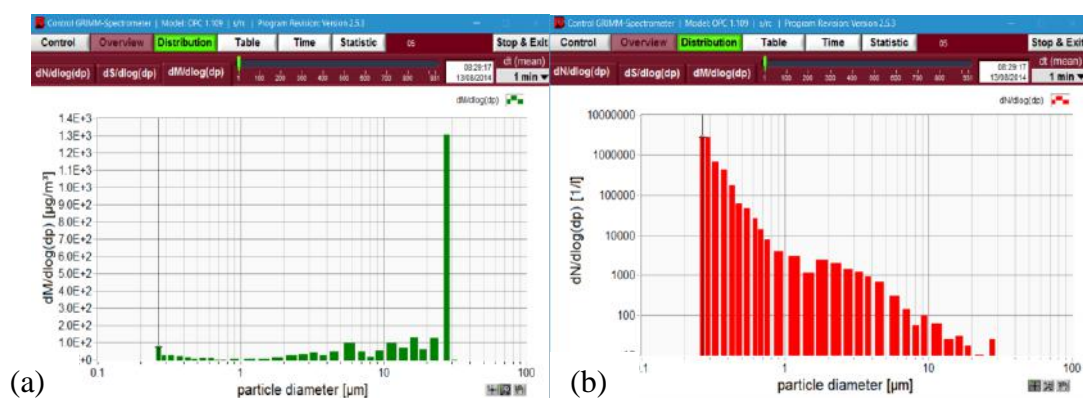



Figure 2.27. Screenshots of the Grimm software displaying particle size distribution in (a) mass and (b) number (Brindisi, 13/08/2014 08:29 AM).

## 2.4 Gaseous pollutants

At the Brindisi site both remote-sensing and high temporal resolution measurements of gaseous concentrations were taken. Concentrations of  $\text{O}_3$  (Teledyne-API 400E analyser),  $\text{NO}$ ,  $\text{NO}_2$ ,  $\text{NO}_x$  (Teledyne-API 200E analyser), and  $\text{SO}_2$  (Teledyne-API M100E analyser), were measured at 5 min resolution (Fig. 2.28). Calibration of the analysers at the start of the measurements and regular zero and span checks every 2-3 days was performed. Output concentrations were given in ppb/ppm at Standard Temperature and Pressure (STP) of  $0^\circ\text{C}$  and 760 mmHg, therefore a conversion from volume/volume units to weight/volume (in  $\mu\text{g}/\text{m}^3$ ) at  $20^\circ\text{C}$  was applied according to the relative analyser manuals (Tab. 2.3).

Table 2.3. Conversion factors between ppb and  $\mu\text{g}/\text{m}^3$  used in post-processing data (source: Teledyne API-series manuals from <http://www.teledyne-api.com/manuals/>).



Gas	Conversion factor	Operation principle
Ozone ( $\text{O}_3$ )	1 ppb = $2.14 \mu\text{g}/\text{m}^3$	UV Spectroscopy
Nitrogen oxides ( $\text{NO}_x$ )	1 ppb = $2.05 \mu\text{g}/\text{m}^3$	Chemiluminescence
Nitrogen monoxide (NO)	1 ppb = $1.34 \mu\text{g}/\text{m}^3$	Chemiluminescence
Nitrogen dioxide ( $\text{NO}_2$ )	1 ppb = $2.05 \mu\text{g}/\text{m}^3$	Chemiluminescence (indirect)
Sulphur dioxide ( $\text{SO}_2$ )	1 ppb = $2.66 \mu\text{g}/\text{m}^3$	UV Fluorescence

Figure 2.28. Gas analysers in the Mobile Laboratory.

#### 2.4.1 Gas analysers

Ozone analysers (Fig. 2.29) are photometers, which use the fact that ozone molecules adsorb light in UV region. The analyser measures reference and sample air alternating measurements in a cycle, using the same cell. In the first part of the cycle, sample air is scrubbed by means of a manganese dioxide ( $\text{MnO}_2$ ) scrubber to remove ozone. Then, the scrubbed sample air enters the measurement cell to establish a reference light intensity at zero ozone concentration. In the second part of the cycle, sample air is re-directed to bypass the scrubber and enters the sample cell directly for measurement of the attenuated light intensity. Ozone concentration is calculated by the Lambert-Beer law, quantifying reduction of the intensity of light (difference between sample and scrubbed air) reaching the detector at 254 nm.



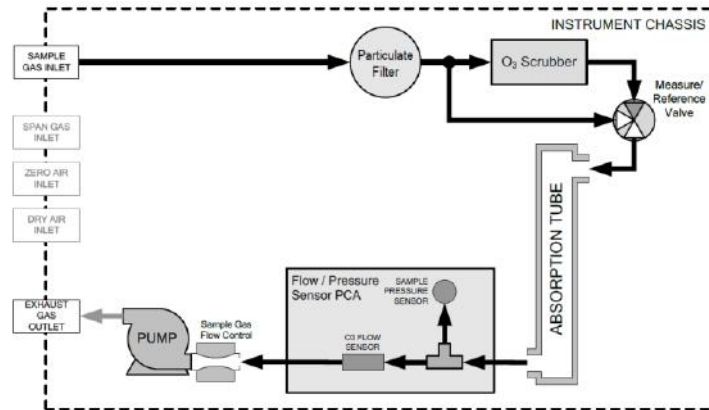


Figure 2.29. Operation scheme for ozone measurements (source: Teledyne-API 400E Operator's manual).

The reactive oxides of nitrogen in the atmosphere are largely nitric oxide (NO) and nitrogen dioxide (NO<sub>2</sub>), known together as NO<sub>x</sub>. Measurement technique is based on two cycles (Fig. 2.30). The first NO cycle passes sample air to reaction chamber, in which NO concentration is measured. In particular, at wavelengths greater than 600 nm, chemiluminescence given off when the sample gas is exposed to ozone (O<sub>3</sub>) is detected, according to the reaction (Eq. 1):



Another portion of ambient air follows the NO<sub>x</sub> cycle, in which a catalytic-reactive converter (molybdenum converter) reduces any NO<sub>2</sub> in the sample gas to NO. Again NO concentration is determined by chemiluminescence as described above. Therefore, NO<sub>2</sub> concentration is indirectly calculated as difference between NO<sub>x</sub> and NO detections.

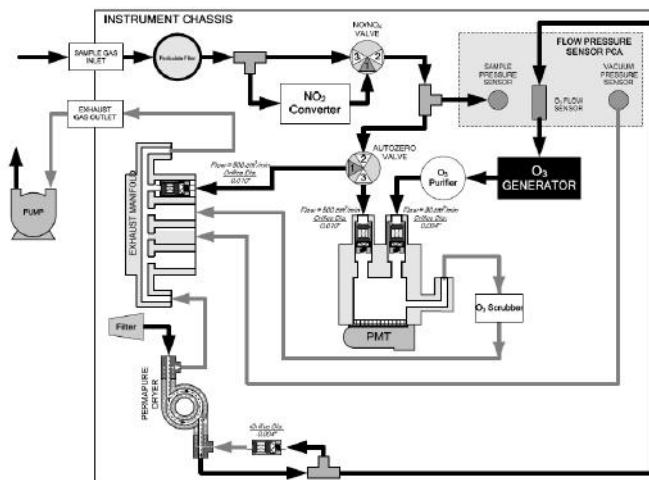


Figure 2.30. Pneumatic diagram of nitrogen oxides analyser (source: Teledyne-API 200E Operator's manual).

Sulphur dioxide (SO<sub>2</sub>) measurements are based on the fluorescence principle. Incoming air passes through a filter (kicker) to remove any hydrocarbons from the sample (Fig. 2.31). Afterwards, in reaction cell molecules of SO<sub>2</sub> are excited adsorbing UV light at 214 nm, switching from a fundamental state to an excited state for few second fractions (Eq. 2.3). When molecules decay at lower energetic state (fluorescence), emit UV radiation at 330 nm, proportional to SO<sub>2</sub> concentration (Eq. 2.4).

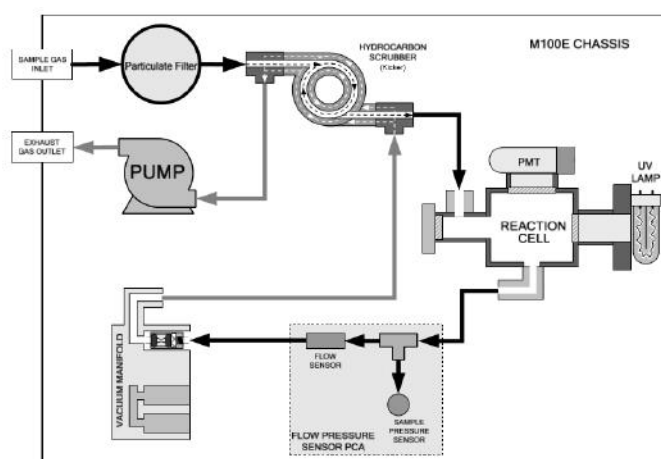
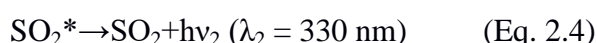
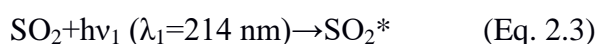


Figure 2.31. Basic configuration of sulphur dioxide analyser (source: Teledyne-API M100E Operator's manual).

#### 2.4.2 DOAS system

Detection of columnar concentrations of nitrogen dioxide (NO<sub>2</sub>) and sulphur dioxide (SO<sub>2</sub>) over the harbour area was performed in Brindisi by a Differential Optical Absorption Spectroscopy (DOAS) system to validate the emission inventory estimates and to evaluate the inter-annual trend on the emissions in summer 2012 and in summer 2014 (Merico et al., 2016). The DOAS system is an investigative method to determine atmospheric concentrations of trace gases by measuring their specific narrow band absorption structures in the UV and visible wavelength range along an optical path.

The instrumental setup included two parts (Fig. 2.32): the UV-Vis remote sensing spectrometer, called TROPOGAS (TROPOspheric Gas Analyser Spectrometer) and the platform SODCAL (Scanning Optical Device Collecting Atmospheric Light).

The TROPOGAS belongs to a new series of DOAS instruments developed at ISAC-CNR (Masieri et al., 2014). It is composed by: a spectrometer with spherical holographic grating (1200 lines/mm, mean dispersion 2.4 nm/mm); a CCD (SITE Charge Coupled Device) sensor R2V-Marconi cooled up to  $-40^{\circ}\text{C}$ ; an electronic device that manages all the CCD and spectrometer functions (e.g. grating movement; control of the sensor temperature; spectral position in front of CCD, using an internal Hg lamp; control of the temperature of the entire optical part of the spectrometer).

The CCD sensor consists in a back-illuminated rectangular matrix of  $256 \times 1054$  diodes, of which  $30 \times 10$  are taken dark as reference. Light collected is dispersed by the grating along the X dimension of the sensor and the 246 lines are summed/binned in groups of 41 to reduce the signal to noise ratio.

The SODCAL is a platform containing a small telescope with azimuthal and zenithal movements, therefore able to receive the diffused sun radiation from every direction. It is based on a  $45^{\circ}$  rotating mirror objective with a diameter of 60 mm resulting in a field-of-view of  $1.5^{\circ}$ , connected via a quartz optical fiber to the optical entrance of the spectrometer. The *Input module* allows to the TROPOGAS system to select sequentially the incoming optical radiation from three different sources (including the connection with the SODCAL).

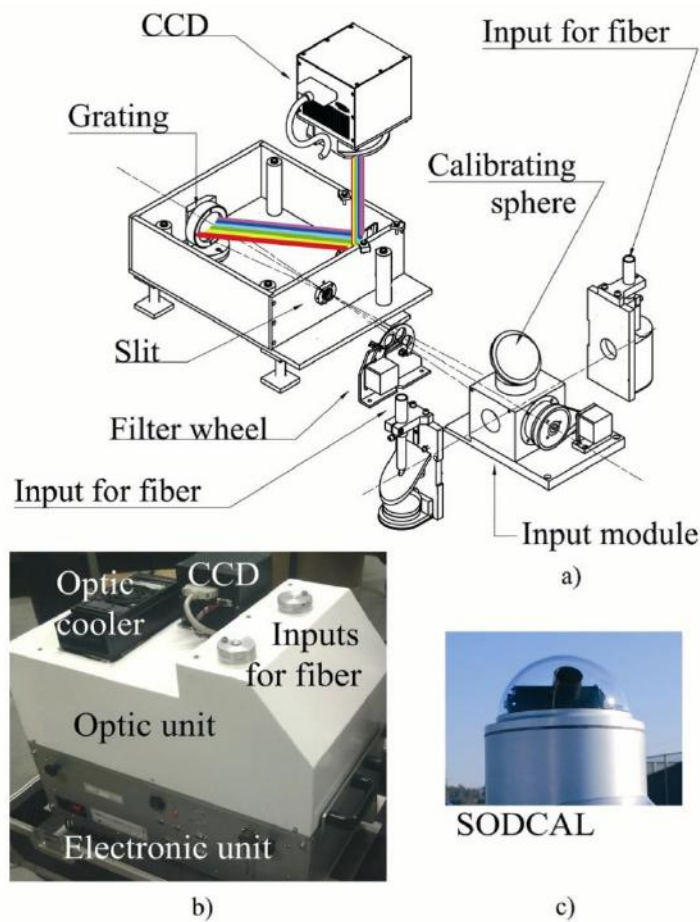


Figure 2.32. Elements of the spectrometric apparatus used: a) exploded internal and b) external view of the spectrometer, c) SODCAL.

Using the approach developed by Premuda et al. (2011), the DOAS system measures flow-rate-emission (FRE) of  $\text{NO}_2$  and  $\text{SO}_2$  of ships. In practice, sunlight scattered radiation is used to retrieve the slant column densities (SCDs) from oblique measurements along a vertical plane intersecting the ship plume at different elevations. An initial elevation of  $45^\circ$  is used, decreasing at steps of  $5^\circ$  and increasing the number of positions next to the horizon.

In Brindisi campaign, the SODCAL was positioned on the roof of the Mobile Laboratory (Fig. 2.33a), connected to the spectrometer recovered inside the van.

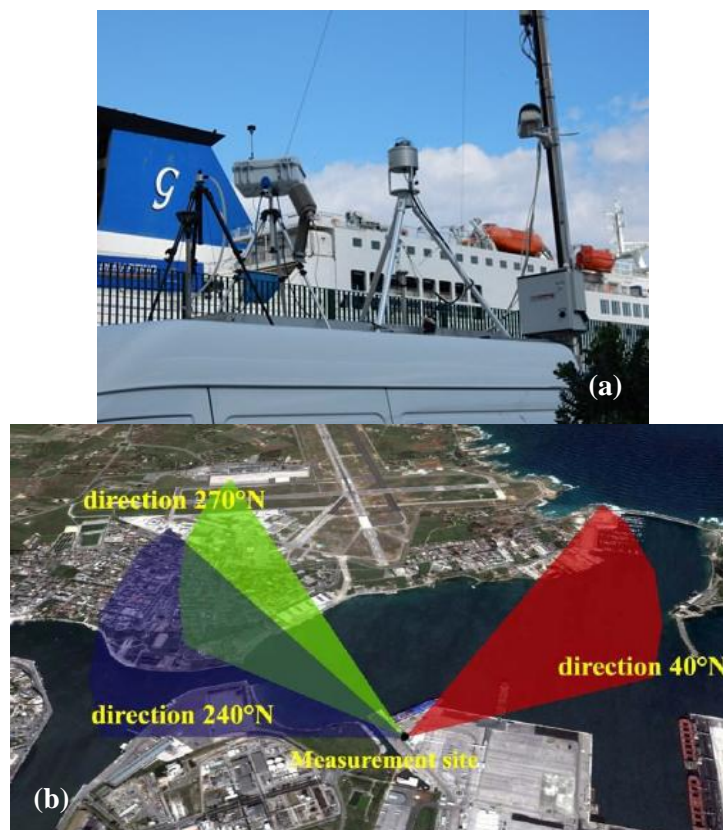


Figure 2.33. (a) The SODCAL setup used and (b) scheme of the scanning planes selected.

Measurements were taken choosing three vertical scanning planes (Fig. 2.33b), in order to intercept the greatest number of ships as possible taking into account docks positions in the port area.

The first plane was at  $40^{\circ}\text{N}$  at the entrance of the harbour; the second was at  $240^{\circ}\text{N}$ , to evaluate the urban concentration background and finally the third was chosen at  $270^{\circ}\text{N}$ , covering the hotelling zone of the ferries close to the measurement site. The set of oblique measurements were carried out in diurnal hours, from one hour after sunrise to one hour before sunset. The detailed FRE-methodology is described in Chapter 3 (section 3.4).

## 2.5 Ships and vehicular traffic

To monitor movements (arrival/departure) of ships and vehicles at the measurements sites, a network infrared video camera (AXIS 221), with a multi-focal lens, CCD with progressive scan 1-3", up to 0.65 colour lux, was used. It was able to operate during night and day collecting photos every 30 s of the quay areas (in Brindisi) and of the channel (in Venice). At Sacca San Biagio site, the video camera was installed

on the sampling station (wooden cabin) at 1.7 m above ground level whereas in Brindisi was fixed on the telescopic mast at about 3 m height (Fig. 2.16).

Actually, from the Venice site only passages of ships were recorded (Fig. 2.34) since that ships docked at the cruise terminal Stazione Marittima, opposite to the site. Collected data of ship traffic were integrated with timetable of ship movements recorded in the detailed database of the Venice Port Authority.



Figure 2.34. Photo frames of a cruise ship departure from the tourist harbour in Venice (12/07/2009).

It is important to highlight that, in Brindisi harbour, only three docks were framed (Fig. 2.35): Prolungamento di Nuovo Sporgente, Costa Morena Terrare and Costa Morena Terrare Punta (see Section 2.1.1). Data traffic about the remaining harbour areas were provided by the local Port Authorities (in Brindisi and Venice) and obtained by MarineTraffic.com. Integrating all data, a comprehensive traffic database was built, including information about:

- ship name (and other features) and GT;
- ship arrival/departure time;

- average manoeuvring time (depending on ship type and departure/arrival dock);
- hotelling duration (time usually spent in loading/unloading operations);
- dock name.

Data furnished by the Avvisatore Marittimo and Port Authority of Brindisi also included average fuel consumption and fleet distribution by GT and type, both for 2010 and 2014. The additional information was used to emission inventories estimates for maritime sector, whose methodology is described in Chapter 3 (section 3.2).

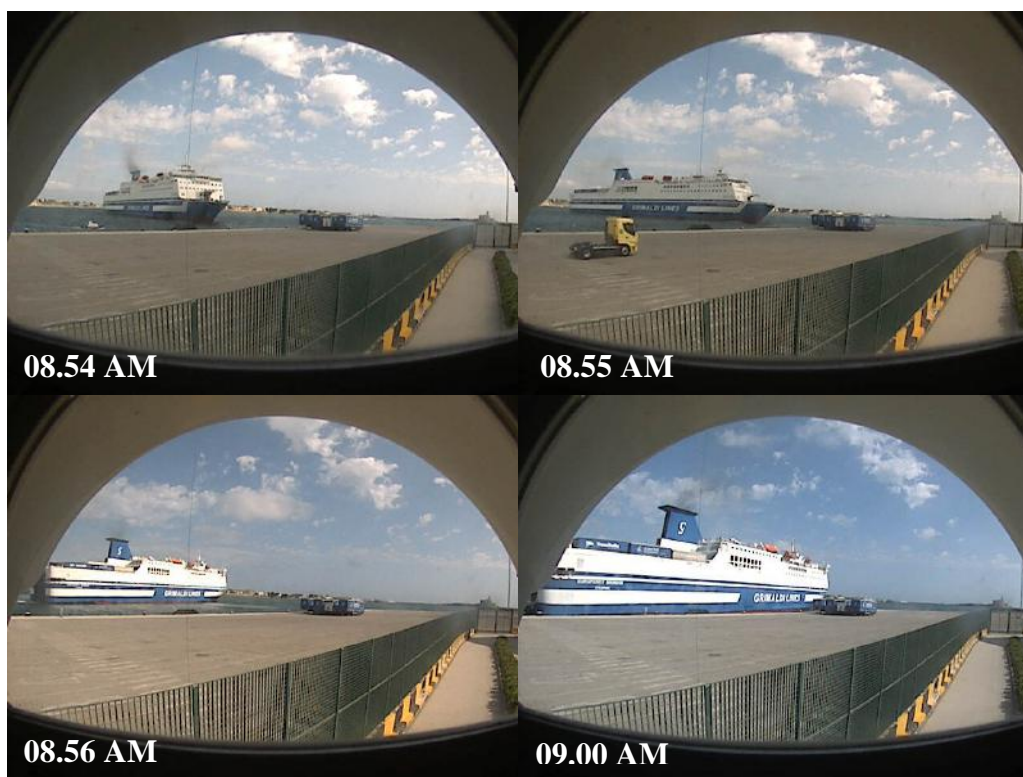


Figure 2.35. Photo frames of ship manoeuvring in arrival in the Brindisi harbour (27/06/2014).

In addition, from video camera snapshots, vehicular movements (e.g. cars, trucks) associated to loading and unloading of ships were also monitored in the area facing the dock in Brindisi (Fig. 2.36). In order to estimate a possible influence on measurements, a threshold of at least 10 vehicles (in the 30-min period) was considered. Loading/unloading activities were included in the calculation of total contribution, separating it from contribution of ships alone. No distinction by vehicle type, fuel used, queue time, engines turned off/on was applied.

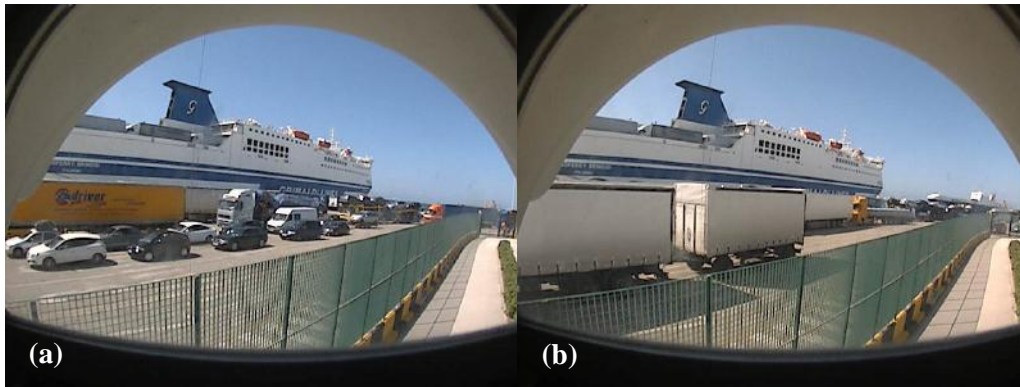


Figure 2.36. Photo frames of (a) loading operations and (b) simultaneous passage of another ship in the Brindisi harbour (27/06/2014).



## **Methods to estimate shipping contribution to air pollution**

Several experimental methods have been developed to better understand and quantify the real impact of shipping emissions on pollutant levels in the harbour areas. Within this scope, most of the literature has been concerned with in laboratory conditions on engine test beds (Kasper et al., 2007; Petzold et al., 2010), on-boards measurements (Fridell et al., 2008; Moldanova et al., 2009; Murphy et al., 2009), in-plume measurements by aircraft or ship (Sinha et al., 2003; Berg et al., 2012) or in-port measurements (Alföldy et al., 2013; Ault et al., 2010; Merico et al., 2016; Donateo et al., 2014; Jonsson et al., 2011).

Furthermore, inventory estimates (Miola et al., 2009; Dalsøren et al., 2009; Dore et al., 2007; Wang et al., 2007; Eyring et al., 2005; Corbett et al., 2003) have been recognized as the main tool for evaluating total emissions from ships. However, dispersion models (Jalkanen et al., 2012; Johansson et al., 2013; Jalkanen et al., 2014) have been demonstrated useful to simulate aerosol emission, formation, transport and deposition at different spatial and temporal scale. In fact, they have the significant advantage to produce future emission scenarios to evaluate the impact of emission abatement strategies.

### **3.1 Source Apportionment approach**

Generally, source apportionment tools, either by means of receptor models or by using chemical tracers (Mazzei et al., 2008; Viana et al., 2009; Pandolfi et al., 2011; Moreno et al., 2010; Becagli et al., 2012; Salameh et al., 2015; Cesari et al., 2014; Bove et al., 2014; Bove et al., 2016), have been used for evaluating contribution to PM concentrations, whereas dispersion modelling has been more appropriate for gaseous pollutants. Chemical tracers of shipping emissions are vanadium (V) and nickel (Ni), but others found are thorium (Th), lead (Pb), zinc (Zn) and sulphate (Isakson et al., 2001; Hellebust et al., 2010; Viana et al., 2008; Becagli et al., 2012). However, maritime emissions are not univocally identified because they are often mixed with other combustion sources present close to (or inside) harbour areas (i.e. petroleum refinery, industrial complexes) and characterised by similar tracers. For this reason, diagnostic tracer ratios have been sometimes used. Typical ratio used are

V/Ni (Agrawal et al., 2009; Viana et al., 2009; Zhao et al., 2013), vanadium/elemental carbon - V/EC (Viana et al., 2009), non-sea-salt (nss)SO<sub>4</sub><sup>2-</sup>/V and others less used (i.e. OC/EC, V/S, Pb/Zn, Zn/Ni). The V/N ratio is universally recognized as robust IFO engine emissions tracer. It has been found around 3 in PM<sub>10</sub> and PM<sub>2.5</sub> fractions (Pandolfi et al., 2011), in Barcelona the value of 2.98 (Pèrez et al., 2016) and between 2.3 and 4.5 for different fuelled main and auxiliary engines at different speed (Agrawal et al., 2008a). Recently, Johnson et al. (2014) found a new set of indicator ratios (V/BC and V\*S/BC) for identifying emission sources burning low quality residual fuel oil.

The source apportionment analysis relies on the application of receptor models such as the Positive Matrix Factorization (PMF). However, these statistical approaches are not always conclusive, because of one of the main limitation in the presence of shared markers between different sources and consequently the inability to discriminate sources with similar profiles. For example, in Viana et al. (2008) was highlighted that the not unique interpretation of the V/Ni/SO<sub>4</sub><sup>2-</sup> factor among different studies, because of the same tracers for industrial and regional background. Especially in harbours, the co-presence of several and various activities, whose emissions are not completely characterised (i.e. exhausts gas from different ships), complicates the analysis.

Additional chemical information (chemical composition of PM and fuels) and meteorological parameters (i.e. wind speed and wind direction) should be included in the analysis to “resolve better” similar source profiles (Cesari et al., 2014; Gregoris et al., 2015).

Based on previous works (Zhao et al., 2013; Agrawal et al., 2009; Pandolfi et al., 2011), the V is considered a tracer of ships' engines combustion. Following the formula obtained by Agrawal et al. (2009), the primary PM contribution (PM<sub>a</sub>) can be calculated (Eq. 3.1):

$$PM_a = R * V_a / F_{V, HFO} \quad (\text{Eq. 3.1})$$

where

R = 8205.8, as suggested in Agrawal et al. (2009) as a value internationally applied to locations with HFO-burning ship emissions;

$V_a$  is in situ ambient concentration of V ( $\mu\text{g}/\text{m}^3$ )

$F_{V, \text{HFO}}$  is the average V content (in ppm) in HFOs used by vessels in port; it ranges from 58 ppm (Furuyama et al., 2011) to 65 ppm (Zhao et al., 2013), to 75 ppm (Murphy et al., 2009) and finally to 100 ppm as reported in Visschedijk et al. (2013).

In Cesari et al. (2014) a value equal to  $65 \pm 25$  ppm was chosen for the Brindisi harbour due to the absence of specific chemical analyses of fuels used.

By applying Eq. 3.1, the primary contribution of shipping was between 0.26 and 0.59  $\mu\text{m}/\text{m}^3$  to  $\text{PM}_{2.5}$  in Brindisi (Cesari et al., 2014), from 0.7 to 3.4  $\mu\text{g}/\text{m}^3$  on  $\text{PM}_{10}$  in the Western Mediterranean (Bove et al., 2016), in the range 0.63-3.58  $\mu\text{g}/\text{m}^3$  in Shanghai port (Zhao et al., 2013), from 1.2 to 2.3  $\mu\text{g}/\text{m}^3$  of  $\text{PM}_{2.5}$  at a coastal site with 1 km off sea (Pandolfi et al., 2011), and between 0.18 and 0.42  $\mu\text{g}/\text{m}^3$  at a site near main shipping line (Minguillón et al., 2008).

Ship emissions are also considered to be a significant contributor to secondary particles mainly due to the sulphate derived from conversion of  $\text{SO}_2$  emissions. Sulphur content fuel is directly implied in secondary particles formation, because they derive from the nucleation process of sulphuric acid formed by reaction catalysed by vanadium (Isakson et al., 2001) between  $\text{SO}_3$  and water vapour during dilution and cooling. Secondary sulphate particles remain in the atmosphere on relatively long time span (Restad et al., 1998) and therefore they spread out on large spatial scales. Also in this case, differentiation of  $\text{SO}_4^{2-}$  originating from regional-scale aerosols or local anthropogenic emissions such as industry or shipping is not clear (Viana et al., 2008).

Characterisation of secondary aerosol (mainly  $\text{nssSO}_4^{2-}$ ) associated with ship emission has been investigated in limited studies (Becagli et al., 2012; Viana et al., 2009; Cesari et al., 2014; Marmer and Langman, 2005; Yau et al., 2013). A recent review (Viana et al., 2014) showed that, in European coastal areas, shipping emissions contribute with 1-7% of  $\text{PM}_{10}$  levels, 1-14% of  $\text{PM}_{2.5}$ , and up to 11% of  $\text{PM}_1$ .  $\text{PM}_{10}$  characterisation in Western Mediterranean discriminated between the sulphate of secondary origin (about 60% of the total sulphate) and those attributed to heavy oil combustion, which was approximately 20% (Bove et al., 2016).

In order to estimate the secondary contribution, the correlation between primary oil combustion contribution and concentrations of  $\text{nssSO}_4^{2-}$  was evaluated (Cesari et al., 2014; Kim and Hopke, 2008; Viana et al., 2009). Practically, the minimum value of  $\text{nssSO}_4^{2-}$  concentration expected per unit contribution of oil combustion–industrial particles was obtained.

In the Central Mediterranean, the secondary contribution has been found to be more accentuated with respect to those to the primary, confirming that impact of shipping activities increases with decreasing particle size. In Lampedusa Island the secondary contribution was 30% of total sulphate (Becagli et al., 2012), in Brindisi (Italy) it accounted of 40% of the total  $\text{nssSO}_4^{2-}$  (Cesari et al., 2014). Further, in the Melilla harbour (Spain) it was found that the secondary contribution of ship emissions was two times the primary one (Viana et al., 2009). Ship-borne measurements performed following a ship route on western Mediterranean (Bove et al., 2016) recorded the highest shipping contribution to  $\text{nssSO}_4^{2-}$  in August-September period, contributing to  $\text{PM}_{10}$  with 25% and 18% in August and September, respectively. In Tab. 3.1 primary and secondary contributions to  $\text{PM}_{10}$  and  $\text{PM}_{2.5}$  obtained with different approaches in some Mediterranean port-cities are reported.

Table 3.1. Primary and secondary shipping contribution to  $\text{PM}_{10}$  and  $\text{PM}_{2.5}$  obtained in different studies.

Site	$\text{PM}_{10}$		$\text{PM}_{2.5}$		PNC	Reference
	Primary	secondary	primary	secondary		
Venice (3 sites: 2 lagoon inlets for ships and near the harbour)			2.4-3.3%			Gregoris et al. (2015)
Barcelona	9%	0-1%	17%	0.3%		Pèrez et al. (2016)
Western Mediterranean	12%	7%				Bove et al. (2016)
Brindisi (harbour)	7.3%		9.3%		48%	Merico et al. (2016)
Brindisi (urban area)			2.8%	11%		Cesari et al. (2014)
Brindisi (harbour)	7.4%		9.3%		39%	Donateo et al. (2014)

Barcelona	2.7%	12%				Pey et al. (2013)
Lampedusa	3.9%		8%			Becagli et al. (2012)
Venice (3 ship passage points along the Giudecca Channel included the cruise terminal)	1-8%					Contini et al. (2011)
Algeciras urban/industrial	3-7%	6-10%	5-10%	7-12%		Pandolfi et al. (2011)
Cork			1.5%		18%	Healy et al. (2010)
Melilla urban	2%	4%	14%			Viana et al. (2009)
Melilla urban	5%		6%			Amato et al. (2009)
Italy, UK, Portugal	5-10%					Fagerli and Tarrason (2001)
4 Adriatic-Ionian harbours (Brindisi, Patras, Rijeka, Venice)	0.3-5.8%		0.5-7.4%			Merico et al. (2017)
4 Mediterranean harbours (Venice, Barcelona, Genoa, Marseille, Thessaloniki)			10-20%			APICE project

### 3.2 High resolution measurement approach

Particles emitted by ships showed a bimodal shape in number size distribution in several studies on different engines and ships (Kasper et al., 2007; Petzold et al., 2008; Kivekäs et al., 2014; Pirjola et al., 2014) with a first mode at 0.04-0.06  $\mu\text{m}$  and a second one at 0.1-0.2  $\mu\text{m}$ . However, an additional nucleation mode (at around 0.01  $\mu\text{m}$ ) was found at the banks of the Elbe in an ECA area in Germany (Diesch et al., 2013) and only a single mode in Gothenburg (Sweden) at 0.035  $\mu\text{m}$  (Jonsson et al., 2011). These differences are likely due to the different fuels and engine

performances. On the other hand, larger particles dominate mass size distribution because they are very few in number and difficult to detect by counting methods (Fridell et al., 2008).

Murphy et al. (2009) individuated a significant contribution up to 6  $\mu\text{m}$  whereas a bimodal shape in mass distribution was found in Lyyaranen et al. (1999) and in Moldanova et al. (2009) with a first mode at around 0.4-0.5  $\mu\text{m}$  and a coarse mode at 7-10  $\mu\text{m}$ . However, a third mode at 0.1-0.2  $\mu\text{m}$  was added by Fridell et al. (2008).

The relative variability of the typical size of the different modes could be related to the temperature of exhausts or to aging of the plume. The influence of sulphur content in fuel on particle size distributions has been little investigated. Comparison of emissions using HFO and MDO showed that the largest particle emissions values were attributed to HFO-burning compared to distillate fuels (Winnes and Fridell, 2009) and the modes in the number concentration were shifted to larger diameters (Anderson et al., 2015).

The impact on particle number concentrations have been investigated in few works (Donateo et al., 2014; Healy et al., 2010; Hallquist et al., 2013; Merico et al., 2016; Westerlund et al., 2015) especially in the Mediterranean area. This is probably due to difficulties in performing accurate measurements as well as lack in information about ship operating conditions influencing particle size distribution of emissions.

Typical particle size distributions from in-plume measurements (Sinha et al., 2003) or on ships at berth (Cooper et al., 2003) and for different fuels and loads (Kasper et al., 2007; Petzold et al., 2011; Anderson et al., 2015) were available.

Gonzàles et al. (2011) analysed ultrafine particles ( $D_p < 100$  nm) pollution in downwind urban area of Santa Cruz de Tenerife (Canary Islands) splitting the total number concentration into two source components (vehicles exhausts and ships emissions) as done in Rodríguez and Cuevas (2007). Shipping contributed from 55% to 65% of the total particle number concentration during the morning and from 65% to 70% during breeze events, with a simultaneous increase in  $\text{SO}_2$  concentrations.

Studies on contributions of shipping to gaseous pollutants have been conducted at large domains (from regional to global scale), essentially by using modelling tools. Being the modelling simulations based on emission inventories (more or less updated), large uncertainties in estimates are frequent (see Section 3.3).

In Europe most of studies on gaseous pollutants have been concentrated in Northern regions (Hammingh et al., 2012; Isakson et al., 2011; Saxe and Larsen, 2004; Eyring et al., 2010) with respect to the Mediterranean works focused on PM and chemical composition.

It was demonstrated that ship manoeuvring operations contributed about 6% of NO<sub>x</sub> and 10% of SO<sub>2</sub> to total shipping emissions in U.S. (Corbett and Fischbeck, 1997). Also, along the waterways of the port of Rotterdam shipping determined an enhancement of the surface NO<sub>2</sub> mixing ratio of 5–7 ppb (Keuken et al., 2005). The local effect of sea breeze was shown by an increase of SO<sub>2</sub> levels at midday by a factor of 3-4 compared to daily concentrations in Barcelona (Reche et al., 2011).

The application of a 3-D Lagrangian particle dispersion model in Taranto port (Italy) determined a contribution of 9% for SO<sub>2</sub> and NO<sub>2</sub> from harbour activities (Gariazzo et al., 2007).

Not homogeneous knowledge complicates the decisional process in orienting reduction strategies at international level which needs comparable results.

In this work, a novel statistical approach, based on simultaneous analysis of aerosol and gaseous concentrations, wind directions, integrated with the timetable of ship movements synchronized with concentration measurements, was applied to estimate shipping primary contribution. This represents a new methodology based on stationary measurements (inside the harbour) at high temporal resolution processed by an ad-hoc developed statistical approach which included also meteorological data. The method was developed and firstly applied to estimate shipping contribution to PM in Venice (Contini et al., 2011) and then extended to the Brindisi harbour in 2012 (Donateo et al., 2014). Thus, a qualitative and quantitative analysis was performed by using different statistical tools in order to evaluate the directionality in the shipping contribution on concentration data and quantifying it in relative terms, respectively. A comparable method was implemented in the port of Brisbane (Australia), obtaining wind rose distributions of each chemical species (Johnson et al., 2014). However, daily average chemical concentration data integrated with the daily mean wind velocity were plotted oppositely to this study in which high-resolution data were elaborated as described in the following.

In our analysis, bivariate polar plots were obtained relatively to 2014 by using the extension “openair” - version 1.1-4 (<http://www.openair-project.org>) of the open-source RStudio software (version 3.1.2), described in more details in Carslaw et al. (2015). Highlighting the joint wind speed-direction dependence of concentrations, a graphical impression of potential sources influences at the location site is provided. In fact, in these graphs three variables can be plotted: the colour scale reports the average concentration, the distance from the centre is proportional to the wind velocity and the angular position indicates the wind directions. Resulting plots are shown as a continuous surface calculated through modelling using smoothing techniques.

The analysis of primary contribution was performed on 30 min averages, starting from high resolution measurements (each variable with its sampling frequency). The two main reasons for that are reported in the following:

1) the intermittent nature of shipping emissions and related harbour activities. In fact, any correlation was observed between daily PM concentrations and ship traffic in the Brindisi harbour in previous campaigns (Donateo et al., 2014) and multiple short peaks (less than 10 min) in manoeuvring phase associated to the same ship were detected in Venice (Contini et al., 2015);

2) 30 min was a suitable period to separate hotelling and manoeuvring phases and to have stable wind direction. Therefore, high resolution measurements allowed to “capture” single peaks associated to different phases (i.e. arrival/departure) and modulated by harbour activities such as hotelling phase.

Further, since that direct contribution of ships was dependent on wind direction, the periods when the site was downwind were firstly selected. The wind direction sector  $292.5^{\circ}$ - $67.5^{\circ}$  (WNW-ENE) for the Brindisi site and  $315^{\circ}$ - $45^{\circ}$  (NW-NE) for Venice were chosen.

Definitively, the approach developed in Contini et al. (2011) for the Venice harbour and then applied in Brindisi (Donateo et al., 2014) was followed, using the formula (Eq. 3.2):



$$\varepsilon_C = \frac{(C_{DP} - C_{DSP})F_P}{C_D} = \frac{\Delta_P F_P}{C_D} \quad (\text{Eq. 3.2})$$

where  $C_{DP}$  is the average concentration in the selected wind direction sector in periods potentially influenced by ship;  $C_{DSP}$  is the average concentration not significantly influenced by ship;  $C_D$  is the average concentration in the specific wind direction sector;  $F_P$  is the fraction of cases influenced by ship emissions.

This approach was followed in Brindisi for the estimation of the contribution from gaseous (only in 2014) and from particle concentrations (both in mass and in number). In Brindisi measurements this contribution was calculated also for size segregated particle mass and number concentration. In Venice this approach was adopted for  $PM_{2.5}$  and PNC.

Since the availability of detailed ship traffic data in Brindisi, the estimation could be separated in two cases: manoeuvring, in which selected periods for estimation were only relative to manoeuvring phase; manoeuvring plus hotelling, in which hotelling periods were included in the calculation of the contributions potentially influenced by ships. The latter was determined in downwind conditions when at least a ship was at berth in one of the docks framed by the video camera. Specific wind directions sectors were associated to the docks:  $292.5^\circ - 0^\circ$ ,  $270^\circ - 345^\circ$  and  $10^\circ - 45^\circ$  in 2014;  $292.5^\circ - 10^\circ$  and  $15^\circ - 60^\circ$  in 2012. When the total (manoeuvring plus hotelling) contribution was computed, vehicular traffic associated to loading and unloading activities, was also included. A threshold of 10 vehicles (car, trucks) in the 30-min interval was fixed to assume a possible influence on the measurements. The uncertainties of the estimated contributions were calculated by looking at the variability of the results for different elaborations with slight changes ( $\pm 10^\circ$ ) in the wind direction sector definition and also eliminating data of wind calm (velocities  $< 0.5$  m/s) or low winds (velocities  $< 1$  m/s).

In addition, for 2014 campaign, it was possible to obtain contribution to PNC considering three size ranges:  $PNC_{<0.25}$  ( $0.009 < D_p < 0.25 \mu\text{m}$ ), as difference between particles counted by the CPC and by the OPC;  $PNC_{1-0.25}$  ( $0.25 < D_p < 1.0 \mu\text{m}$ ) and  $PNC_{>1}$  ( $D_p > 1 \mu\text{m}$ ).

Since that the OPC indirectly calculates mass particle concentrations by means of optical light scattering of particles, a correction is needed to be applied to measurements by a gravimetric factor – the so-called C-factor. This factor depends on the particle density, shape, and refractive index of the particles and can be easily determined by means of the built-in gravimetric filter according to the procedure from the constructor or set using typical values obtained for different dust types also retroactively with the software. However, a default value equal to 1 is used by the instrument in case of unknown C-factor. Finally, all particle mass concentrations calculated will be multiplied for this factor and thus corrected. The general formula used by the OPC (Grimm model 1.109) is (Eq. 3.3):

$$C - factor = \frac{gravimetricdustweightonfilter(loadedfilter - emptyfilter)}{calculateddustweight(shownbyinstrument)} \quad (Eq. 3.3)$$

In this work, the default value (1) for the C-factor was applied and number particle concentrations were used to obtain mass concentrations using instrument-specific factors given by the manufacturer. This was done when the OPC run in mass mode, allowing add a virtual size channel by extrapolation of the size distribution with a nominal lower size cut at 0.225  $\mu\text{m}$ .

The step was to convert particle number concentrations (in #/L) given at different optical geometric sizes (representing the channels) to mass concentrations (in  $\mu\text{g}/\text{m}^3$ ). This was done multiplying count data  $n$  for spherical particle volume, considering geometric diameter ( $d_{geom}$ ) and the particle density  $\rho$  as proportionality constant, following the equation (Eq. 3.4):

$$m = \rho * \frac{n * \pi}{6} * d_{geom}^3 \quad (Eq. 3.4)$$

Since that the OPC provides particle and mass distribution in channels representing geometric particle diameter, to convert optical equivalent size into aerodynamic diameter was necessary. In some cases, for specific test dusts, a calibrated OPC provided a direct read-out dust mass vs. aerodynamic diameter and - by weighting the appropriate size bins with the standard transmission curve - as total  $\text{PM}_{2.5}$  mass (Binnig et al., 2007).

As also explained in Burkart et al. (2010), a conversion factor equal to 1.65 (for OPC 1.109) is suitable (and therefore applied to the measurements), being obtained from

earlier calibration measurements with polystyrene-latex aerosols and include particle density as well as a correction for the complex refractive index of other aerosols.

Practically, optical geometric diameter is considered proportional to aerodynamic diameter ( $d_{aerod}$ ) according to the particle density  $\rho$  (which is the conversion factor) expressed as (Eq. 3.5):

$$d_{aerod} = \rho^{0.5} * d_{geom} \quad (\text{Eq. 3.5})$$

The aerodynamic diameter was substitute in Eq. 3.5 to calculate mass concentrations referred to aerodynamic size.

### 3.3 Emission inventories approach

A reliable and up-to-date ship emission inventory is a fundamental input in assessing maritime emissions and the effectiveness of emission control options.

However, IMO claimed that shipping emissions were significantly under-reported (IMO, 2007) so that improvement of accuracy in estimation is a challenge (Wang et al., 2008).

Even today, significant discrepancies are present among the reported estimates, especially during the last 10 years, because of different approaches used and input data (Fig. 3.1). For example, IMO 2014 report estimated global emissions in good agreement with those reported in Corbett and Koehler (2003), in contrast with values reported in a previous report (IMO, 2007).

There is a still open debate about some important issues: representativeness of bunker statistics, engine operational profiles for different ship classes and size (Corbett and Koehler, 2003; 2004; Endresen et al., 2003; 2004a; Eyring et al., 2005a), comparability between past, present and future levels of emissions, completeness of information on the world fleet traffic (Corbett and Koehler, 2003; Endresen et al., 2003; Dalsøren et al., 2007), allocation of ships or ship voyages between domestic and international shipping (IMO, 2014) and reliability of large scale models estimates (Beirle et al., 2004; Chen et al., 2005; Dalsøren et al., 2007).

The current methodologies available may quantify and spatially allocate shipping emissions by a “fuel-based” or “activity-based” approach.

The first studies used a full top-down approach distributing calculated emissions according to global traffic statistics (Corbett et al., 1999; Endresen et al., 2003) but it was not reliable. On the contrary, a full bottom-up approach estimates emissions from individual ship movements on defined routes (Whall et al., 2002; Endresen et al., 2003; Dalsøren et al., 2007) and aggregates data over the total fleet and time. This approach is more accurate, however, it requires large efforts for data mining. Actually, hybrid systems are generally used. For example, a model could be top-down in the evaluation of total emissions and bottom-up in the geographic characterisation or vice versa. In the former, total emissions are the sum of emissions from individual cells (on the basis of the global activity or route) with some assumptions to assign total emissions to the different ships.

Another model considers total emissions from all ships, then geographically allocated, based on assumptions, i.e. ship activities or single geographic cells. Also, maritime data may be refined by the use of the terrestrial and satellite AIS data (Goldsworthy L. and Goldsworthy B., 2015).

In general, a top-down approach is able to produce multiscale inventories more quickly and to assess regional and global impacts but it is limited by the accuracy of the global emissions totals, which have large uncertainties, whereas the bottom-up approach is not representative for extracted periods (Wang et al., 2007).

A new global model called STEEM (Waterway Network Ship Traffic, Energy and Environment Model) overcomes the weaknesses of both previous approaches, by using an empirical waterway network based on shipping routes travelled for many years (Wang et al., 2008).

Comparative analysis of current methods (Moreno-Gutiérrez et al., 2015; IMO, 2009; Wang et al., 2008) showed that the most uncertainties were associated to engine's load factor and specific fuel oil consumption. An example of differences in estimations of fuel consumption is reported in Fig. 3.2. A realistic model should use not theoretical emission factors (as the majority of the available studies) but it should consider the engine's maintenance condition (i.e. load factor, real consumption, instantaneous speed) (Moreno-Gutiérrez et al., 2015).

Also AIS error should be considered so that the Third IMO GHG Study 2014 (<http://www.imo.org/en/OurWork/Environment/PollutionPrevention/AirPollution/Do>

cuments/Third%20Greenhouse%20Gas%20Study/GHG3%20Executive%20Summary%20and%20Report.pdf) confirmed the importance in improving the AIS coverage from the increased use of satellite and shore-based receivers to maximize the accuracy in bottom-up approach.

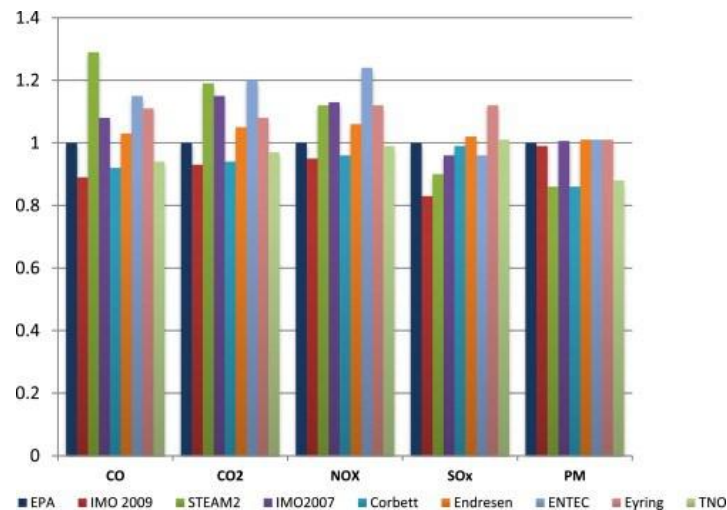


Figure 3.1. Comparison in relative total emissions (main and auxiliary engines). Baseline coefficient from EPA (2000) equal to 1 (source: Moreno-Gutiérrez et al., 2015).

The Third IMO GHG Study 2014 removed any uncertainty attributable to the use of average values, representing a significant improvement in the resolution of shipping activity, fuel consumption and emissions data. According this study, the discrepancy between the bottom-up and top-down approach may be solved through the respective methods' uncertainties and rigorous testing of results quality against noon reports and LRIT (Long-Range Identification and Tracking) data.

Ultimately, a consensus value was assumed as the best estimate for all years' emissions of pollutants.

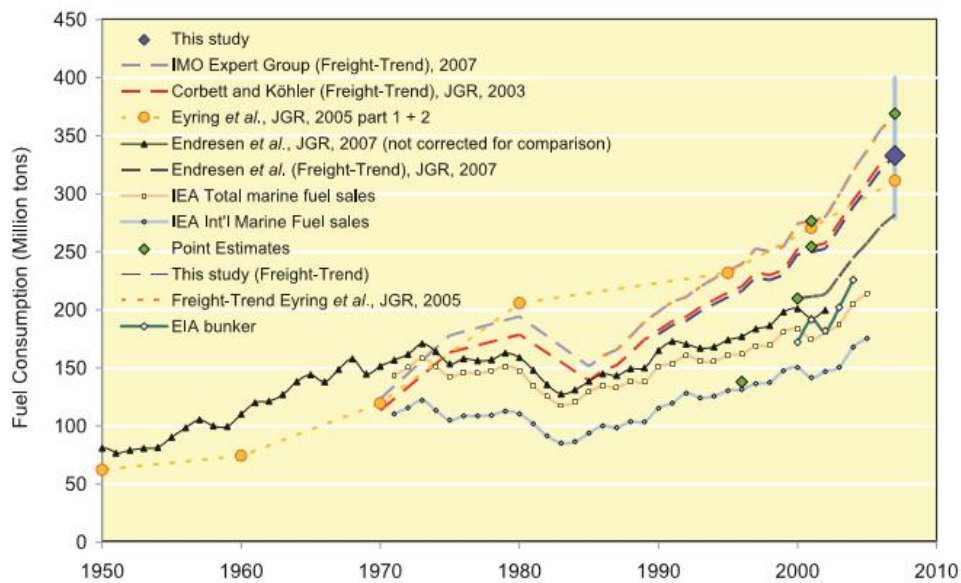


Figure 3.2. Bottom-up and top-down estimates in fuel consumption (source: IMO, 2009).

Starting from the emission inventory, available from the Regional Agency for Environmental Protection of the Apulia region (ARPA Puglia), it was possible to extract estimates of maritime sector (included in SNAP08 in the CORINAIR classification) at municipality level.

The emission inventory was compiled on the basis of the INEMAR (Inventario Regionale delle Emissioni in Atmosfera) database, developed by a consortium of Italian Regions ([www.inemar.eu](http://www.inemar.eu)) led by the Lombardy Region (Caserini et al. 2002; Caserini et al. 2005), which allowed to have a municipality resolution level. Following the CORINAIR methodology (EEA, [www.eea.europa.eu](http://www.eea.europa.eu)), estimates were almost completely computed by a bottom-up approach (i.e. industrial point sources, domestic heating, traffic, airports and harbour traffic), and partially based on activity indicators and emission factors (diffuse sources and activities). Finally, the calculated emissions are grouped and classified by SNAP code (activity typology) and fuel consumption.

Shipping emissions were estimate using the methodology described in the Emission inventory guidebook 2013 (EMEP/EEA, 2013) with shipping activity data obtained from the database of ship movements provided by the local Port Authority, using six ship classes: cargo, passengers and Ro-Ro, fishing boats, tanker, cruise and other.

The traffic data concerned arrival and departure time, ship typology and size (as GT), and dock occupied.

Emissions from manoeuvring and hotelling phases were computed separately, also considering the different regulation limit in sulphur content in fuels. In this perspective, the reference year was 2010 in order to take into account the European legislation regarding the use of low-sulphur content fuel (Directive 2005/33/EC) came in force in 01/01/2010 in Italy.

Specifically, in manoeuvring phase were considered limits in sulphur content fuel equal to 1.5% for all passenger ships (including cruise ships) and to 3.5% for all other ship typologies. For hotelling phase a unique value of 0.1% for all ship typologies was assumed.

The emission factors used (kg/ton) for NO<sub>x</sub>, NMVOC, PM and CO are those proposed in the Emission Inventory Guidebook 2013 for different combinations of engine type (gas and steam turbines, diesel engines at low, medium and high speed) and fuel (Bunker Fuel Oil - BFO, Marine Diesel Oil - MDO, and Marine Gas Oil - MGO). If there was not specification in the database of the engine and the type of fuel used, the statistical distributions of the world fleet in 2010 was followed (EMEP/EEA 2013). Values applied are reported in Tab. 3.2 and 3.3. Emission factors for SO<sub>2</sub> were calculated using the formula (Eq. 3.4):

$$EF = 20 * S \quad (\text{Eq. 3.4})$$

where S represents the percentage of content sulphur by mass in the fuel. A schematic representation of the overall methodology is reported in Fig. 3.3.

In the detailed MEET methodology (Trozzi and Vaccaro, 1998, Chapter 3), ship emissions are obtained as (Eq. 3.5):

$$E_i = \sum_{jklm} E_{ijklm} \quad (\text{Eq. 3.5})$$

With

$$E_{ijklm} = S_{jkm}(GT) * t_{jklm} * F_{ijlm}$$

where

$i$  is pollutant (NO<sub>x</sub>, SO<sub>x</sub>, CO, VOC, PM);

$j$  is fuel (BFO, MDO, MGO, GF);

$k$  is ship class for use in consumption classification (Solid Bulk, Liquid Bulk, General Cargo, Container, Passenger/Ro-Ro/Cargo, Passenger, High speed ferries, Inland Cargo, Sail ships, Tugs, Fishing, Other);

$l$  is engines type class for use in emission factors characterisation (Steam turbines, High speed motor engines, Medium speed motor engines, Slow speed motor engines);

$m$  is operating mode (cruising, manoeuvring, hotelling);

$E_i$  is total emissions of pollutant  $i$ ;

$E_{ijklm}$  is total emissions of pollutant  $i$  from use of fuel  $j$  on ship class  $k$  with engines type  $l$  in mode  $m$ ;

$S_{jkm}(GT)$  is daily consumption of fuel  $j$  in ship class  $k$  in mode  $m$  as a function of gross tonnage (GT), calculated as (Tab. 3.4):

$$S_{jkm} = C_{jk}(GT) * p_{km}$$

where

$C_{jk}(GT)$  is daily consumption at full power of fuel  $j$  in ship class  $k$  as a function of gross tonnage (GT);

$p_{km}$  is fraction of maximum fuel consumption of ships of class  $k$  in mode  $m$  (0.40 for manoeuvring, 0.20 for hotelling and 0.32 for hotelling of passenger ship – Trozzi and Vaccaro, 1998).

$t_{jklm}$  is days operating of ships of class  $k$  with engines type  $l$  using fuel  $j$  in mode  $m$ ;

$F_{ijlm}$  is average emission factors of pollutant  $i$  from fuel  $j$  in engines type  $l$  in mode  $m$ .



Table 3.2. Tier 3 Emission factors for NO<sub>x</sub>, NMVOC, PM for different engine types/fuel combinations and vessel phases (cruising, hotelling, manoeuvring). Sources: ENTEC (2002), ENTEC (2007), IPCC (1997).

Engine	Phase	Engine type	Fuel type	NO <sub>x</sub> EF 2000 (kg/tonne)	NO <sub>x</sub> EF 2005 (kg/tonne)	NO <sub>x</sub> EF 2010 (kg/tonne)	NMVOC EF (kg/tonne)	TSP, PM <sub>10</sub> , PM <sub>2.5</sub> EF (kg/tonne)	
Main	Cruise	Gas turbine	BFO	20.0	19.3	18.6	0.3	0.3	
			MDO/MGO	19.7	19.0	18.3	0.3	0.0	
		High-speed diesel	BFO	59.6	57.7	55.6	0.9	3.8	
			MDO/MGO	59.1	57.1	55.1	1.0	1.5	
		Medium-speed diesel	BFO	65.7	63.4	61.3	2.3	3.8	
			MDO/MGO	65.0	63.1	60.6	2.4	1.5	
		Slow-speed diesel	BFO	92.8	89.7	86.5	3.0	8.7	
			MDO/MGO	91.9	88.6	86.5	3.2	1.6	
		Steam turbine	BFO	6.9	6.6	6.4	0.3	2.6	
			MDO/MGO	6.9	6.6	6.4	0.3	1.0	
		Manoeuvring Hotelling	Gas turbine	BFO	9.2	8.9	8.6	1.5	4.5
				MDO/MGO	9.1	8.8	8.5	1.5	1.6
	High-speed diesel		BFO	43.6	42.3	40.6	2.5	10.3	
			MDO/MGO	43.0	41.7	40.1	2.6	4.0	
	Medium-speed diesel		BFO	47.9	46.2	44.6	6.3	10.3	
			MDO/MGO	47.5	45.7	44.3	6.6	4.0	
Slow-speed diesel	BFO		67.4	65.1	62.9	8.2	11.2		
	MDO/MGO		66.7	64.2	62.1	8.6	4.4		
Steam turbine	BFO		5.1	4.8	4.7	0.9	7.1		
	MDO/MGO		5.0	5.0	4.7	0.9	2.8		
Auxiliary	Cruise Manoeuvring Hotelling	High-speed diesel	BFO	51.1	49.4	47.6	1.7	3.5	
			MDO/MGO	50.2	48.6	46.8	1.8	1.4	
		Medium-speed diesel	BFO	64.8	62.5	60.4	1.7	3.5	
			MDO/MGO	64.1	62.0	59.7	1.8	1.4	

Table 3.3. Statistical distribution of the world fleet in 2010, by ship category and fuel type (source: Trozzi, 2010).

Ship category	SSD MDO/MGO	SSD BFO	MSD MDO/MGO	MSD BFO	HSD MDO/MGO	HSD BFO	GT MDO/MGO	GT BFO	ST MDO/MGO	ST BFO
Liquid bulk ships	0.87	74.08	3.17	20.47	0.52	0.75	0.00	0.14	0.00	0.00
Dry bulk carriers	0.37	91.63	0.63	7.29	0.06	0.02	0.00	0.00	0.00	0.00
Container	1.23	92.98	0.11	5.56	0.03	0.09	0.00	0.00	0.00	0.00
General cargo	0.36	44.59	8.48	41.71	4.30	0.45	0.00	0.10	0.00	0.00
Ro Ro cargo	0.17	20.09	9.86	59.82	5.57	2.23	2.27	0.00	0.00	0.00
Passenger	0.00	3.81	5.68	76.98	3.68	1.76	4.79	3.29	0.00	0.02
Fishing	0.00	0.00	84.42	3.82	11.76	0.00	0.00	0.00	0.00	0.00
Others	0.48	30.14	29.54	19.63	16.67	2.96	0.38	0.20	0.00	0.00
Tugs	0.00	0.00	39.99	6.14	52.80	0.78	0.28	0.00	0.00	0.00

SSD – Slow Speed Diesel, MSD – Medium Speed Diesel, HSD – High Speed Diesel, GT – Gas Turbine, ST – Steam Turbine; MDO – Marine Diesel Oil, MGO – Marine Gas Oil, BFO – Bunker Fuel Oil

Table 3.4. Daily consumption as function of GT (source: Trozzi and Vaccaro, 1998).

Ship types	Average consumption (t/day)	Consumption at full power (t/day) as function of gross tonnage (GT)
Solid bulk	33.80	$C_{jk} = 20.186 + 0.00049 * GT$
Liquid bulk	41.15	$C_{jk} = 14.685 + 0.00079 * GT$
General cargo	21.27	$C_{jk} = 9.8197 + 0.00143 * GT$
Container	65.88	$C_{jk} = 8.0552 + 0.00235 * GT$
Passenger/Ro-Ro/Cargo	32.28	$C_{jk} = 12.834 + 0.00156 * GT$
Passenger	70.23	$C_{jk} = 16.904 + 0.00198 * GT$
High speed ferry	80.42	$C_{jk} = 39.483 + 0.00972 * GT$
Inland cargo	21.27	$C_{jk} = 9.8197 + 0.00143 * GT$
Sail ships	3.38	$C_{jk} = 0.4268 + 0.00100 * GT$
Tugs	14.35	$C_{jk} = 5.6511 + 0.01048 * GT$
Fishing	5.51	$C_{jk} = 1.9387 + 0.00448 * GT$
Other ships	26.40	$C_{jk} = 9.7126 + 0.00091 * GT$
All ships	32.78	$C_{jk} = 16.263 + 0.00100 * GT$

Uncertainties are generally related to emission factors, ship traffic data, engine and fuel characteristics. According to different pollutants, uncertainties may range from 20% to 50% (Cooper and Gustaffson, 2004; ENTEC, 2002). However, a reasonable uncertainty value could be assumed as done in Broome et al. (2016) to balance over- and underestimation.

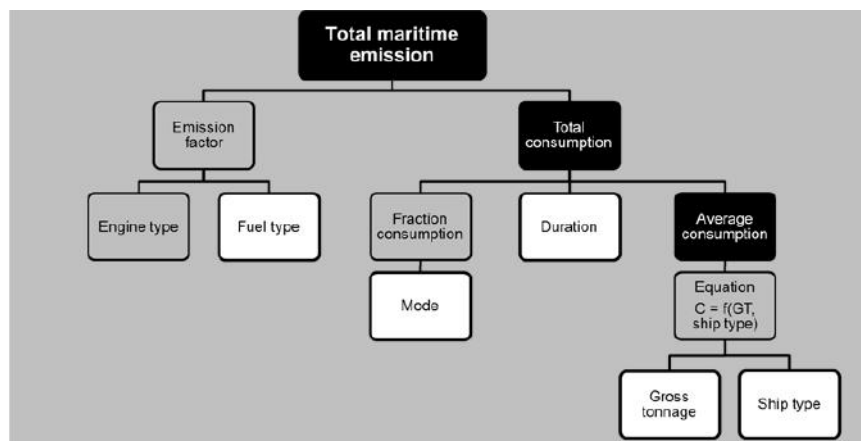


Figure 3.3. Flow diagram of the approach used.

The emission inventory for passenger ships in Venice was built by the Regional Agency for Environmental Protection of the Veneto region (ARPAV) within the project APICE in 2013. Maritime emissions were extrapolated from the total emissions at municipality level obtained from the INEMAR database of ARPAV (Osservatorio Regionale Aria, Regione Veneto - Dipartimento Ambiente, Sezione Tutela Ambiente, Settore Tutela Atmosfera).

The methodology applied was detailed in the EMEP/CORINAIR emission inventory guidebook (EMEP/EEA, 2006, 2009), developed within the MEET project (Trozzi and Vaccaro, 1998) as described previously for Brindisi. In absence of the information about fuel and engine type, the necessary emission factors without the dependency on fuel were found in the study conducted by Entec UK Ltd on behalf of the European Commission: “Quantification of emissions from ships associated with ship movements between ports in the European Community” (EC, 2002).

Emissions from ships were calculated over a domain of 100x100 km<sup>2</sup> in three phases: cruise, manoeuvring and hotelling. However, for comparison purposes with Brindisi, only manoeuvring and hotelling operational modes were considered.

### 3.4 Modelling approach

Although global and continental scale modelling studies (Eyring et al., 2007; Dalsøren et al., 2009) established the importance of ship emissions, few studies are conducted on smaller scales using high-resolution models and considering the non-linear chemical effects concerning NO<sub>x</sub> and O<sub>3</sub> evolution during ship plume

dispersion (Huszar et al., 2010). Modelling is particularly used in atmospheric deposition of pollutants released and for future scenarios (i.e. to evaluate the effectiveness of mitigation measures or regulations).

Within the framework of the POSEIDON project, a modelling approach was followed to assess the impact of maritime on the air quality of the Central and Eastern Mediterranean (Merico et al., 2017). Numerical simulations were performed by the University of Patras and University of Thessaloniki.

In addition, simulation cells (6 x 6 km) that better represented each port-city were extracted for the summer and winter periods, to highlight eventual seasonal patterns in shipping emissions of different pollutants analysed.

The modelling system used integrated the Weather Research and Forecast - Advanced Research Weather model (WRF version 3.5.1) and the photochemical Comprehensive Air Quality Model with Extensions (CAM<sub>x</sub> version 5.3). The WRF and CAM<sub>x</sub> models were employed over two modelling domains (CAM<sub>x</sub> nested in WRF domain) covering the Central and Eastern Mediterranean area (Fig. 3.4).

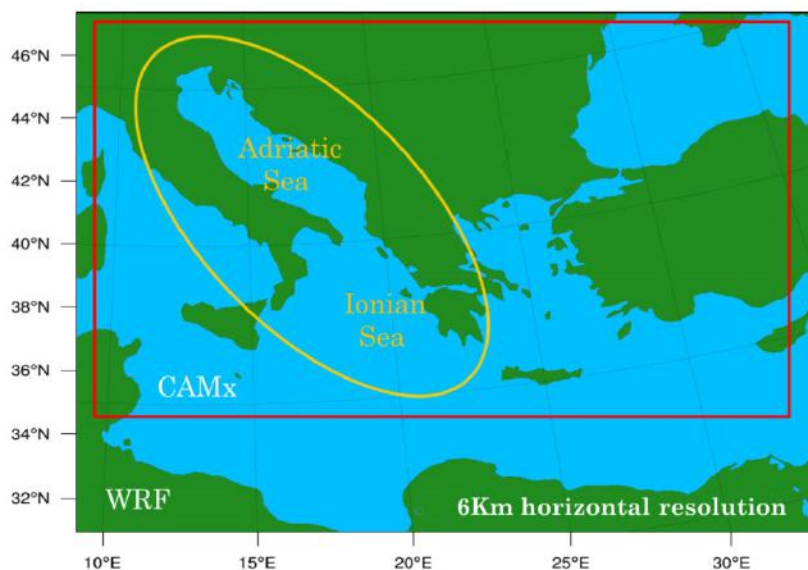


Figure 3.4. The WRF and CAM<sub>x</sub> modelling domains.

The numerical model WRF is a next-generation Numerical Weather Prediction modelling system developed to serve both operational forecasting and atmospheric research needs. The model's dynamics solver integrates the compressible non-hydrostatic Euler equations (Ooyama, 1990), which are formulated on the Arakawa C grid using a terrain following mass vertical coordinate system (Laprise, 1992). The

model develops initial and boundary conditions based on the re-analysis forecast of ECMWF in 0.125° spatial resolution. The projection is the Lambert Conformal, and model runs were performed in 6 km spatial resolution over the defined domain. A detailed description of the model can be found elsewhere (Skamarock et al., 2008).

The Eulerian photochemical dispersion model CAM<sub>x</sub> unifies into a single system several features required by other air quality models. Practically, it simulates emission, dispersion, chemical reactions and removal of pollutants in the troposphere, by solving the pollutant continuity equation for each chemical species on a system of three-dimensional grid(s) (ENVIRON, 2010). CAM<sub>x</sub> was applied over a domain of 367x227 grid cells of 6 km spatial resolution with 17 vertical layers in total extending up to about 10 km above ground level. The CAM<sub>x</sub> gaseous and PM chemical boundary conditions were derived from results of the IFS-MOZART global modelling system produced in the framework of the EU FP7 project Monitoring Atmospheric Composition and Climate Interim Implementation (MACC II) (Morcrette et al., 2009).

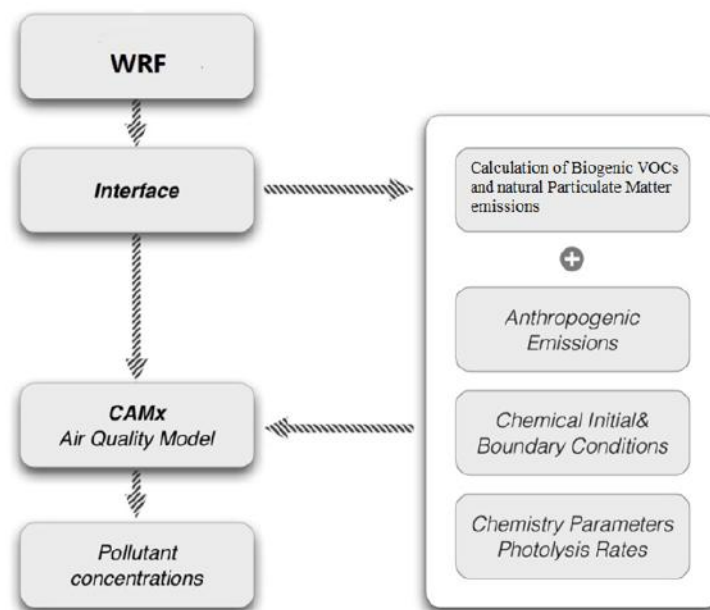


Figure 3.5. The WRF-CAM<sub>x</sub> modelling system flow chart.

The Natural Emission Model (NEMO), developed by the Laboratory of Atmospheric Physics of the Department of Physics of the Aristotle University of Thessaloniki, was used in order to estimate spatially (6 km) and temporally (hourly) resolved, biogenic

NMVOCs, sea salt and wind-blown dust emissions driven by the WRF meteorology (Liora et al., 2014; 2013; Poupkou et al., 2010; Markakis et al., 2009).

The anthropogenic emissions (CO, NO<sub>x</sub>, SO<sub>2</sub>, NH<sub>3</sub>, NMVOCs, PM<sub>10</sub> and PM<sub>2.5</sub>) were extracted from the European scale database prepared by The Netherlands Organization (TNO) for the reference year 2009 in the framework of MACC II (Kuenen et al., 2014). Emission data, available on annual basis and 1/8°x1/16° spatial resolution, were spatially allocated (in 6 km resolution), temporally analysed (hourly values) and chemically speciated using the MOSESS anthropogenic emission model (Markakis et al., 2013).

Following, the overall scheme of the modelling approach applied (Fig. 3.5) and the parametrizations (Tab. 3.5) are presented.

Table 3.5. Parametrization schemes applied in the WRF-CAM<sub>x</sub> modelling system.

Model	Data/process	Parametrization/source	Reference
WRF	Microphysics processes	New Thompson et al. scheme	Thompson et al., 2008
	Convention	Grell-Devenyi ensemble scheme	Grell and Devenyi, 2002
	Shortwave/longwave radiation	RRTMG shortwave/longwave scheme	Iacono et al., 2008
	Surface layer	Eta similarity scheme	Janjic, 2002
	Planetary boundary layer	Mellor-Yamada-Janjic scheme	Janjic, 1994
	Land surface processes	Noah Land Surface Model	Tewari et al., 2004
CAM <sub>x</sub>	Gaseous and PM chemical boundary conditions	Results of the IFS-MOZART global modelling	Morcrette et al., 2009
	Gas-phase chemical mechanism	Carbon Bond 2015 version (CB05)	Yarwood et al., 2005
	Aerosol size distribution	Static two-mode coarse/fine scheme	-
	Aerosol aqueous inorganic chemistry	RADM-AQ aqueous chemistry algorithm	Chang et al., 1987

	Gas/aerosol phase partitioning of the inorganic aerosol constituents	ISORROPIA thermodynamic module	Nenes et al., 1998
	Secondary organic aerosol formation	SOAP scheme	Strader et al., 1999

The relative impact of shipping on air quality in the study domain was computed by using the approach called “zero-out method”. It was based on the concentration differences between two scenarios computed for winter (January 2012) and summer (July 2012) periods. In the first scenario, the natural and all anthropogenic emission sources data were included, while in the second scenario the shipping pollutant emissions were excluded. The hourly CAM<sub>x</sub> data (surface concentrations) were averaged for each time period and emission scenario and the contribution of shipping emissions calculated as follows (Eq. 3.6):

$$\delta(\%) = \frac{Conc_{with} - Conc_{no}}{Conc_{with}} * 100 \quad (\text{Eq. 3.6})$$

where Conc<sub>with</sub> and Conc<sub>no</sub> the averaged surface concentrations with and without shipping emissions respectively.

### 3.5 Remote sensing approach

The use of remote sensing techniques has been proposed for several years by many authors (Giovanelli et al., 1979; Mc Gonigle et al., 1985; Bobrowski et al., 2003; Ibrahim et al., 2010), also adapting on-road use instruments for measuring non road sources such as ocean-going vessels (Burgard et al., 2016). In general terms, the advantage of this approach is that all the transiting ships can be monitored with the same instrument, avoiding the problem of possible offsets if single in-situ instruments were installed on board each ship. In addition, measurements can be performed at different distances from the target ship, also taking into account the background concentrations of the harbour.

The FRE-DOAS (Flow Rate Emission with Differential Optical Absorption Spectroscopy) methodology used is a particular application of the Off-axis technique

(Honninger et al., 2004), devoted to the calculation of the flow rate emitted by a point source. Starting from a set of spectral measurements taken by a Multi axis DOAS remote sensing system, the methodology has been generally used to evaluate gaseous pollutant flow rates from moving sources such as ships when passing along canals, navigable rivers, or at the entrance of the harbours.

Remote sensing measurements of gaseous columnar concentrations of NO<sub>2</sub> and SO<sub>2</sub> were available for the Brindisi site in 2012 and 2014. A presentation of results obtained within the CESAPO and POSEIDON projects is reported in Chapter 4 (Section 4.4) as well as an inter-annual comparison with emission inventories estimates.

The instrumental apparatus used was placed on the roof of the Mobile Laboratory (see Section 2.4.2). Previously, the same approach was used during different field measurement campaigns at the Giudecca channel (tourist harbour of Venice). Results obtained in Brindisi were compared with those obtained in the two campaigns carried out (2012-2014). Furthermore, a comparison with the emission inventory estimates of NO<sub>2</sub> and SO<sub>2</sub> in the same periods was possible.

Since that measurements can be performed only in diurnal hours (in good light conditions and with low clouds), excluding also the first light hour after sunrise and the last before sunset, it must be considered that in that intervals the multiple scattering can influence the quality of measurements of slanted diffuse solar radiation, especially along the trajectories of measurement near the horizon (Premuda, 2012).

The system SODCAL, combined with the spectrometer TropoGAS, performs a set of oblique measurements of diffuse solar radiation at different zenithal angles along same vertical plane, which cuts ideally almost orthogonally the plume size of the ship. The scan starts at an elevation angle (zenith position - 90°) of 45°, continuing down in intervals of 5° increasing the number of positions, next to the horizon. To calculate the optical thicknesses two spectral ranges are generally used: the first (308-328 nm) for the optical thickness of SO<sub>2</sub> and O<sub>3</sub> and the second (436-460 nm) for the optical thickness of NO<sub>2</sub> (Fig. 3.6).

The whole measurement procedure is schematically summarized as follows (Premuda et al., 2011; Masieri et al., 2009):



- the instrument automatically performs vertical scans in sequence for the same azimuth value (in this case the azimuth values were three: one for each of the three measurement planes at 40°N, 240°N and 270°N executed alternately) and for the entire daily period of detection;
- for each  $j^{\text{th}}$  vertical section the value of the emission flow (expressed in g/s) of the test gas is defined by the formula (Eq. 3.7), deduced from the theory for measurements of the same kind with regard to the smokestacks of central ground:

$$F_{j,d} = \sum_i (CL)_{i,j} \cdot \Delta z_i \cdot \bar{u}_j \cdot \sin \beta \cdot \cos \vartheta_i \quad (\text{Eq. 3.7})$$

where:

$F_{j,d}$  is the emission flow of the test gas through the  $j^{\text{th}}$  ( $j = 1, 2, \dots, V$ ) vertical section of the  $d^{\text{th}}$  ( $d = 1, 2, \dots, C$ ) day ( $V$  and  $C$  are respectively the number of vertical sections made in the day  $d$ , and the number of measurements days of the entire campaign);

$(CL)_{i,j}$  is the value of  $i^{\text{th}}$  optical thickness of the test gas on the  $j^{\text{th}}$  vertical section, with  $i = 1, 2, \dots, M$  ( $M$  is the number of measurements taken in each vertical section);

$\Delta z_i$  is the vertical increase between the  $i^{\text{th}}$  and the  $(i-1)^{\text{th}}$  measurement calculated according to the distance between the ship and the observation point and accounting also for the different angular values between and ;

$\bar{u}_j$  is the vectorial composition of the average wind speed in the  $j^{\text{th}}$  vertical section (derived from data of the small anemometer placed on the roof of the container) and the speed of the ship, assessed by means of the images of the video camera;

$\beta$  is the azimuth angle of the vertical plane of measurement (its value was chosen to be the basis of the measurement plane almost perpendicular to the direction of the ships berthed in port or in transit);

$\vartheta_i$  is the  $i^{\text{th}}$  zenith angle.

Considering the vertical section that precedes the passage of the ship concerned (for example, the  $r^{\text{th}}$  vessel) and the vertical section after the passage of the same ship, indicated with  $(j-1)$  and  $j$ , the value (i.e. the amount of gas emitted in 'unit of time' expressed in g/s from the chimney of the ship) can be calculated by subtracting the value  $F_{j,d}$  from the value of  $F_{j-1,d}$ , considering the latter as the background concentration for the measurement of the flow released from the ship (Eq. 3.8):

$$\mathfrak{S}_{r,d} = F_{j,d} - F_{j-1,d} = \sum_i (CL)_{i,j} \cdot \Delta z_i \cdot \bar{u}_j \cdot \sin \beta \cdot \cos \vartheta_i - \sum_i (CL)_{i,(j-1)} \cdot \Delta z_i \cdot \bar{u}_{(j-1)} \cdot \sin \beta \cdot \cos \vartheta_i \quad (\text{Eq. 3.8})$$

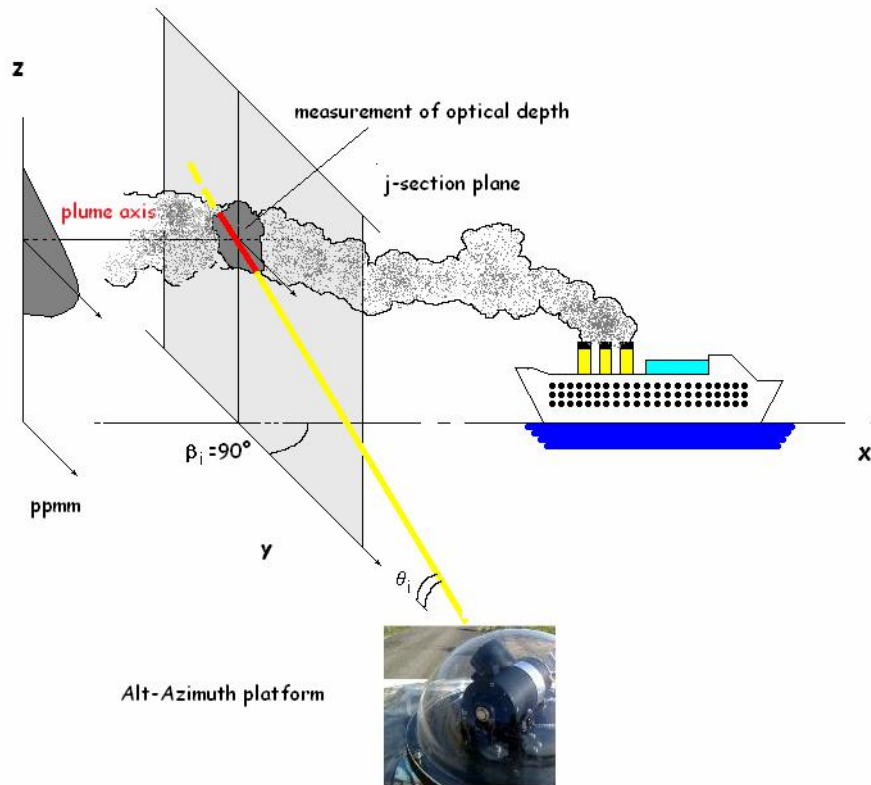


Figure 3.6. Schematic representation of ship plume measurement performed with TropoGAS and SODCAL system.

Applying a method generally used for sources moving along the channels or at the entrance of ports, it was also possible to evaluate flow rate emissions during hotelling time of ferries.

To calculate the mass (in grams) of the gas released from the  $r^{\text{th}}$  ship, during its period of operation for docking or departure as (Eq. 3.9):

$$Q_{r,d} = \mathfrak{V}_{r,d} \cdot \delta t_r \text{ (Eq. 3.9)}$$

where

$\delta t_r$  is the time employed by the  $r^{\text{th}}$  ships for the docking or leaving.

In order to have a daily measure of the gaseous emissions, the approach was then modified assuming that ships stationed in the harbour and moored overnight. In this case, the flow rate values obtained during the diurnal hours were extended for night periods. This estimation was based on the great regularity of the ferries observing the arrival and departure schedule (confirmed by the video camera frames), and by their similar size/tonnage.

The errors associated with the mass amount of gas released from the ships in motion or berthed in the harbour are calculated using the general formula of error propagation for independent measures, obtaining values the order of 30% for SO<sub>2</sub> and 20% for NO<sub>2</sub>.

## 4.1 Results in Brindisi

In the following sections the impact of shipping on measured pollutants concentrations was reported distinguishing two operational modes (manoeuvring and hotelling phases). Micrometeorological data were used to individuate correlation between measurements at different temporal resolution and wind characteristics. Finally, high temporal measurements of SO<sub>2</sub> were useful to estimate plume age.

### 4.1.1 Meteorological conditions

The local meteorology in Brindisi has not specific breeze patterns because a clear daily cycle of wind direction is not present, although relatively extended periods with wind coming from the NW-NE sector or from the S-SW sector are recorded. Episodes of strong winds blowing from the Adriatic Sea (NW-NE directions) can also occur.

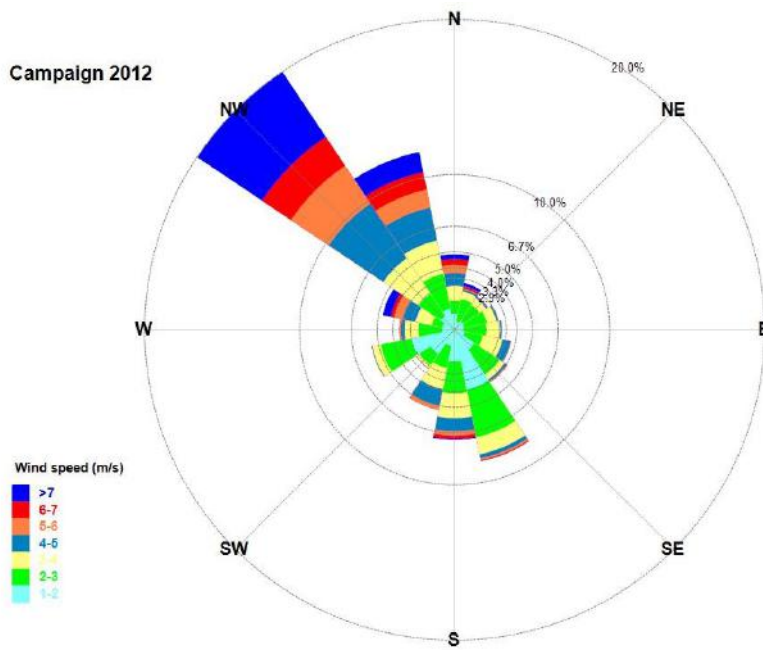
During the campaigns (in summer 2012 and in summer 2014), the meteorological conditions, specifically wind velocity and direction, temperature and relative humidity (RH) were provided by the micrometeorological station located inside the harbour area (see Section 2.2) at 10 m height on 30-min averages. All measurements at the Terminal Passeggeri were done in reasonably similar meteorological conditions (Tab. 4.1), being taken in the same season and in the same site. In this way, micrometeorological differences between 2012 and 2014 campaigns were minimized and, consequently, the comparison of the results was consistent.

However, in 2014 a decrease (2°C) in temperature and an increase (5%) in RH were observed. In addition, the prevalent wind direction was slightly changed from NW to NNW from 2012 to 2014 (Fig. 4.1). Further, in 2012 stronger winds with a more well-defined direction, corresponding to the prevalent one, were detected. For example, more than 15% of cases with wind speed greater than 7 m/s from the prevalent direction (NW) were observed in 2012.

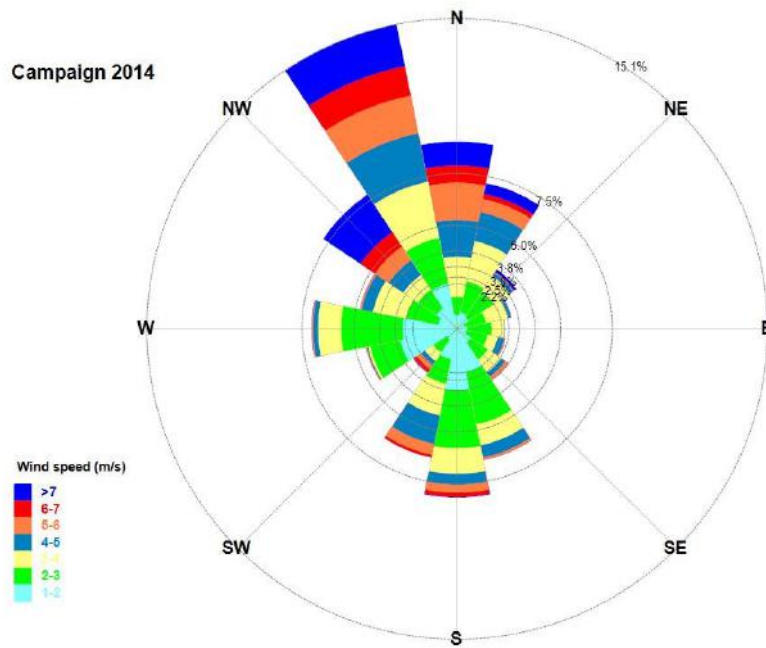
Table 4.1. Main meteorological conditions in the 2012 and 2014 campaigns in Brindisi (in parenthesis the standard deviation is reported).

	<b>2012</b>	<b>2014</b>
Prevalent wind direction (°)	315	337.5
Downwind of ship releases occurrences (%)	47.8	48.4

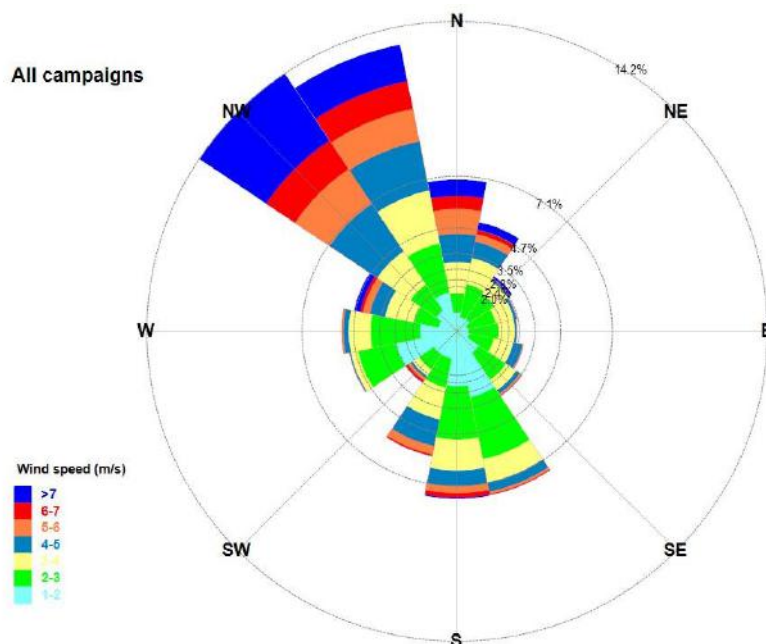
Wind calms (%) (occurrences with wind velocity lower than 0.5 m/s)	0.9	1.6
Mean wind velocity (m/s)	3.4 (2.1)	3.3 (1.9)
Mean temperature (°C)	25.6 (4.0)	23.6 (3.4)
RH (%)	68.0 (14.2)	72.8 (13.4)



(a)



(b)



(c)

Figure 4.1. Wind roses for summer campaigns in a) 2012; b) 2014 and both campaigns together (c) in Brindisi.

In order to identify the direct contribution of ship exhausts to concentrations, wind directions were selected putting the site downwind from WNW-ENE ( $292.5^{\circ}$ - $67.5^{\circ}$ )

(Fig. 4.2). These cases represented 47.8% and 48.4% of the total in 2012 and 2014, respectively. Relatively scarce wind calm (wind lower than 0.5 m/s) periods were present both in 2012 (0.9%) and in 2014 (1.6%): These periods were removed from the successive analysis.



Figure 4.2. Wind direction sector selected for the contribution analysis.

#### 4.1.2 Gaseous and particulate matter concentration

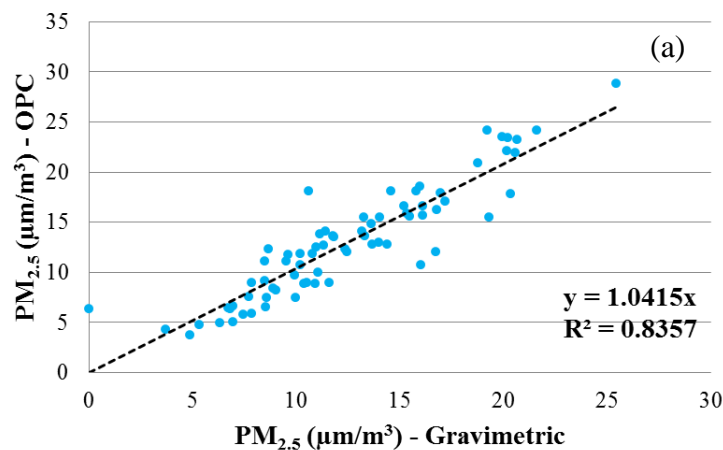
Measurements in the Brindisi site were taken at different temporal resolution, according to the specific instrument used (see Section 2.4.1). However, post-processing of the acquired data was based on 30-min averages to have a reasonably homogeneity and comparability between the datasets in the two campaigns (2012 and 2014). As previously described in Section 2.2, gaseous measurements were added in 2014, therefore only a comparison for  $PM_{2.5}$  and PNC concentrations has been possible.

The average daily concentrations were comparable between 2012 and 2014 (Tab. 4.2), however, a decrease (9.3%) in PNC and in  $PM_{2.5}$  concentrations (pDR determination) (19.8%) were observed in the last campaign. This could be due to several factors, such as different micrometeorological conditions (i.e. more frequent wind calms) or related to ships and harbour activities (i.e. volume of ship and vehicular traffic, fuel and ship type).

Table 4.2. Average concentrations measured in 2012 and 2014 (in parenthesis the standard deviation is reported).

	2012	2014
<b>PM<sub>1</sub> (µm/m<sup>3</sup>)</b>	n.a.	11.0 (6.7)
<b>PM<sub>2.5</sub> (µm/m<sup>3</sup>)</b>	16.7 (10.6)	13.4 (9.6)
<b>PNC (#/cm<sup>3</sup>)</b>	14,467 (22,316)	13,123 (22,738)
<b>NO (µm/m<sup>3</sup>)</b>	n.a.	11.5 (28.3)
<b>NO<sub>2</sub> (µm/m<sup>3</sup>)</b>	n.a.	18.9 (20.9)
<b>O<sub>3</sub> (µm/m<sup>3</sup>)</b>	n.a.	76.7 (26.3)
<b>SO<sub>2</sub> (µm/m<sup>3</sup>)</b>	n.a.	3.1 (9.4)

PM<sub>2.5</sub> concentrations determined by using the OPC (in 2014) were compared with those obtained from gravimetric determination (Fig. 4.3a) and the nephelometer pDR (Fig. 4.3b). The gravimetric results were compared to the pDR concentrations (Fig. 4.3c). The correlation coefficient  $R^2$  is reported in the figures, showing a good agreement among all measurements, with higher correlation values between the OPC and gravimetric data ( $R^2 = 0.85$ ) and the OPC and pDR data ( $R^2 = 0.77$ ).





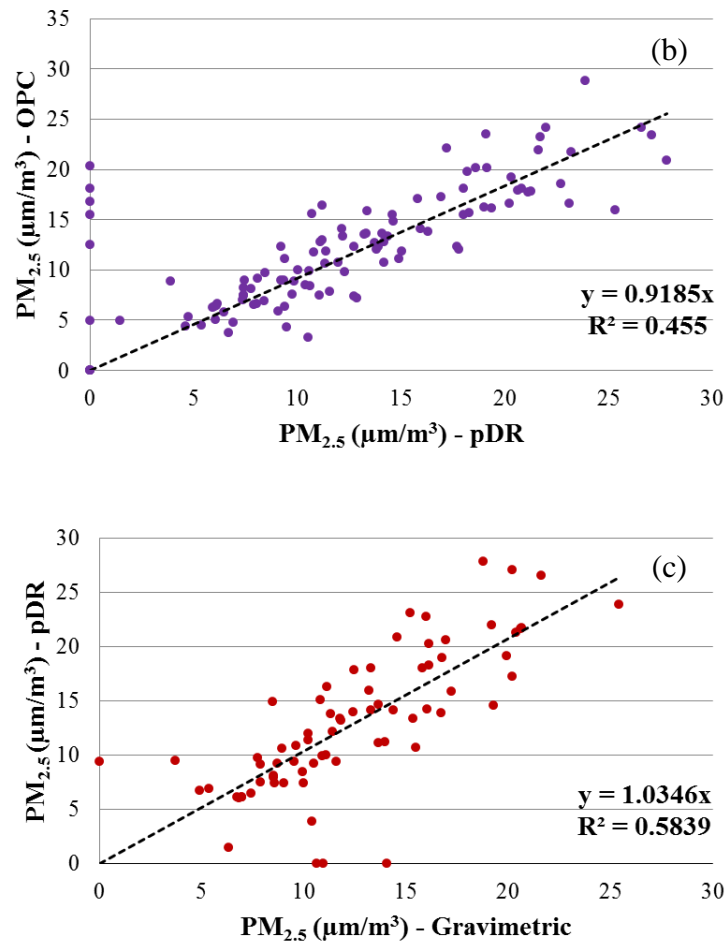


Figure 4.3. Correlation between daily concentrations obtained from a) OPC, b) pDR and c) gravimetric analysis.

Daily  $PM_{10}$  concentrations (data provided by ARPA Puglia – [www.arpa.puglia.it](http://www.arpa.puglia.it) – for the same sampling period) and measured  $PM_{2.5}$ , PNC concentrations at the Terminal Passeggeri showed no correlation with daily ship traffic (as cumulative Gross Tonnage) recorded in 2012 (Donateo et al., 2014). This revealed that shipping contribution may not be identified simply using long-term averages.

Looking at high resolution measurements, it was clear a plume-like behaviour described by short and intense peaks modulated by harbour activities (arrival/departure phases). This outcome was more accentuated if the specific downwind direction was selected, highlighting the effect of the local meteorology on measurements. It is clear that high wind velocity promotes a quick transport and dispersal of plume emitted by ships reducing local concentrations.

Arrival and departure phases were clear either on PNC and  $PM_{2.5}$  in 2012 and

especially on SO<sub>2</sub> concentrations in 2014. After ship arrival at berth an unloading activity by cars and trucks follows and this contribution was visible with lower concentrations (for 30-40 min) but more accentuated on PNC. The same effect could be seen before ship departure with loading activities. Even though concentrations associated to hotelling phase were lower with respect to manoeuvring mode, they were more extended in time (from 3 to 6 hours). Regarding high resolution measurements of gaseous pollutants concentration (Fig. 4.5), it was shown that ship movements in the harbour substantially contributed to SO<sub>2</sub> concentrations at arrival and departure of ships. Instead, hotelling phase has only a limited contribution on SO<sub>2</sub> since that low-sulphur content fuel is mandatory at berth.

On the other hand, peaks of nitrogen oxides were visible either in manoeuvring phase (arrival/departure) and hotelling phase. Loading/unloading of ships can produce higher nitrogen oxides concentrations due to vehicular emissions, in addition to those associated to plume released by ships.

The concentration peaks were more evident on NO with respect to NO<sub>2</sub> and this provokes a depletion of O<sub>3</sub> (see Section 4.1.4) that is evident for both the hotelling and the manoeuvring phases. Further, the contribution on PNC was firstly investigated considering three size ranges: PNC<sub><0.25</sub> (0.009 < D<sub>p</sub> < 0.25 μm), PNC<sub>1-0.25</sub> (0.25 < D<sub>p</sub> < 1 μm), PNC<sub>>1</sub> (D<sub>p</sub> > 1 μm).

The first range, obtained as the difference between particles counted by the CPC and the OPC (see Section 3.1), was the majority (on average, 99%) of particles in number but only 11.7% of the total mass concentration. On the other hand, PNC<sub>1-0.25</sub> and PNC<sub>>1</sub> contributed significantly to PM<sub>2.5</sub> and PM<sub>10</sub> mass concentrations that are included in European air quality standards (2008/50/EC).

Investigating the impact of the different phases, the three size ranges showed some significant differences. In detail, the first range was affected by both phases. Moreover, PNC<sub><0.25</sub> were well-correlated with NO and NO<sub>2</sub> trends, demonstrating a clear dependency on vehicular traffic (during loading/unloading phases) and ship manoeuvring.

PNC<sub>1-0.25</sub> showed a trend much more similar to SO<sub>2</sub> with evident peaks due to manoeuvring phases but limited changes during hotelling. Oppositely, larger particles (PNC<sub>>1</sub>) increased during hotelling, being almost unchanged during

manoeuvring.

Definitively, the results of different size ranges of PNC suggested that particles primary emissions have a strong dependency on size and operational phase. This is likely due to the differences in the emissions of auxiliary and main engines, to the different engine loads and to the use of low-sulphur content fuel mandatory during hotelling in European harbours.

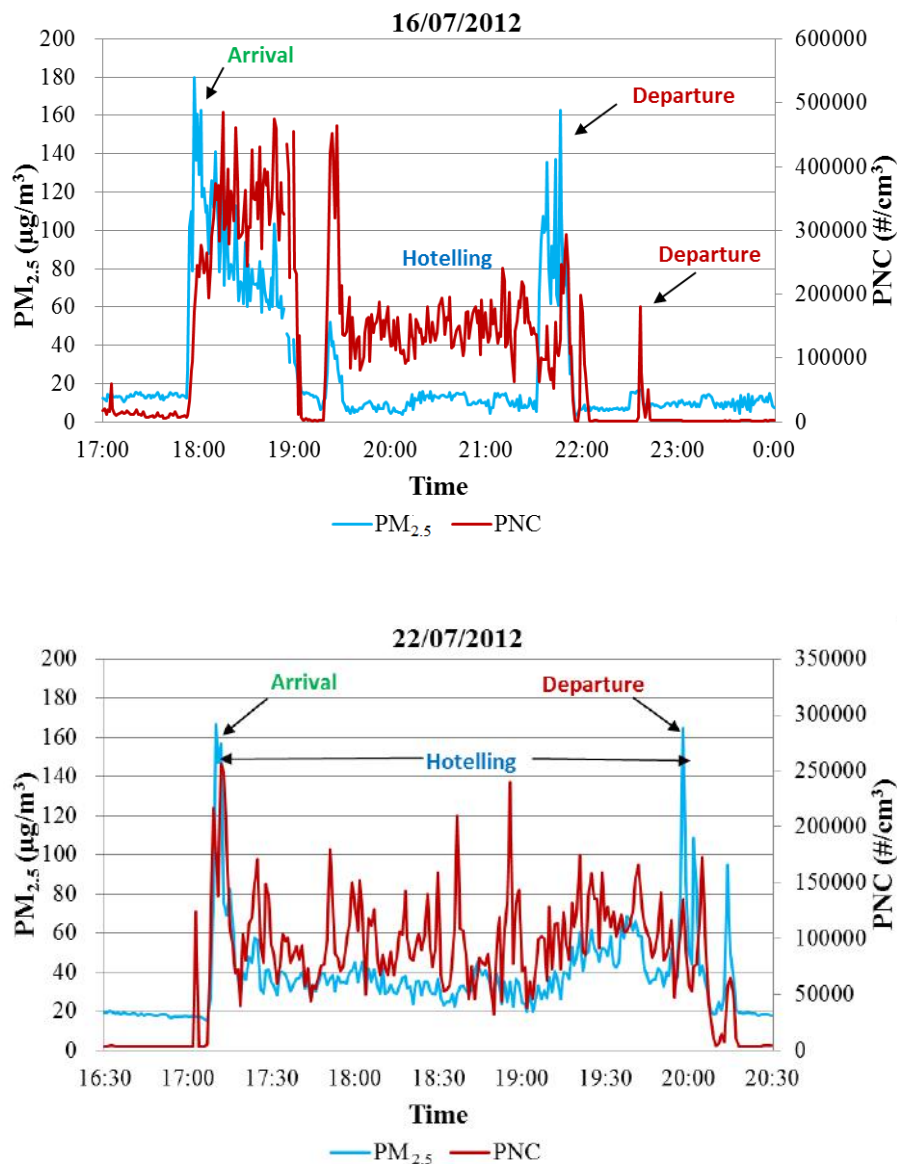
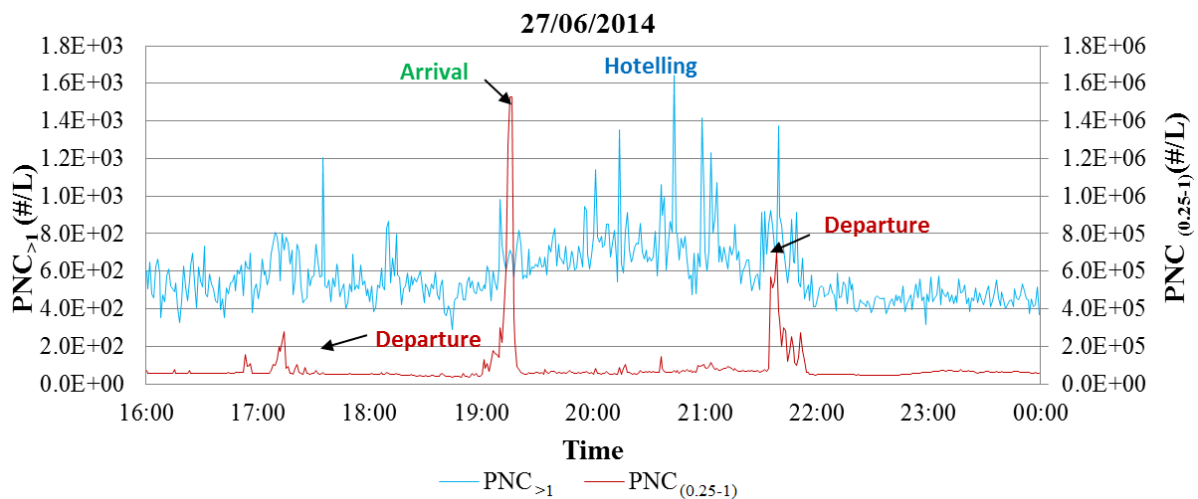
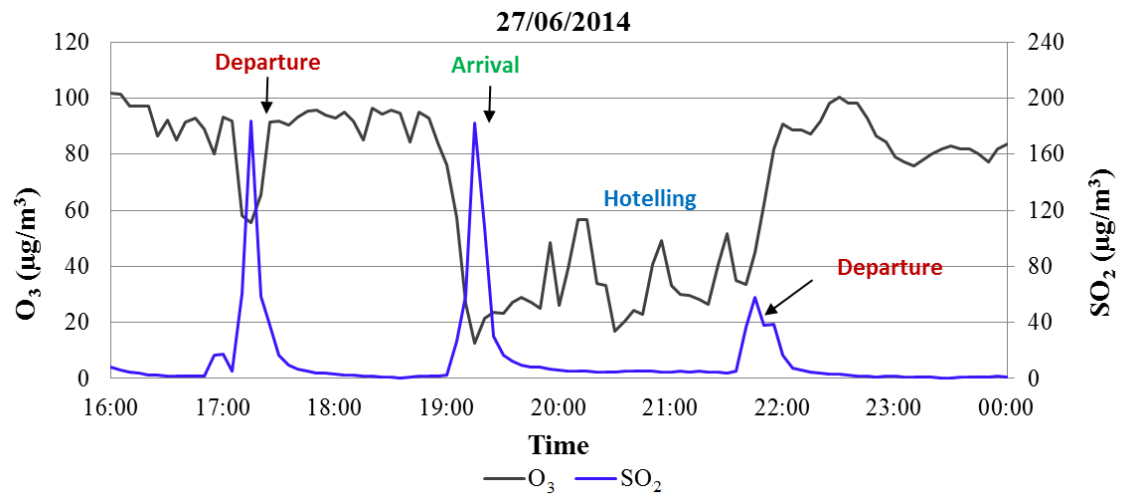
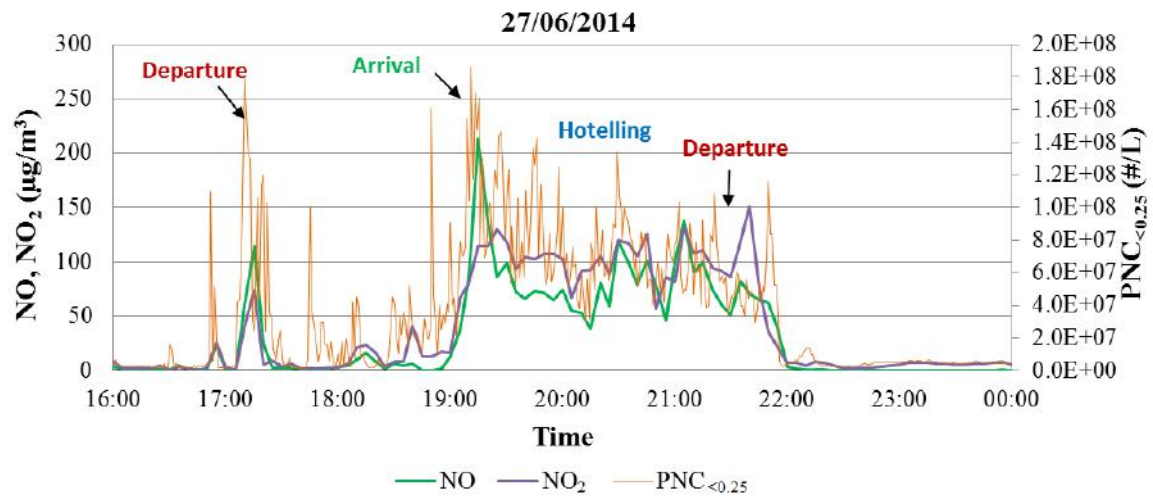
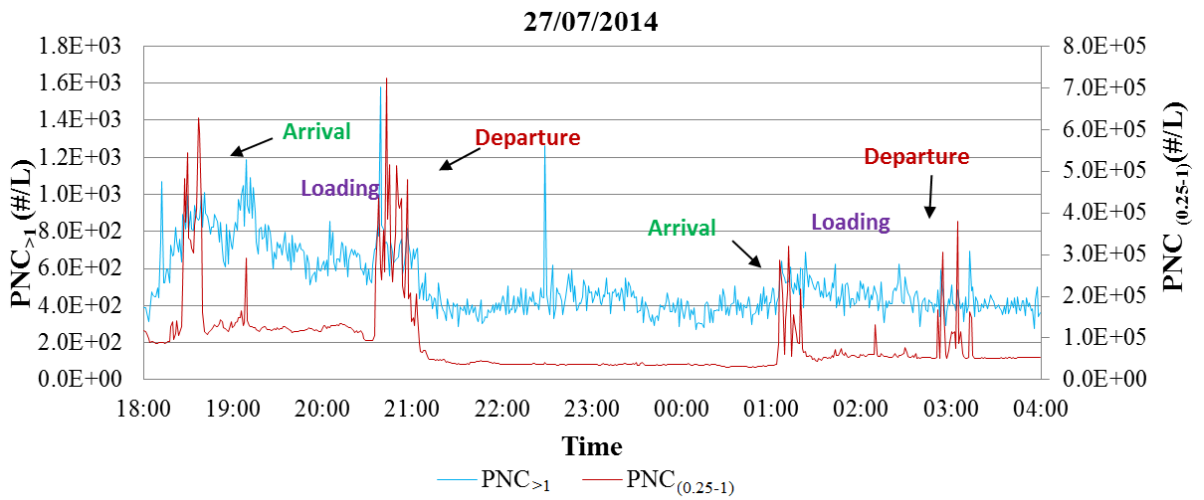
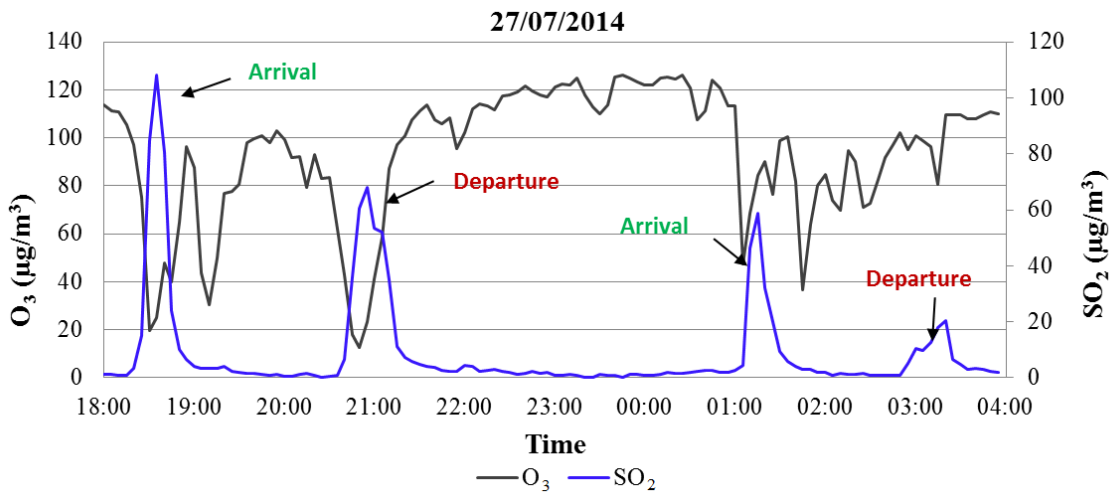
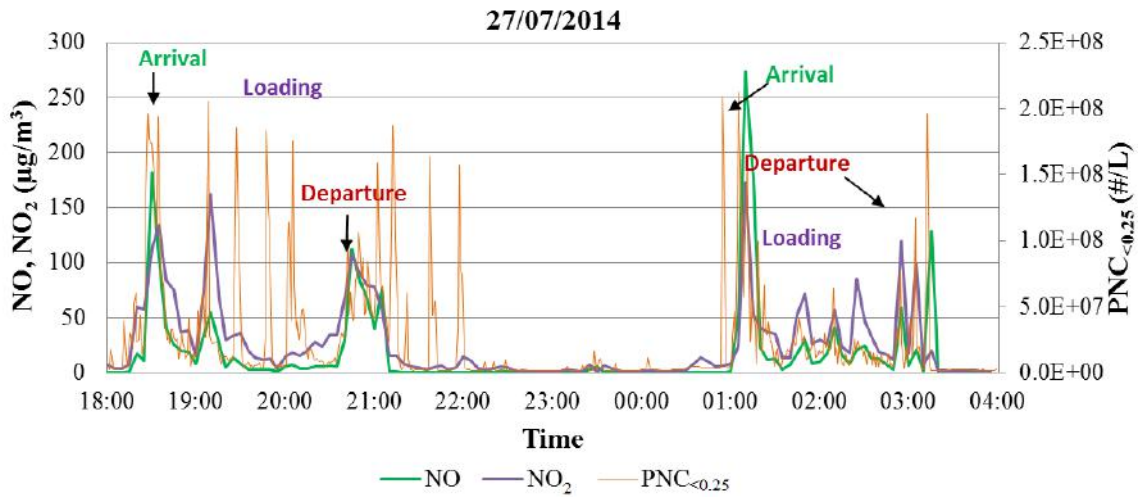


Figure 4.4. Examples of concentration peaks of PNC and PM<sub>2.5</sub> (1-min resolution) associated to arrival/departure of ships and loading/unloading activities in 2012.





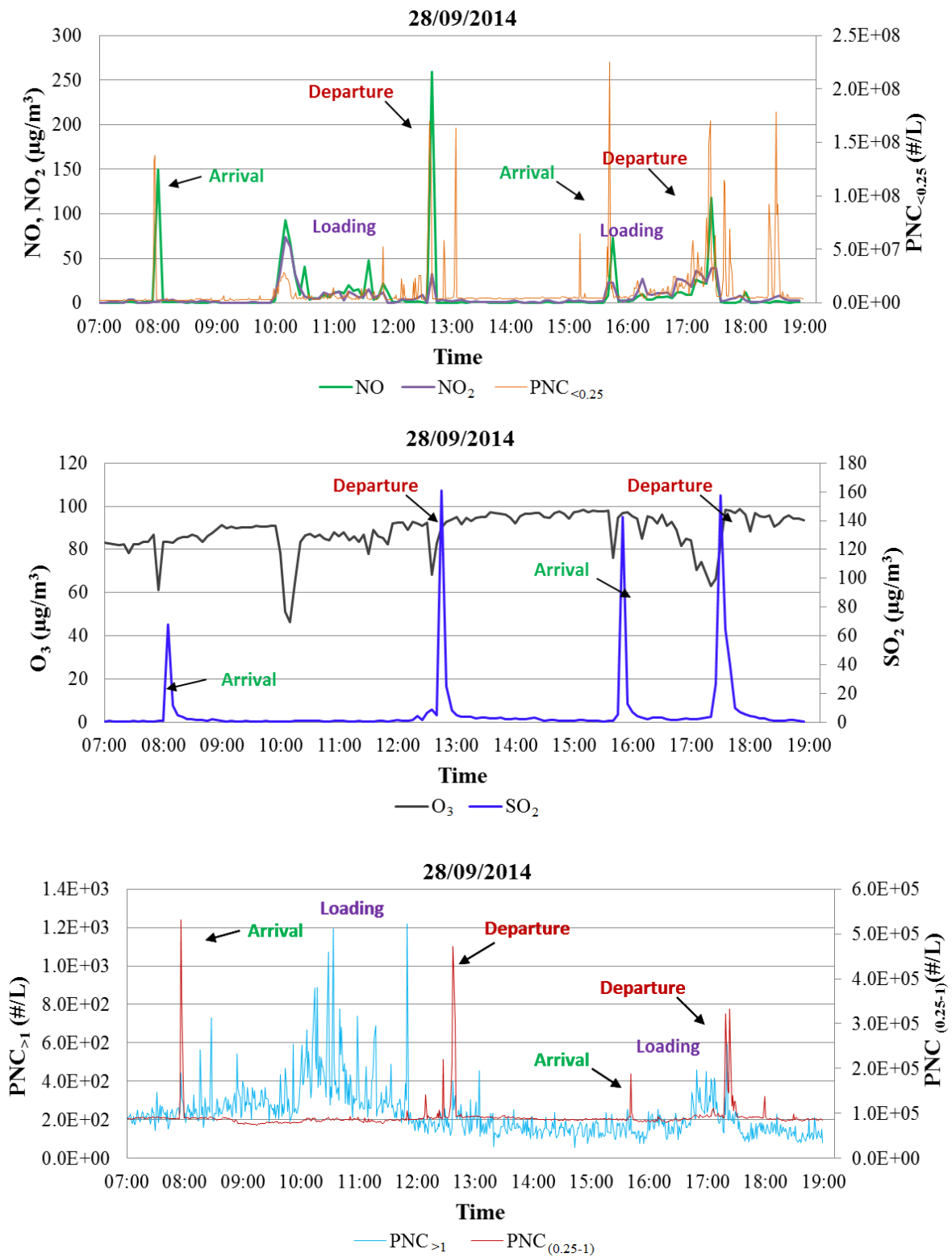


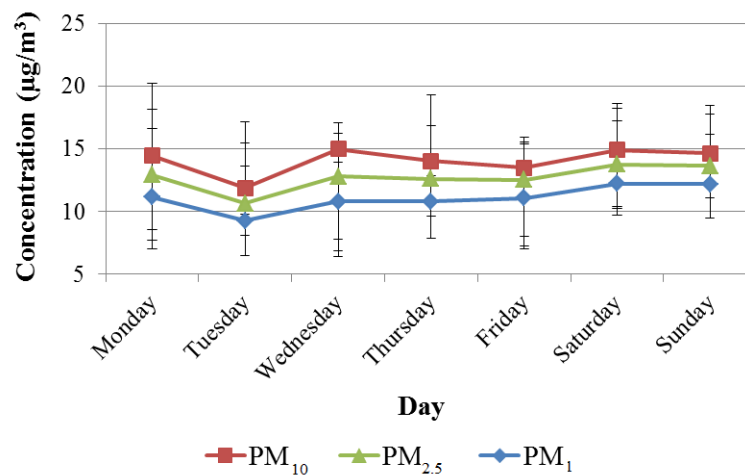
Figure 4.5. Examples of concentration peaks of gaseous pollutants (5-min resolution) and particles of different sizes (1-min resolution) associated to arrival/departure of ships and loading/unloading activities in 2014.

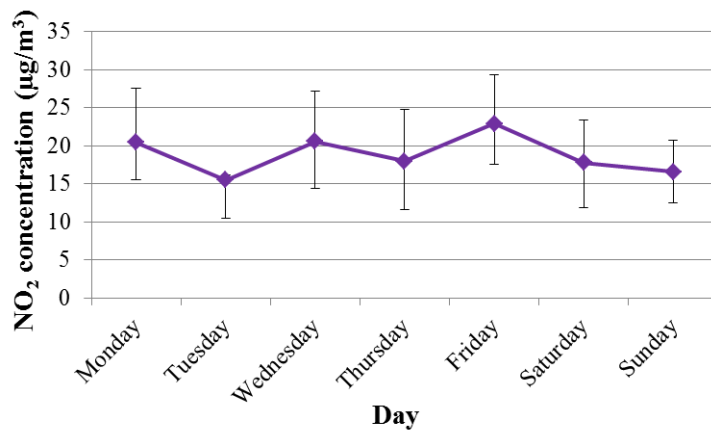
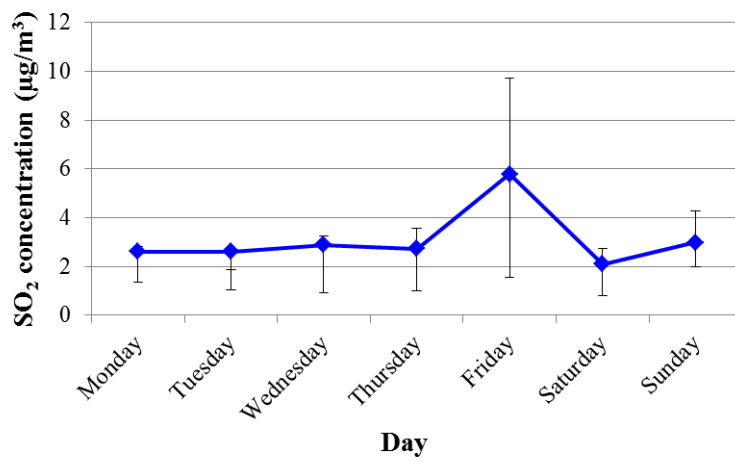
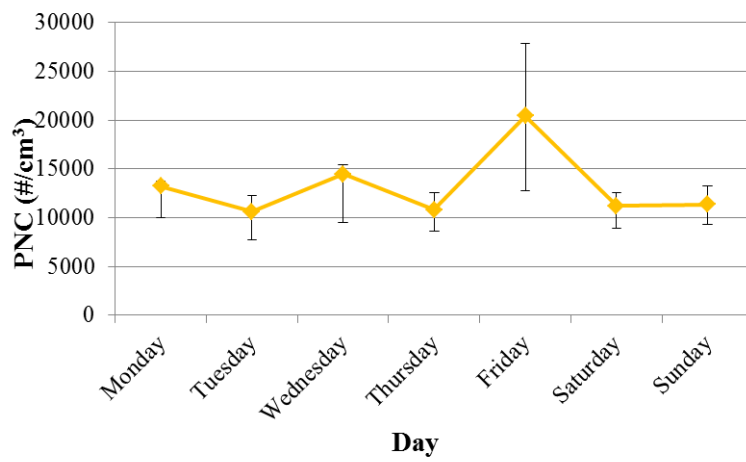
Chemical characterisation of  $PM_{2.5}$ , whose results are reported elsewhere (Cesari et al., 2014), were useful to evaluate the contribution of ships emissions to primary  $PM_{2.5}$  and secondary  $nssSO_4^{2-}$  using receptor models (see Section 3.1).

#### 4.1.3 Patterns of ship traffic and concentrations

Concentration peaks obtained at high temporal resolution (i.e. 5 minutes for gases) allowed “capture” ship releases of gaseous and particles but they were not useful in correlating measurements with ship phases because of different temporal resolution. In order to have information on temporal correlation between measured concentrations and ship traffic, weekly (period Monday-Sunday) and daily (hourly interval 0-23) patterns were obtained. Starting from 30-min average data, patterns were computed for gaseous pollutants, ship traffic (in terms of cumulative GT) and particles (both in mass and number) measurements. Further, to “isolate” the direct contribution of ship operations (i.e. manoeuvring, hotelling mode), only data associated to the selected wind direction sector indicating downwind conditions ( $292.5^\circ$ - $67.5^\circ$ ) were included. Finally, comparison between hourly patterns of 2012 and 2014 is reported in Section 4.3.

In general terms, weekly patterns did not show evident trends neither in gaseous and PM concentrations, in agreement with no significant changes in ship traffic during the week (Fig. 4.6).







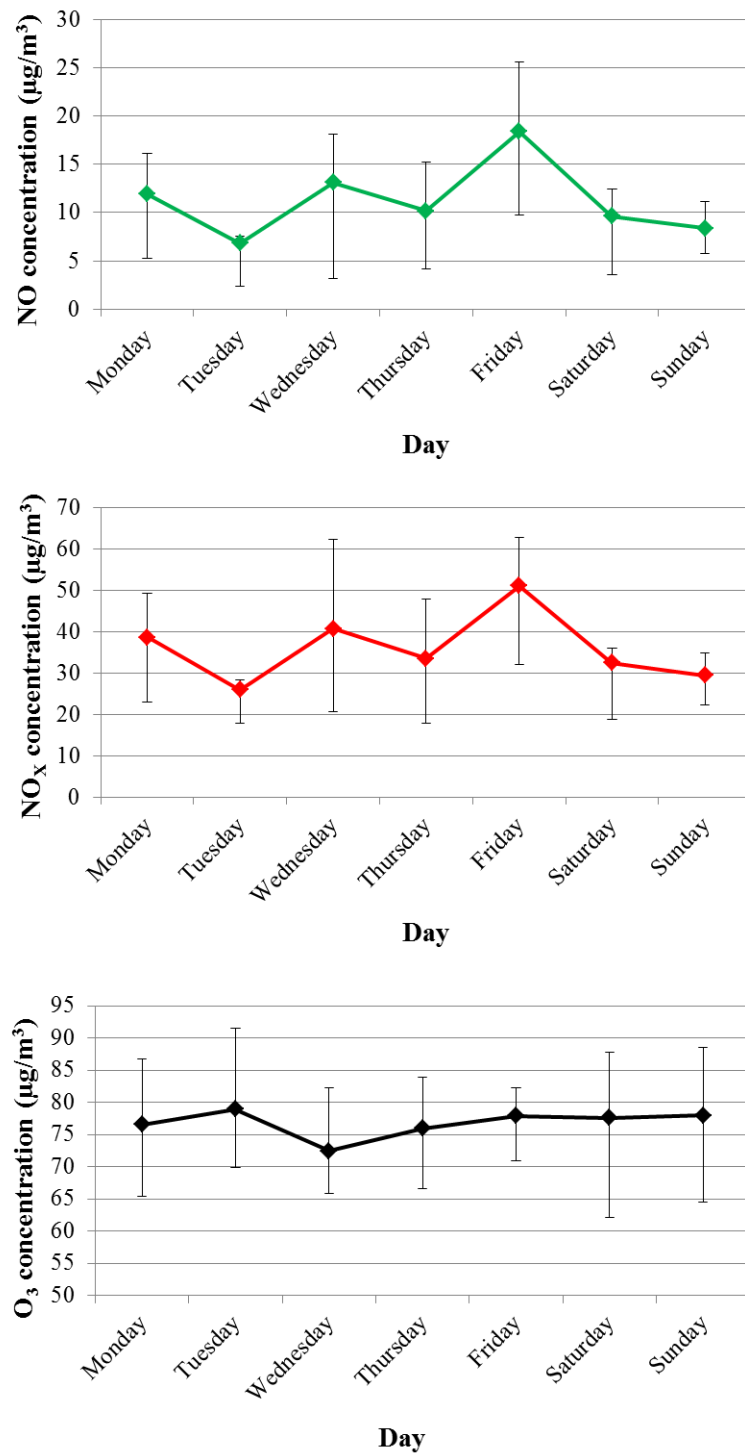
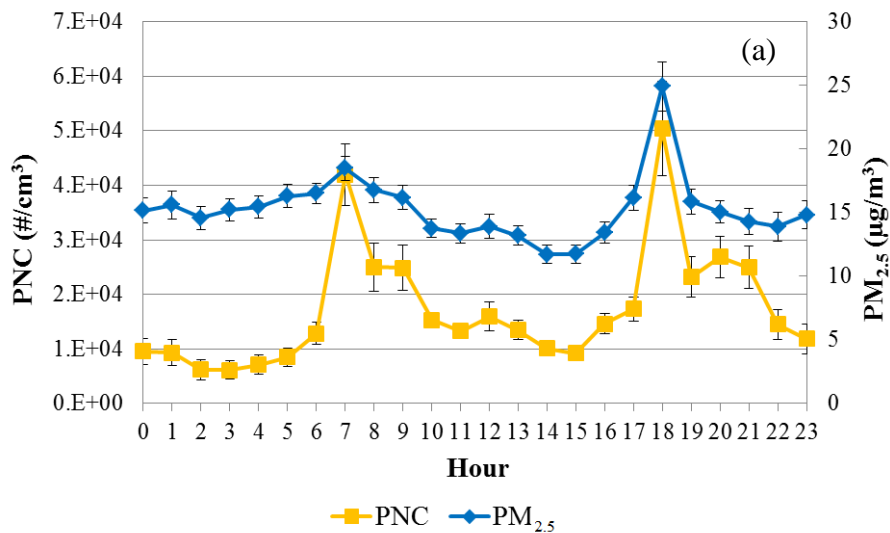


Figure 4.6. Weekly pattern of PM<sub>2.5</sub>, PNC and gaseous (SO<sub>2</sub>, NO<sub>2</sub>, NO, NO<sub>x</sub>, O<sub>3</sub>) concentrations measured during the 2014 campaign (error bars indicate the inter-quartile range).

On the basis of hourly averages, daily patterns were obtained for all pollutants and ship traffic in both campaigns performed at the Terminal Passeggeri site. In 2012, a very clear pattern was evident for particle concentrations (both in mass and number),

following the same daily trend of ship traffic. The detected peaks were characterised by an increase of 3-4 times in  $PM_{2.5}$  concentrations and up to a factor 10 for PNC. The effect particularly marked on PNC with respect to  $PM_{2.5}$  concentrations suggested that shipping contribution was higher on fine and ultrafine particles. In fact, two distinct peaks of PNC were present at 7.00 a.m. and 6.00 p.m. (Fig. 4.7a) in correspondence to the maximum values of ship traffic (around 160 vessels with a total GT over 3 million tonnes), either in number of ships and cumulative GT (Fig. 4.7b).

In detail, during all measurement period, the majority of ship arrivals were recorded in the morning whereas departures occurred in the afternoon. Considering that the two peaks of vessels number and cumulative GT were very similar in magnitude, it was likely that the same ships were involved in arrival and departure traffic data. That was probably due to the fact that ships berthed at the framed docks were Ro-Ro ferries with fixed timetables or at least constant through the measurement campaign. Regarding to the  $PM_{2.5}$  daily pattern, it was comparable to those of PNC only for the second peak in the afternoon whereas the first peak in the morning was more smoothed.



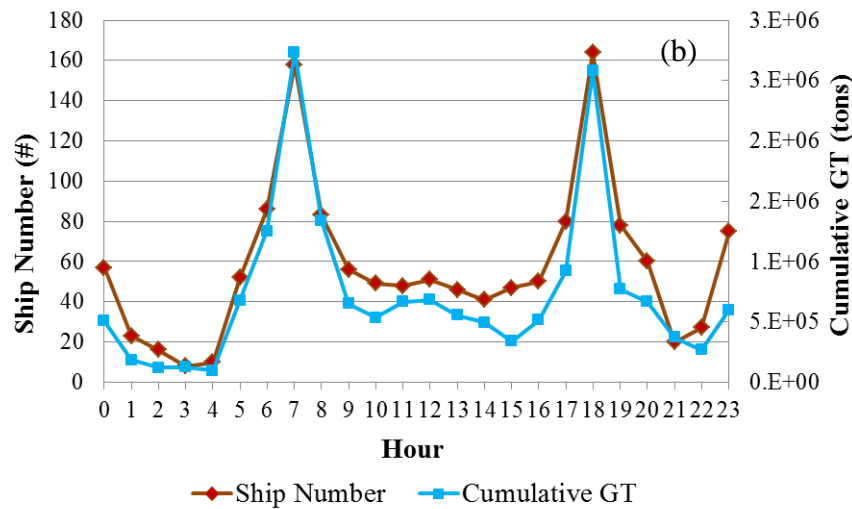


Figure 4.7. Daily patterns of (a) PNC,  $PM_{2.5}$  (data referred to the wind direction sector WNW-ENE) and (b) ship traffic (in number of ships and cumulative GT) obtained in 2012 (source: Donateo et al., 2014).

Average hourly GT in 2012 and 2014 was compared in order to identify substantial changes in ship traffic during the day (Fig. 4.8). Effectively, results indicated an increase (8%) in the average traffic (as GT) per day from 2012 (172 ktons/day) to 2014 (186 ktons/day) in the same period. However, ship traffic was significantly changed in terms of distribution during the day. In 2012, ship traffic volume was concentrated essentially at two definite time intervals, corresponding to arrival and departure of ships, as described previously. On the contrary, in 2014 ships movements were recorded almost indifferently in day-time, with peaks at 8 a.m. in the morning and at 7 p.m. in the evening. Other peaks were visible at midday and between 3 p.m. and 5 p.m. confirming larger and more distributed ship traffic in 2014 compared to 2012. This could be probably due to different ship types hosting through the day at the three docks considered or changes in timetables. Moreover, hourly peaks in 2014 were shifted by one hour in the morning (at 8 a.m.) and in the afternoon (at 7 p.m.) with respect to 2012. Finally, taking into account that the evening peak was approximately equal between the two years and the first one in the morning was significantly less pronounced in 2014, a growth in ship traffic volume was found to be especially focused in the afternoon hours.

Daily  $PM_{2.5}$  pattern showed two small peaks at 7 a.m. for both years and a peak at 6 a.m. and 7 a.m. in 2012 and 2014, respectively (Fig. 4.9a). It is interesting to note

that concentration peaks reflected the well-defined daily ship traffic in 2012 but a peak shifted by one hour before in the morning (at 7 a.m.) was observed in 2014.

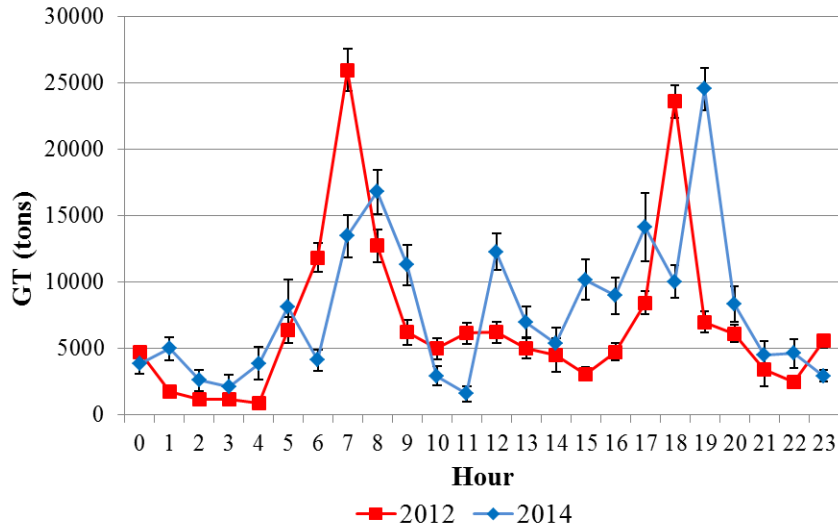


Figure 4.8. Daily pattern of average GT in both campaigns.

As seen for  $PM_{2.5}$  concentrations, daily patterns of PNC in 2014 did not show significant peaks through the day oppositely to 2012 (Fig. 4.9b). In fact, two relevant peaks were visible in 2012 in agreement with ship traffic data.

These differences could be related to micrometeorological effects (i.e. atmospheric stability) which make difficult to separate shipping contribution as well as the simultaneous presence of other sources in the same wind direction sector. In this perspective, an integrated analysis including synchronized wind direction data, measurements and effective ships passage was needed.

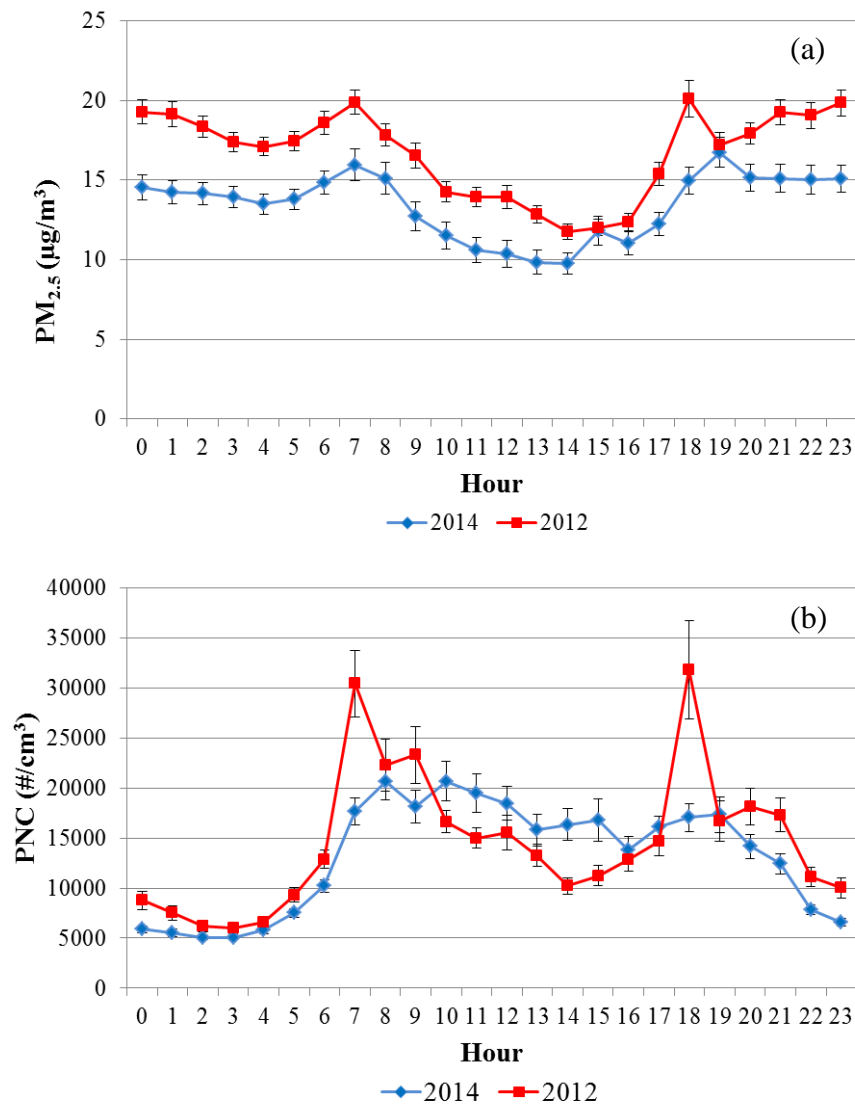


Figure 4.9. Daily pattern of (a)  $PM_{2.5}$  and (b) PNC in both campaigns.

Gaseous pollutants concentrations of NO, NO<sub>2</sub>, NO<sub>x</sub>, SO<sub>2</sub> and O<sub>3</sub> were also analysed. Daily pattern of nitrogen oxides presented a marked peak at 8 a.m. and at a more smoothed time interval between 5 p.m. and 7 p.m. in which NO<sub>2</sub> concentrations were slightly higher. All nitrogen oxides followed the ship traffic pattern especially in the morning with a less evident effect on concentrations in the evening. However, in general NO<sub>2</sub> seemed to be more influenced in the afternoon. Loading and unloading activities could affect NO<sub>2</sub> concentrations, being the oxidized product of NO primary emissions from vehicles such as cars and trucks.

Daily cycle of O<sub>3</sub> shows larger concentrations in diurnal hours as expected, whereas SO<sub>2</sub> concentrations followed the daily pattern of ship traffic (Fig. 4.10b) with the

same peaks, except for peaks at 5 a.m. and 5 p.m. This confirms that shipping is one of the main contributor to  $\text{SO}_2$  at local air quality, being directly associated to sulphur content in ship fuel.

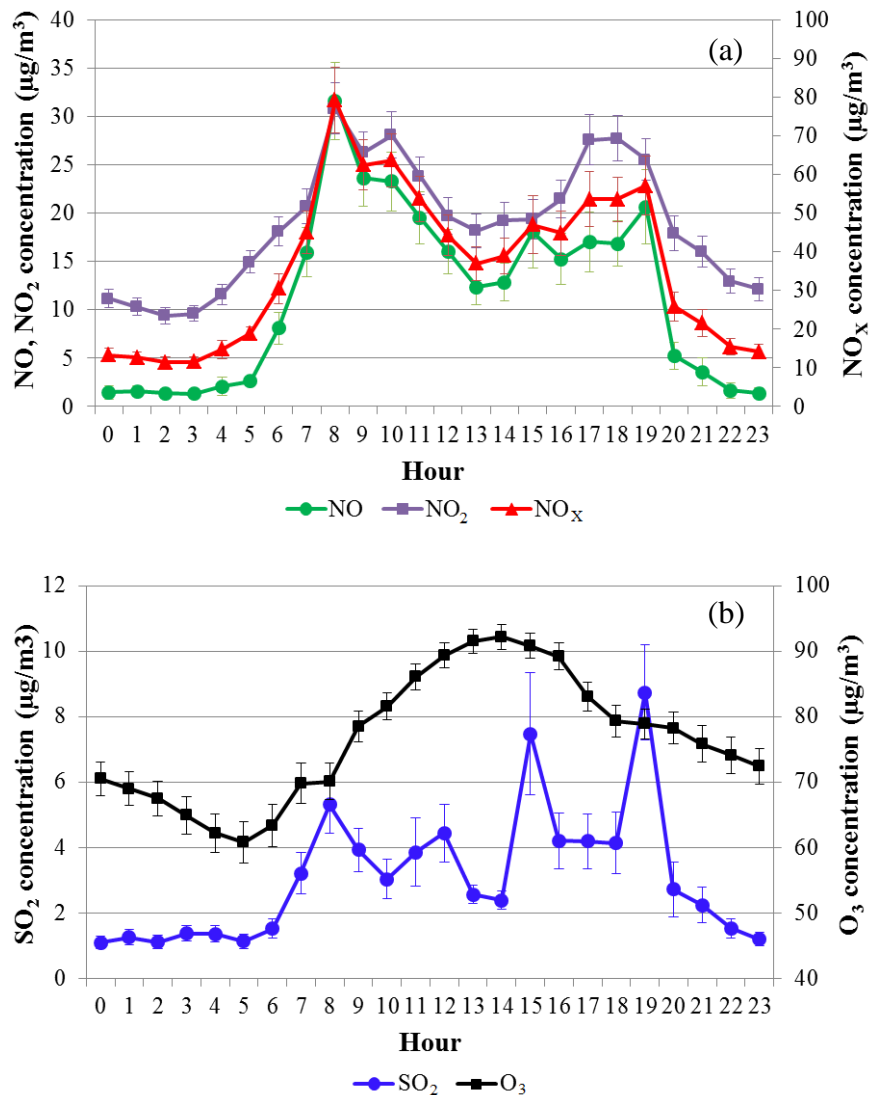


Figure 4.10. Daily pattern of (a) NO, NO<sub>2</sub>, NO<sub>x</sub>; (b) SO<sub>2</sub> and O<sub>3</sub> in 2014.

#### 4.1.4 Primary contribution to pollutants of ship traffic

In this work, 30-min averages were chosen to estimate shipping contribution because in this time interval stable wind direction were typically found and ship operational phases (manoeuvring and hotelling) were easily separated. On the basis of the ship traffic database built integrating data provided by the local Port Authority (arrival/departure time at one of the three docks framed: Prolungamento di Nuovo

Sporgente, Costa Morena Terrare and Costa Morena Terrare Punta) and pictures from the video camera, the arrival/departure time of each ship and hotelling duration were calculated. Actually, arrival and departure time available from the Port Authority were referred to the ship entrance and exit recorded in correspondence of the outer harbour zone, respectively. Because of this, the actual arrival and departure data from the images were considered. However, in case of necessity (i.e. pictures not clear, missing frames), data from the Port Authority database were integrated, considering an addition and a subtraction of 30 min to the arrival and departure time reported respectively, being the average time in manoeuvring phase obtained from ship movements in the harbour for all ship types during the entire measurement campaign. As described in Section 3.2, using 30-min averages, a qualitative and quantitative analysis of primary contribution on gaseous and particles concentration (both in mass and number) were performed.

For 2014 campaign, polar plots provided a qualitative individuation of shipping contribution to the measured concentrations (Fig. 4.11). For doing this, a separated data elaboration was carried out in cases not influenced and influenced by ships, including in the latter also data associated to hotelling phase. Considering hotelling plus manoeuvring cases, concentration data were statistically relevant and distributed at all wind velocities, especially for PNC, NO, SO<sub>2</sub>. Instead, PM<sub>2.5</sub> concentrations seemed less affected by ships compared to the other pollutants, showing the maximum share from the Southern sector, corresponding to the urban and industrial areas. PNC and NO had a similar pattern with a marked evidence of contribution from the harbour sector. The SO<sub>2</sub> concentration distribution was associated both at low and high wind velocities but more smoothed with respect to NO and PNC. This was likely explained by the fact that hotelling phase (when the sulphur-content fuel should be lower) was included in the calculation, lowering the average concentration in correspondence of the harbour sector.

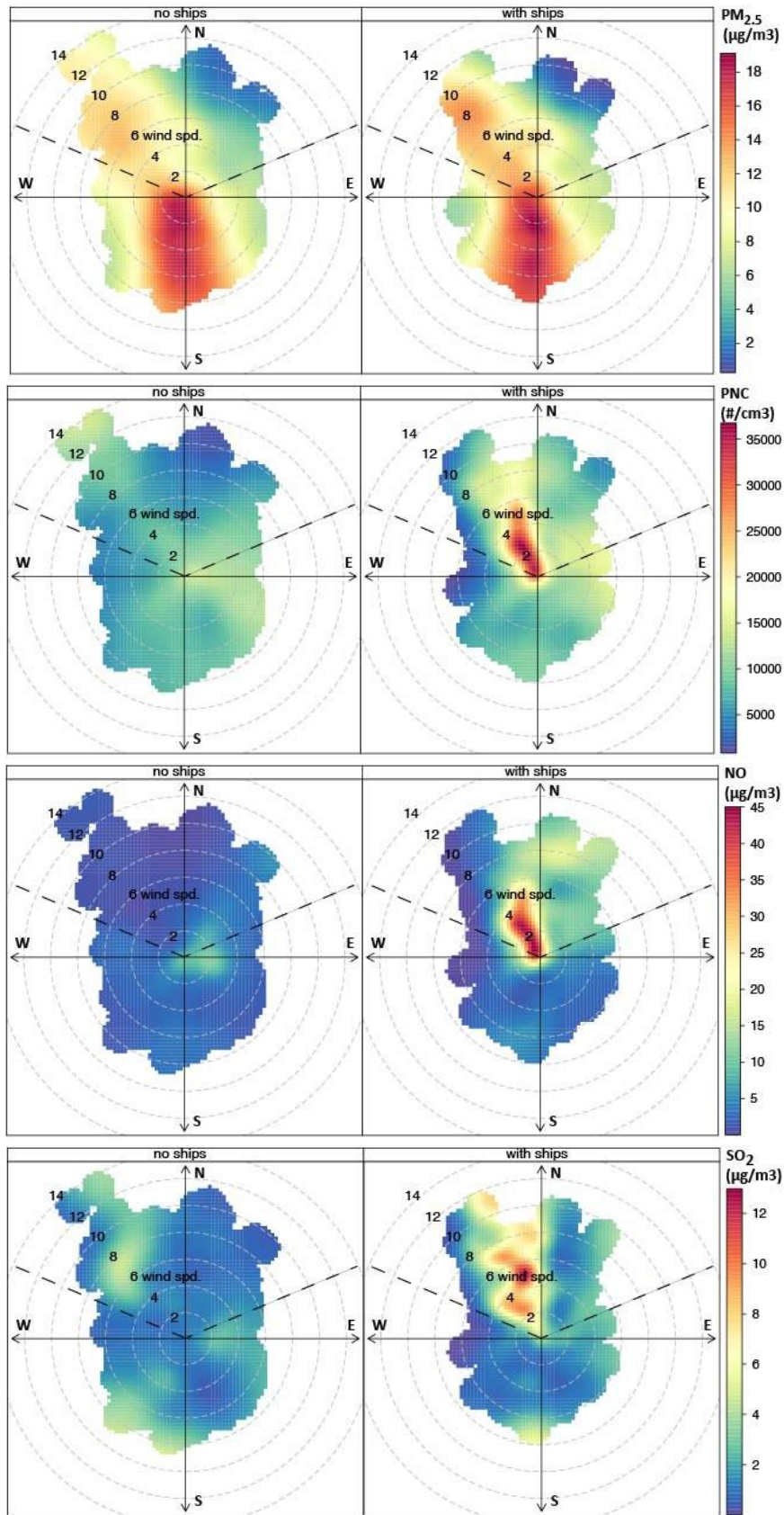


Figure 4.11. Polar plots for PM<sub>2.5</sub>, PNC, NO, SO<sub>2</sub> (in order) with dotted lines indicating the wind direction sector associated to the harbour (WNW-ENE) for the 2014 campaign.



By applying the approach developed in Contini et al. (2011) the average relative contribution was estimated distinguishing between only ship traffic (ship arrival/departure) and total contribution (ship traffic plus hotelling periods) for both campaigns in 2012 (Tab. 4.2) and 2014 (Tab. 4.3).

In 2012, the relative contribution of ship traffic was 7.4% ( $\pm 0.5\%$ ) to  $PM_{2.5}$  and 26% ( $\pm 1\%$ ) to PNC, confirming the highest weight on particle number rather than particle mass of ship emissions.

Adding related harbour activities (loading/unloading by cars, trucks), the total impact increased to 9.3% ( $\pm 0.5\%$ ) on  $PM_{2.5}$  and to 39% ( $\pm 1\%$ ) on PNC, more reflecting the hotelling importance on air pollution in the harbour. In this analysis hotelling in periods potentially influenced by ships were considered when the site was downwind. For this reason, two wind direction sectors associated to docks were individuated:  $292.5^{\circ}$ - $10^{\circ}$  and  $15^{\circ}$ - $60^{\circ}$ .

In 2014, a more detailed analysis was possible evaluating also shipping contribution on gaseous pollutants and particles of different sizes. As resulted in summer 2012 (Donateo et al., 2014) and as shown in other studies carried out in other harbours (Contini et al., 2015; Healy et al., 2009; Kivekäs et al., 2014; Healy et al., 2010), the ship traffic contribution was significantly larger on particle number concentration ( $23\% \pm 1\%$ ) with respect to  $PM_{2.5}$  ( $7.8\% \pm 0.6\%$ ) either considering manoeuvring than including harbour activities. This is because primary particles emitted by ships may cover the size range from the nucleation to the coarse mode (i.e.  $0.005$  to  $>3 \mu m$ ; Petzold et al., 2004; Kasper et al., 2007; Healy et al., 2009, Petzold et al., 2008; Reche et al., 2011). The primary particles in the accumulation mode are included in PNC measurements and seem better conserved during dispersion (Zhang et al., 2004; Kumar et al., 2008; Wehner et al., 2009). These reasons lead to propose PNC as a more suitable metric to evaluate shipping impact instead of  $PM_{2.5}$  and  $PM_{10}$  concentrations included in the European Air Quality Standards.

Table 4.2. Estimated average contribution of ship traffic and harbour activities on  $PM_{2.5}$  and PNC in 2012.

	<b><math>PM_{2.5}</math></b>	<b>PNC</b>
Only ship traffic (%)	7.4% ( $\pm 0.5\%$ )	26% ( $\pm 1\%$ )
Ship traffic + hotelling and loading/unloading periods (%)	9.3% ( $\pm 0.5\%$ )	39% ( $\pm 1\%$ )

It is important to take into account that the contribution to  $PM_{10}$  reported in Tab. 4.3 was not directly measured rather, it was evaluated assuming that ship emissions are mainly characterised by sub-micrometric particles; therefore, the absolute contribution to  $PM_{2.5}$  and  $PM_{10}$  is essentially the same. Therefore, the differences in the relative contributions could be obtained from the ratio  $PM_{2.5}/PM_{10}$  that is about 0.78 in the site analysed.

The size distribution of the impact on particle number concentration is discussed in Section 4.1.5. The impact on gaseous concentration of NO, NO<sub>2</sub> and SO<sub>2</sub> was significantly higher compared to particles concentration in mass and number, particularly for hotelling phase (Fig. 4.12).

The contribution on NO was larger than those to NO<sub>2</sub> because of the short distance between the emission point and sampling site, compatibly to the “fresh” plumes observed at the site (see Section 4.1.6). In fact, NO is the main (around 80% of nitrogen oxides) primary component in ship emissions but it is rapidly oxidized to NO<sub>2</sub> in the atmosphere depending on local meteorology (mainly solar radiation, temperature and relative humidity) and on the distance from the emission source. Hotelling phase represented 43% and 40% of the increase in contribution on NO and NO<sub>2</sub> concentration respectively. Also  $PNC_{<0.25}$  was strongly affected by the hotelling and related activities (loading/unloading) in the harbour.

The negative impact on O<sub>3</sub> represented a local depletion occurring very close to the emissions, due to the fast reaction between NO producing NO<sub>2</sub>, as also demonstrated in other sites (Diesch et al., 2013; Eckhardt et al., 2013). However, the opposite effect (that is production of O<sub>3</sub>) was observed at larger distances by modelling simulations (Huszar et al., 2010; Gencarelli et al., 2014) in diurnal hours (and more accentuated in summertime) being correlated with the excess of NO<sub>2</sub> emitted by ships.

Finally, shipping impact on O<sub>3</sub> is not unequivocal suggesting be dependent on the spatial resolution used. For example, the meso-scale study by Huszar et al. (2010) found that shipping contributed to O<sub>3</sub> production at most of the remote domain and to destruction by over 50% over the main shipping routes.

In our case, hotelling mode contributed to amplify the ozone destruction process, doubling (+56%) the negative contribution (2.2% in manoeuvring phase). The impact

of the harbour-related activities is lower on SO<sub>2</sub> and particle mass compared to the other species, being 9% and 1.8% (on average) respectively greater than considering only manoeuvring phase.

Table 4.3. Estimated average contribution of ship traffic and harbour activities on all pollutants in 2014.

	<b>PM<sub>1</sub></b>	<b>PM<sub>2.5</sub></b>	<b>PM<sub>10</sub></b>	<b>PNC</b>	<b>SO<sub>2</sub></b>	<b>NO</b>	<b>NO<sub>2</sub></b>	<b>NO<sub>x</sub></b>	<b>O<sub>3</sub></b>
Only ship traffic (%)	8.4 (±0.5)	7.8 (±0.6)	6.0 (±0.5)	23 (±1)	48 (±1)	37 (±1.7)	20 (±1.4)	29 (±1.6)	-2.2 (±0.2)
Manoeuvring + hotelling and loading/unloading activities (%)	11.1 (±1.8)	9.3 (±1.8)	7.3 (±1.4)	48 (±3.5)	57 (±1.5)	80 (±4.5)	55 (±7.0)	69 (±6.0)	-5.0 (±1.8)

In conclusion, results indicated that logistic in the harbour, like the organization and optimization of arrival and departure scheduling and hotelling time as well as the emissions of ships and road vehicles associated with the loading/unloading phases, was a relevant share, ranging from 15% to 60% of the total impact to atmospheric pollutants. The ratio (manoeuvring plus hotelling/manoeuvring) reported in Fig. 4.12 provided a direct evidence of the impact of hotelling operations in cases with values larger than 1. It was clear as NO<sub>2</sub>, NO, O<sub>3</sub>, PNC<sub><0.25</sub> and PNC<sub>>1</sub> were the most affected pollutants and PNC<sub>1-0.4</sub> the lesser one.

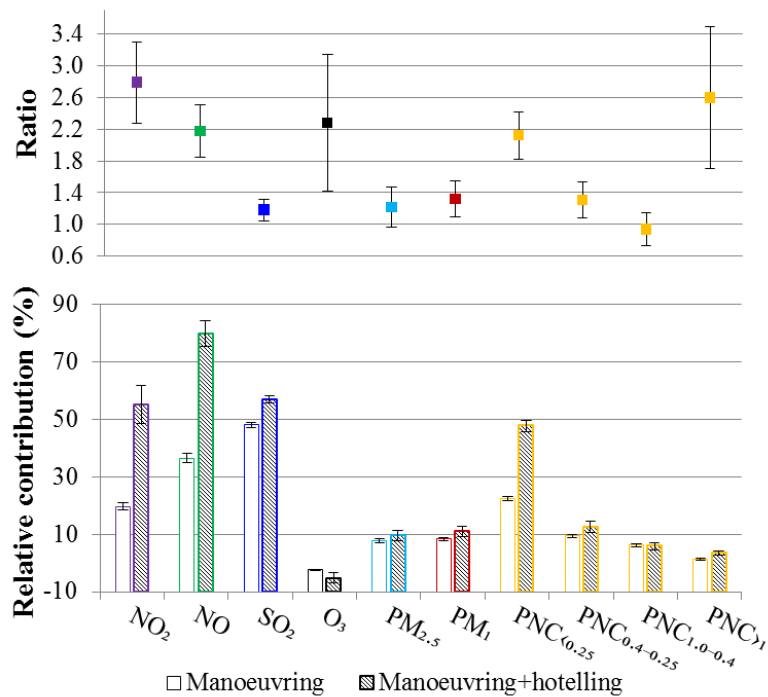


Figure 4.12. Ratio of the contributions of manoeuvring and hotelling plus manoeuvring phase and relative contributions for all pollutants analysed (from up to bottom).

#### 4.1.5 Particle size distribution

Also for measurements provided by the OPC, weekly and daily patterns were obtained on 30-min and 24-h averages from raw data at 1-min resolution. Evaluating PM concentrations ( $PM_{10}$ ,  $PM_{2.5}$  and  $PM_1$ ), no significant trend was observed (Fig. 4.13a), apart from a minimum on Tuesday, more evident on larger particles ( $PM_{10}$ ), but within the uncertainty interval (error bars as interquartile range). Particles counts, represented in majority by particles up to around  $0.4 \mu m$ , increased in the weekend (Friday-Sunday), reached the lowest value on Tuesday and then had a relatively constant trend between Wednesday and Thursday (Fig. 4.13b).

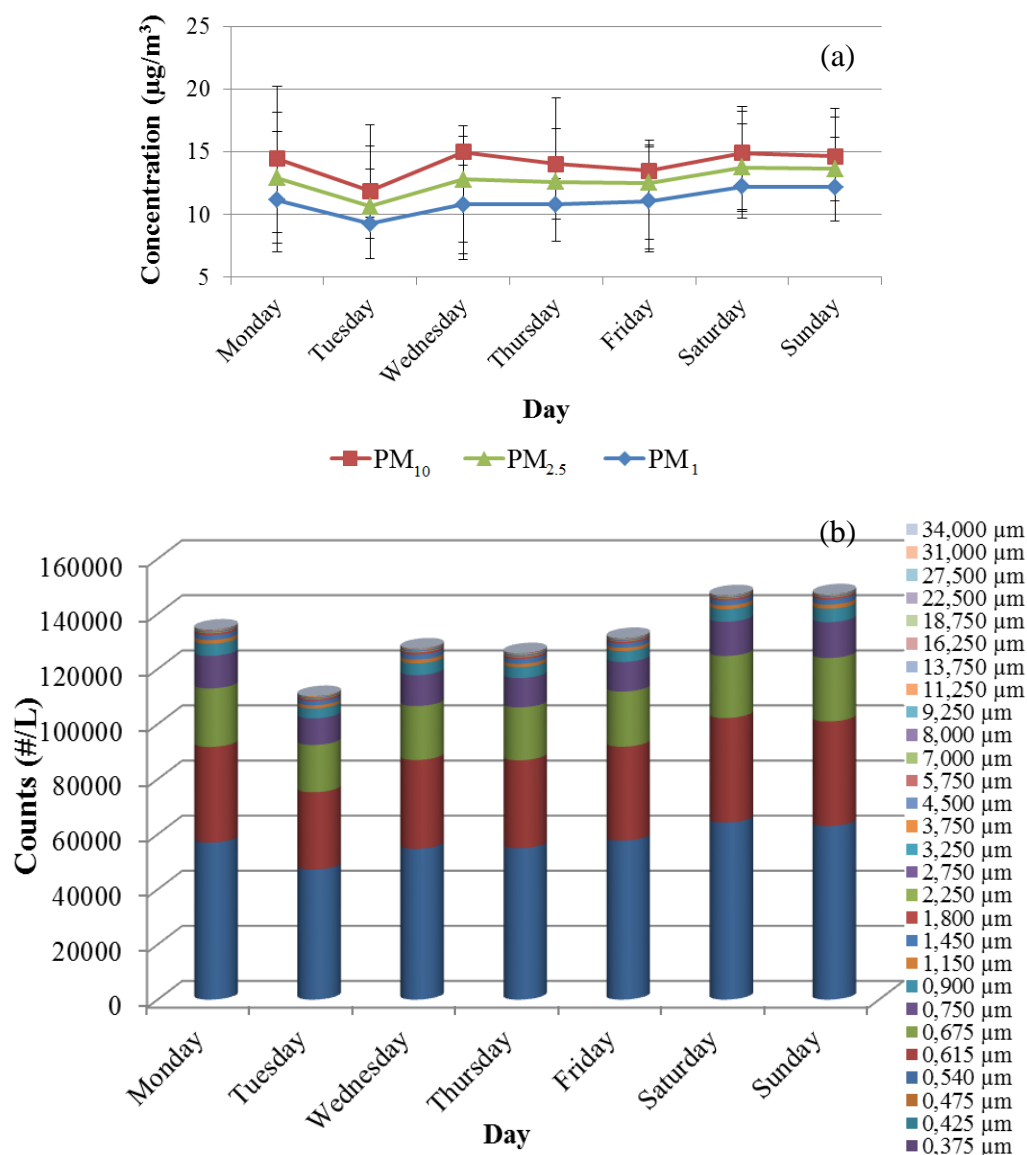


Figure 4.13. Weekly patterns of (a) PM and (b) number particle concentration in different size ranges measured by the OPC.

Daily patterns of PM showed no accentuated peaks but some small differences in concentration values were visible. In fact, the absolute highest PM concentrations were recorded at 7 a.m. in agreement with the ship traffic peak detected in the evening, as well as a relative peak at 3 a.m. (Fig. 4.14a). In general terms, concentrations of PM were greater in evening and nocturnal hours.

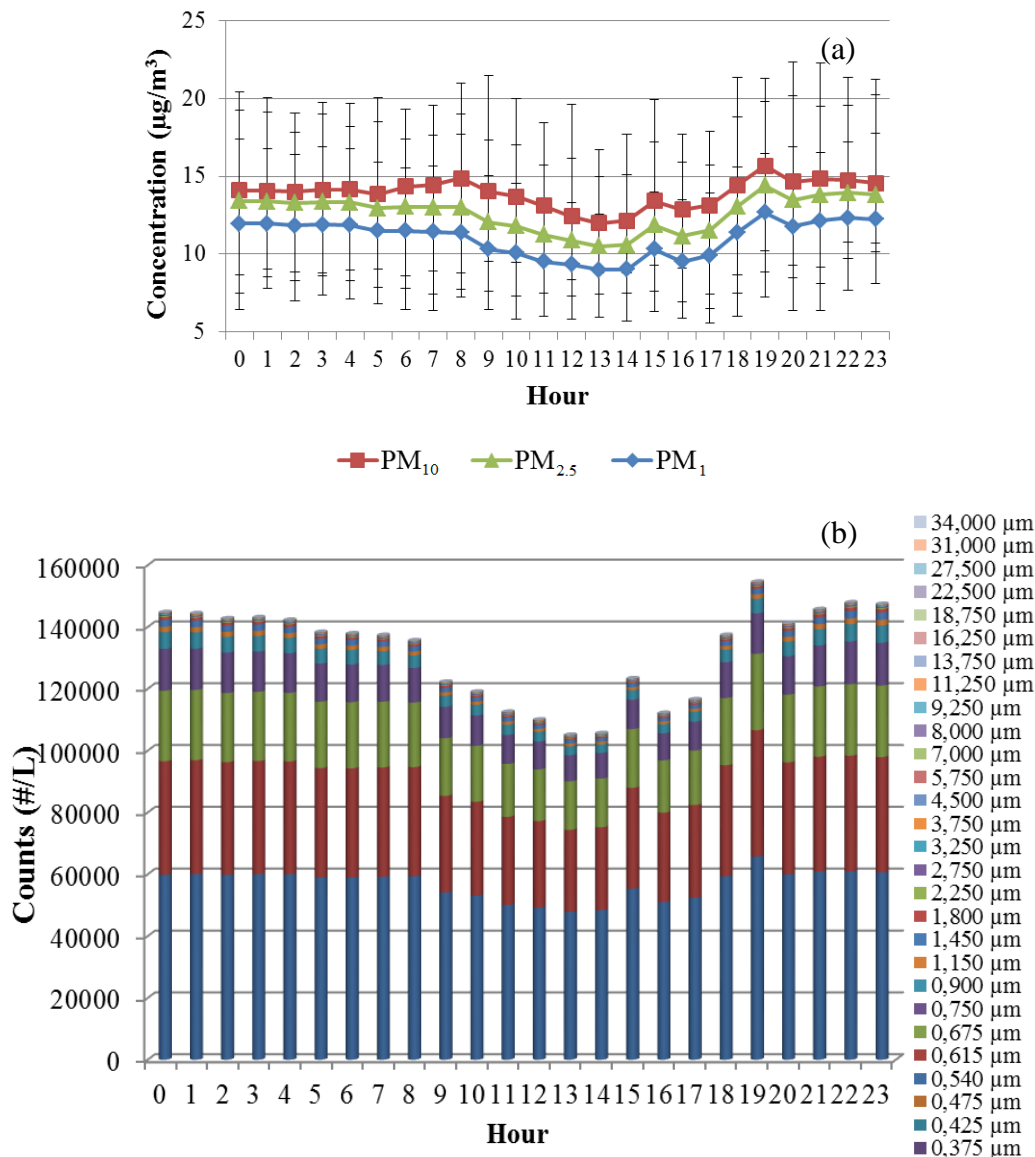


Figure 4.14. Daily patterns of (a) PM and (b) particle number concentrations in different sizes measured by the OPC.

Looking at overall particle number concentration for different sizes (Fig. 4.14b), the lowest values in day-time were more clear especially for particles larger than  $0.3 \mu\text{m}$ . Particle counts exceeded 130,000 #/L per hour at 7 a.m., as seen for mass concentrations, with more particles of smaller sizes with respect to the previous and following hours. In night-time particle number concentrations remained almost unchanged in total amount.

Contribution analysis was performed for particle number concentrations in absolute (#/L) and relative terms (%) as function of particle diameter (in  $\mu\text{m}$ ). Also, distinction between manoeuvring and manoeuvring plus hotelling phases was

performed to highlight different shipping contribution.

It must be considered that the filled marks at  $0.13 \mu\text{m}$  in Fig. 4.15a and Fig. 4.15b were obtained considering measurements both from the CPC and the OPC. Taking into account that the lower limit of CPC is  $0.009 \mu\text{m}$  and those of the OPC is  $0.25 \mu\text{m}$ , particle number concentrations in the range  $0.009\text{-}0.25 \mu\text{m}$  (after reporting as  $\text{PNC}_{<0.25}$ ) is represented by the difference between measurements at the first channel of the OPC and those of the CPC. A simplified scheme is reported in Fig. 4.16.

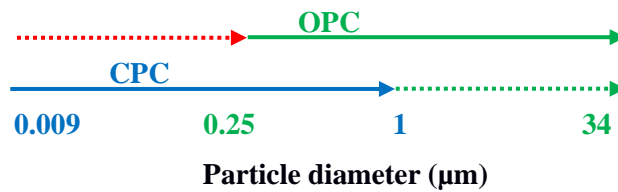
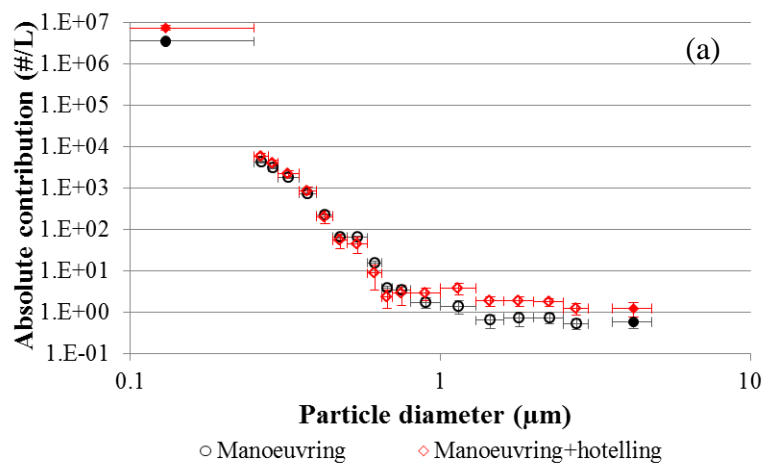


Figure 4.16. Upper and lower detection limits for the CPC (in blue) and the OPC (in green). Red arrow indicates the range in which particle number concentrations were derived (see text).

Similarly, the filled marks at  $4.2 \mu\text{m}$  corresponded the cumulative particle number concentration summing measurements at channels with  $D_p > 3.25 \mu\text{m}$ .

This was justified by the fact that very few particles ( $< 1 \text{ #/L}$ ), were found at these channels which had an average diameter of  $4.2 \pm 0.6 \mu\text{m}$ , representing 30% of measurements.



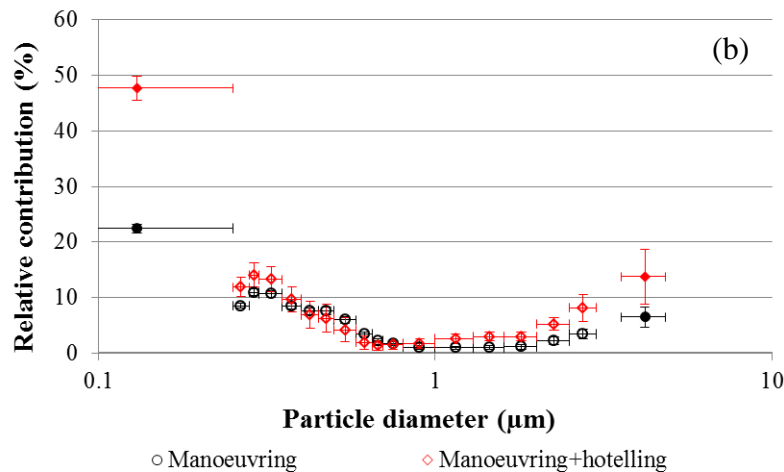


Figure 4.15. Absolute (a) and (b) relative contribution to particle number concentration as function of particle size.

Segregation of manoeuvring and manoeuvring plus hotelling phases allowed estimate the hotelling “weight” on different particle size classes. Both in absolute and relative terms, the two phases have a broad similarity in the size distribution of contributions, however, some differences could be related to different engine emissions according to specific engine type (at two or four strokes) or loads (main and auxiliary engines) or fuel type burnt.

In absolute terms, the size distribution showed an absolute maximum for  $PNC_{<0.25}$  and a secondary one at around  $0.35 \mu\text{m}$ , with around 1,500,000 #/L and almost 10,000 #/L respectively (Fig. 4.17a). Hotelling phase became significant with respect to manoeuvring on particles larger than  $0.9 \mu\text{m}$ .

By analysing the relative contribution, the minimum values were at  $0.8\text{-}0.9 \mu\text{m}$  and increased for super micrometric particles (Fig. 4.17b). Ideally, four size intervals could describe contributions on particle number concentrations at different sizes:  $PNC_{<0.25}$ ,  $PNC_{0.4\text{-}0.25}$ ,  $PNC_{1\text{-}0.4}$ ,  $PNC_{>1}$ . At the first (particles smaller than  $0.25 \mu\text{m}$ ) and the last (particles larger than  $1 \mu\text{m}$ ) size interval both operation modes contributed almost in the same way. Hotelling phase impact was 53% on ultrafine particles ( $PNC_{<0.25}$ ) and 61% on coarse particles ( $PNC_{>1}$ ). That was probably explained by vehicular emissions during loading/unloading activities and associated dust resuspension. Also, large amounts of relatively large particles may be attributed to re- entrained soot particles from walls in the engine systems (Fridell et al., 2008).



The intermediate interval ( $PNC_{0.4-0.25}$ ) representing particles in the accumulation mode (between  $0.25 \mu\text{m}$  and  $0.4 \mu\text{m}$ ) showed a reduced contribution of hotelling to 23% of the total contribution. Finally, hotelling mode did not contribute on particles with diameter between  $0.4$  and  $1 \mu\text{m}$  ( $PNC_{1-0.4}$ ).

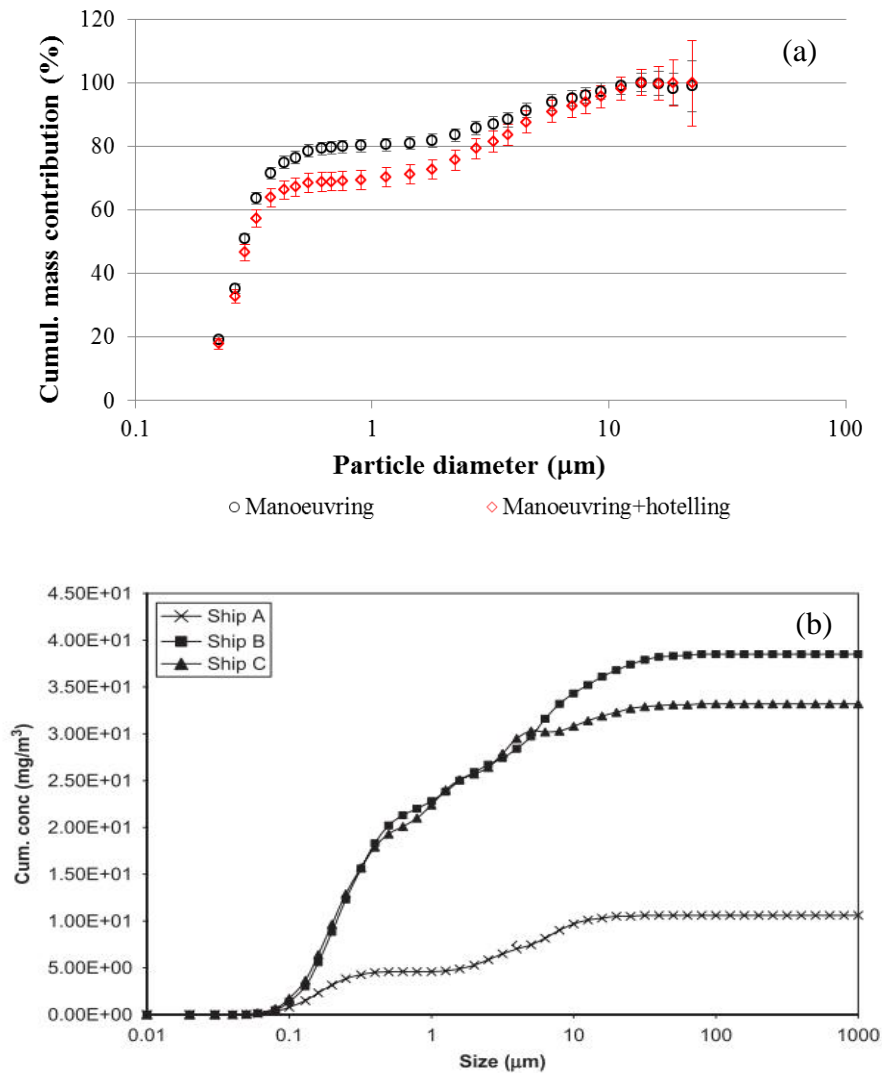


Figure 4.17. Cumulative mass contribution as function of particle size (a) obtained in this study (in %) and (b) from Fridell et al. (2008) (in  $\text{mg}/\text{m}^3$ ).

The cumulative contribution on mass concentrations (Fig. 4.17a) was characterised by a step increase up to  $0.4 \mu\text{m}$  in which the impact of different phases was not distinguishable. After this, a first plateau was reached at around  $0.8-1 \mu\text{m}$  and a second one at  $10 \mu\text{m}$ . This trend was comparable to those observed elsewhere

(Fridell et al., 2008) for the main engines of three different ships (Fig. 4.17b).

The total contribution to mass concentration was mainly due to manoeuvring phase, especially on particles between 0.4  $\mu\text{m}$  and 8  $\mu\text{m}$ , which are included in  $\text{PM}_{10}$  concentration measurements. This means that the absolute contribution to  $\text{PM}_{10}$  could effectively be considered equivalent (within 3-4%) to the total impact to PM mass concentration. Therefore,  $\text{PM}_1$  and  $\text{PM}_{2.5}$  measurements could actually underestimate total mass contribution. In fact,  $\text{PM}_1$  corresponded, on average, to 80% of the total impact to mass concentration and  $\text{PM}_{2.5}$  expressed 83.5% for manoeuvring phase. Similarly, to the value observed in Kasper et al. (2007),  $\text{PM}_{0.4}$  represented 71% (manoeuvring) and 64% (manoeuvring+hotelling) of the total impact to PM. If the hotelling phase is added these percentages reduce to 69.5% for  $\text{PM}_1$  and 75.6% for  $\text{PM}_{2.5}$ .

#### 4.1.6 Aging of the plume

Different studies essentially focused on exhaust plumes dynamics from emission to aging phase by measurements at stack (Cooper et al., 2001; Fridell et al., 2008; Hallquist et al., 2013), in harbour (stationary) (Jonsson et al., 2011; Diesch et al., 2013; Merico et al., 2016; Alföldy et al., 2013; Lu et al., 2006; Ault et al., 2010; Agrawal et al., 2009; Healy et al., 2009), by aircraft or ships for individual single plume characterisation (Murphy et al., 2009; Moldanova et al., 2009; Lack et al., 2009; Petzold et al., 2008).

It is known that ship exhausts composition changes according to airborne or in-stack measurements are considered (Murphy et al., 2009). This is because chemical and physical processes can occur in the atmosphere (Fig. 4.18), involving primary emissions of soot, PM, NO, CO and  $\text{SO}_2$ .

Generally, emitted soot particles (unimodal distribution) are the main primary components of plumes and they are unchanged also after several days since the release, being chemically inactive.

However, at the stack exit, due to lower temperature, condensation on pre-existing particles or condensation of vapours occur forming primary volatile particles. After a rapid dilution of volatile components, plume evolution (and therefore dispersion) is highly variable in time and space. Coagulation and condensation phenomena may

contribute to change size distribution towards larger particles (Petzold et al., 2008). The aging process can involve many processes such as wet and dry deposition and cycle of evaporation-condensation, according to the physical and chemical properties of particles and atmospheric conditions. Particle-gas conversion can produce more volatile compounds which can remain in gas phase or re-condense into particle phase after oxidation (i.e.  $\text{SO}_2$  converted in aerosol nitrate). In latter case, secondary particulate is formed.

During the aging of the plume, if condensation process prevails, particles in accumulation mode are formed by coagulation of particles with each other or with pre-existing particles in the atmosphere, thus decreasing particle number concentration.

Other important mechanisms involved in aging plume process may be also wet and dry deposition.

Comprehensive studies described plume evolution models, parameterizations and validation processes followed, with particular attention to chemical composition and particle size distribution (von Glasow et al., 2003; Murphy et al., 2009; Healy et al., 2009).

Typical “signature” of fresh soot emissions (particles of elemental carbon), detected by tests on vehicles burning gasoline and diesel fuel (Toner et al., 2006, Sodeman et al., 2005), has been individuated in low content in sulphate and nitrate ions (Ault et al., 2010). Off-line studies (Agrawal et al., 2008; Murphy et al., 2009) demonstrated that 70-80% of emitted PM mass was composed by sulphuric acid or sulphate and 20%-30% of organic carbon in fresh plumes. However, chemical composition and particles size are strongly related to fuel type and operational conditions. Residual fuels were found to be cause of higher OC-V-sulphate levels with respect to distillates (i.e. diesel) which can produce more Ca-EC/OC particles (Ault et al., 2010).

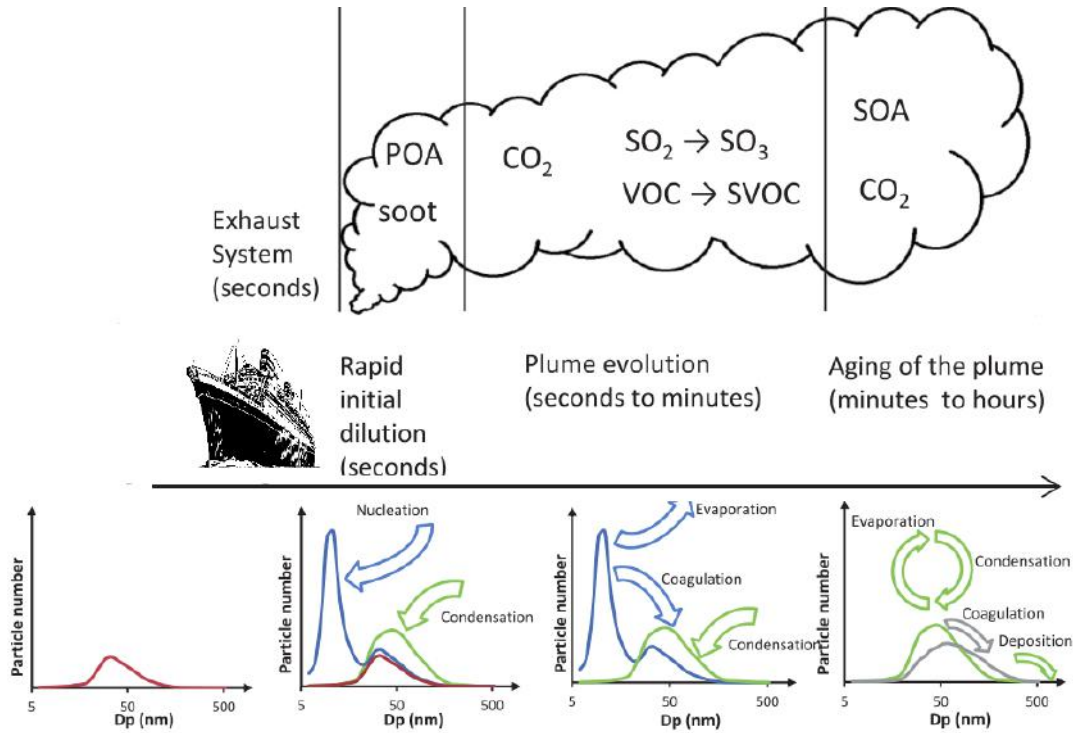


Figure 4.18. Plume life time characterisation with particle size distribution and processes involved (adapted from Westerlund, 2015).

On the basis of the width of  $SO_2$  concentration peaks, directly related to arrival/departure phases (Fig. 4.19), plume analysis was performed. Practically, the difference between the start and end time of each peak represented plume duration. For the 2014 measurement period, the average was  $40 \pm 15$  min during manoeuvring and  $8.5 \pm 6$  h during hotelling.

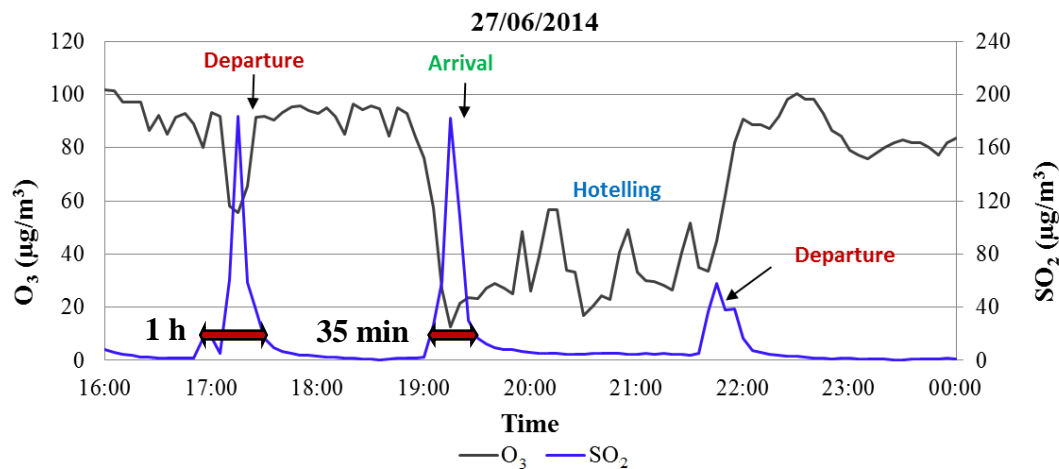


Figure 4.19. Duration plume calculated on  $SO_2$  concentration peaks at arrival and departure operations.

Then, plume age was determined from a simple calculation based on the ratio between the distance dock-measurements site and the wind velocity recorded in correspondence of detected  $\text{SO}_2$  peaks.

The minimum and maximum distances corresponded to the linear distance (calculated by Google Earth tools) from the Terrare (56 m) and Costa Morena Diga (870 m) docks (Fig. 4.20). Knowing space and velocity data, the minimum and maximum plume age was obtained. In this case, the plumes detected were slightly aged because of an age variable between 15s and 300s.



Figure 4.20. Maximum ( $d_{\max}$ ) and minimum ( $d_{\min}$ ) distance between the measuring site and the nearest docks.

This is confirmed by the higher NO concentration peaks compared to those of  $\text{NO}_2$  (see Section 4.1.2). In fact, nitrogen oxides are mostly emitted as NO (about 90%) and then rapidly oxidized into  $\text{NO}_2$ , in a mixing ratio variable in space and time also according to meteorological conditions.

Separating concentration data of NO and  $\text{NO}_2$  in cases with and without  $\text{SO}_2$  peaks, the NO/ $\text{NO}_2$  ratio was computed inside and outside of the plume. The average NO/ $\text{NO}_2$  ratio was 1.0 ( $\pm 1.3$ ) in plumes cases and 0.35 ( $\pm 0.6$ ) in absence of releases.

Taking into account that the typical value observed at ship exhausts was found to be

equal to 4 (Alföldy et al., 2013), relatively fresh plume could be considered individuated with measurements taken at the sampling site.

## 4.2 Results in Venice

Similarly to Brindisi, experimental data collected in the period between 2007 and 2013 were processed to investigate tourist ship traffic contribution to measured PM concentrations (in mass and number). The three campaigns performed in similar meteorological conditions allowed obtain temporal patterns of concentrations and ship traffic. In addition, comparing results through the years it was possible to evaluate the effects of local mitigation actions and of the European legislation on low-sulphur content fuel at local scale.

### 4.2.1 Meteorological conditions

The circulation in the Venice Lagoon is characterised by a typical breeze regime with two prevalent wind directions. In particular, winds come from NNE-NE, following a circulation from the Alps, mainly during the night and from the Adriatic Sea (SSE-SE) during the day.

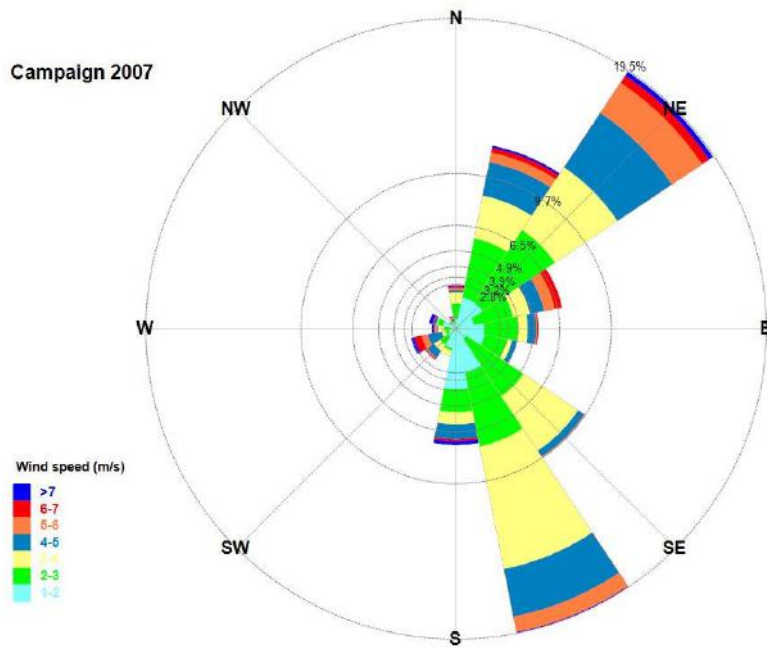
This was observed in all three campaigns performed in 2007 (Fig. 4.21a), 2009 (Fig. 4.21b) and 2012 (Fig. 4.21c) at the Sacca San Biagio site (Cescon et al., 2008; Contini et al., 2011) as well as in other sites in the Lagoon (Gambaro et al., 2007; Prodi et al., 2009; Donateo et al., 2012). The overall wind rose is reported in Fig. 4.22, considering together all the data available in the three campaigns. The average of the main meteorological parameters (temperature, relative humidity, precipitation, sensible heat flux, friction velocity) was calculated for each measurement campaign period (Tab. 4.4).

Micrometeorological conditions were very similar between all campaigns with differences lower than the standard errors. However, wind calms periods were more frequent in 2009 and the highest average wind velocity was recorded in 2007. The relative humidity varied very little among the field campaigns, however, rain periods were more present in 2007.

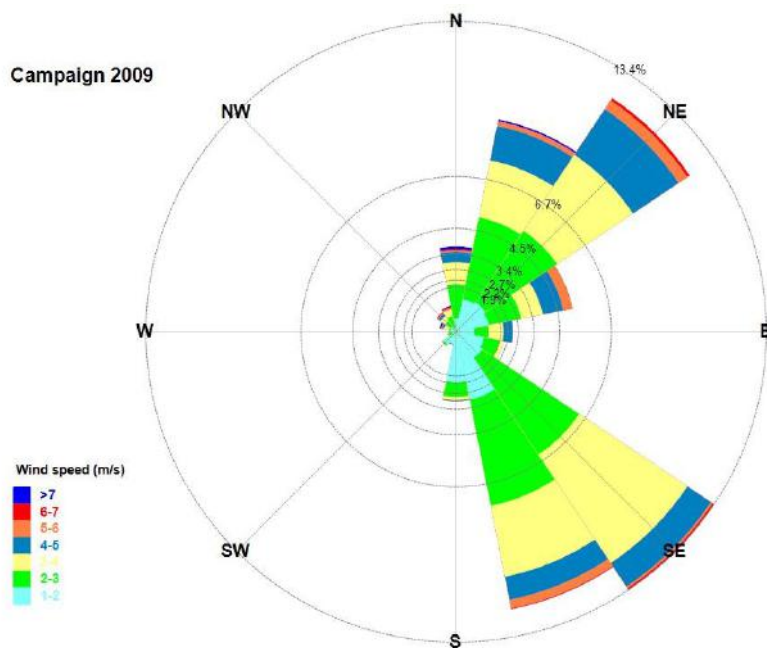
Table 4.4. Main meteorological conditions in the 2007, 2009 and 2012 campaigns in Venice (in parenthesis the inter-quartile range is reported).

	<b>2007</b>	<b>2009</b>	<b>2012</b>
Prevalent wind direction (°)	135	135	45
Wind calms (%) (occurrences with wind velocity lower than 0.5 m/s)	0.2	27.6	8.0
Mean wind velocity (m/s)	3.1 (0.6-10.1)	2.8 (0.4-9.8)	2.8 (0.1-10.1)
Mean temperature (°C)	22.5 (11.5-34.6)	26.6 (17.9-33.8)	24.9 (13.9-34.0)
RH (%)	67.6 (24.6-98.0)	65.9 (36.3-96.2)	65.9 (28.2-98.5)
Rain (>0.5 mm/h) (%)	3.6	1.0	1.6

Starting from hourly measurements, hourly patterns were obtained and compared for all years (Fig. 4.23). The patterns of temperature and relative humidity had very similar behaviors whereas the sensible heat flux (H) showed slightly lower averages in diurnal hours in 2007. Negative values of the sensible heat flux, corresponding to instability conditions, were present late in the evening and the first hours of the night. The friction velocity ( $u^*$ ) trend was similar during all campaigns with the maximum values in the central hours of the day. However, during the 2009 campaign, lower values were observed in the time interval 6-11 p.m. compared to the other years.



(a)



(b)



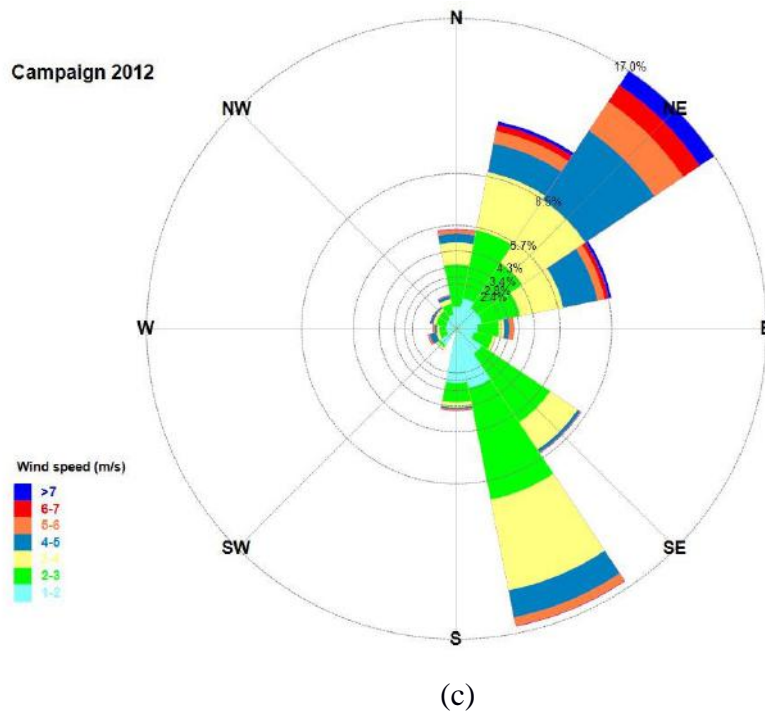


Figure 4.21. Wind rose of the (a) 2007, (b) 2009 and (c) 2012 campaigns in Venice.

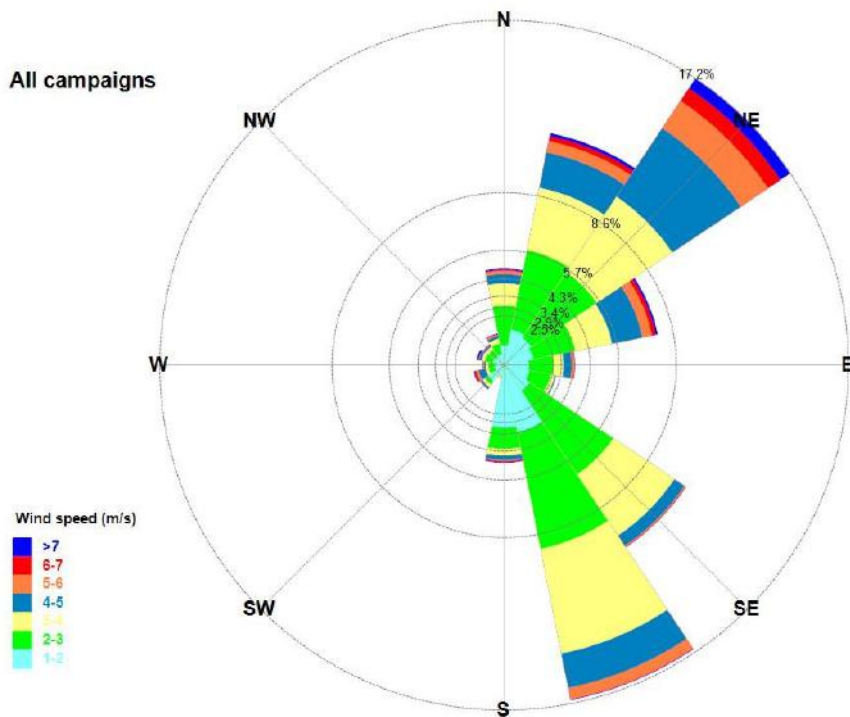
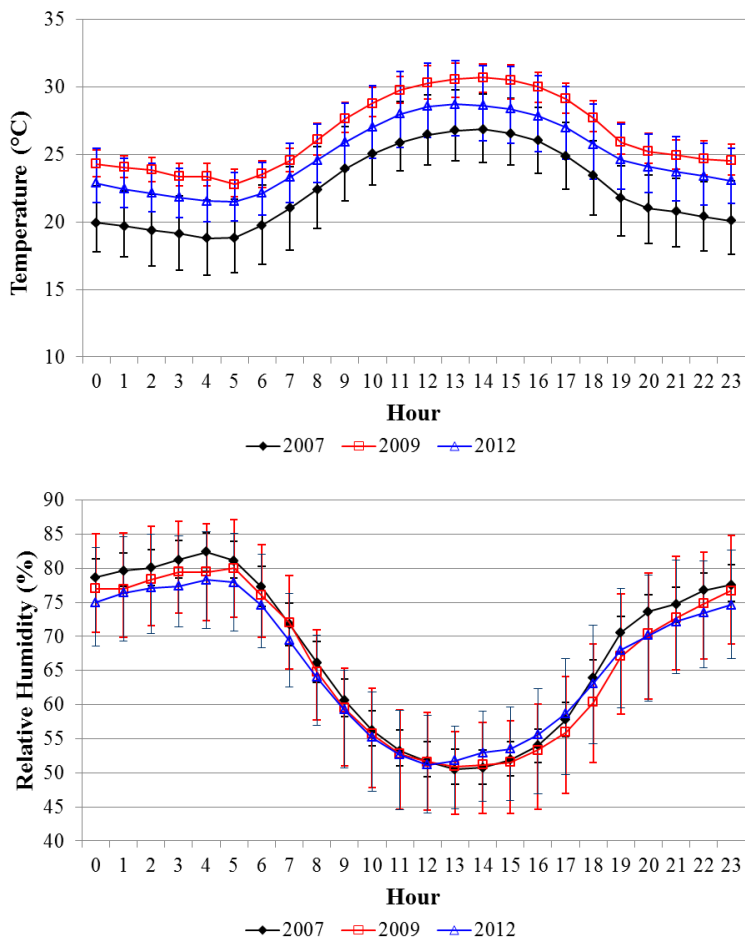


Figure 4.22. Wind rose of the three campaigns in Venice.

Wind velocity was more variable in 2007, however, a general trend was followed in all campaigns (Fig. 4.24a) with a decrease visible in the morning (8-12 a.m.) and an

increase in the afternoon. Further, a single peak was observed in 2007 at 10 p.m. The two prevalent wind directions, characterising the breeze regime, were easily identified (Fig. 4.24b). In 2009, a small variation in wind direction was recorded after midday with respect to 2007 and 2012. Considering the position of the sampling site with respect to the harbour and daily pattern of wind direction, it was determined that the site was downwind during morning during all campaigns.



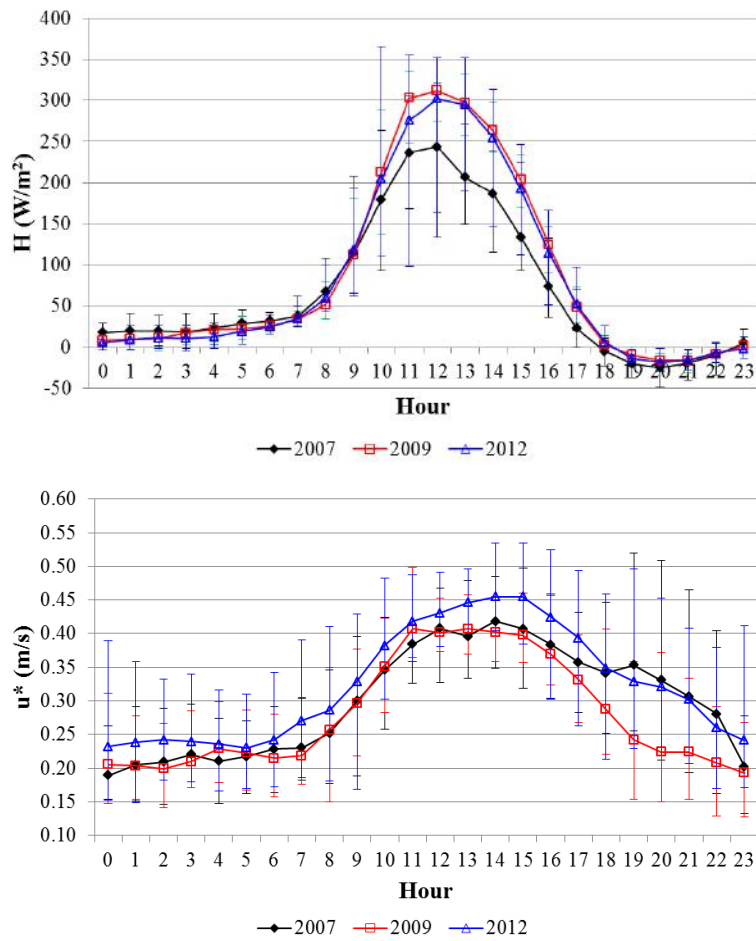
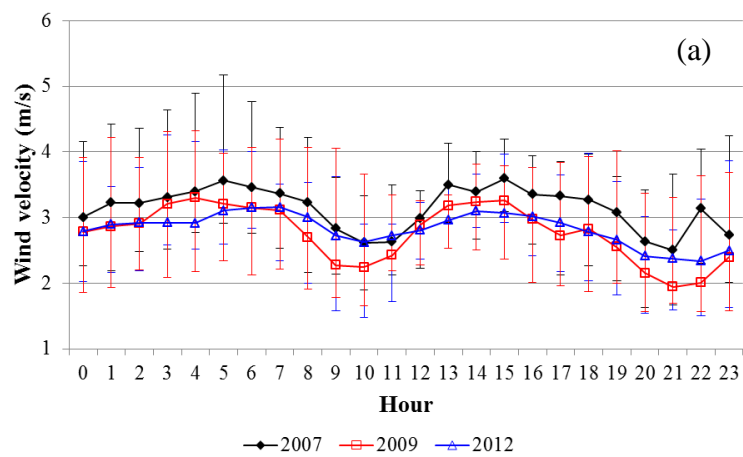


Figure 4.23. Hourly pattern of the main meteorological parameters for the three campaigns (error bars represent the inter-quartile range).



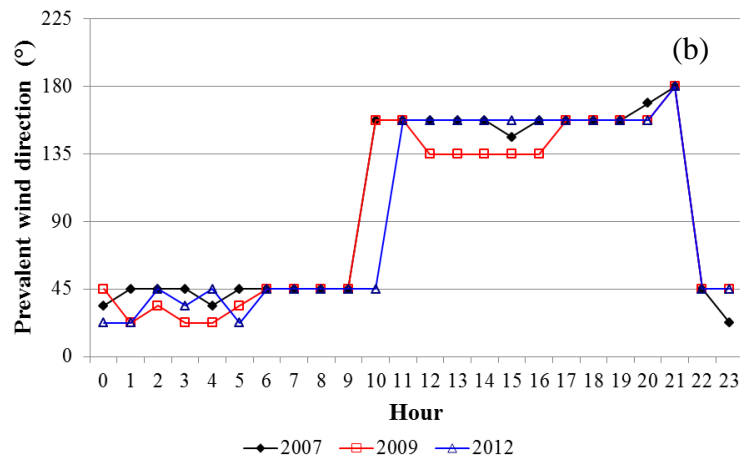


Figure 4.24. Hourly pattern of the (a) wind velocity and (b) wind direction in Venice.

#### 4.2.2 Particulate matter concentrations and ship traffic

As mentioned before for the Brindisi harbour (Donateo et al., 2014), no correlation between daily  $PM_{2.5}$  concentrations and the daily ship traffic was observed in Venice. Consequently, short-duration peaks were considered more suitable to describe shipping impacts associated to arrival or departure of ships (Fig. 4.25).

Generally,  $PM_{2.5}$  and PNC peaks were caused by ship manoeuvring and mooring phases. Since that several manoeuvres occur in the waters off the sampling site at Sacca San Biagio, plume releases during manoeuvring of the same ship were visible as multiple and consecutive peaks long less than 10 min each. Often manoeuvring phase can last long, depending on ship type, space availability for manoeuvrers and position of the berth assigned.

Instead, arrival and departure operations were more clearly identified by higher and shorter (between 5 and 10 min) peaks of  $PM_{2.5}$  and PNC measurements. In particular, PNC were strongly affected, showing a larger increase, in relative terms, of concentrations with respect to those of  $PM_{2.5}$  (Contini et al., 2015).

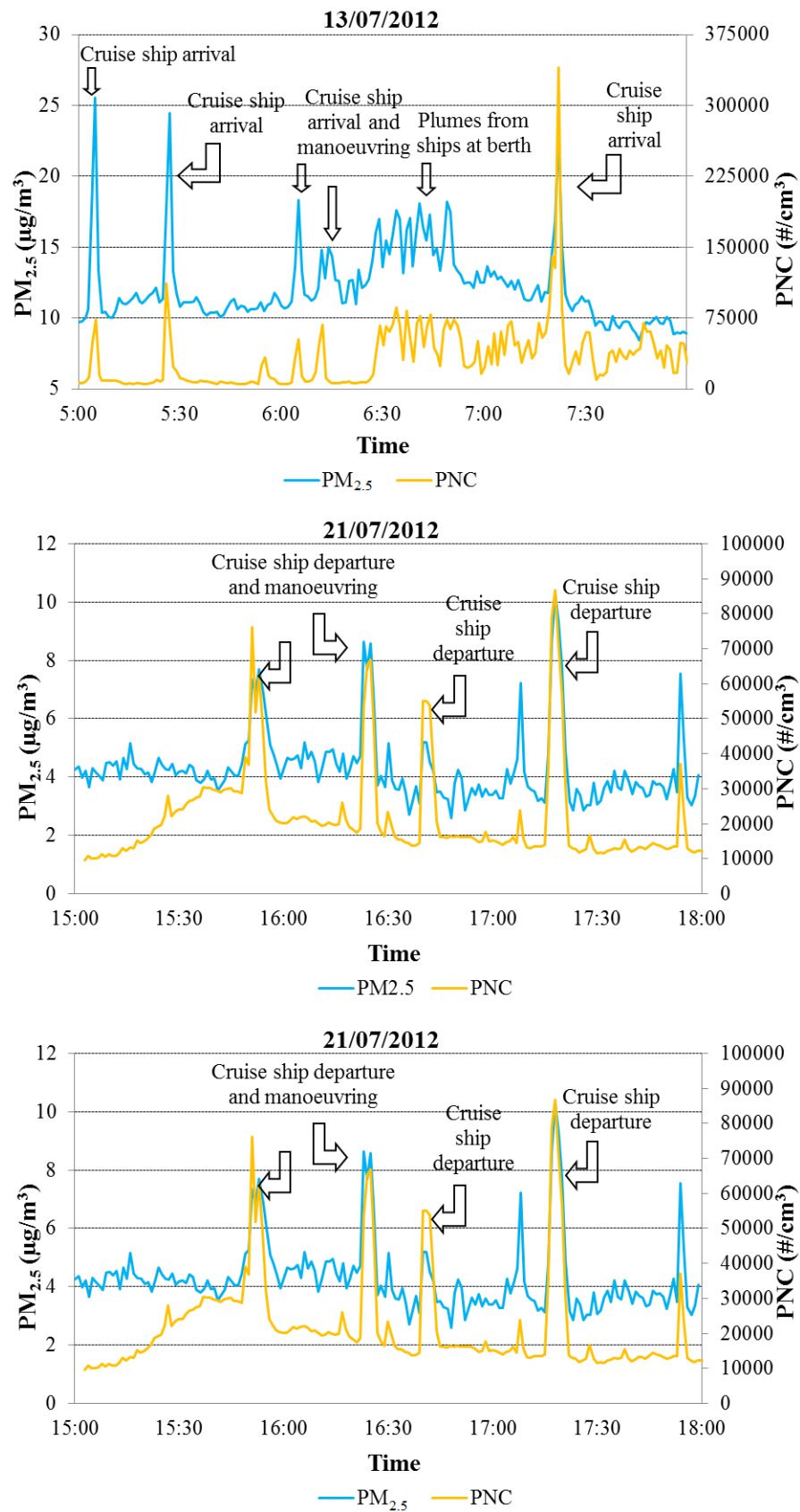


Figure 4.25. Two examples of concentration peaks of PM<sub>2.5</sub> and PNC associated to different ship phases during the 2012 campaign. Adapted from Contini et al., 2015.

Being one of the most tourist destination worldwide, ship traffic in Venice is mainly related to large cruise ships (in 2012, 61.3% of cruise ships larger than 40,000 tons and 22.5% over 100,000 tons). Further, the traffic concentration is greater during spring and summer (83.1% of berths between May and October), as reported in Fig. 4.26.

The total ship traffic, including arrivals and departures in terms of GT, was evaluated on weekly and daily averages for all the three measurement campaigns. The average ship traffic in 2007 was 262.7 ktons/day, 329.5 ktons/day in 2009 and 387.4 ktons/day in 2012. Therefore, a growing trend was recorded especially between 2007 and 2009 (+25.4%) compared to the period 2009-2012 (+17.6%).

The average weekly pattern of ship traffic was very similar among the measurement periods (Fig. 4.27a). A marked increase was visible during weekends (from Friday to Sunday), with the relative maximum on Saturday. Except for 2007, on Sunday started to decrease up to Thursday, to which the minimum ship traffic volume was associated. Practically, comparing the average GT during the time intervals Friday-Sunday and Monday-Thursday, it grew in the weekend by 83.7% in 2007, 152.8% in 2009 and 95% in 2012.

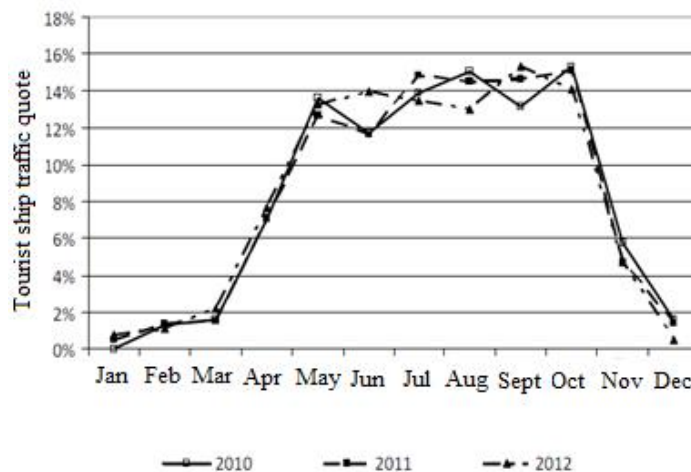


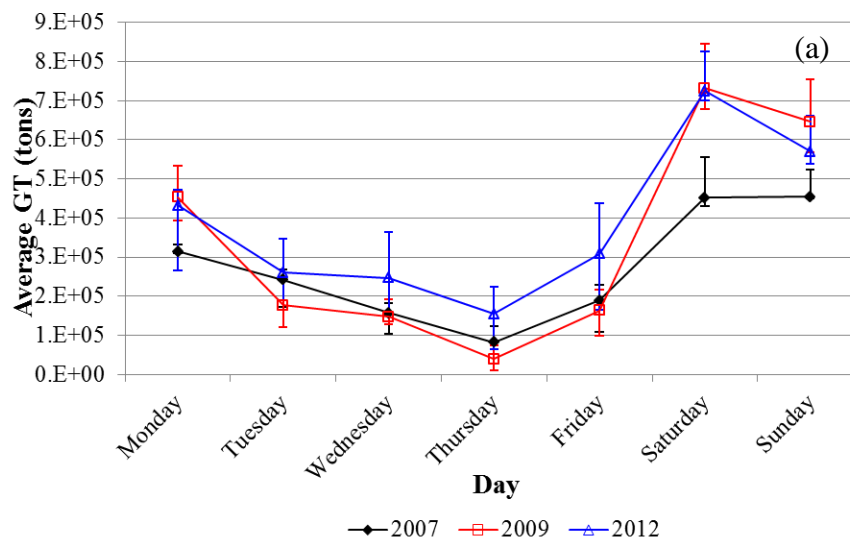
Figure 4.26. Seasonality of tourist ship traffic in Venice, period 2010-2012 (source: Venice Port Authority, 2013).

Besides weekly trend of ship traffic, the average daily patterns were computed for all

measuring years (Fig. 4.27b). In this case, it was possible to highlight some differences. All trends were characterised by two clear peaks, one in the morning and one in the late afternoon corresponding to arrivals and departures of ships respectively. However, a third peak was present at midday in 2012.

The more well-defined pattern was detected in 2009 whereas other minor peaks were present in 2007 at 10 a.m. and 3 p.m.

In detail, the first peak in the morning was shifted one hour before in 2007 (at 6 a.m.) with respect to 2009 and 2012 (at 7 a.m.) and the peak associated to arrivals was shifted at different time during the 2007 (at 6 p.m.), 2009 (at 5 p.m.) and 2012 (at 4 p.m.) campaign. This could be due some changes in the timetable and the presence of other peaks in daytime, especially in 2007 and 2012.



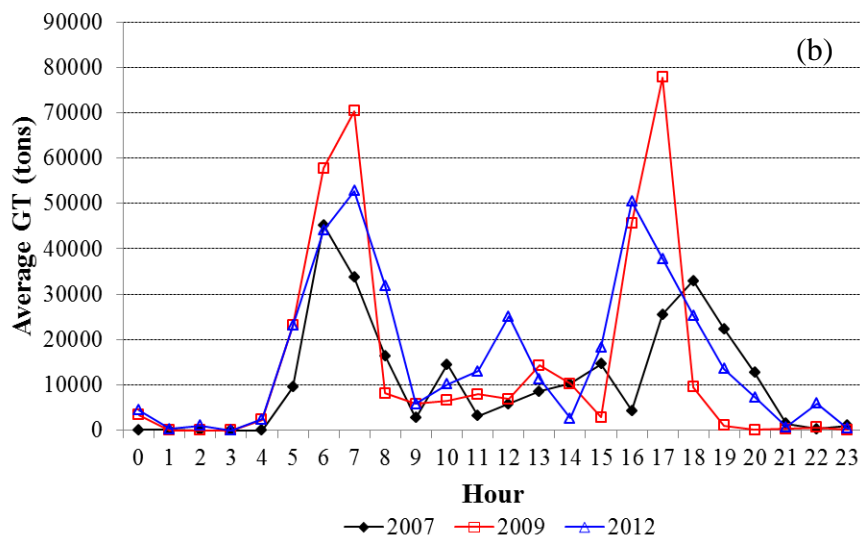


Figure 4.27. Average (a) weekly and (b) daily patterns of tourist ship traffic in Venice during the three campaigns (source: Contini et al., 2015).

The average  $PM_{2.5}$  concentration during the entire measurement periods was  $8.4 \mu\text{g}/\text{m}^3$  (interquartile range  $0.96\text{-}12.37 \mu\text{g}/\text{m}^3$ ) in 2007,  $19.5 \mu\text{g}/\text{m}^3$  (interquartile range  $12.24\text{-}25.55 \mu\text{g}/\text{m}^3$ ) in 2009 and  $12.4 \mu\text{g}/\text{m}^3$  (interquartile range  $5.02\text{-}16.53 \mu\text{g}/\text{m}^3$ ) in 2012. However, weekly and daily patterns were useful to correlate concentrations with ship traffic in time. Weekly trend of  $PM_{2.5}$  concentrations (Fig. 4.28a) showed a different behaviour through the years. In 2007 from Saturday to Tuesday  $PM_{2.5}$  concentrations were comparable (around  $10 \mu\text{g}/\text{m}^3$ ) with the minimum values (around  $5 \mu\text{g}/\text{m}^3$ ) in the middle of the week. A more similar pattern was shown in 2012 with an average variation between the maximum and the minimum values about  $5 \mu\text{g}/\text{m}^3$ . However, the decreasing trend lasted also during the weekend. Finally, the highest concentration values were observed in 2009, with an evident increase between Thursday and Friday. In this case, an increase between  $5 \mu\text{g}/\text{m}^3$  and  $10 \mu\text{g}/\text{m}^3$  could be seen.

Analysing the average daily pattern (Fig. 4.28b), it was evident a general increase during the night and the first morning (between 6 a.m. and 7 a.m.) in all campaigns. Specifically, two small peaks (about  $25 \mu\text{g}/\text{m}^3$ ) were present at 2 a.m. and 7 a.m. (corresponding to the traffic peak in the morning) in 2009. However, only one more smoothed peak was recorded in 2012 at 7 a.m., in correspondence of ships arrivals. The trend obtained in 2007 and 2012 were more similar compared to those for 2009, however, the increasingly pattern appeared shifted towards early night hours, with



the maximum concentrations visible between 4 a.m. and 6 a.m.

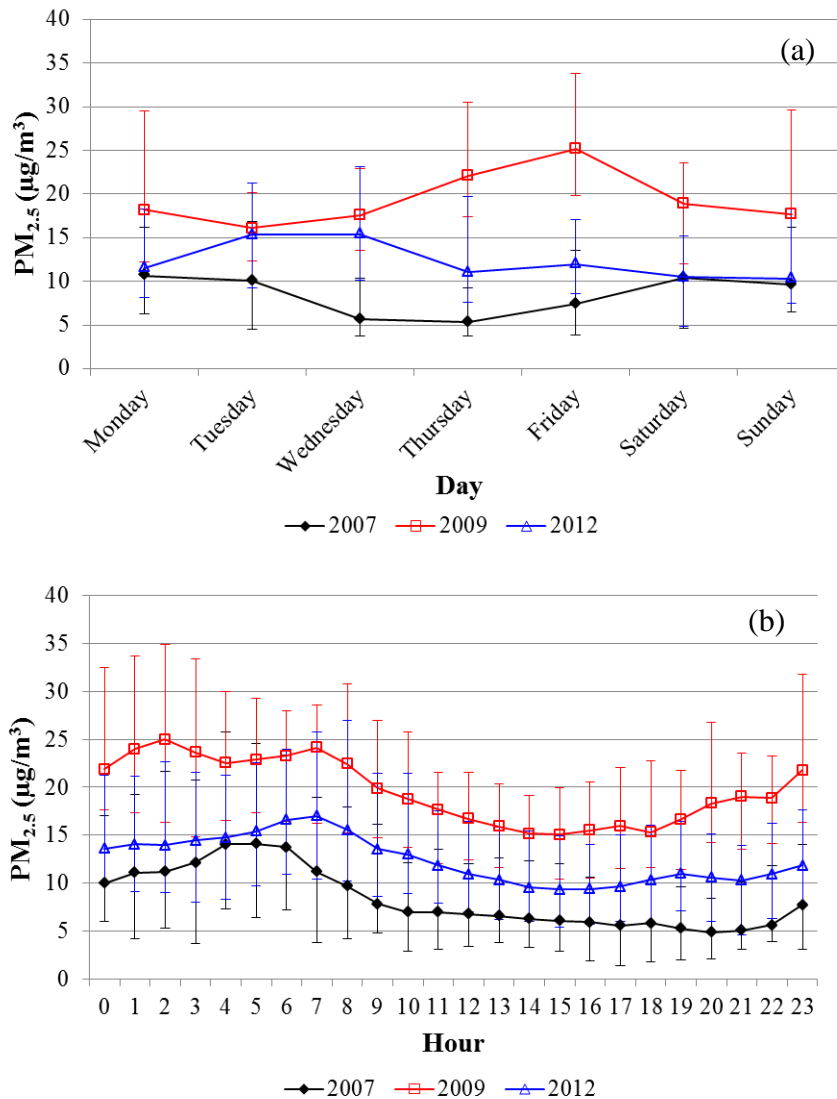


Figure 4.28. Weekly (a) and daily (b) pattern of PM<sub>2.5</sub> concentrations in Venice during the three campaigns.

The average particle number concentration during the measurement period in 2012 was 9,688 #/cm<sup>3</sup> (interquartile range 11,300 #/cm<sup>3</sup>). Weekly and daily trend were computed and showed very different behaviours. No significant differences were recorded through the week (Fig. 4.29a), except for Thursday which showed the lowest PNC values (around 8,000 #/cm<sup>3</sup>) compared to the other days (over 9,000 #/cm<sup>3</sup>).

The daily pattern of PNC (Fig. 4.29b) was characterised by one peak in the morning

at 7 a.m. more pronounced with respect to those of  $PM_{2.5}$  concentrations.

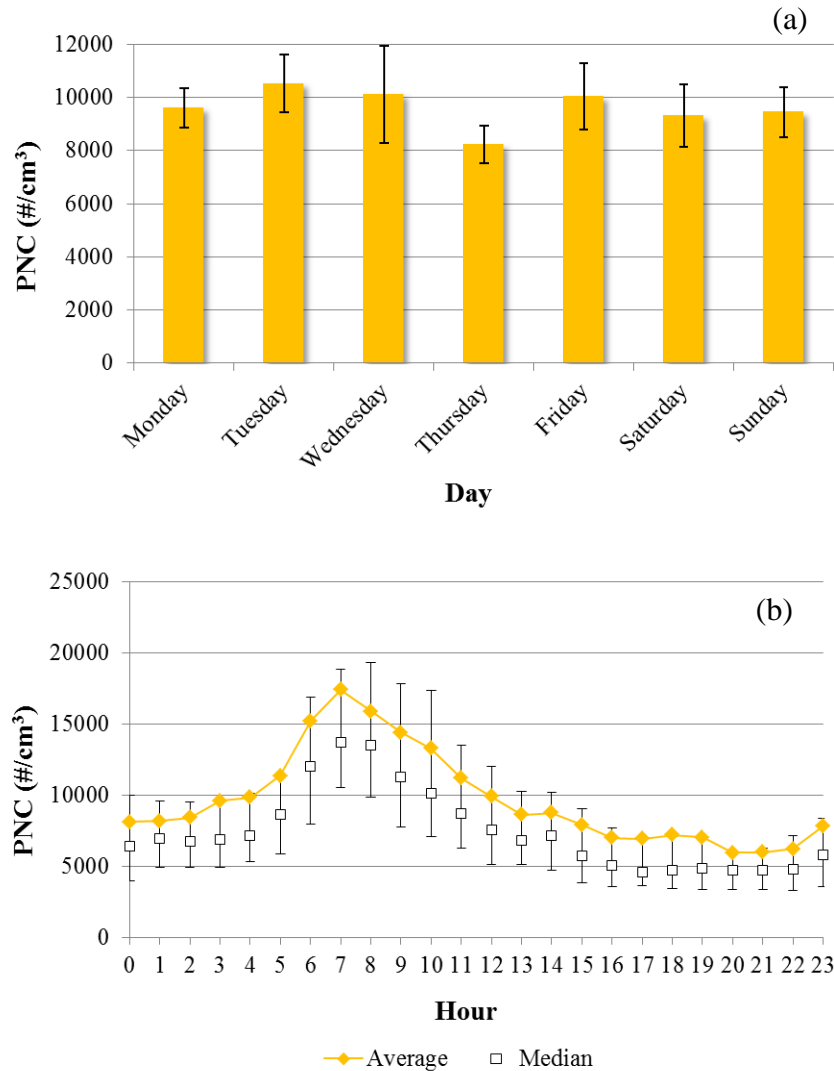


Figure 4.29. Weekly (a) and daily (b) pattern of PNC in Venice during the 2012 campaign.

This was probably due to contribution from other sources present in the area, therefore, the selection of the specific wind direction sector associated to the harbour was needed to evaluate the effective shipping influence to measurements. The correlation between PNC,  $PM_{2.5}$  and ship traffic was not observed (Fig. 4.30) on daily averages, confirming the usefulness of high-resolution measurements.

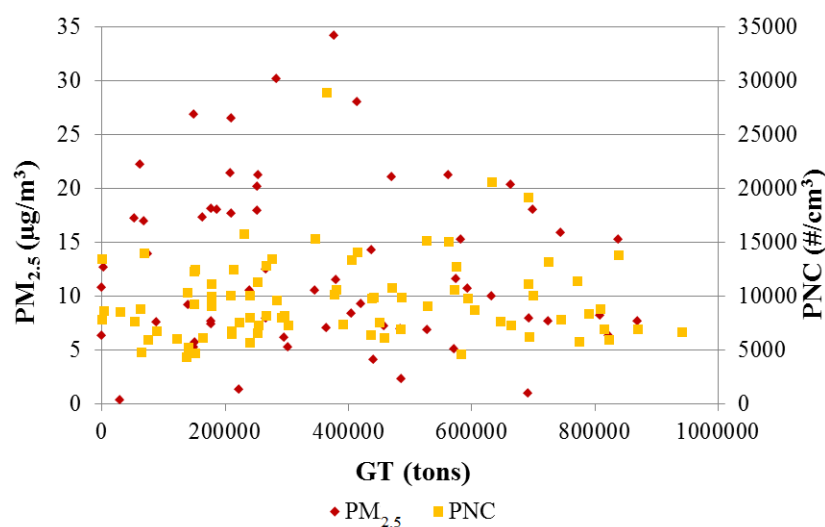


Figure 4.30. Correlation between daily averages of  $PM_{2.5}$ , PNC and ship traffic in Venice during the 2012 campaign.

#### 4.2.3 Primary contribution to pollutants of ship traffic

As demonstrated before, the contribution of ships was not extractable from the atmospheric aerosol daily averages, therefore the estimates were done using data associated to the same wind direction sector and, consequently, to similar periods of day, thus limiting biases (see Section 3.2).

The primary contribution was computed for  $PM_{2.5}$  and PNC concentrations in the different three campaigns following the same methodology applied in Brindisi. In general terms, results confirmed, as already shown for Brindisi, that ship traffic contribution was larger on particle number concentration with respect to  $PM_{2.5}$ . A very clear decrease of the primary ship contribution to  $PM_{2.5}$ , was found moving from 2007 to 2012 (50%), larger than the uncertainties of the estimates, and between 2007 and 2009 (30%) but smaller than the calculated uncertainties (Fig. 4.31), although an increasingly ship traffic (48% in total). Results are discussed in Section 4.3.

#### 4.3 Inter-annual trends in impacts

Experimental data available for Venice and Brindisi in different years were compared to investigate temporal trends in shipping contributions to aerosol and gaseous concentrations. This was possible because of comparable measurement

conditions at the two sites during all campaigns. Similar instrumental equipment, overlapping sampling periods and micrometeorological parameters allowed apply the same statistical methodology and compare estimations.

In the Brindisi harbour results were reported for  $PM_{10}$ ,  $PM_{2.5}$  and PNC concentrations. Being relative to summer 2012 and 2014, the effectiveness of the European Directive (2005/33/EC), entered into force on 01/01/2010, was not verified at the site. Further, hotelling and manoeuvring phases were analysed separately. In this way an evaluation of the influence of different fuels and engine loads could be possible.

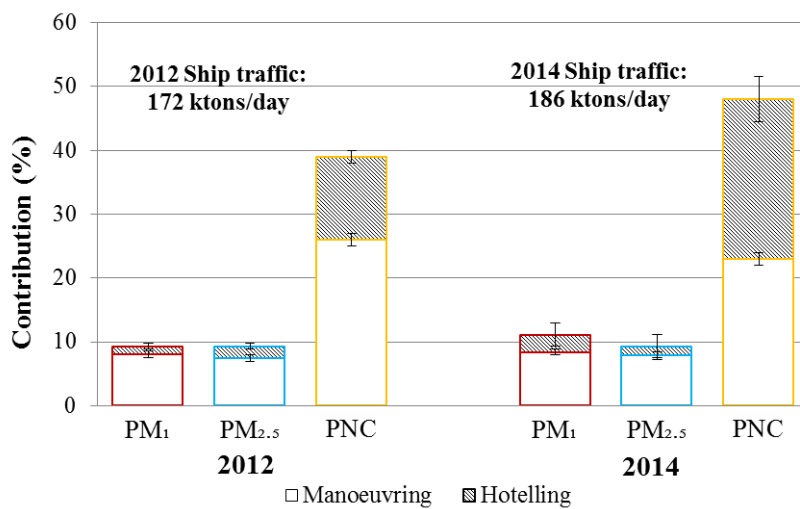


Figure 4.32. Trends of shipping contributions to  $PM_{10}$ ,  $PM_{2.5}$  and PNC concentration (with indication of ship traffic) separated by phase (manoeuvring and hotelling) in Brindisi.

As discussed in Section 4.1.3 some changes in ship traffic were evident from 2012 to 2014. Overall the total Gross Tonnage increased by 8%, moving from 172 ktons/day to 186 ktons/day. Although the growth in the traffic volume, the inter-comparison of average relative primary contributions (Fig. 4.32) showed an almost constant contribution to mass concentrations ( $PM_{10}$  and  $PM_{2.5}$ ) and an increase of contribution to PNC.

No significant differences (from  $7.4 \pm 0.5\%$  to  $7.8 \pm 0.6\%$  for manoeuvring and from  $9.3 \pm 0.5\%$  to  $9.3 \pm 1.8\%$  including hotelling) of the contribution to  $PM_{2.5}$  were observed between the two years. However, if the smaller fraction ( $PM_{10}$ ) was considered, changes slightly increased especially related to hotelling phase. In fact, results indicated an average contribution to  $PM_{10}$  concentrations due to only

manoeuvring raised from  $8.0 \pm 0.5\%$  in 2012 to  $8.4 \pm 0.5\%$  in 2014, therefore with a small increase by  $0.4 \pm 0.5\%$ . Hotelling phase (and related activities) caused a change from  $9.3 \pm 0.5\%$  to  $11.1 \pm 1.8\%$  in the total impact, recording a growth by 1.7%.

It was interesting to note the different primary contributions to PNC for the two operational modes moving from 2012 to 2014. In general, it was clear as both phases affected strongly particle number concentrations with respect mass concentrations. The total contribution (manoeuvring plus hotelling) increased by 9%, changing from  $39 \pm 1\%$  in 2012 to  $48 \pm 3.5\%$  in 2014, although a decreasing trend in manoeuvring contribution (from  $26 \pm 1\%$  in 2012 to  $23 \pm 1\%$  in 2014).

However, a detailed analysis revealed that the impact of hotelling phase grew significantly (12%) with respect to manoeuvring mode (-3%) in 2014, being an increasingly contributor to PNC concentrations.

This was a confirmation of the relevance of the logistics in the harbour, especially on PNC and of the limited effectiveness of the use of low-sulphur content fuels during mooring to reduce in-port emissions. It must be considered that during hotelling many activities occur such as loading/unloading operations carried out by cars, trucks, ship refueling, repair and maintenance services. Therefore, optimization of harbour logistics could be a viable tool to mitigate in-port shipping-related emissions and, consequently, air quality at local scale.

Further, some considerations were possible: a) ship timetable changes observed between 2012 and 2014 did not reduce the total impact to PNC; b) the increased ship traffic (as total GT) between the two years was reflected essentially by particle number concentrations; c) shipping had a growing impact on particles number emissions in port areas when lower loads are used by ships as also observed by Anderson et al. (2015); d) manoeuvring mode affected mainly  $PM_{2.5}$  and  $PM_1$  mass concentrations.

In Venice area, shipping contribution results obtained with the same methodology applied in Brindisi were discussed (Fig. 4.33). In this case, measurements taken at the Sacca San Biagio site in three different years (2007, 2009, and 2012) in comparable conditions allowed evaluate the effectiveness of some mitigation actions implemented at local and international level. However, no trend of contribution to

PNC was evaluated, being measurements available only in 2012. Further, no distinction between phases was reported, because of scarce details in ship traffic data.

In general, as seen in Brindisi, the shipping impact was greater on smaller particles ( $PM_{2.5}$ ), showing a decrease from  $7 \pm 1\%$  in 2007 to  $5 \pm 1\%$  and to  $3.5 \pm 1\%$  in 2012. The decline in  $PM_{2.5}$  contribution was slightly higher moving from 2007 to 2009 ( $2 \pm 1\%$ ) whereas a reduction of  $1.5 \pm 1\%$  was visible between 2009 and 2012. The estimated contribution to  $PM_{10}$  concentrations was more gradually reduced by  $1.6 \pm 1\%$  from 2007 to 2009 and by  $1.1 \pm 1\%$  from 2009 to 2012.

Taking into account that among the campaign periods tourist ship traffic gradually increased between 2007 and 2009 (from 262.7 ktons/day to 329.5 ktons/day, +25.4%) and also moving from 2009 to 2012 (387.4 ktons/day, +17.6%), the effect of some reduction strategies was very clear.

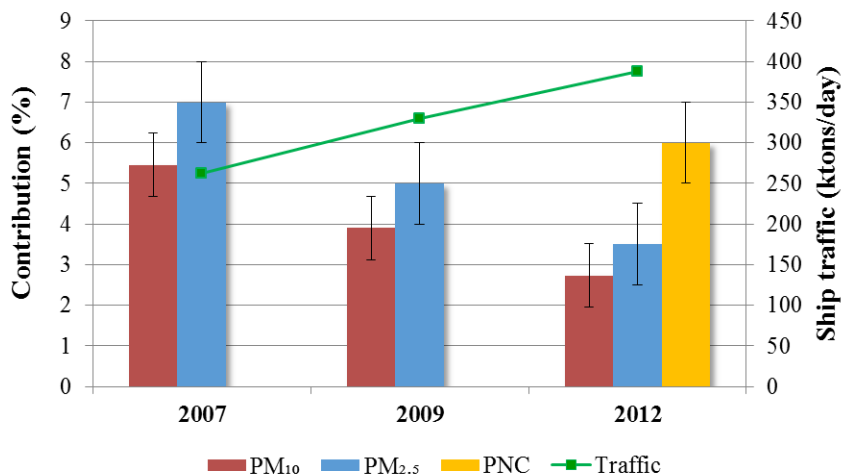


Figure 4.33. Trend of shipping contributions to  $PM_{10}$ ,  $PM_{2.5}$  and PNC concentration (with indication of ship traffic) in Venice. A  $PM_{10}$  to  $PM_{2.5}$  ratio equal to 0.78 was assumed in calculation of the contribution to  $PM_{10}$ .

In particular, between the first two campaigns (2007-2009) the Venice Blue Flag agreement was implemented in the area, consisting in the use of cleaner fuels.

Briefly, the most important improvement was applied to fuels during berth, which passed from 4.5% of sulphur allowed, with no difference between berth and navigation, in 2007 to 1.5% at berth in the period 2008-2009 (see Section 1.6.3).

This voluntary action applied at local level anticipated the implementation (starting from 01/01/2010) of the European Directive 2005/33/EU regarding the use of low-sulphur content fuels which fixed the maximum limit of 0.1% sulphur in harbour (see Section 1.6.2).

Apart from the direct contribution of tourist ship traffic, a further analysis was performed (Contini et al., 2015). In order to reduce the effects of ship traffic variability on the results, the contribution previously obtained was normalized (by ratio) by the average daily ship traffic (Mtons/day). Doing this, the reduction of the primary contributions was more accentuated between 2007 and 2012 (66%) and by 44% from 2007 to 2009 (Fig. 4.34). Therefore, the effectiveness of the adoption of strategies to use “cleaner” fuels was reflected by a significant decrement in the impact of particulate matter which is directly related to sulphur-content in fuels. This led to conclude that also the impact to secondary sulphate and particles smaller than  $PM_{2.5}$  associated to ship emissions could be lowered greater than the primary one.

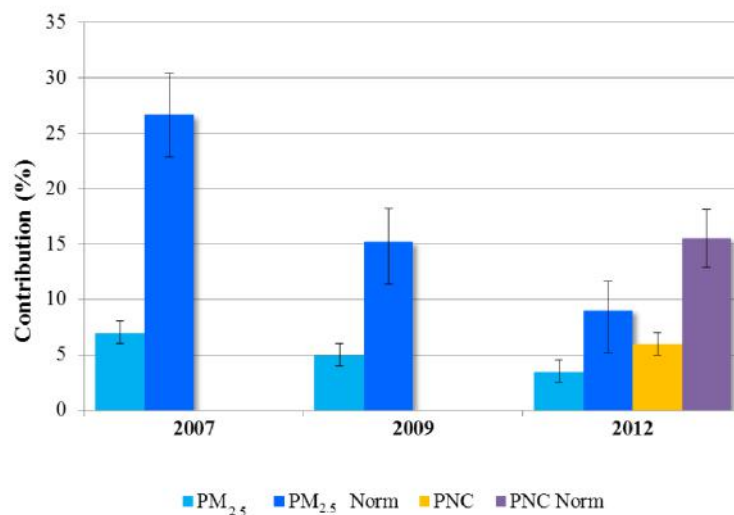


Figure 4.34. Direct (a) and (b) normalized (as difference) primary contribution of tourist ship traffic to  $PM_{2.5}$  and PNC in Venice.

#### 4.4 Comparison of emission inventories data

Emissions from maritime sector for  $NO_x$ ,  $SO_2$  and  $PM_{2.5}$  were computed for the year 2010 (after the implementation of the European Directive 2005/33/EC) at Municipality level (high resolution), according the methodology explained in Chapter 3 (Section 3.3).

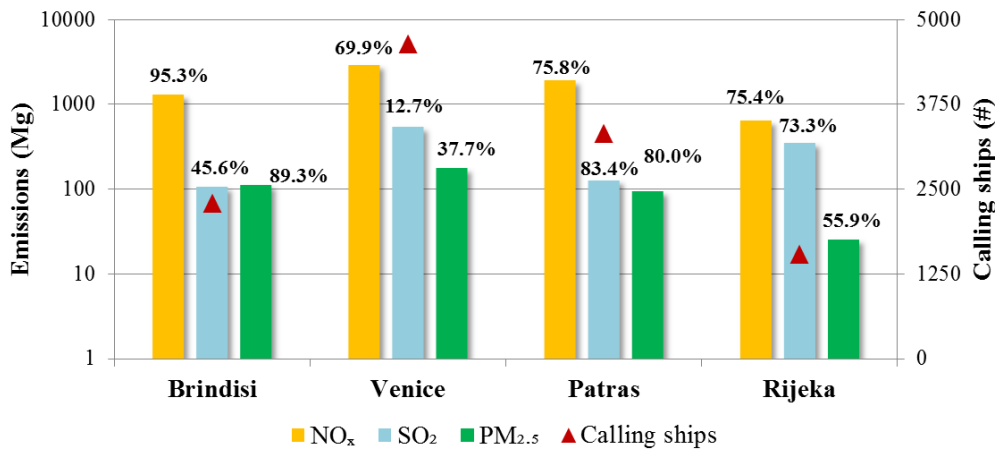


Figure 4.35. Annual emissions (reference year 2010) of NO<sub>2</sub>, SO<sub>2</sub> and PM<sub>2.5</sub> (columns) with indication of % of emissions in hotelling phase, for the four port-cities. Also calling ships (marks) is reported.

In Fig. 4.35 results for each port-city of the POSEIDON project are shown for the main atmospheric pollutants as well as total number of ships calling. In all port-cities, NO<sub>x</sub> were the main shipping emissions in absolute terms with high percentage values (ranging from 69.9% to 95.3%) related to hotelling phase. Instead, SO<sub>2</sub> and PM<sub>2.5</sub> emissions were comparable in Brindisi and Patras whereas they were slightly different in Venice and even more in Rijeka. Overall, Venice was the port-city most affected by maritime emissions, followed by Patras and Brindisi which seemed very similar. Oppositely, Rijeka showed the highest SO<sub>2</sub> emission values and the lowest ones for PM<sub>2.5</sub>.

The estimates were evaluated taking into account ship traffic volume in each site. In this case, the observed emission values were in agreement with the total number of ship calling at the four harbours, with the maximum ships number in Venice and Patras.

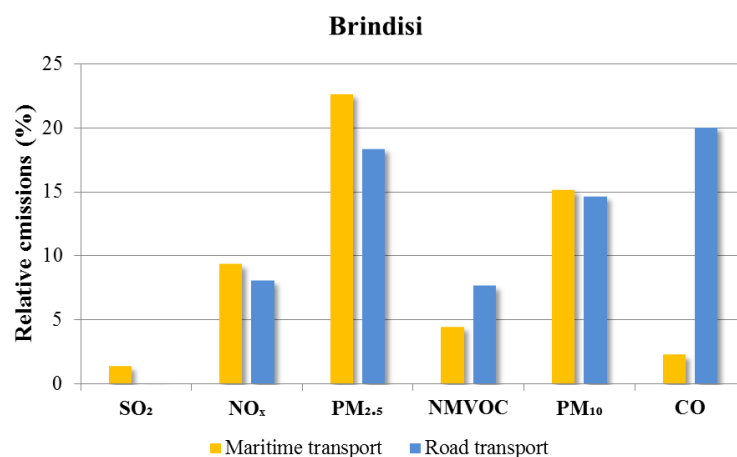
However, the variability of emissions was also related to different ship categories (which characterised the ship traffic volume in the harbour areas considered. In fact, Venice and Patras are two important cruise ports whereas Brindisi and Rijeka have a commercial vocation (with cargo, containers, tankers, bulk carriers).

Hotelling mode was a significant factor that influenced total emissions with a large variability among the sites, ranging from about 70% to 95% for NO<sub>x</sub>, from 13% to



83% for SO<sub>2</sub>, from 38% to 89% for PM<sub>2.5</sub>. The relevant differences could be due to the specific logistics and ship typologies involved in each harbour. It was clear the greatest influence of hotelling phase in Patras, especially on SO<sub>2</sub> emissions. On the contrary, in Venice when ships were at berth the lowest SO<sub>2</sub> emissions were recorded. This is a confirmation of the effect of local agreements to use low-sulphur content fuels in harbour. Besides SO<sub>2</sub>, the major differences were detected for PM<sub>2.5</sub> associated to hotelling phase.

Yearly shipping emissions were compared with those from road traffic at Municipality level (Fig. 4.36), indicating maritime sector as a significant additional emission source in port-cities. In general, the two modes of transport were comparable for PM<sub>2.5</sub> and NO<sub>x</sub> emissions, except for Rijeka (probably related to the context of local emissions). Brindisi and Venice (in which road traffic included also water traffic from public transport) showed a high similarity of relative emissions of both transportation modes. On the other hand, Patras had higher CO relative emissions for maritime sector and lower for PM<sub>10</sub> compared to other sites which had the opposite behaviour. Obviously, shipping was the main responsible of SO<sub>2</sub> emissions in all areas.



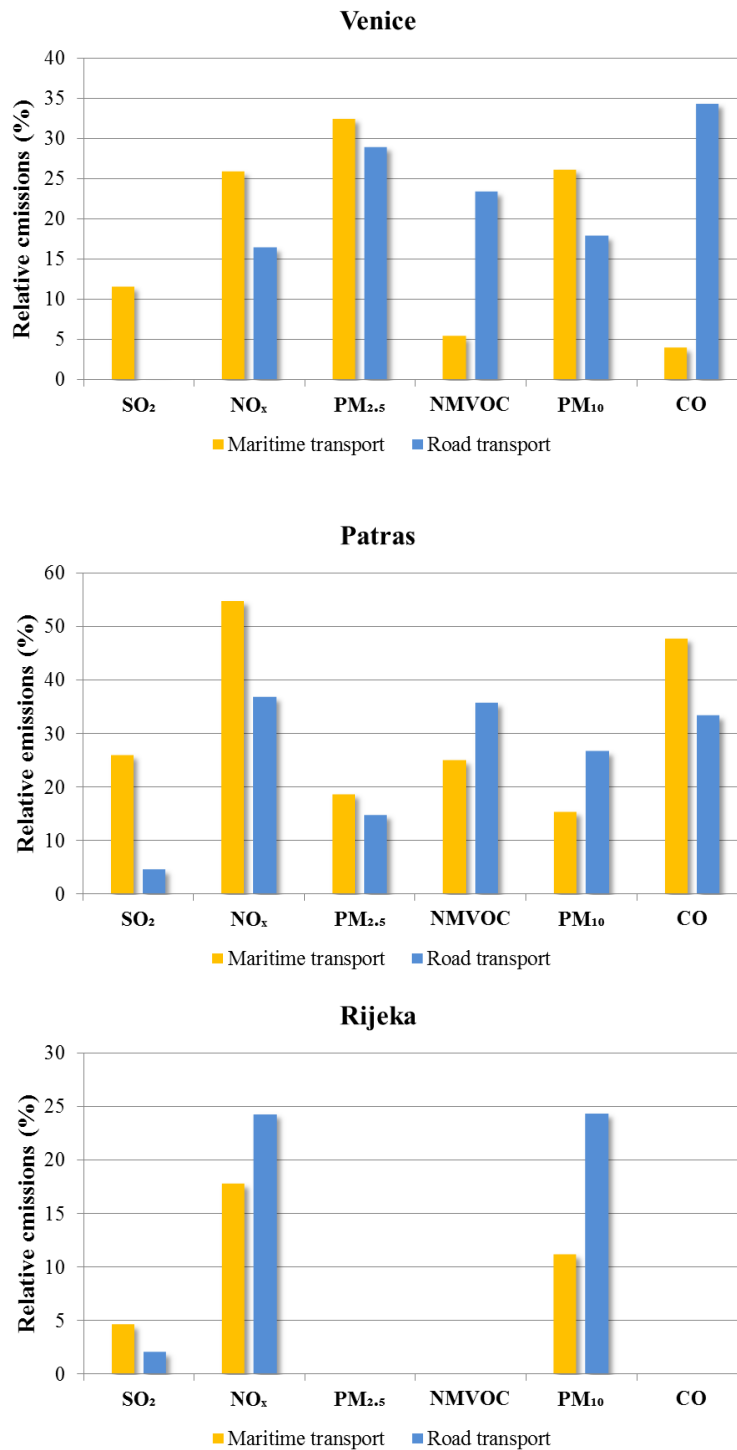


Figure 4.36. Comparison of relative emissions associated to maritime and road transport in the four port cities.

In addition, in Fig. 4.37 the maritime estimates for Brindisi and Venice were further detailed distinguishing manoeuvring and hotelling phase. In general terms, Venice showed the greatest emission values but PM and NO<sub>x</sub> emissions from road and

maritime sectors were comparable at both sites. However, the more visible difference between the two port-cities was the smallest contribution of hotelling phase in Venice, representing less than 50% of total emissions (except for  $\text{NO}_x$ ). This could be the positive effect of mitigation actions implemented in the area in the previous years as well as of the European legislation entered into force in 2010.

In Brindisi, shipping represented 23% of total emissions of  $\text{PM}_{2.5}$ , 9% of  $\text{NO}_x$  and 1% of  $\text{SO}_2$ . Manoeuvring phase was the smallest share of the estimated shipping emissions, representing less than 10% of total emissions for all pollutants, except for  $\text{SO}_2$ . The mandatory use of low-sulphur content fuel at berth limits the weight of hotelling on total emissions.

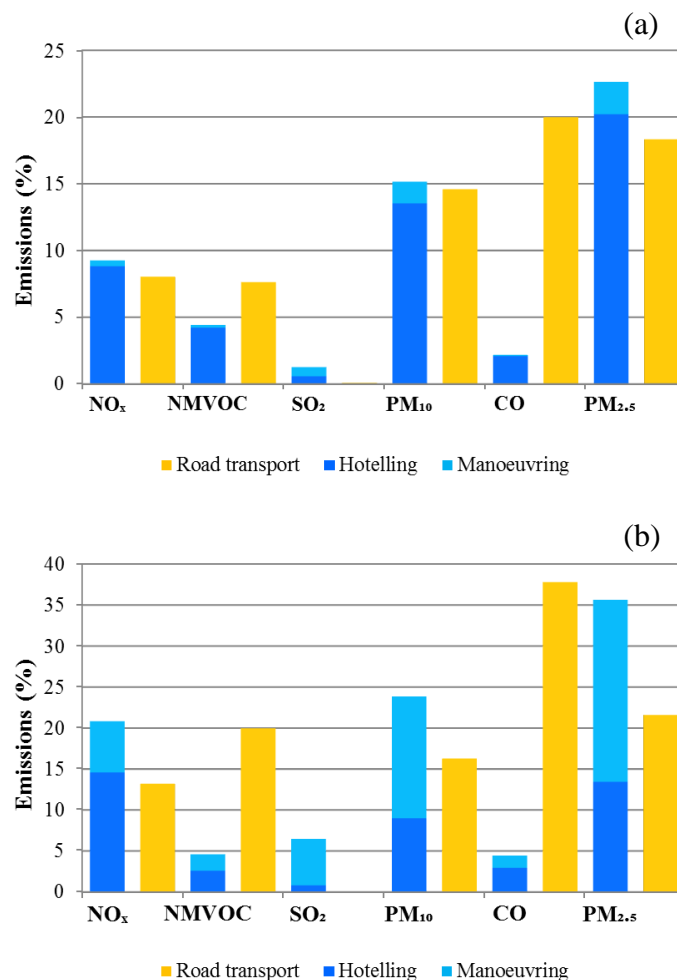


Figure 4.37. Comparison between road and maritime transport separated in manoeuvring and hotelling phase in (a) Brindisi and (b) Venice (reference year 2010).

Emission fluxes of  $\text{SO}_2$  and  $\text{NO}_2$ , measured with DOAS remote sensing system in summer 2012 and 2014, were compared with the estimated emissions from emission

inventories (Fig. 4.38). Also, emission inventory estimates for  $PM_{2.5}$  are shown. It is important to note that  $NO_2$  values of emission inventory were indirectly obtained from  $NO_x$  emissions using the measured in-plume ratio  $NO/NO_2$ . No evident changes were present between the two periods for all pollutants, considering the uncertainties. Effectively, both  $SO_2$  and  $NO_2$  emissions measured by DOAS decreased between 8.6% and 10.4% respectively in 2014, whereas emission inventory estimates of  $NO_2$  were reduced only by 2.5% and those of  $SO_2$  increased by 6.3%. Finally,  $PM_{2.5}$  emissions were lowered of 2.5% in 2014.

Comparison between emission inventory estimates and measurements by DOAS showed a good agreement (better than the uncertainties). It was observed that DOAS measurements were always higher than estimates, excluding  $NO_2$  emissions in 2014 (-4.5%). However, the differences were limited for  $NO_2$  in 2012 (+1.9%) and  $SO_2$  in 2014 (+1%). Only in 2012, a more visible change was calculated for  $SO_2$  (+19.8%).

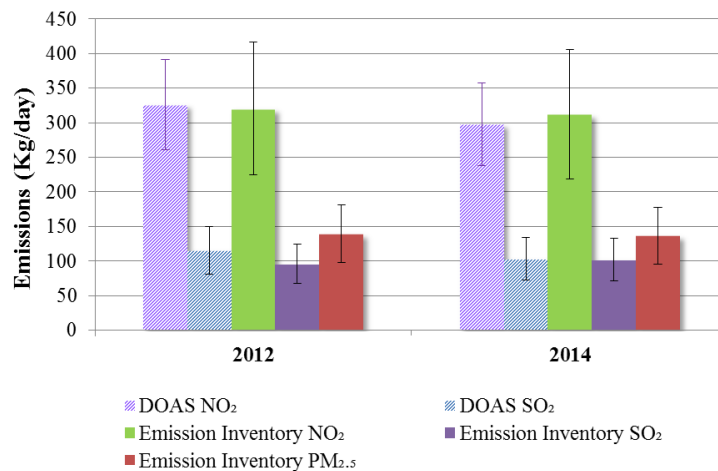


Figure 4.38. Comparison between estimated and measured (by DOAS) gaseous ( $NO_2$ ,  $SO_2$ ) and  $PM_{2.5}$  emissions.

#### 4.5 Modelling results over all the Adriatic/Ionian area

Numerical simulations performed by using the WRF-CAM<sub>x</sub> system were run over a modelling domain covering the Central and Eastern Mediterranean area. As explained in Section 3.3, the zero-out modelling method was implemented involving simulations performed once including and once omitting the ship emissions data. Two different periods were considered (July and January 2012) to illustrate

seasonality (winter/summer) in modelled results, also correlating the different ship traffic volume.

Overall, the shipping impact seemed to be higher on gaseous pollutants (NO, NO<sub>2</sub>, NO<sub>x</sub> and SO<sub>2</sub>) concentration with respect to particulate matter (PM<sub>10</sub> and PM<sub>2.5</sub>) during both periods. In addition, the contribution was quite strong during the warm part of the year, due to the more intense ship traffic.

In relative terms, NO<sub>2</sub> and NO<sub>x</sub> modelling results in July were very similar, with the impact reaching 90% along the main international routes (Southern part of the domain) and 70% on the Adriatic/Ionian area. The influence of shipping on NO<sub>2</sub> and NO<sub>x</sub> could be between 30-50% near the Adriatic/Ionian coasts. Results were very significant for SO<sub>2</sub> simulations, that is 60% was observed in the Adriatic and Ionian Seas decreasing along the coasts to about 40%.

PM<sub>2.5</sub> and PM<sub>10</sub> surface concentrations were impacted by more than 15% and 13% respectively, covering the main shipping routes (between Sicily and Tunisia) and more than 5% and 3% respectively in the Adriatic-Ionian area. The contributions to PM<sub>2.5</sub> and PM<sub>10</sub> decreased to less than 3% along the coasts of the Adriatic/Ionia area. During winter, the contributions dropped especially for SO<sub>2</sub> surface concentrations, which described essentially only the international traffic in that period. Over the international shipping routes the decrease was more than 80% but for the Adriatic and Ionian Seas this percentage reached 60% and along coastal areas was below 10%. However, PM<sub>2.5</sub> and PM<sub>10</sub> concentrations reached a reduction of about 10% and 5% respectively, at the largest scale. Regarding the Adriatic and Ionian Seas, the reduction was below 5% and 3% for PM<sub>2.5</sub> and PM<sub>10</sub> respectively, lowering to 4% (PM<sub>2.5</sub>) and to less than 3% (PM<sub>10</sub>) near the coasts.

In Fig. 4.39 and Fig. 4.40 results are reported for July and January 2012, respectively.

Chapter 4. Results and discussion

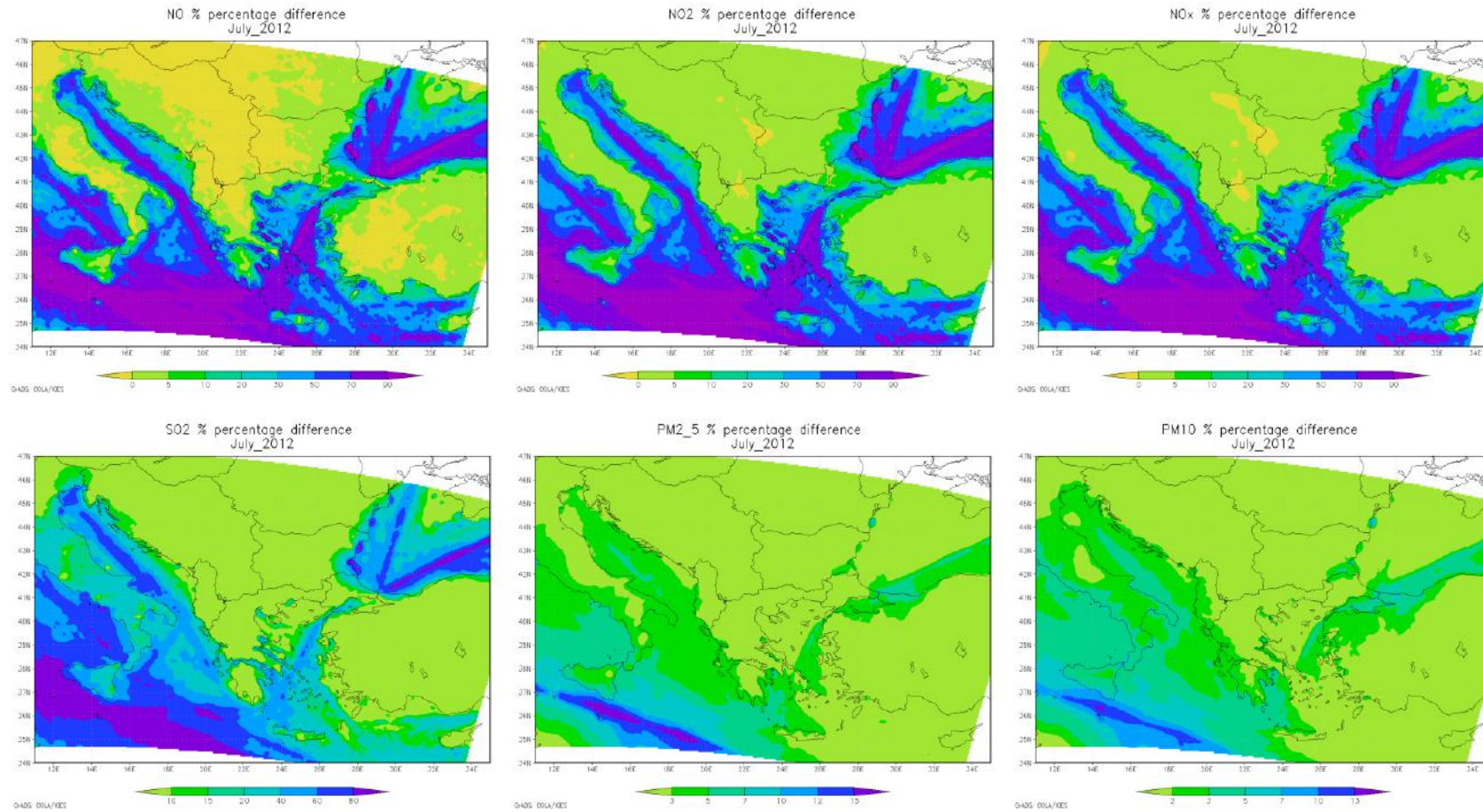


Figure 4.39. Modelled relative impact on atmospheric pollutants on a regional scale for July 2012.

Chapter 4. Results and discussion

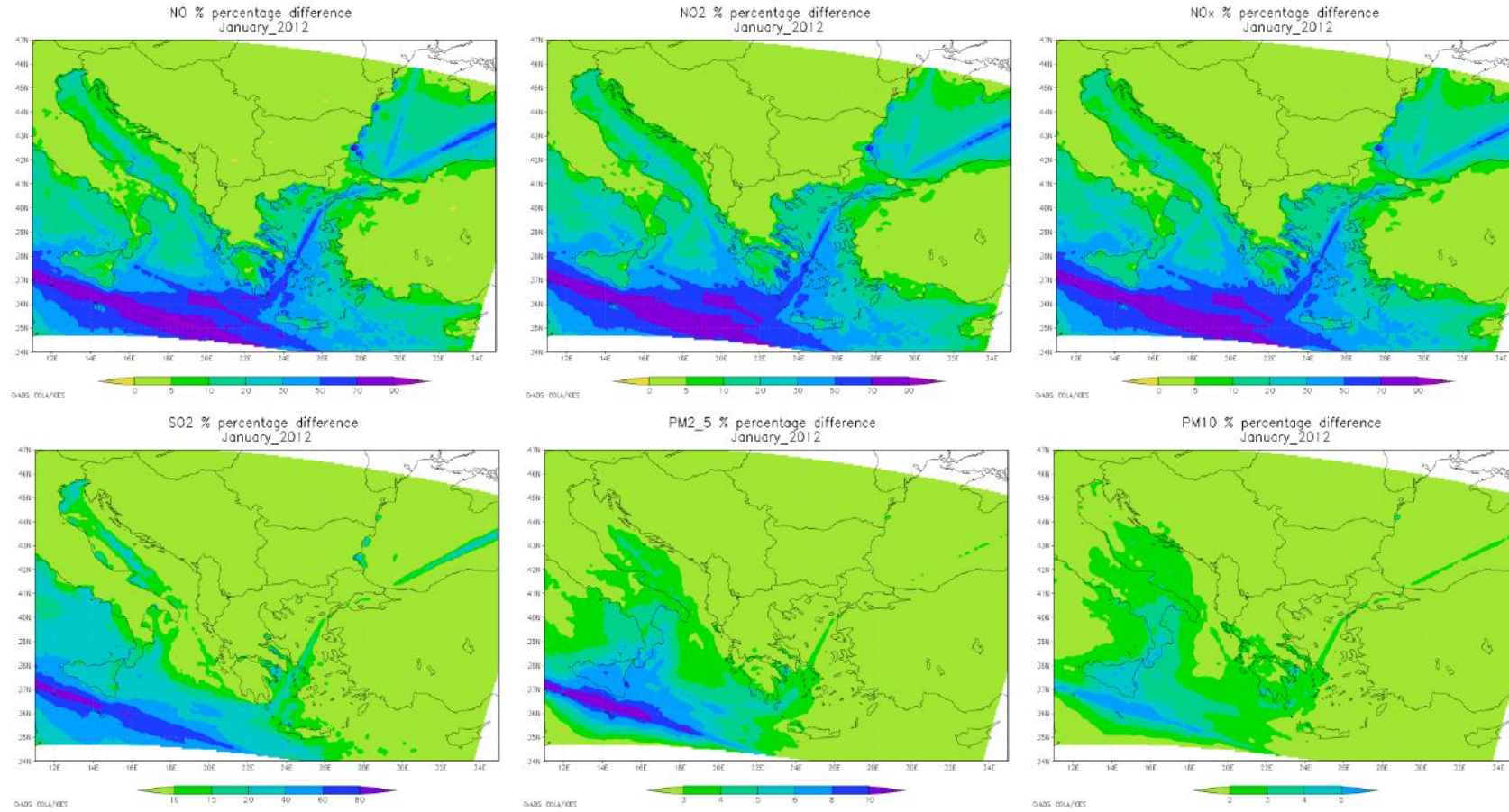


Figure 4.40. Modelled relative impact on atmospheric pollutants on a regional scale for January 2012.

In order to investigate impacts on the measurement sites simulation cells of 6x6 km were extracted for each port-city and for winter and summer periods.

In Tab. 4.5 besides to Venice and Brindisi, modelled results for Patras and Rijeka (studied in POSEIDON project) are also reported. As expected, a clear seasonality was observed in all sites and the highest impacts on gaseous pollutants compared to particulate matter were recorded.

Table 4.5. Modelled contribution to atmospheric pollutants concentration in the four port-cities computed for January (winter) and July (summer) 2012.

Area	Period	NO (%)	NO <sub>2</sub> (%)	NO <sub>x</sub> (%)	SO <sub>2</sub> (%)	PM <sub>2.5</sub> (%)	PM <sub>10</sub> (%)
Brindisi	Winter	17.9	16.7	16.5	23.5	5.0	3.9
	Summer	23.1	32.5	31.7	46.3	4.7	3.7
Venice	Winter	5.7	2.8	3.6	5.2	1.2	1.2
	Summer	5.0	9.1	8.9	16.5	2.6	2.3
Patras	Winter	15.4	14.6	14.3	8.8	2.6	2.1
	Summer	18.2	22.5	21.6	24.7	3.4	2.5
Rijeka	Winter	12.9	9.7	10.2	2.4	1.1	1.0
	Summer	14.3	21.9	21.7	4.1	2.2	2.0

Modelled results were in reasonable agreement with estimated impacts on PM<sub>2.5</sub> (Venice) and PM and gaseous concentrations in Brindisi.

Brindisi had the greatest values either in summer and winter periods for all pollutants whereas Venice was one of the less impacted from shipping. However, the seasonality of contribution to PM<sub>2.5</sub> and PM<sub>10</sub> was not significant in Brindisi compared to the other pollutants and harbours. Only in Brindisi, PM<sub>10</sub> and PM<sub>2.5</sub> were lower during summer whereas NO<sub>2</sub>, NO<sub>x</sub> and SO<sub>2</sub> doubled. In Patras SO<sub>2</sub> emissions were three times lower in winter and NO<sub>2</sub> more than two times reduced in Rijeka. In Venice the difference between gaseous and particulate pollutants was weaker with respect to the other sites and the shipping contribution to SO<sub>2</sub> was lower than those observed for Patras and Brindisi in both winter and summer periods.



## **Conclusions and perspectives**

The main objective of this thesis is the analysis of how harbour emission sources contributed to particulate matter, PM, (both in mass and number) and to gaseous concentrations measured in the Adriatic port-cities of Brindisi and Venice. A common state-of-the-art methodology based on emission inventories, numerical modelling and experimental results has been used to obtain comparable information at the two sites. This allowed to investigate inter-annual trends and the efficiency of mitigation strategies as well as to furnish with the aim to propose plan future actions for sustainable development and management of harbours in the study region. The two port-cities analysed are very different in traffic volume and vocation, being Venice the first cruise home-port of the Mediterranean Sea and Brindisi essentially a commercial port. A multidisciplinary approach which integrated experimental data of different field campaigns performed in Venice (2007, 2009, and 2012) and Brindisi (2012 and 2014), estimates of emission inventories and modelling simulations was applied. This allowed obtaining comparable results through the years and sites.

Results obtained in Venice suggested that the influence of the increasing tourist ship traffic (48% from 2007 to 2012) could be mitigated by local strategies implemented in the area on reducing sulphur-content in ship fuels. In fact, between 2007 and 2009, the decrease (2%) of shipping impact was likely due to the voluntary agreement “Venice Blue Flag”. In addition, the declining trend (-1.5% with respect to 2009) continued in 2012, probably associated to the adoption (starting from 01/01/2010) of the European legislation (2005/33/EC Directive) on low-sulphur content fuel in harbour areas. Finally, numerical simulations for Venice revealed the weaker relative difference between shipping influence on gaseous and PM concentrations, oppositely to the other sites.

In Brindisi, it was determined how much shipping emissions compromised air quality of coastal areas in different phases such as navigation along the coast and while manoeuvring and mooring in harbours. Moreover, during the 2014 campaign, further impact analysis was carried out on gaseous pollutants and particulate matter of different sizes (0.009-32  $\mu\text{m}$ ). The average contribution estimated was larger on gaseous concentrations ( $\text{SO}_2$  and  $\text{NO}_x$ ) than to particle concentrations (in mass and number) in both measurement periods. The contributions to gases ( $\text{NO}$ ,  $\text{NO}_2$  and

SO<sub>2</sub>) were more accentuated on NO and NO<sub>2</sub> during hotelling phase, provoking a local depletion of O<sub>3</sub>. The shipping influence on PM and SO<sub>2</sub> did not show important changes between the two phases.

The impact on PNC was about 4 times larger with respect to the impact on PM<sub>2.5</sub>. Since that actually, the current European legislation of Air Quality Standards (2008/50/EC) sets limits only for PM<sub>10</sub> and PM<sub>2.5</sub>, results lead to propose PNC as a more suitable metric for evaluating the impact of shipping as pollution source to be included in future international policies.

As expected, mass concentration was essentially determined by particles in accumulation and coarse modes whereas particles in the ultrafine fraction ( $D_p < 0.25 \mu\text{m}$ ) were the large majority (around 99%) of particle number concentration. However, particle size ranges seemed to be impacted differently, according to different ship operational phase. Hotelling phase contributed to PNC of smaller particles than  $0.25 \mu\text{m}$  and larger than  $1 \mu\text{m}$  but it was not relevant on particles between  $0.4$  and  $1 \mu\text{m}$ . With regards to mass contribution, manoeuvring phase was significant especially for particles larger than  $0.4 \mu\text{m}$  up to  $8-9 \mu\text{m}$ . In this range manoeuvring impact exceeded those of hotelling phase, consisting, on average, 80% of PM<sub>1</sub> and 83.5% of PM<sub>2.5</sub>.

Definitively, the impact of harbour-related activities was a relevant share of the total contribution to the different pollutants inside the harbour area. This indicated the decisive role of harbour logistics indicating arrival/departure schedules of ships, loading/unloading operations. Therefore, it is needed to adopt good harbour management practices at short-time and sustainable development plans in the air quality policy for the future.

The inter-comparison analysis between 2012 and 2014 summer period measurements at Brindisi port showed a slightly growth of the primary contribution to PM<sub>2.5</sub> and a significant increase of those to PNC during hotelling phase compared to manoeuvring.

In addition, the comparison between DOAS remote sensing emissions and estimates of shipping emissions from emission inventories suggested DOAS as a very good technique to monitor gaseous emissions from ships.

The impact on PM<sub>2.5</sub> concentrations for the simultaneous campaigns in 2012 was less than half in Venice compared to those in Brindisi. Actually, impact results for PM<sub>2.5</sub> in Brindisi appeared more comparable with those obtained in Venice before the implementation of the European Directive 2005/33/EC (campaigns 2007 and 2009). The dissimilarity was more significant for PNC in the same year with an impact higher by 20% ± 1% in Brindisi. However, an important factor to consider was the greatest distance between the sampling site and ship emissions in Venice with respect to Brindisi.

Emission inventories at Municipality level highlighted that maritime activities should be seriously considered as significant air pollution source as much as road traffic. This is particularly clear for PM and NO<sub>x</sub>, with the highest yearly absolute values in Venice (in line with ship traffic volume) with respect to the other sites considered in POSEIDON project. Further, it was interesting to note that in Venice area hotelling contribution on total maritime emissions was the smallest one for all pollutants investigated, with the main evidence for SO<sub>2</sub>, of which shipping is the major emitter worldwide.

Numerical modelling confirmed the seasonal trend of ship traffic in the Adriatic/Ionian area with more intense activity in summertime and, therefore, the maximum impacts. Finally, the estimated impacts were reasonably comparable with those from simulations. Results obtained in Brindisi and Venice were in agreement with typical values of other European harbours and, regarding PNC, they confirmed the predominance of ultrafine particles within ship emissions as found in other works (Healy et al., 2009; Diesch et al., 2013).

One of the objective of this work was to develop an integrated methodological tool to investigate the impact of shipping to air quality that could be exported to other port-cities providing information potentially useful for defining new strategies to reduce these impacts at Mediterranean level. The Adriatic-Ionian macro-region, focus area in this work, represents a growing shipping market for tourism and commerce. However, few studies have been focused on air pollution from shipping and therefore on relative mitigation policies.

Generally, specific reduction strategies can be addressed to minimize critical points identified in each site, taking into account enforceability, implement ability,

cost-effectiveness, infrastructural investments, emissions reduction potential. In most cases, a mix of solutions is chosen, involving public institutions, ship companies and associations.

Although no future emission scenario was provided in this study, some possible mitigation actions may be adopted at short-term and at local scale in the port-cities studied. However, further cost-benefits analyses are necessary to individuate long-term solutions for an “environment friendly” port development (i.e. use of LNG, On-Shore Supply).

At the present, the most simple and reliable action, already successfully implemented in Venice area, is the use of low-sulphur fuel by ships in harbour. Also the application of retrofitting technologies such as seawater scrubbers during hotelling and manoeuvring could be a valid alternative to other more costly and complex actions. Greater attention should be taken to develop and adopt targeted guidelines for harbour logistics such as optimization of docking position, of approach and departure routes, hotelling time. Other urgent measures should consider road traffic (heavy duty vehicles, road freight, passenger traffic) induced by port activities, which has great detrimental effects on local air quality as observed in Brindisi. For example, an efficient management of traffic flow by regulating port access or minimizing queue time with the engine running could be useful.

In conclusion, a fundamental issue is represented by the need of networking of port and environmental Authorities of the different port-cities in order to exchange and update information, to adopt shared measures to achieve common goals of sustainable port growth. In fact, a transnational collaboration could allow an efficient mitigation policy of shipping at large scale (i.e., for example, Mediterranean Basin) without hindering competitiveness of the harbours involved.

Finally, in the context of climate change maritime sector will play an increasingly decisive role considering its growth rate and potential effects at different scales. However, different scientific approaches should be applied to investigate separately shipping impacts associated to open-sea navigation and related to in-port activities. Since the differences in terms of emissions and exposure levels, it is important to specifically characterise and regulate them from a technical and legislative point of view.

## References

- Adamo, K., Garonna, P., 2009. Euro-Mediterranean Integration and Cooperation: Prospects and Challenges, No 2009\_9, UNECE Annual Report Economic Essays, UNECE. Available at [http://www.unece.org/fileadmin/DAM/oes/nutshell/2009/9\\_EuroMediterranean.pdf](http://www.unece.org/fileadmin/DAM/oes/nutshell/2009/9_EuroMediterranean.pdf).
- Agrawal, H., Eden, R., Zhang, X., Fine, P.M., Katzenstein, A., Miller, J.W., Ospital, J., Teffera, S., Cocker, D.R., 2009. Primary particulate matter from ocean-going engines in the Southern California air basin. *Environ. Sci. Technol.* 43(14), 5398–5402. <http://pubs.acs.org/doi/abs/10.1021/es8035016>.
- Agrawal, H., Malloy, Q.G.J., Welch, W.A., Miller, J.W., Cocker III, D.R., 2008a. In-use gaseous and particulate matter emissions from a modern ocean going container vessel. *Atmos. Environ.* 42, 5504–5510. <http://dx.doi.org/10.1016/j.atmosenv.2008.02.053>.
- Alföldy, B., Lööv, J.B., Lagler, F., Mellqvist, J., Berg, N., Beecken, J., Weststrate, H., Duyzer, J., Bencs, L., Horemans, B., Cavalli, F., Putaud, J.-P., Janssens-Maenhout, G., Csordás, A.P., Van Grieken, R., Borowiak, A., Hjorth, J., 2013. Measurements of air pollution emission factors for marine transportation in SECA. *Atmos. Meas. Tech.* 6, 1777–1791. <http://dx.doi.org/10.5194/amt-6-1777-2013>.
- Amato, F., Pandolfi, M., Escrig, A., Querol, X., Alastuey, A., Pey, J., Pérez, N., Hopke, P., 2009. Quantifying road dust resuspension in urban environment by multilinear engine: a comparison with PMF2. *Atmos. Environ.* 43, 2770–2780. <http://dx.doi.org/10.1016/j.atmosenv.2009.02.039>.
- Anderson, M., Salo, K., Hallquist, Å.M., Fridell, E., 2015. Characterization of particles from a marine engine operating at low loads. *Atmos. Environ.* 101, 65–71. <http://dx.doi.org/10.1016/j.atmosenv.2014.11.009>.
- Andreasen, A., Mayer, S., 2007. Use of seawater scrubbing for SO<sub>2</sub> removal from marine engine exhaust gas. *Energ. Fuel.* 21(6), 3274–3279. <http://pubs.acs.org/doi/abs/10.1021/ef700359w>.
- APICE Project Final Publication, 2013. Reducing atmospheric pollution in the Mediterranean port cities. ISBN 978-88-7504-166-3. <http://www.apice-project.eu/>
- Arduino, G., Murillo, D.C., Ferrari, C., 2011. Key factors and barriers to the adoption of cold ironing in Europe. [http://ww2.unime.it/sefisast/SEFISAST/Conference\\_Paper\\_files/Arduino\\_Carrillo\\_Murillo\\_Ferrari.pdf](http://ww2.unime.it/sefisast/SEFISAST/Conference_Paper_files/Arduino_Carrillo_Murillo_Ferrari.pdf).
- ATI, Instruction manual P/N 1800114, September 2010, Revision B. <http://www.atitest.com/wp-content/uploads/2016/05/1800114-Manual-Diffusion-Dryer-rev-C.pdf>.
- Ault, A.P., Gaston, C.J., Wang, Y., Dominguez, G., Thiemens, M.H., Prather, K.A., 2010. Characterization of the single particle mixing state of individual ship plume events measured at the Port of Los Angeles. *Environ. Sci. Technol.* 44, 1954–1961. <http://pubs.acs.org/doi/abs/10.1021/es902985h>.

- Ballini, F., Bozzo, R., 2015. Air pollution from ships in ports: The socio-economic benefit of cold-ironing technology. *Res. Trans. Bus. Manage.* 17, 92-98.
- Bartolomé, A., McAleer, M., Ramos, V., Rey-Maqueira, J., 2009. Cruising in Risky business. CIRJE Discussion paper. <http://www.cirje.e.u-tokyo.ac.jp/research/dp/2009/2009cf664.pdf>.
- Becagli, S., Sferlazzo, D.M., Pace, G., di Sarra, A., Bommarito, C., Calzolari, G., Ghedini, C., Lucarelli, F., Meloni, D., Monteleone, F., Severi, M., Traversi, R., Udisti, R., 2012. Evidence for heavy fuel oil combustion aerosols from chemical analyses at the island of Lampedusa: a possible large role of ships emissions in the Mediterranean. *Atmos. Chem. Phys.* 12(7), 3479–3492. <http://dx.doi.org/10.5194/acp-12-3479-2012>.
- Beirle, S., Platt, U., von Glasow, R., Wenig, M., Wagner, T., 2004. Estimate of nitrogen oxide emissions from shipping by satellite remote sensing. *Geophys. Res. Lett.* 31, L18102. <http://dx.doi.org/10.1029/2004GL020312>.
- Berg, N., Mellqvist, J., Jalkanen, J.-P., Balzani, J., 2012. Ship emissions of SO<sub>2</sub> and NO<sub>2</sub>: DOAS measurements from airborne platforms. *Atmos. Meas. Tech.* 5, 1085–1098. <http://dx.doi.org/10.5194/amt-5-1085-2012>.
- Binnig, J., Meyer, J., Kasper, G., 2007. Calibration of an optical particle counter to provide PM<sub>2.5</sub> mass for well-defined particle materials. *J. Aerosol Sci.* 38, 325-332. <http://dx.doi.org/10.1016/j.jaerosci.2006.12.001>.
- Blasco, J., Durán-Grados, V., Hampel, M., Moreno-Gutiérrez, J., 2014. Towards an integrated environmental risk assessment of emissions from ships' propulsion systems. *Environ. Int.* 66, 44-47. <http://dx.doi.org/10.1016/j.envint.2014.01.014>.
- Bobrowski, N., Honninger, G., Galle, B., Platt, U., 2003. Detection of bromine monoxide in a volcanic plume. *Nature*, 423 (6937), 273-276. <http://dx.doi.org/10.1038/nature01625>.
- Bond, T.C., Doherty, S.J., Fahey, D.W., Forster, P.M., Berntsen, T., De Angelo, B.J., Flanner, M.G., Ghan, S., Kärcher, B., Koch, D., Kinne, S., Kondo, Y., Quinn, P.K., Sarofim, M.C., Schultz, M.G., Schulz, M., Venkataraman, C., Zhang, H., Zhang, S., Bellouin, N., Guttikunda, S.K., Hopke, P.K., Jacobson, M.Z., Kaiser, J.W., Klimont, Z., Lohmann, U., Schwarz, J.P., Shindell, D., Storelvmo, T., Warren, S.G., Zender, C.S., 2013. Bounding the role of black carbon in the climate system: A scientific assessment. *J. Geophys. Res.* 118, 5380–5552. <http://dx.doi.org/10.1002/jgrd.50171>.
- Bove, M.C., Brotto, P., Calzolari, G., Cassola, F., Cavalli, F., Fermo, P., Hjorth, J., Massabò, D., Nava, S., Piazzalunga, A., Schembari, C., Prati, P., 2016. PM<sub>10</sub> source apportionment applying PMF and chemical tracer analysis to shipborne measurements in the Western Mediterranean. *Atmos. Environ.* 125 (Part A), 140–151. <http://dx.doi.org/10.1016/j.atmosenv.2015.11.009>.
- Bove, M.C., Brotto, P., Cassola, F., Cuccia, E., Massabò, D., Mazzino, A., Piazzalunga, A., Prati, P., 2014. An integrated PM<sub>2.5</sub> source apportionment study: Positive Matrix factorization vs. chemical transport model CAMx. *Atmos. Environ.* 94, 274-286. <http://dx.doi.org/10.1016/j.atmosenv.2014.05.039>.

- Broome, R.A., Cope, M.E., Goldsworthy, B., Goldsworthy, L., Emmerson, K., Jegasothy, E., Morgan, G.G., 2016. The mortality effect of ship-related fine particulate matter in the Sidney greater metropolitan region of NSW, Australia. *Environ. Int.* 87, 85-93. <http://dx.doi.org/10.1016/j.envint.2015.11.012>.
- Brunekreef, B., Beelen, R., Hoek, G., Schouten, L., Bausch-Goldbohm, S., Fischer, P., Armstrong, B., Hughes, E., Jerrett, M., van den Brandt, P., 2009. Effects of long-term exposure to traffic-related air pollution on respiratory and cardiovascular mortality in the Netherlands: the NLCS-AIR study. *Res. Rep. Health Eff. Inst.* 139, 5–71. <http://dSPACE.library.uu.nl/handle/1874/39242>.
- Buhaus, Ø., Corbett, J.J., Endresen, Ø., Eyring, V., Faber, J., Hanayama, S., Lee, D.S., Lindstad, H., Mjelde, A., Pålsson, C., Wanquing, W., Winebrake, J.J., Yoshida, K., 2008. Updated Study on Greenhouse Gas Emissions from Ships: Phase I Report. International Maritime Organization (IMO), London, UK, 1 September, p. 129.
- Burgard, D.A., Bria, C.R.M., 2016. Bridge-based sensing of NO<sub>x</sub> and SO<sub>2</sub> emissions from ocean-going ships. *Atmos. Environ.* 136, 54-60. <http://dx.doi.org/10.1016/j.atmosenv.2016.04.014>.
- Burkart, J., Steiner, G., Reischl, G., Moshhammer, H., Neuberger, M., Hitzenberger, R., 2010. Characterizing the performance of two optical particle counters (Grimm OPC1.108 and OPC1.109) under urban aerosol conditions. *J. Aerosol Sci.* 41 (10), 5751-5759. <http://dx.doi.org/10.1016/j.jaerosci.2010.07.007>.
- C.C.I.A.A., 2014. Brindisi, Servizio Economia Locale. Rapporto della provincia di Brindisi 2014. L'economia reale dal punto di osservazione delle Camere di Commercio.
- CAFE (Clean Air For Europe), 2005. Impact Assessment. Available at: [http://ec.europa.eu/environment/air/cafe/pdf/ia\\_report\\_en050921\\_final.pdf](http://ec.europa.eu/environment/air/cafe/pdf/ia_report_en050921_final.pdf), p. 31.
- Capaldo, K., Corbett, J.J., Kasibhatla, P., Fischbeck, P., Pandis, S.N., 1999. Effects of ship emissions on sulphur cycling and radiative climate forcing over the ocean. *Nature* 400(6746), 743-746.
- CARB, 2006. Emission reduction plan for ports and goods movement in California. California Air Resources Board, Sacramento.
- Carić, H., Mackelworth, P., 2014. Cruise tourism environmental impacts - The perspective from the Adriatic Sea. *Ocean Coast. Manage.* 102, 350-363. <http://dx.doi.org/10.1016/j.ocecoaman.2014.09.008>.
- Carslaw, D.C., 2015. The openair manual - open-source tools for analysing air pollution data. Manual for version 1.1-4, King's College London. Available at [http://www.openair-project.org/PDF/OpenAir\\_Manual.pdf](http://www.openair-project.org/PDF/OpenAir_Manual.pdf).
- Caserini, S., Monguzzi, A., 2002. PCDD/Fs Emissions inventory in the Lombardy Region: results and uncertainties. *Chemosphere* 48, 779-786. [http://dx.doi.org/10.1016/S0045-6535\(02\)00127-3](http://dx.doi.org/10.1016/S0045-6535(02)00127-3).

- Caserini, S., Monguzzi, A.M., Fraccaroli, A., Moretti, M., Angelino, E., Fossati, G., Giudici, A., 2005. L'inventario delle emissioni in atmosfera in Lombardia: stato dell'arte e prospettive. *Ingegneria Ambientale* XXXIV/5, 222-233.
- Castells, M., Usabiaga, J.J., Martínez de Osés, F.X., 2013. Manoeuvring and Hoteling External Costs: Enough for Alternative Energy Sources? *Marit. Pol. Manage.* <http://dx.doi.org/10.1080/03088839.2013.782441>.
- Cesari, D., Genga, A., Ielpo, P., Siciliano, M., Mascolo, G., Grasso, F.M., Contini, D., 2014. Source apportionment of PM<sub>2.5</sub> in the harbour–industrial area of Brindisi (Italy): Identification and estimation of the contribution of in-port ship emissions. *Sci. Total Environ.* 497–498, 392–400. <http://dx.doi.org/10.1016/j.scitotenv.2014.08.007>.
- Cescon, P., Prodi, F., Belosi, F., Gambaro, A., Contini, D., Giovanelli, G., Donateo, A., Cesari, D., Santachiara, G., Dimatteo, L., Kostadinov, I., Masiero, S., Cairns, W., Stortini, A., De Pieri, S., Radaelli, M., Zuccon, E., Zampieri, V., Ongaro, I., Pastrello, E., Freda, A., Silverio, P., Grasso, F.M., Ravegnani, F., Premuda, M., Zangrando, R., 2008. Misurazione del PM<sub>10</sub> e PM<sub>2.5</sub> nell'area portuale della Laguna di Venezia. Final report Venice Port Authority with Department of Environmental Sciences, University Ca' Foscari, Venice.
- Chakrabarti, B., Fine, M.P., Delfino, R., Sioutas, C., 2004. Performance evaluation of the active-flow personal DataRAM PM<sub>2.5</sub> mass monitor (Thermo Anderson pDR-1200) designed for continuous personal exposure measurements. *Atmos. Environ.* 38, 3329–3340. <http://dx.doi.org/10.1016/j.atmosenv.2004.03.007>.
- Chang, J.S., Brost, R.A., Isaksen, I.S.A., Madronich, S., Middleton, P., Stockwell, W.R., Walcek, C.J., 1987. A Three-dimensional Eulerian Acid Deposition Model: Physical Concepts and Formulation. *J. Geophys. Res.* 92, 14681–14700. <http://dx.doi.org/10.1029/JD092iD12p14681>.
- Chen, G., Huey, L.G., Trainer, M., Nicks, D., Corbett, J.J., Ryerson, T., Parrish, D., Neuman, J.A., Nowak, J., Tanner, D., Holloway, J., Brock, C., Crawford, J., Olson, J.R., Sullivan, A., Weber, R., Schauffler, S., Donnelly, S., Atlas, E., Roberts, J., Flocke, F., Hubler, G., Fehsenfeld, F., 2005. An investigation of the chemistry of ship emission plumes during ITCT 2002. *J. Geophys. Res.* 110, D10S90. <http://dx.doi.org/10.1029/2004JD005236>.
- Collet, I., Engelbert, A., 2013. Coastal regions: people living along the coastline, integration of NUTS 2010 and latest population grid. *EUROSTAT Stat. Focus* 30(2013), ISSN:2314-9647.
- Contini, D., Belosi, F., Gambaro, A., Cesari, D., Stortini, A., Bove, M.C., 2012. Comparison of PM<sub>10</sub> concentrations and metal content in three different sites of the Venice Lagoon: an analysis of possible aerosol sources. *J. Environ. Sci.* 24(11), 1954–1965. [http://dx.doi.org/10.1016/S1001-0742\(11\)61027-9](http://dx.doi.org/10.1016/S1001-0742(11)61027-9)  
doi:10.1016/S1001-0742(11)61027-9
- Contini, D., Cesari, D., Genga, A., Siciliano, M., Ielpo, P., Guascito, M.R., Conte, M., 2014. Source apportionment of size-segregated atmospheric particles based on the major water-soluble components in Lecce (Italy). *Sci. Total Environ.* 472, 248–61. <http://dx.doi.org/10.1016/j.scitotenv.2013.10.127>.



- Contini, D., Gambaro, A., Belosi, F., De Pieri, S., Cairns, W.R.L., Donato, A., Zanutto, E., Citron, M., 2011. The direct influence of ship traffic on atmospheric PM<sub>2.5</sub>, PM<sub>10</sub> and PAH in Venice. *J. Environ. Manage.* 92, 2119–2129. <http://dx.doi.org/10.1016/j.jenvman.2011.01.016>.
- Contini, D., Gambaro, A., Donato, A., Cescon, P., Cesari, D., Merico, E., Belosi, F., Citron, M., 2015. Inter annual Trend of the Primary Contribution of Ship Emissions to PM<sub>2.5</sub> Concentrations in Venice (Italy): Efficiency of Emissions Mitigation Strategies. *Atmos. Environ.* 102, 183–190. <http://dx.doi.org/10.1016/j.atmosenv.2014.11.065>.
- Cooper, D.A., 2001. Exhaust emissions from high-speed passenger ferries. *Atmos. Environ.* 35, 4189–4200. [http://dx.doi.org/10.1016/S1352-2310\(01\)00192-3](http://dx.doi.org/10.1016/S1352-2310(01)00192-3).
- Cooper, D.A., 2003. Exhaust emissions from ships at berth. *Atmos. Environ.* 37(27), 3817–3830. [http://dx.doi.org/10.1016/S1352-2310\(03\)00446-1](http://dx.doi.org/10.1016/S1352-2310(03)00446-1).
- Cooper, D.A., Gustaffson, T., 2004. Methodology for Calculating Emissions from Ships. 2. Emission factors for 2004 reporting: on behalf of the Swedish Environmental Protection Agency; Report series for SMED and SMED&SLU, 4, ISSN: 1652-4179. Available at [http://www.smed.se/wp-content/uploads/2011/05/SMED\\_Report\\_2004\\_4.pdf](http://www.smed.se/wp-content/uploads/2011/05/SMED_Report_2004_4.pdf).
- Corbett, J. J., 2003. New Directions: designing ship emissions and impacts research to inform both science and policy. *Atmos. Environ.* 37(33), 4719–4721. <http://dx.doi.org/10.1016/j.atmosenv.2003.08.003>.
- Corbett, J. J., Koehler, H.W., 2003. Updated emissions from ocean shipping. *J. Geophys. Res.* 108(D20), 4650–4666. <http://dx.doi.org/10.1029/2003JD003751>.
- Corbett, J., Winebrake, J., Green, E., Kasibhatta, P., Eyring, V., Lauer, A., 2007. Mortality from ship emissions: a global assessment. *Environmental Science & Technology* 41, 8512–8518.
- Corbett, J.J., Fischbeck, P.S., 1997. Emissions from ships. *Science* 278, 3723–3731.
- Corbett, J.J., Fischbeck, P.S., Pandis, S.N., 1999. Global nitrogen and sulfur inventories for oceangoing ships. *J. Geophys. Res. Atmos.* 104(D3), 3457–3470. <http://dx.doi.org/10.1029/1998JD100040>.
- Corbett, J.J., Koehler, H.W., 2004. Considering alternative input parameters in an activity-based ship fuel consumption and emission model: reply to comment by Øyvind Endresen et al. on “Updated emissions from ocean shipping”. *J. Geophys. Res.* 109(D23303). <http://dx.doi.org/10.1029/2004JD005030>.
- COSES (Consortio per la ricerca e la formazione), 2009. Turismo sostenibile a Venezia. Studio per il coordinamento delle strategie turistiche del Comune di Venezia.
- Cullinane, K., Bergqvist, R., 2014. Emission control areas and their impact on maritime transport. *Transport. Res. Part D: Transp. Environ.* 28, 1–5. <http://dx.doi.org/10.1016/j.trd.2013.12.004>.
- Cullinane, K., Cullinane, S., 2013. Atmospheric Emissions from Shipping: The Need for Regulation and Approaches to Compliance. *Transport Rev.* 33(4), 377–401. <http://dx.doi.org/10.1080/01441647.2013.806604>.

- Dalsøren, S.B., Eide, M.S., Endresen, Ø., Mjelde, A., Gravir, G., Isaksen, I.S.A., 2009. Update on emissions and environmental impacts from the international fleet of ships: the contribution from major ship types and ports. *Atmos. Chem. Phys.* 9, 2171–2194. <http://dx.doi.org/10.5194/acpd-8-18323-2008>.
- Dalsøren, S.B., Endresen, Ø., Isaksen, I.S.A., Gravir, G., Sørsgard, E., 2007. Environmental impacts of the expected increase in sea transportation, with a particular focus on oil and gas scenarios for Norway and northwest Russia. *J. Geophys. Res.* 112(D02310). <http://dx.doi.org/10.1029/2005JD006927>.
- Davis, D.L., Kjellstrom, T., Sloof, R., McGartland, A., Atkinson, D., Barbour, W., Hohenstein, W., Nalgelhout, P., Woodruff, T., Divita, F., Wilson, J., Deck, L., Schwartz, J., 1997. Short term improvements in public health from global-climate policies on fossil-fuel combustion: an interim report. *The Lancet* 350(9088), 1341–1349. [http://dx.doi.org/10.1016/S0140-6736\(97\)10209-4](http://dx.doi.org/10.1016/S0140-6736(97)10209-4).
- Deniz, C., Kilic, A., Cıvkaroglu, G., 2010. Estimation of shipping emissions in Candarli Gulf, Turkey. *Environ. Monit. Assess.* 171, 219–228. <http://dx.doi.org/10.1007/s10661-009-1273-2>.
- Di Natale, F., Carotenuto, C., 2015. Particulate matter in marine diesel engines exhausts: Emissions and control strategies. *Transport. Res. Part D: Transport Environ.* 40, 166-191. <http://dx.doi.org/10.1016/j.trd.2015.08.011>.
- Diesch, J.M., Drennick, F., Klimach, T., Borrmann, S., 2013. Investigation of gaseous and particular emissions from various marine vessel types measured on the banks of the Elbe in Northern Germany. *Atmos. Chem. Phys.* 13, 3603–3618. <http://dx.doi.org/10.5194/acp-13-3603-2013>.
- Donateo, A., Contini, D., Belosi, F., 2006. Real time measurements of PM<sub>2.5</sub> concentrations and vertical turbulent fluxes using an optical detector. *Atmos. Environ.* 40, 1346-1360. <http://dx.doi.org/10.1016/j.atmosenv.2005.10.026>.
- Donateo, A., Contini, D., Belosi, F., Gambaro, A., Santachiara, G., Cesari, D., Prodi, F., 2012. Characterisation of PM<sub>2.5</sub> concentrations and turbulent fluxes on a island of the Venice lagoon using high temporal resolution measurements. *Meteorol. Z.* 21(4), 385-398. <http://dx.doi.org/10.1127/0941-2948/2012/0354>.
- Donateo, A., Gregoris, E., Gambaro, A., Merico, E., Giua, R., Nocioni, A., Contini, D., 2014. Contribution of harbour activities and ship traffic to PM<sub>2.5</sub>, particle number concentrations and PAHs in a port city of the Mediterranean Sea (Italy). *Environ. Sci. Pollut. Res.* 21(15), 9415-9429. <http://dx.doi.org/10.1007/s11356-014-2849-0>.
- Dore, A.J., Vieno, M., Tang, Y.S., Dragosits, U., Dosio, A., Weston, K.J., Sutton, M.A., 2007. Modelling the atmospheric transport and deposition of sulphur and nitrogen over the United Kingdom and assessment of the influence of SO<sub>2</sub> emissions from international shipping. *Atmos. Environ.* 41, 2355-2367. <http://dx.doi.org/10.1016/j.atmosenv.2006.11.013>.
- EC, 2008a. Assessment of Options for the Legislation of CO<sub>2</sub> Emissions from Light Commercial Vehicles. Final Report to European Commission by AEA, London. [http://ec.europa.eu/clima/events/docs/0019/final\\_report\\_lcv\\_co2\\_250209\\_en.pdf](http://ec.europa.eu/clima/events/docs/0019/final_report_lcv_co2_250209_en.pdf).

- ECC (European Cruise Council), 2012. Making a Real Social and Economic Contribution to Europe's Economy. Ashcroft & Associates Ltd, PO Box 57940, London W4 5RD, United Kingdom. Available at [http://sete.gr/\\_fileuploads/entries/Online%20library/GR/ecc.pdf](http://sete.gr/_fileuploads/entries/Online%20library/GR/ecc.pdf).
- Eckhardt, S., Hermansen, O., Grythe, H., Fiebig, M., Stebel, K., Cassiani, M., Baecklund, A., Stohl, A., 2013. The influence of cruise ship emissions on air pollution in Svalbard – a harbinger of a more polluted Arctic? *Atmos. Chem. Phys.* 13, 8401-8409. <http://dx.doi.org/10.5194/acp-13-8401-2013>.
- EEA (European Environment Agency), 2006. EMEP/CORINAIR Emission Inventory Guidebook 2006. Technical Report No 30/2006. Available at <http://www.eea.europa.eu/publications/EMEPCORINAIR4>.
- EEA (European Environment Agency), 2013. The Impact of International Shipping on European Air Quality and Climate Forcing. Technical report No 4/2013, p. 88, European Environmental Agency, Copenhagen, Denmark. Available at <http://www.eea.europa.eu/publications/the-impact-of-international-shipping>.
- Eide, M.S., Endresen, Ø., Mjelde, A., Mangset, L.E., Gravir, G., 2007. Ship emissions of the future. Technical Report 2007-1325, Det Norske Veritas for EC QUANTIFY Project.
- EMEP/EEA, 2009. Air pollutant emission inventory guidebook 2009. European Environment Agency. Technical report No 9/2009. Available at <http://www.eea.europa.eu/publications/emep-eea-emission-inventory-guidebook-2009>.
- EMEP/EEA, 2013. EMEP/EEA Air Pollutant Emission Inventory Guidebook 2013. Technical guidance to prepare national emission inventories. Technical report No 12/2013. European Environment Agency, Luxembourg. Available at <http://www.eea.europa.eu/publications/emep-eea-guidebook-2013>.
- Endresen, Ø., Dalsøren, S.B., Eide, M., Sørsgård, E., Isaksen, I.S.A., 2008. The environmental impacts of increased international maritime shipping - Past trends and future perspectives. OECD/ ITF Global Forum on Transport and Environment in a Globalising World; November 10-12, 2008, Guadalajara, Mexico. Available at <http://www.oecd.org/greengrowth/greening-transport/41380820.pdf>.
- Endresen, Ø., Sorgard, E., Bakke, J., Isaksen, I.S.A., 2004. Substantiation of a lower estimate for the bunker inventory: comment on “Updated emissions from ocean shipping” by James J. Corbett and Horst W. Koehler. *J. Geophys. Res.* 109(D23302). <http://dx.doi.org/10.1029/2004JD004853>.
- Endresen, Ø., Sørsgård, E., Sundet, J.K., Dalsøren, S.B., Isaksen, I.S.A., Berglen, T.F., Gravir, G., 2003. Emission from international sea transportation and environmental impact. *J. Geophys. Res.* 108(D17), 4560. <http://dx.doi.org/10.1029/2002JD002898>.
- ENTEC UK Limited, 2002. Quantification of emissions from ships associated with ship movements between ports in the European Community. Final report to the European Commission, London UK. Available at [http://ec.europa.eu/environment/air/pdf/chapter1\\_ship\\_emissions.pdf](http://ec.europa.eu/environment/air/pdf/chapter1_ship_emissions.pdf).

- ENTEC UK Limited, 2007. CONCAWE ship emissions inventory e Mediterranean Sea, Final Report.
- ENVIRON, 2010. User's guide CAMx - Comprehensive Air Quality Model with extensions, Version 5.30, ENVIRON International Corporation, 415.899.0700, December 2010.
- EPA (European Protection Agency), 2000. Analysis of Commercial Marine Vessels Emissions and Fuel Consumption Data. Prepared for EPA under contract to Sierra Research by Energy and Environmental Analysis, Inc. EPA Contract No. 68-C7-0051, EPA420-R-00-002, February 2000. <https://www3.epa.gov/otaq/models/nonrdmdl/c-marine/r00002.pdf>.
- ESPO (European Sea Ports Organization), 2013. Top environmental priorities of European ports for 2013. ESPO Publication. Available at [http://www.ecoport.com/templates/frontend/blue/images/pdf/Analysis\\_of\\_top\\_environmental\\_priorities\\_2013.pdf](http://www.ecoport.com/templates/frontend/blue/images/pdf/Analysis_of_top_environmental_priorities_2013.pdf).
- European Parliament and Council, 2015. Regulation (EU) 2015/757 on the monitoring, reporting and verification of carbon dioxide emissions from maritime transport and amending Directive 2009/16/EC (29/04/2015). Available at <http://eur-lex.europa.eu/legal-content/EN/TXT/PDF/?uri=CELEX:32015R0757&from=EN>.
- Eurostat, 2014. Eurostat Yearbook 2014. Available at <http://ec.europa.eu/eurostat/documents/3217494/5786385/KS-HA-14-001-10-EN.PDF>.
- Eurostat, 2015. Eurostat statistics explained. Available at <http://ec.europa.eu/eurostat/statistics-explained/index.php/Transport>.
- Eyring, V., Isaksen, I., Berntsen, T., Collins, W.J., Corbett, J.J., Endresen, O., Stevenson, D.S., 2010. Transport impacts on atmosphere and climate: Shipping. *Atmos. Environ.* 44, 4735–4771. <http://dx.doi.org/10.1016/j.atmosenv.2009.04.059>.
- Eyring, V., Koehler, H.W., van Aardenne, J., Lauer, A., 2005. Emissions from international shipping: 1. The last 50 years, *J. Geophys. Res.* 110(D17), D17305. <http://dx.doi.org/10.1029/2004JD005619>.
- Eyring, V., Stevenson, D.S., Lauer, A., Dentener, F.J., Butler, T., Collins, W.J., Ellingsen, K., Gauss, M., Hauglustaine, D.A., Isaksen, I.S.A., Lawrence, M.G., Richter, A., Rodriguez, J.M., Sanderson, M., Strahan, S.E., Sudo, K., Szopa, S., van Noije, T.P.C., Wild, O., 2007. Multi-model simulations of the impact of international shipping on Atmospheric Chemistry and Climate in 2000 and 2030. *Atmos. Chem. Phys.* 7, 757–780. <http://dx.doi.org/10.5194/acp-7-757-2007>.
- Fagerli, H., Tarrason, L., 2001. The influence of ship traffic emissions on the air concentrations of particulate matter. Preliminary Estimate from EMEP/MSC-W, Requested by DG Environment. <http://ec.europa.eu/environment/air/pdf/particulates.pdf>.
- Farahmand-Razavi, 2008. Land Transport Options between Europe and Asia. Presentation to Worldnet Beijing Workshop, 8 May.

- Feng, A., Gordon, D., Hui, H., Drew, K., Rutherford D., 2007. Passenger Vehicle Greenhouse Gas and Fuel Economy Standards: A Global Update. Prepared for The International Council on Clean Transportation (ICCT). Available at [http://www.theicct.org/sites/default/files/publications/PV\\_standards\\_2007.pdf](http://www.theicct.org/sites/default/files/publications/PV_standards_2007.pdf).
- Frey, H.C., 2008. Identification and evaluation of potential best practices for greenhouse gas emissions reductions in freight transportation. Available at <http://www.arb.ca.gov/research/seminars/frey/frey.pdf>.
- Fridell, E., Steen, E., Peterson, K., 2008. Primary particles in ship emissions. *Atmos. Environ.* 42, 1160-1168. <http://dx.doi.org/10.1016/j.atmosenv.2007.10.042>.
- Fuglestedt, J., Berntsen, T., Eyring, V., Isaksen, I., Lee, D.S., Sausen, R., 2009. Shipping emissions: from cooling to warming of climates - and reducing impacts on health. *Environ. Sci. Technol.* 43(24), 9057-9062. <http://dx.doi.org/10.1021/es901944r>.
- Fuglestedt, J., Berntsen, T., Myhre, G., Rypdal, K., Skeie, R.B., 2008. Climate forcing from the transport sectors. *Proc. Natl. Acad. Sci.* 105(2), 454-458. <http://dx.doi.org/10.1073/pnas.0702958104>.
- Fullenbaum, R., Fallon, J., Flanagan, B., 2013. Oil & Natural Gas Transportation & Storage Infrastructure: Status, Trends, & Economic Benefits. In: IHS Global Inc (Ed.), American Petroleum Institute, Washington, DC, p. 86. <http://www.api.org/~media/files/policy/soae-2014/api-infrastructure-investment-study.pdf>.
- Furuyama, Y., Fujita, H., Taniike, A., Kitamura, A., 2011. Ion beam analyses of particulate matter in exhaust gas of a ship diesel engine. *Nucl. Instrum. Methods. Phys. Res. B* 269, 3063-6. <http://dx.doi.org/10.1016/j.nimb.2011.04.071>.
- Gambaro, A., Manodori, L., Toscano, G., Contini, D., Donateo, A., Belosi, F., Prodi, F., Cescon, P., 2007. Organic and inorganic compounds in the Venice lagoon PM2.5 and their correlation with micrometeorology. *Annali di Chimica* 97(5-6), 343-358.
- Gariazzo, C., Papaleo, V., Pelliccioni, A., Calori, G., Radice, P., Tinarelli, G., 2007. Application of a Lagrangian particle model to assess the impact of harbour, industrial and urban activities on air quality in the Taranto area, Italy. *Atmos. Environ.* 41, 6432-6444. <http://dx.doi.org/10.1016/j.atmosenv.2007.06.005>.
- Gencarelli, C.N., De Simone, F., Hedgecock, I.M., Sprovieri, F., Pirrone, N., 2014. Development and application of a regional-scale atmospheric mercury model based on WRF/Chem: a mediterranean area investigation. *Environ. Sci. Pollut. Res.* 21, 4095-4109. <http://dx.doi.org/10.1007/s11356-013-2162-3>.
- Giovanelli, G., Tirabassi, T., Sandroni, S., 1979. Sulphur Dioxide plume structure by mask correlation spectroscopy. *Atmos. Environ.* 13(9), 1311-1318. [http://dx.doi.org/10.1016/0004-6981\(79\)90087-8](http://dx.doi.org/10.1016/0004-6981(79)90087-8).
- Goldsworthy, L., Goldsworthy, B., 2015. Modelling of ship engine exhaust emissions in ports and extensive coastal waters based on terrestrial AIS data – An Australian case study. *Environ. Modell. Softw.* 63, 45-60. <http://dx.doi.org/10.1016/j.envsoft.2014.09.009>.

- González, Y., Rodríguez, S., García, J.C.G., Trujillo, J.L., García, R., 2011. Ultrafine particles pollution in urban coastal air due to ship emissions. *Atmos. Environ.* 45, 4907-4914. <http://dx.doi.org/10.1016/j.atmosenv.2011.06.002>.
- Graham, S., 2014. Competitiveness of Ro-Ro and container sectors in Europe and the Baltic. Proceedings from the Baltic Ports Conference 2014, Bornholm, Denmark. Available at [http://www.mdst.co.uk/attachments/insight/MDST\\_CompetitivenessOfRoRoAndContainerSectorsInEuopeAndTheBaltic\\_September14.pdf](http://www.mdst.co.uk/attachments/insight/MDST_CompetitivenessOfRoRoAndContainerSectorsInEuopeAndTheBaltic_September14.pdf).
- Gregoris, E., Barbaro, E., Morabito, E., Toscano, G., Donateo, A., Cesari, D., Contini, D., Gambaro, A., 2015. Impact of maritime traffic on polycyclic aromatic hydrocarbons, metals and particulate matter in Venice air. *Environ. Sci. Pollut. Res.* 23(7), 6951-6959. <http://dx.doi.org/10.1007/s11356-015-5811-x>.
- Grell, G.A., Devenyi, D., 2002. A generalized approach to parameterizing convection combining ensemble and data assimilation techniques. *Geophys. Res. Lett.* 29(14), 381-384. <http://dx.doi.org/10.1029/2002GL015311>.
- GRIMM Aerosol. <http://www.wmo-gaw-wcc-aerosol-physics.org/files/OPC-Grimm-model--1.108-and-1.109.pdf>.
- Gualtieri, M., Capasso, L., D'Anna, A., Camatini, M., 2014. Organic nanoparticles from different fuel blends: in vitro toxicity and inflammatory potential. *J. Appl. Toxicol.* 34(11), 1247-1255. <http://dx.doi.org/10.1002/jat.3067>.
- Hallquist, A.M., Fridell, E., Westerlund, J., Hallquist, M., 2013. Onboard measurements of nanoparticles from a SCR-equipped marine diesel engine. *Environ. Sci. Technol.* 47, 773-780. <http://dx.doi.org/10.1021/es302712a>.
- Hammingh, M.R., Holland, G.P., Geilenkirchen, J.E., Jonson, R.J.M Maas, 2012. Assessment of the environmental impacts and health ebenfits of a Nitrogen Emission Control Area in the North Sea. Policy studies PBL Netherlands Environmental Assessment Agency (PBL), The Hague , p. 113. Available at [http://www.pbl.nl/sites/default/files/cms/publicaties/pbl-2012-assessment-of-the-environmental-impacts-and-health-benefits-of-a-nitrogen-emission-control-area-in-the-north-sea-500249001-v2\\_0.pdf](http://www.pbl.nl/sites/default/files/cms/publicaties/pbl-2012-assessment-of-the-environmental-impacts-and-health-benefits-of-a-nitrogen-emission-control-area-in-the-north-sea-500249001-v2_0.pdf).
- Hammingh, P., Aben, J.M.M., Blom, W.F., Jimmink, B.A., de Vries, W.J., Visser, M., 2007. Effectiveness of international emission control measures for North Sea shipping on Dutch air quality. MNP Report 500092004/2007, Netherlands Environmental Assessment Agency. Available at <http://www.pbl.nl/sites/default/files/cms/publicaties/500092004.pdf>.
- Healy, R.M., Hellebust, S., Kourtchev, I., Allanic, A., O'Connor, I.P., Bell, J.M., Healy, D.A., Sodeau, J.R., Wenger, J.C., 2010. Source apportionment of PM<sub>2.5</sub> in Cork Harbour, Ireland using a combination of single particle mass spectrometry and quantitative semi-continuous measurements. *Atmos. Chem. Phys.* 10, 9593-9613. <http://dx.doi.org/10.5194/acp-10-9593-2010>.
- Healy, R.M., O'Connor, I.P., Hellebust, S., Allanic, A., Sodeau, J.R., Wenger, J.C., 2009. Characterisation of single particles from in-port ship emissions. *Atmos. Environ.* 43, 6408-6414. <http://dx.doi.org/10.1016/j.atmosenv.2009.07.039>.

- Heim, M., Kasper, G., Reischl, G.P., Gerhart, C., 2004. Performances of a new commercial electrical mobility spectrometer. *Aerosol. Sci. Tech.* 38(S2), 3-14. <http://dx.doi.org/10.1080/02786820490519252>.
- Hellebust, S., Allanic, A., O'Connor, I.P., Jourdan, C., Healy, D., Sodeau, J.R., 2010. Sources of ambient concentrations and chemical composition of PM<sub>2.5-0.1</sub> in Cork Harbour, Ireland. *Atmos. Res.* 95, 136-149. <http://dx.doi.org/10.1016/j.atmosres.2009.09.006>.
- Hinds, W.C., 1999. *Aerosol technology: properties, behaviour, and measurement of airborne particles*. J. Wiley & Sons Inc., Hoboken, USA.
- Holland, M., Watkiss, P., 2002. Benefits Table Database: Estimates of the Marginal External Costs of Air Pollution in Europe. Created for the European Commission, DG Environment, Brussels. Available at <http://ec.europa.eu/environment/enveco/air/pdf/betaec02a.pdf>.
- Hönninger, G., Von Friedeburg, C., Platt, U., 2004. Multi axis differential optical absorption spectroscopy (MAX-DOAS). *Atmos. Chem. Phys.* 4, 231-254. <http://dx.doi.org/10.5194/acp-4-231-2004>.
- Horvat, M., Covelli, S., Faganeli, J., Logar, M., Mandić, V., Rajar, R., Sirca, A., Zagar, D., 1999. Mercury in contaminated coastal environments; a case study: the Gulf of Trieste. *Sci. Total Environ.* 237-238, 43-56. [http://dx.doi.org/10.1016/S0048-9697\(99\)00123-0](http://dx.doi.org/10.1016/S0048-9697(99)00123-0).
- Huszar, P., Cariolle, D., Paoli, R., Halenka, T., Belda, M., Schlager, H., Miksovsky, J., Pisoft, P., 2010. Modeling the regional impact of ship emissions on NO<sub>x</sub> and ozone levels over the Eastern Atlantic and Western Europe using ship plume parameterization. *Atmos. Chem. Phys.* 10, 6645-6660. <http://dx.doi.org/10.5194/acp-10-6645-2010>.
- Iacono, M.J., Delamere, J.S., Mlawer, E.J., Shephard, M.W., Clough, S.A., Collins, W.D., 2008. Radiative forcing by long-lived greenhouse gases: Calculations with the AER radiative transfer models. *J. Geophys. Res.* 113, D13103. <http://dx.doi.org/10.1029/2008JD009944>.
- Ibrahim, O., Shaiganfar, R., Sinreich, R., Stein, T., Platt, U., Wagner, T., 2010. Car MAX-DOAS measurements around entire cities: quantification of NO<sub>x</sub> emissions from the cities of Mannheim and Ludwigshafen (Germany). *Atmos. Meas. Tech.* 3, 709-721. <http://dx.doi.org/10.5194/amt-3-709-2010>.
- ICCT (International Council on Clean Transportation), 2011. Reducing Greenhouse Gas Emissions from Ships – Cost Effectiveness of Available Options, White Paper. International Council on Clean Transportation, Washington, DC. Available at [http://www.theicct.org/sites/default/files/publications/ICCT\\_GHGfromships\\_jun2011.pdf](http://www.theicct.org/sites/default/files/publications/ICCT_GHGfromships_jun2011.pdf).
- IEA (International Energy Agency), 2009. Transport, Energy and CO<sub>2</sub>, ISBN: 978-92-64-07316-6 OECD IEA Publications, Paris. Available at <https://www.iea.org/publications/freepublications/publication/transport2009.pdf>.

- IEA (International Energy Agency), 2012. International Energy Agency Energy Prices and Taxes. In: Agency, I.E. (Ed.). ESDS International, University of Manchester, Paris, France.
- IEA (International Energy Agency), 2014. CO<sub>2</sub> emissions from fuel combustion 2014. Paris. Available at [http://www.connaissancedesenergies.org/sites/default/files/pdf-actualites/co2\\_emissions\\_from\\_fuel\\_combustion\\_2014.pdf](http://www.connaissancedesenergies.org/sites/default/files/pdf-actualites/co2_emissions_from_fuel_combustion_2014.pdf).
- Im, U., Kanakidou, M., 2011. Summertime impacts of Eastern Mediterranean megacity emissions on air quality. *Atmos. Chem. Phys. Discuss.* 11, 26657–26690. <http://dx.doi.org/10.5194/acp-12-6335-2012>.
- IMO, 2007. Report on the outcome of the Informal Cross Government/Industry Scientific Group of Experts established to evaluate the effects of the different fuel options proposed under the revision of MARPOL Annex VI. Review of MARPOL Annex VI and the NO<sub>x</sub> Technical Code, IMO/BLG 12/INF.11. Available at <http://www.sjofartsverket.se/pages/13677/12-6-1.pdf>.
- IMO, 2009. Second IMO GHG Study 2009: Update of the 2000 IMO GHG Study. Final report covering Phase 1 and Phase 2 (No. MEPC 59/INF.10). Available at [https://www.transportenvironment.org/docs/mepc59\\_ghg\\_study.pdf](https://www.transportenvironment.org/docs/mepc59_ghg_study.pdf).
- IMO, 2011. The International Convention for the Prevention of Pollution from Ships, MARPOL, Consolidated Edition (73/78). [http://www.imo.org/en/Publications/Documents/Supplements%20and%20CDs/English/QD520E\\_092015.pdf](http://www.imo.org/en/Publications/Documents/Supplements%20and%20CDs/English/QD520E_092015.pdf).
- IMO, 2014. Reduction of GHG emissions from ships - Third IMO GHG Study 2014. Final report. London. Available at <http://www.imo.org/en/OurWork/Environment/PollutionPrevention/AirPollution/Documents/Third%20Greenhouse%20Gas%20Study/GHG3%20Executive%20Summary%20and%20Report.pdf>.
- IMO, 2016. Studies on the feasibility and use of LNG as a fuel for shipping. London.
- IPCC, 2007. Climate Change. The physical science basis. Contribution of Working Group I to the Fourth Assessment Report of the IPCC 978 0521 88009-1 (Hardback; 978 0521 70596-7 Paperback, 2007).
- IPCC, 2014. Climate Change 2014: Synthesis Report. Contribution of Working Groups I, II and III to the Fifth Assessment Report of the Intergovernmental Panel on Climate Change [Core Writing Team, R.K. Pachauri and L.A. Meyer (eds.)]. IPCC, Geneva, Switzerland, 151 pp. Available at [https://www.ipcc.ch/pdf/assessment-report/ar5/syr/SYR\\_AR5\\_FINAL\\_full\\_wcover.pdf](https://www.ipcc.ch/pdf/assessment-report/ar5/syr/SYR_AR5_FINAL_full_wcover.pdf).
- Isakson, J., Persson, T.A., Lindgren, E.S., 2001. Identification and assessment of ship emissions and their effects in the harbour of Göteborg, Sweden. *Atmos. Environ.* 35, 3659-3666. [http://dx.doi.org/10.1016/S1352-2310\(00\)00528-8](http://dx.doi.org/10.1016/S1352-2310(00)00528-8).
- ISL, 1994. Shipping Statistics Yearbook 1994. Inst. of Shipping Econ. and Logistics, Bremen, Germany.
- Jalkanen, J.P., Johansson, L., Kukkonen, J., 2014. A Comprehensive Inventory of the Ship Traffic Exhaust Emissions in the Baltic Sea from 2006 to 2009. *Ambio* 43, 311–324. <http://dx.doi.org/10.1007/s13280-013-0389-3>.



- Jalkanen, J.P., Johansson, L., Kukkonen, J., 2016. A Comprehensive Inventory of the Ship Traffic Exhaust Emissions in the European area in 2011. *Atmos. Chem. Phys.* 16, 71-84. <http://dx.doi.org/10.5194/acp-16-71-2016>.
- Jalkanen, J.-P., Johansson, L., Kukkonen, J., Brink, A., Kalli, J., and Stipa, T., 2012. Extension of an assessment model of ship traffic exhaust emissions for particulate matter and carbon monoxide, *Atmos. Chem. Phys.* 12, 2641–2659. <http://dx.doi.org/10.5194/acp-12-2641-2012>.
- Janjic, Z.I., 1994. The Step–Mountain Eta Coordinate Model: Further developments of the convection, viscous sublayer, and turbulence closure schemes. *Mon. Weather Rev.* 122, 927–945. [http://dx.doi.org/10.1175/1520-0493\(1994\)122<0927:TSMECM>2.0.CO;2](http://dx.doi.org/10.1175/1520-0493(1994)122<0927:TSMECM>2.0.CO;2).
- Janjic, Z.I., 2002. Nonsingular implementation of the Mellor-Yamada Level 2.5 Scheme in the NCEP Meso model. National Centers for Environmental Prediction (NCEP) Office Note No. 437, pp. 61. Available at [http://www2.mmm.ucar.edu/wrf/users/phys\\_refs/SURFACE\\_LAYER/eta\\_part4.pdf](http://www2.mmm.ucar.edu/wrf/users/phys_refs/SURFACE_LAYER/eta_part4.pdf).
- Johansson, L., Jalkanen, J.-P., Kalli, J., Kukkonen, J., 2013. The evolution of shipping emissions and the costs of regulation changes in the northern EU area. *Atmos. Chem. Phys.* 13, 11375–11389. <http://dx.doi.org/10.5194/acp-13-11375-2013>.
- Johnson, G.R., Juwono, A.M., Friend, A.J., Cheung, H.C., Stelcer, E., Cohen, D., Ayoko, G.A., Morawska, L., 2014. Relating urban airborne particle concentrations to shipping using carbon based elemental emission ratios. *Atmos. Environ.* 95, 525-536. <http://dx.doi.org/10.1016/j.atmosenv.2014.07.003>.
- Jonson, J.E., Jalkanen, J.P., Johansson, L., Gauss, M., Denier van der Gon, H.A.C., 2015. Model calculations of the effects of present and future emissions of air pollutants from shipping in the Baltic Sea and the North Sea. *Atmos. Chem. Phys.* 15, 783–798. <http://dx.doi.org/10.5194/acp-15-783-2015>.
- Jonsson, A.M., Westerlund, J., Hallquist, M., 2011. Size-resolved particle emission factors for individual ships. *Geophys. Res. Lett.* 38, L13809. <http://dx.doi.org/10.1029/2011GL047672>.
- Kaiser, J., 2005. Mounting Evidence Indicts Fine- Particle Pollution. *Science* 307(5717), 1858-1861. <http://dx.doi.org/10.1126/science.307.5717.1858a>.
- Kasper, A., Aufdenblatten, S., Forss, A., Mohr, M., Burtcher, H., 2007. Particulate emissions from a low-speed marine diesel engine. *Aerosol Sci. Technol.* 41(1), 24–32. <http://dx.doi.org/10.1080/02786820601055392>.
- Kerker M., 1969. The scattering of light and other electromagnetic radiation. In: *Physical Chemistry: A Series of Monographs*, vol. 16, ISBN: 978-0-12-404550-7, Academic Press, New York.
- Keuken, M., Wesseling, J., Van den Elshout, S., Hermans, L., 2005. Impact of shipping and harbour activities on air quality – a case study in the Rijnmond Area (Rotterdam). In: Canepa, E., Georgieva, E. (Eds.), *Proceeding of the 1st Int. Conference on Harbours & Air Quality*, ISBN 88-89884 00-2 Genova, Italy, June 15–17.

- Kim, E., Hopke, P.K., 2008. Source characterization of ambient fine particles at multiple sites in the Seattle area. *Atmos. Environ.* 42, 6047–56. <http://dx.doi.org/10.1016/j.atmosenv.2008.03.032>.
- Kivekäs, N., Massling, A., Grythe, H., Lange, R., Rusnak, V., Carreno, S., Skov, H., Swietlicki, E., Nguyen, Q.T., Glasius, M., Kristensson, A., 2014. Contribution of ship traffic to aerosol particle concentrations downwind of a major shipping lane. *Atmos. Chem. Phys.* 14, 8255–8267. <http://dx.doi.org/10.5194/acp-14-8255-2014>.
- Klein, R.A., 2005. *Cruise Sheep Squeeze. The New Pirates of the Seven Seas.* New Society Publishers, Gabriola Island, Canada.
- Krewski, D., Jerrett, M., Burnett, R.T., Ma, R., Hughes, E., Shi, Y., Turner, M.C., Pope 3rd, C.A., Thurston, G., Calle, E.E., Thun, M.J., Beckerman, B., DeLuca, P., Finkelstein, N., Ito, K., Moore, D.K., Newbold, K.B., Ramsay, T., Ross, Z., Shin, H., Tempalski, B., 2009. Extended follow-up and spatial analysis of the American Cancer Society study linking particulate air pollution and mortality. *Res. Rep. Health Eff. Inst.* 140, 5–114.
- Kuenen, J.J.P., Visschedijk, A.J.H., Jozwicka, M., Denier van der Gon, H.A.C., 2014. TNO-MACC\_II emission inventory: a multi-year (2003–2009) consistent high resolution European emission inventory for air quality modelling. *Atmos. Chem. Phys.* 14, 10963–10976. <http://dx.doi.org/10.5194/acp-14-10963-2014>.
- Kumar, P., Fennell, P., Britter, R., 2008. Measurements of particles in the 5-1000 nm range close to road level in an urban street canyon. *Sci. Total Environ.* 390, 437–447. <http://dx.doi.org/10.1016/j.scitotenv.2007.10.013>.
- Lack, D.A., Corbett, J.J., Onasch, T., Lerner, B., Massoli, P., Quinn, P.K., Bates, T.S., Covert, D.S., Coffman, D., Sierau, B., Herndon, S., Allan, J., Baynard, T., Lovejoy, E., Ravishankara, A.R., Williams, E., 2009. Particulate emissions from commercial shipping: chemical, physical, and optical properties. *J. Geophys. Res.* 114(D7). <http://dx.doi.org/10.1029/2008JD011300>.
- Laprise, R., 1992. The Euler equations of motion with hydrostatic pressure as an independent variable. *Mon. Weather Rev.* 120, 197–207. [http://dx.doi.org/10.1175/1520-0493\(1992\)120<0197:TEEOMW>2.0.CO;2](http://dx.doi.org/10.1175/1520-0493(1992)120<0197:TEEOMW>2.0.CO;2).
- Lauer, A., Eyring, V., Hendricks, J., Jöckel, P., Lohmann, U., 2007. Global model simulations of the impact of ocean-going ships on aerosols, clouds, and the radiation budget. *Atmos. Chem. Phys.* 7, 5061–5079. <http://dx.doi.org/10.5194/acp-7-5061-2007>.
- Lee, C.-Y., Lee, H., Zhang, J., 2013. The impact of slow ocean steaming on delivery reliability and fuel consumption. Social Science Research Network. [http://papers.ssrn.com/sol3/papers.cfm?abstract\\_id=2060105](http://papers.ssrn.com/sol3/papers.cfm?abstract_id=2060105).
- Liora, N., Markakis, K., Poupkou, A., Dimopoulos, S., Giannaros, T., Melas, D., 2013. Particulate matter emissions from natural sources in Europe – A case study of the impact of natural sources to PM pollution levels. ACCENT-Plus Symposium, Bringing together the European Research in atmospheric

- composition change Challenges for the next decade, 17 -20 September 2013, Urbino, Italy.
- Liora, N., Poupkou, A., Markakis, K., Giannaros, T., Melas, D., 2014. Sea salt and windblown dust emissions in the Eastern Mediterranean – Study of the natural PM emissions dependence on meteorology. In: Proceedings of the 12th International Conference of Meteorology, Climatology and Physics of the Atmosphere (COMECAP 2014), 28 – 31 May 2014, Heraklion, Greece (M. Kanakidou, N. Mihalopoulos, P.Nastos Eds), Crete University Press, ISBN: 978-960-524-430-9, vol. 2, pp. 137-141.
- Lloyd's Maritime Information System (LMIS), 2002. The Lloyd's Maritime Database [CD ROM], Lloyd's Register–Fairplay Ltd., London.
- Lloyd's Register – Fairplay, World Fleet Statistics, various publications.
- LMIU (Lloyd's Marine Intelligence Unit), 2008. Report prepared for the Regional Marine Pollution Emergency Response Centre for the Mediterranean Sea (REMPEC) by Lloyd's Marine Intelligence Unit under Task 2.3 O of Activity 2 of the European Union financed MEDA regional project “Euromed co-operation on Maritime Safety and Prevention of Pollution from Ships – SAFEMED”.
- Lu, G., Brook, J.R., Alfarra, M.R., Anlauf, K., Leitch, W.R., Sharma, S., Wang, D., Worsnop, D.R., Phinney, L., 2006. Identification and characterization of inland ship plumes over Vancouver, BC. *Atmos. Environ.* 40(15), 2767–2782. <http://dx.doi.org/10.1016/j.atmosenv.2005.12.054>.
- Lyyranen, J., Jokiniemi, J., Kauppinen, E.I., Joutsensaari, J., 1999. Aerosol characterization in medium-speed diesel engines operating with heavy fuel oils. *J. Aerosol Sci.* 30 (6), 771–784. [http://dx.doi.org/10.1016/S0021-8502\(98\)00763-0](http://dx.doi.org/10.1016/S0021-8502(98)00763-0).
- Maffii, S., 2007. External costs and climate impacts of maritime transport. In: TRT Trasporti e Territorio Srl, Milan e Italy Transport and Climate Change: A Greens/ EFA Conference, Bruxelles, 14th June 2007.
- MAN Diesel & Turbo, 2011. Basic Principles of Ship Propulsion. MAN Diesel & Turbo, Copenhagen SV, Denmark. Available at <https://marine.man.eu/docs/librariesprovider6/propeller-aftship/basic-principles-of-propulsion.pdf?sfvrsn=0>.
- Markakis, K., Giannaros, T., Poupkou, A., Liora, N., Melas, D., Sofiev, M., Soares, J., 2009. Evaluating the impact of particle emissions from natural sources in the Balkan region. European Aerosol Conference 2009, 6-9 September 2009, Karlsruhe, Germany.
- Markakis, K., Katragkou, E., Poupkou, A., Melas, D., 2013. MOSESS: A new emission model for the compilation of model-ready emission inventories. Application in a coal mining area in Northern Greece. *Environ. Model. Assess.* 18(5), 509-521. <http://dx.doi.org/10.1007/s10666-013-9360-8>.
- Marmer, E., Langman, B., 2005. Impact of ship emissions on the Mediterranean summertime pollution and climate: a regional model study. *Atmos. Environ.* 39, 4659–4669. <http://dx.doi.org/10.1016/j.atmosenv.2005.04.014>.

- Marušić Z., Sever I., Ivandić N., 2012. Mediterranean cruise itineraries and the position of Dubrovnik. In: Papathanassis, A., Luković, T., Vogel, M. (Eds.), *Cruise Tourism and Society: a Socio-economic Perspective*. Springer, Heidelberg.
- Masieri, S., Palazzi, E., Ravegnani, F., Bortoli, D., Petritoli, A., Premuda, M., Kostadinov, I., Pisoni, E., Carnevale, C., Volta, M., Giovanelli, G., 2014. Vertical distribution of lower tropospheric NO<sub>2</sub> derived from diffuse solar radiation measurements: a geometrical retrieval approach. *IEEE TGRS* 52(8), 4846-4857. <http://dx.doi.org/10.1109/TGRS.2013.2285282>.
- Masieri, S., Premuda, M., Bortoli, D., Kostadinov, I., Petritoli, A., Ravegnani, F., Giovanelli, G., 2009. Cruise ships flow rate emission evaluated by means of a passive DOAS instrument. In: *Remote Sensing for Environmental Monitoring, GIS Applications, and Geology IX*. Ulrich, M., Civco, D. L., Eds.; Proceedings of SPIE, 7478. SPIE, Bellingham, WA.
- Mazzei, F., D'Alessandro, A., Lucarelli, F., Nava, S., Prati, P., Valli, G., Vecchi, R., 2008. Characterization of particulate matter sources in an urban environment. *Sci. Total Environ.* 401, 81-89. <http://dx.doi.org/10.1016/j.scitotenv.2008.03.008>.
- McArthur, D.P., Osland, L., 2013. Ships in a city harbour: an economic valuation of atmospheric emissions. *Transport. Res. Part D: Transp. Environ.* 21, 47–52. <http://dx.doi.org/10.1016/j.trd.2013.02.004>.
- McConnell, J.R., Edwards, R., Kok, G.L., Flanner, M.G., Zender, C.S., Saltzman, E.S., Banta, J.R., Pasteris, D.R., Carter, M.M., and Kahl, J.D.W., 2007. 20th-Century Industrial Black Carbon Emissions Altered Arctic Climate Forcing. *Science* 317, 1381-1384. <http://dx.doi.org/10.1126/science.1144856>.
- McGonigle, A.J.S., Oppenheimer, C., Galle, B., Mather, T.A., Pyle, D.M., 2002. Walking traverse and scanning DOAS measurements of volcanic gas emission rates. *Geophys. Res. Lett.* 29(20), 1985. <http://dx.doi.org/10.1029/2002GL015827>.
- McKinnon, A., 2010. Environmental sustainability: A new priority for logistics managers. In: A. McKinnon, S. L. Cullinane, A. Whiteing, & M. Browne (Eds.), *Green logistics: Improving the environmental sustainability of logistics* (pp. 3–30). London: Kogan Page.
- MedCruise, 2015. Cruise activities in Medcruise Ports: statistics 2014. A MedCruise report: Piraeus 2015. Available at [http://www.medcruise.com/sites/default/files/cruise\\_activities\\_in\\_medcruise\\_ports-edition\\_2015\\_1.pdf](http://www.medcruise.com/sites/default/files/cruise_activities_in_medcruise_ports-edition_2015_1.pdf).
- Meech, R., 2008. Designation of the Mediterranean Sea as a SO<sub>x</sub> Emission Control Area (SECA) under MARPOL Annex VI Guidelines & Procedures regarding the ratification process of Annex VI & the preparations required for the submission of an Application to IMO for the Mediterranean Sea to be designated as a SECA SAFEMED Task 3.7. Report prepared under the Project EUROMED Cooperation on Maritime Safety and Prevention of Pollution from Ships SAFEMED (MED 2005/109-573) financed by the

- European Commission under an IMO/EC contract presented to REMPEC (SAFEMED). Available at <http://www.safemedproject.org>.
- Merico, E., Donato, A., Gambaro, A., Cesari, D., Gregoris, E., Barbaro, E., Dinoi, A., Giovanelli, G., Masieri, S., Contini, D., 2016. Influence of in-port ships emissions to gaseous atmospheric pollutants and to particulate matter of different sizes in a Mediterranean harbour in Italy. *Atmos. Environ.* 139, 1-10. <http://dx.doi.org/10.1016/j.atmosenv.2016.05.024>.
- Merico, E., Gambaro, A., Argiriou, A., Alebic-Juretic, A., Barbaro, E., Cesari, D., Dimopoulos, S., Dinoi, A., Donato, A., Gregoris, E., Karagiannidis, A., Ivosevic, T., Liora, N., Melas, D., Mifka, B., Orlic, I., Poupkou, A., Sarovic, K., Contini, D., 2016. Atmospheric impact of ship traffic in four Adriatic-Ionian port-cities: comparison and harmonization of different approaches. *Transport. Res. Part D*, 50, 431-445. <http://dx.doi.org/10.1016/j.trd.2016.11.016>.
- Mestl, T., Løvoll, G., Stensrud, E., Le Breton, A., 2013. The Doubtful Environmental Benefit of Reduced Maximum Sulfur Limit in International Shipping Fuel. *Environ. Sci. Technol.* 47(12), 6098-6101. <http://dx.doi.org/10.1021/es4009954>.
- Minguillón, M.C., Arhami, M., Schauer, J.J., Sioutas, C., 2008. Seasonal and spatial variations of sources of fine and quasi-ultrafine particulate matter in neighborhoods near the Los Angeles-Long Beach harbor. *Atmos. Environ.* 42(32), 7317-7328. <http://dx.doi.org/10.1016/j.atmosenv.2008.07.036>.
- Miola, A., Ciuffo, B., 2011. Estimating air emissions from ships: meta-analysis of modelling approaches and available data sources. *Atmos. Environ.* 45, 2242-2251. <http://dx.doi.org/10.1016/j.atmosenv.2011.01.046>.
- Miola, A., Paccagnan, V., Mannino, I., Massarutto, A., Perujo, A., Turvani, M., 2009. External Cost of transportation-Case study: Maritime Transport. Brussels: JRC European Commission. Available at [http://www.eurosfair.prdd.fr/7pc/doc/1269355029\\_eur\\_23837\\_en.pdf](http://www.eurosfair.prdd.fr/7pc/doc/1269355029_eur_23837_en.pdf).
- Moldanová, J., Fridell, E., Popovicheva, O., Demirdjian, B., Tishkova, V., Faccineto, A., Focsa, C., 2009. Characterisation of particulate matter and gaseous emissions from a large ship diesel engine. *Atmos. Environ.* 43, 2632-2641. <http://dx.doi.org/10.1016/j.atmosenv.2009.02.008>.
- Morcrette, J.-J., Boucher, O., Jones, L., Salmond, D., Bechtold, P., Beljaars, A., Benedetti, A., Bonet, A., Kaiser, J. W., Razinger, M., Schulz, M., Serrar, S., Simmons, A. J., Sofiev, M., Suttie, M., Tompkins, A.M., Untch, A., 2009. Aerosol analysis and forecast in the European Centre for Medium-Range Weather Forecasts Integrated Forecast System: Forward modeling. *J. Geophys. Res.* 114, D06206. <http://dx.doi.org/10.1029/2008JD011235>.
- Moreno, T., Querol, X., Alastuey, A., de la Rosa, J., Sánchez de la Campa, A.M., Minguillón, M.C., et al., 2010. Variations in vanadium, nickel and lanthanoid element concentrations in urban air. *Sci. Total Environ.* 408, 4569-4579. <http://dx.doi.org/10.1016/j.scitotenv.2010.06.016>.
- Moreno-Gutiérrez, J., Calderay, F., Saborido, N., Boile, M., Rodríguez Valero, R., Durán-Grados, V., 2015. Methodologies for estimating shipping emissions

- and energy consumption: A comparative analysis of current methods. *Energy* 86, 603-616. <http://dx.doi.org/10.1016/j.energy.2015.04.083>.
- Murphy, S., Agrawal, H., Sorooshian, A., Padro, L.T., Gates, H., Hersey, S., Welch, W.A., Jung, H., Miller, J.W., Cocker, I.D.R., Nenes, A., Jonsson, H.H., Flagan, R.C., Seinfeld, J.H., 2009. Comprehensive simultaneous shipboard and airborne characterization of exhaust from a modern container ship at sea. *Environ. Sci. Technol.* 43(13), 4626-4640. <http://dx.doi.org/10.1021/es802413j>.
- Nel, A., 2005. Air pollution-related illness: effects of particles. *Science* 308, 804-806. <http://dx.doi.org/10.1126/science.1108752>.
- Nenes A., Pilinis C., Pandis S.N., 1998. ISORROPIA: A New Thermodynamic Model for Multiphase Multicomponent Inorganic Aerosols. *Aquat. Geochem.* 4, 123-152. <http://dx.doi.org/10.1023/A:1009604003981>.
- Nicholls, R.J., Small, C., 2002. Improved estimates of coastal population and exposure to hazards released. *Eos – Trans. Am. Geophys. Union* 83(28), 301-305. <http://dx.doi.org/10.1029/2002EO000216>.
- Ooyama, K.V., 1990. A thermodynamic foundation for modeling the moist atmosphere. *J. Atmos. Sci.* 47, 2580-2593. [http://dx.doi.org/10.1175/1520-0469\(1990\)047<2580:ATFFMT>2.0.CO;2](http://dx.doi.org/10.1175/1520-0469(1990)047<2580:ATFFMT>2.0.CO;2).
- Ostro, B., 2004. Outdoor air pollution: Assessing the environmental burden of disease at national and local levels. *Environmental burden of disease series*, No. 5, World Health Organization: Geneva.
- Pandolfi, M., Gonzalez-Castanedo, Y., Alastuey, A., de la Rosa, J., Mantilla, E., Sanchez de la Campa, A., Querol, X., Pey, J., Amato, F., Moreno, T., 2011. Source apportionment of PM<sub>10</sub> and PM<sub>2.5</sub> at multiple sites in the strait of Gibraltar by PMF: impact of shipping emissions. *Environ. Sci. Pollut. Res.* 28, 260-269. <http://dx.doi.org/10.1007/s11356-010-0373-4>.
- Pérez, N., Pey, J., Reche, C., Cortés, J., Alastuey, A., Querol, X., 2016. Impact of harbour emissions on ambient PM<sub>10</sub> and PM<sub>2.5</sub> in Barcelona (Spain): Evidences of secondary aerosol formation within the urban area. *Sci. Total Environ.* 571, 237-250. <http://dx.doi.org/10.1016/j.scitotenv.2016.07.025>.
- Petzold, A., Feldpausch, P., Fritze, L., Minikin, A., Lauer, P., Kurok, C., Bauer, H., 2004. Particle emissions from ship engines. *J. Aerosol Sci.* <http://www.puertos.es> Abstracts of the European conference, S1095eS1096. Puertos del Estado, Official Manager of Ports in Spain.
- Petzold, A., Hasselbach, J., Lauer, O., Baumann, R., Franke, K., Gurk, C., Schlager, H., Weingartner, E., 2008. Experimental studies on particle emissions from cruising ship, their characteristic properties, transformation and atmospheric lifetime in the marine boundary layer. *Atmos. Chem. Phys.* 8, 2387-2403. <http://dx.doi.org/10.5194/acp-8-2387-2008>.
- Petzold, A., Lauer, P., Fritsche, U., Hasselbach, J., Lichtenstern, M., Schlager, H., Fleischer, F., 2011. Operation of marine diesel engines on biogenic fuels: modification of emissions and resulting climate effects. *Environ. Sci. Technol.* 45(24), 10394-10400. <http://dx.doi.org/10.1021/es2021439>.

- Petzold, A., Weingartner, E., Hasselbach, J., Lauer, P., Kurok, C., and Fleischer, F., 2010. Physical properties, chemical composition and cloud forming potential of particulate emissions from a marine diesel engine at various load conditions. *Environ. Sci. Tech.* 44, 3800–3805. <http://dx.doi.org/10.1021/es903681z>.
- Pey, J., Pérez, N., Cortés, J., Alastuey, A., Querol, X., 2013. Chemical fingerprint and impact of shipping emissions over a western Mediterranean metropolis: primary and aged contributions. *Sci. Total Environ.* 463-464, 497–507. <http://dx.doi.org/10.1016/j.scitotenv.2013.06.061>.
- Pirjola, L., Pajunoja, A., Jalkanen, J.-P., Rönkkö, T., Kousa, A., Koskentalo, T., 2014. Mobile measurements of ship emissions in two harbour areas in Finland. *Atmos. Meas. Tech.* 7, 149–161. <http://dx.doi.org/10.5194/amt-7-149-2014>.
- Pope, C.A., Burnett, R.T., Thurston, G.D., Thun, M.J., Calle, E.E., Krewski, D., Godleski, J.J., 2004. Cardiovascular mortality and long-term exposure to particulate air pollution. *Circulation* 109, 71–77. <http://dx.doi.org/10.1161/01.CIR.0000108927.80044.7F>.
- Poupkou, A., Giannaros, T., Markakis, K., Kioutsioukis, I., Curci, G., Melas, D., Zerefos, C., 2010. A model for European biogenic volatile organic compound emissions: Software development and first validation. *Environ. Modell. Softw.* 25, 1845-1856. <http://dx.doi.org/http://dx.doi.org/10.1016/j.envsoft.2010.05.004>.
- Premuda, M., Masieri, S., Bortoli, D., Kostadinov, I., Petritoli, A., Giovanelli, G., 2011. Evaluation of vessel emissions in a lagoon area with ground based Multi axis DOAS measurements. *Atmos. Environ.* 45, 5212-5219. <http://dx.doi.org/10.1016/j.atmosenv.2011.05.067>.
- Premuda, M., Palazzi, E., Ravegnani, F., Bortoli, D., Masieri, S., Giovanelli, G., 2012. MOCRA: a Monte Carlo code for the simulation of radiative transfer in the atmosphere. *Opt. Express*, 20(7), 7973-7993. <https://doi.org/10.1364/OE.20.007973>.
- Prodi, F., Belosi, F., Contini, D., Santachiara, G., Di Matteo, L., Gambaro, A., Donato, A., Cesari, D., 2009. Aerosol fine fraction in the Venice Lagoon: Particle composition and sources. *Atmos. Res.* 92, 141-150. <http://dx.doi.org/10.1016/j.atmosres.2008.09.020>.
- Reche, C., Viana, M., Moreno, T., Querol, X., Alastuey, A., Pey, J., Pandolfi, M., Prevot, A., Mohr, C., Richard, A., Artimano, B., Gomez-Moreno, F.J., Cots, N., 2011. Peculiarities in atmospheric particle number and size-resolved speciation in an urban area in the western Mediterranean: results from the DAURE campaign. *Atmos. Environ.* 45, 5282-5293. <http://dx.doi.org/10.1016/j.atmosenv.2011.06.059>.
- Restad, K., Isaksen, I.S.A., Berntsen, T.K., 1998. Global distribution of sulphate in the troposphere. A three-dimensional model study. *Atmos. Environ.* 32, 3593-3609. [http://dx.doi.org/10.1016/S1352-2310\(98\)00081-8](http://dx.doi.org/10.1016/S1352-2310(98)00081-8).
- Rodríguez, S., Cuevas, E., 2007. The contributions of ‘minimum primary emissions’ and ‘new particle formation enhancements’ to the particle number

- concentration in urban air. *J. Aerosol Sci.* 38, 1207-1219. <http://dx.doi.org/10.1016/j.jaerosci.2007.09.001>.
- Rundell, K.W., Hoffman, J.R., Caviston, R., Bulbulian, R., Hollenbach, A.M., 2007. Inhalation of ultrafine and fine particulate matter disrupts systemic vascular function. *Inhal. Toxicol.* 19(2), 133–140. <http://dx.doi.org/10.1080/08958370601051727>.
- Salameh, D., Detournay, A., Pey, J., Pérez, N., Liguori, F., Saraga, D., Bove, M.C., Brotto, P., Cassola, F., Massabò, D., Latella, A., Pillon, S., Formenton, G., Patti, S., Armengaud, A., Piga, D., Jaffrezo, J.L., Bartzis, J., Tolis, E., Prati, P., Querol, X., Wortham, H., Marchand, N., 2015. PM<sub>2.5</sub> chemical composition in five European Mediterranean cities: a 1-year study. *Atmos. Res.* 155, 102–117. <http://dx.doi.org/10.1016/j.atmosres.2014.12.001>.
- Sausen, R., Isaksen, I., Grewe, V., Hauglustaine, D., Lee, D. S., Myhre, G., Köhler, M. O., Pitari, G., Schumann, U., Stordal, F., Zerefos, C., 2005. Aviation radiative forcing in 2000: An update on IPCC (1999). *Meteorol. Z.*, 14, 555–561. <http://dx.doi.org/10.1127/0941-2948/2005/0049>.
- Saxe, H., Larsen, T., 2004. Air pollution from ships in three Danish ports. *Atmos. Environ.* 38, 4057–4067. <http://dx.doi.org/10.1016/j.atmosenv.2004.03.055>.
- Schembari, C., Cavalli, F., Cuccia, E., Hjorth, J., Calzolari, G., Pérez, N., Pey, J., Prati, P., Raes, F., 2012. Impact of a European directive on ship emissions on air quality in Mediterranean harbours. *Atmos. Environ.* 61, 661–669. <http://dx.doi.org/10.1016/j.atmosenv.2012.06.047>.
- Schinas, O., Bani, J., 2012. The Impact of a Possible Extension at EU Level of SECAs to the Entire European Coastline. Detailed Briefing Note prepared for the needs of the European Parliament, Directorate General for Internal Policies; Policy Department B: Structural and Cohesion Policies; Transport and Tourism. <http://dx.doi.org/10.2861/84453>.
- Sharma, D.C., 2006. Ports in a storm. *Environ. Health Persp.* 114(4), A222-231. PMID: PMC1440801.
- Sinha, P., Hobbs, P.V., Yokelson, R.J., Christian, T.J., Kirchstetter, T.W., Bruintjes, R., 2003. Emissions of trace gases and particles from two ships in the southern Atlantic Ocean. *Atmos. Environ.* 37(15), 2139–2148. [http://dx.doi.org/10.1016/S1352-2310\(03\)00080-3](http://dx.doi.org/10.1016/S1352-2310(03)00080-3).
- Sioutas, C., Kim, S., Chang, M., Terrell, L.L., Gong Jr., H., 2000. Field evaluation of a modified Data RAM MIE scattering monitor for real-time PM<sub>2.5</sub> mass concentration measurements. *Atmos. Environ.* 34, 4829-4838. [http://dx.doi.org/10.1016/S1352-2310\(00\)00244-2](http://dx.doi.org/10.1016/S1352-2310(00)00244-2).
- Sippula, O., Stengel, B., Sklorz, M., Streibel, T., Rabe, R., Orasche, J., Lintelmann, J., Michalke, B., Abbaszade, G., Radischat, C., Gröger, T., Schnelle-Kreis, J., Harndorf, H., Zimmermann, R., 2014. Particle emissions from a marine engine: chemical composition and aromatic emission profiles under various operating conditions. *Environ. Sci. Technol.* 48(19), 11721–11729. <http://dx.doi.org/10.1021/es502484z>.
- Skamarock, W.C., Klemp, J.B., Dudhia, J., Gill D.O., Barker D.M., Duda M.G., Huang X.Y., Wang, W., Powers J.G., 2008. A description of the advanced



- researcher WRF version 3. NCAR Technical Note, 88 pages. Available at [http://www2.mmm.ucar.edu/wrf/users/docs/arw\\_v3.pdf](http://www2.mmm.ucar.edu/wrf/users/docs/arw_v3.pdf).
- Slezakova, K., Morais, S., Pereira, M.d.C., 2013. Atmospheric Nanoparticles and their Impacts on Public Health. In: *Current Topics in Public Health*, Alfonso J. Rodriguez-Morales (Ed.), ISBN 978-953-51-1121-4, Intech. <http://dx.doi.org/10.5772/54775>.
- Smith, L., Stephenson, S., 2013. New trans-Arctic shipping routes navigable by midcentury. *PNAS* 110 (13) E1191–E1195. <http://dx.doi.org/10.1073/pnas.1214212110>.
- Sodeman, D.A., Toner, S.M., Prather, K.A., 2005. Determination of Single Particle Mass Spectral Signatures from Light- Duty Vehicle Emissions. *Environ. Sci. Technol.* 39, 4569–4580. <http://dx.doi.org/10.1021/es0489947>.
- Strader, R., Lurmann, F., Pandis, S.N., 1999. Evaluation of secondary organic aerosol formation in winter. *Atmos. Environ.* 33, 4849-4863. [http://dx.doi.org/10.1016/S1352-2310\(99\)00310-6](http://dx.doi.org/10.1016/S1352-2310(99)00310-6).
- Tao, L., Fairley, D., Kleeman, M.J., Harley, R.A., 2013. Effects of switching to lower sulphur marine fuel oil on air quality in the San Francisco Bay area. *Environ. Sci. Technol.* 47, 10171-10178. <http://dx.doi.org/10.1021/es401049x>.
- TEFLES (Technologies and Scenarios for Low Emissions Shipping) project. D7.1: Report on the state of the art ship docked in port scenario. Available at [http://www.transport-research.info/sites/default/files/project/documents/20120405\\_233309\\_61001\\_D-7.1-Report-state-of-the-art.pdf](http://www.transport-research.info/sites/default/files/project/documents/20120405_233309_61001_D-7.1-Report-state-of-the-art.pdf).
- Teledyne, Model 100E UV Fluorescence SO<sub>2</sub> Analyzer, Operation manual, 04515F DCN6048, April 2011. Available at [http://www.teledyne-api.com/manuals/04515F\\_100E.pdf](http://www.teledyne-api.com/manuals/04515F_100E.pdf).
- Teledyne, Model 200E Nitrogen Oxide Analyzer, Technical manual, DCN 5731 04410 Rev D, May 2010. Available at [http://www.teledyne-api.com/manuals/04410D\\_200E.pdf](http://www.teledyne-api.com/manuals/04410D_200E.pdf).
- Teledyne, Model 400E Photometric Ozone Analyzer, Technical manual, 04316F DCN6076, May 2011. Available at [http://www.teledyne-api.com/manuals/04316F\\_400E.pdf](http://www.teledyne-api.com/manuals/04316F_400E.pdf).
- Tewari, M., Chen, F., Wang, W., Dudhia, J., LeMone, M.A., Mitchell, K., Gayno, M., Ek, G., Wegiel, J., Cuenca, R.H., 2004. Implementation and verification of the unified NOAA land surface model in the WRF model. 20th conference on weather analysis and forecasting/16th conference on numerical weather prediction, pp. 11–15.
- Thompson, G., Field, P.R., Rasmussen, R.M., Hall, W.D., 2008. Explicit Forecasts of Winter Precipitation Using an Improved Bulk Microphysics Scheme. Part II: Implementation of a New Snow Parameterization. *Mon. Weather Rev.* 136, 5095–5115. <http://dx.doi.org/10.1175/2008MWR2387.1>.
- Thomson H., Corbett J., Winebrake J., 2015. Natural gas as a marine fuel. *Energ. Policy* 87, 153-167. <http://dx.doi.org/10.1016/j.enpol.2015.08.027>.

- Toner, S.M., Sodeman, D.A., Prather, K.A., 2006. Single Particle Characterization of Ultrafine and Accumulation Mode Particles from Heavy Duty Diesel Vehicles Using Aerosol Time-of-Flight Mass Spectrometry, *Environ. Sci. Technol.* 40, 3912–3921.
- Trozzi, C., Vaccaro, R., 1998. Methodologies for estimating air pollutant emissions from ships. *TECHNE Report MEET RF98*.
- TSI, 2007. Model 3775 Condensation Particle Counter - Operation and Service Manual. P/N 1980527, Revision D. Available at <http://dustmonitors.ru/d/68562/d/cpc-3775r.pdf>.
- Tsujimoto, M., Kuroda, M., Sogihara, N., 2013. Development of a calculation method for fuel consumption of ships in actual seas with performance evaluation. In: *ASME 2013 32nd International Conference on Ocean, Offshore and Arctic Engineering*, Nantes, France, pp. V009T012A047. <http://dx.doi.org/10.1115/OMAE2013-11297>.
- Tzannatos, E., 2010. Ship emissions and their externalities for the port of Piraeus-Greece. *Atmos. Environ.* 44, 400–407. <http://dx.doi.org/10.1016/j.atmosenv.2009.10.024>.
- UNCTAD (United Nations Conference on Trade and Development), 2008. *Review of Maritime Transport 2008*. UNCTAD/RMT/2008. Sales No. E.08.II.D.26, ISBN 978-92-1-112758-4, United Nations Publications, New York and Geneva. Available at [http://unctad.org/en/Docs/rmt2008\\_en.pdf](http://unctad.org/en/Docs/rmt2008_en.pdf).
- UNCTAD (United Nations Conference on Trade and Development), 2015. *Review of Maritime Transport 2015*. UNCTAD/RMT/2015. Sales No. E.14.II.D.6, ISBN 978-92-1-112892-5, United Nations publication, Geneva. Available at [http://unctad.org/en/PublicationsLibrary/rmt2015\\_en.pdf](http://unctad.org/en/PublicationsLibrary/rmt2015_en.pdf).
- UNWTO (United Nations World Tourism Organization), 2010. *Cruise tourism – current situation and trends*. Madrid: World Tourism Organization.
- USEPA (United States Environmental Protection Agency), 2008. *Cruise Ship Discharge Assessment Report*. USEPA Oceans and Coastal Protection Division, Washington. EPA 842-R-07005. Available at <https://nepis.epa.gov/Exe/ZyNET.exe/P1002SVS.TXT?ZyActionD=ZyDocument&Client=EPA&Index=2006+Thru+2010&Docs=&Query=&Time=&EndTime=&SearchMethod=1&TocRestrict=n&Toc=&TocEntry=&QField=&QFieldYear=&QFieldMonth=&QFieldDay=&IntQFieldOp=0&ExtQFieldOp=0&XmlQuery=&File=D%3A%5Czyfiles%5CIndex%20Data%5C06thru10%5CTxt%5C00000006%5CP1002SVS.txt&User=ANONYMOUS&Password=anonymous&SortMethod=h%7C-&MaximumDocuments=1&FuzzyDegree=0&ImageQuality=r75g8/r75g8/x150y150g16/i425&Display=hpfr&DefSeekPage=x&SearchBack=ZyActionL&Back=ZyActionS&BackDesc=Results%20page&MaximumPages=1&ZyEntry=1&SeekPage=x&ZyPURL>.
- van Der Zee, S.C., Dijkema, M.B.A., van Der Laan, J., Hoek, G., 2012. The impact of inland ships and recreational boats on measured NO<sub>x</sub> and ultrafine particle concentrations along the waterways. *Atmos. Environ.* 55, 368-376. <http://dx.doi.org/10.1016/j.atmosenv.2012.03.055>.

- Venice Passenger Terminal S.p.A., 2014. Guide book, February 2014. [http://www.vtp.it/img/2016/03/guide\\_book\\_2016.pdf](http://www.vtp.it/img/2016/03/guide_book_2016.pdf).
- Venice Port Authority, 2013. L'impatto economico della crocieristica a Venezia. Available at [https://www.port.venice.it/files/page/130705apvstudiocrocieristica\\_0.pdf](https://www.port.venice.it/files/page/130705apvstudiocrocieristica_0.pdf).
- Viana, M., Amato, F., Alastuey, A., Querol, X., 2009. Chemical tracers of particulate emissions from commercial shipping. *Environ. Sci. Technol.* 43, 7472–7477. <http://dx.doi.org/10.1021/es901558t>.
- Viana, M., Fann, N., Tobias, A., Querol, X., Rojas-Rueda, D., Plaza, A., Aynos, G., Conde, J.A., Fernandez, L., Fernandez, C., 2015. Environmental and health benefits from designating the Marmara Sea and the Turkish straits as an emission control area (ECA). *Environ. Sci. Technol.* 49(6), 3304–3313. <http://dx.doi.org/10.1021/es5049946>.
- Viana, M., Hammingh, P., Colette, A., Querol, X., Degraeuwe, B., de Vlieger, I., Van Aardenne, J., 2014. Impact of maritime transport emissions on coastal air quality in Europe. *Atmos. Environ.* 90, 96–105. <http://dx.doi.org/10.1016/j.atmosenv.2014.03.046>.
- Viana, M., Kuhlbusch, T.A.J., Querol, X., Alastuey, A., Harrison, R.M., Hopke, P.K., Winiwarter, W., Vallius, M., Szidat, S., Pre'vo't, A.S.H., Hueglin, C., Bloemen, H., Wählín, P., Vecchi, R., Miranda, A.I., Kasper-Giebl, A., Maenhaut, W., Hitzenberger, R., 2008. Source apportionment of PM in Europe: a meta-analysis of methods and results. *J. Aerosol Sci.* 39, 827–849. <http://dx.doi.org/10.1016/j.jaerosci.2008.05.007>.
- Visschedijk, A.H.J., Denier van der Gon, H.A.C., Hulskotte, J.H.J., Quass, U., 2013. Anthropogenic vanadium emissions to air and ambient air concentrations in North-West Europe. *E3SWeb of Conferences* 1, p. 03004. <http://dx.doi.org/10.1051/e3sconf/20130103004>.
- von Glasow, R., Lawrence, M. G., Sander, R., and Crutzen, P. J., 2003. Modelling the chemical effects of ship exhaust in the cloud-free marine boundary layer. *Atmos. Chem. Phys.* 3, 233–250. <http://www.atmos-chem-phys.net/3/233/2003/>.
- Vrgoč, N., Arneri, E., Jukić-Peladić, S., Krstulović Šifner, S., Mannini, P., Marčeta, B., Osmani, K., Piccinetti, C., Ungaro, N., 2004. Review of current knowledge on shared demersal stocks of the Adriatic Sea. *FAO-MiPAF Scientific Cooperation to Support Responsible Fisheries in the Adriatic Sea. GCP/RER/010/ITA/TD-12. AdriaMed Technical Documents* 12, 91 pp. Available at <http://www.ismar.cnr.it/file/file-general/pg/Adriamed%202004.pdf>.
- Wang, C., Corbett, J.J., Firestone, J., 2007. Modeling Energy Use and Emissions from North 530 American Shipping: Application of the Ship Traffic, Energy, and Environment Model. *Environ. Sci. Technol.* 41, 3226–3232. PMID: 17539530.
- Wang, C., Corbett, J.J., Firestone, J., 2008. Improving Spatial Representation of Global Ship Emissions Inventories. *Environ. Sci. Technol.* 42, 193–199. <http://dx.doi.org/10.1021/es0700799>.

- Wehner, B., Uhrner, U., von Löwis, S., Zallinger, M., Wiedensohler, A., 2009. Aerosol number size distributions within the exhaust plume of a diesel and gasoline passenger car under on-road conditions and determination of emission factors. *Atmos. Environ.* 43, 1235-1245. <http://dx.doi.org/10.1016/j.atmosenv.2008.11.023>.
- Westerlund, J., Hallquist, M., Hallquist, Å.M., 2015. Characterization of fleet emissions from ships through multi-individual determination of size-resolved particle emissions in a coastal area. *Atmos. Environ.* 112, 159–166. <http://dx.doi.org/10.1016/j.atmosenv.2015.04.018>.
- Whall, C., Cooper, D., Archer, K., Twigger, L., Thurston, N., Ockwell, D., McIntyre, A., Ritchie, A., 2002. Quantification of emissions from ships associated with ship movements between ports in the European Community. European Commission final report, Entec UK Limited, Winsor House, Gadbrook Business Centre, Gadbrook Road, Norwiche, Cheshire CW9 7NT, UK.
- Winebrake, J.J., Corbett, J.J., Green, E.H., Lauer, A., Eyring, V., 2009. Mitigating the health impacts of pollution from oceangoing shipping: an assessment of low-sulfur fuel mandates. *Environ. Sci. Technol.* 43(13), 4776-4782. <http://dx.doi.org/10.1021/es803224q>.
- Winkel, R., Weddige, U., Johnsen, D., Hoen, V., Papaefthimiou, S., 2016. Shore Side Electricity in Europe: Potential and environmental benefits. *Energ. Policy* 88, 584-593. <http://dx.doi.org/10.1016/j.enpol.2015.07.013>.
- Winnes, H., Fridell, E., 2009. Particle Emissions from Ships: Dependence on Fuel Type. *J. Air Waste Manage. Assoc.* 59, 1391–1398. <http://dx.doi.org/10.3155/1047-3289.59.12.1391>.
- Yarwood, G., Rao, S., Yocke, M., Whitten, G.Z., 2005. Updates to the Carbon Bond chemical mechanism: CB05. Final Report prepared for US EPA, RT-04-00675 Available at [http://www.camx.com/publ/pdfs/CB05\\_Final\\_Report\\_120805.pdf](http://www.camx.com/publ/pdfs/CB05_Final_Report_120805.pdf).
- Yau, P.S., Lee, S.C., Cheng, Y., Huang, Y., Lai, S.C., Xu, X.H., 2013. Contribution of ship emissions to the fine particulate in the community near an international port in Hong Kong. *Atmos. Res.* 124, 61–72. <http://dx.doi.org/10.1016/j.atmosres.2012.12.009>.
- Zanobetti, A., Schwartz, J., 2005. The effect of particulate air pollution on emergency admissions for myocardial infarction: a multicity case-crossover analysis. *Environ. Health Perspect.* 113(8), 978-82. PMID: PMC1280336.
- Zhang, K.M., Wexler, A.S., Zhu, Y.F., Hinds, C., Sioutas, C., 2004. Evolution of particle number distribution near roadways e Part II: the “road-to-ambient” process. *Atmos. Environ.* 38, 6655-6665. <http://dx.doi.org/10.1016/j.atmosenv.2004.06.044>.
- Zhao, M., Zhang, Y., Ma, W., Fu, Q., Yang, X., Li, C., Zhou, B., Yu, Q., Chen, L., 2013. Characteristics and ship traffic source identification of air pollutants in China’s largest port. *Atmos. Environ.* 64, 277–286. <http://dx.doi.org/10.1016/j.atmosenv.2012.10.007>.
- Zimmermann, R., Buters, J., Öder, S., Dietmar, G., Kanashova, T., Paur, H., Dilger, M., Mülhopt, S., Harndorf, H., Stengel, B., Rabe, R., Hirvonen, M.,

Jokiniemi, J., Hiller, K., Sapcariu, S., Berube, K., Sippula, O., Streibel, T., Karg, E., Schnelle-Kreis, J., Lintelmann, J., Sklorz, M., Arteaga Salas, M., Orasche, J., Müller, L., Reda, A., Passig, J., Radischat, C., Gröger, T., Weiss, C., 2013. Ship Diesel Emission Aerosols: A Comprehensive Study on the Chemical Composition, the Physical Properties and the Molecular Biological and Toxicological Effects on Human Lung Cells of Aerosols from a Ship Diesel Engine operated with Heavy or Light Diesel Fuel Oil. American Geophysical Union Fall Meeting Abstract, San Francisco, CA.

## Web links

<http://clima.meteoam.it/Clino61-90.php>

<http://demo.istat.it/>

<http://ec.europa.eu/>

<http://unctad.org/>

<http://www.arb.ca.gov/>

<http://www.comune.venezia.it>

<http://www.ecoports.com/>

<http://www.eea.europa.eu/>

<http://www.es-geo.com/>

<http://www.espo.be/>

<http://www.imo.org/>

<http://www.inemar.eu/>

<http://www.openair-project.org>

<http://www.ops.wpci.nl/>

<http://www.veniceairport.net/>

<http://www.vtp.it/>

<http://www.wartsila.com/>

[https://www.google.com/intl/it\\_it/earth/](https://www.google.com/intl/it_it/earth/)

<https://www.port.venice.it/it/crociere.html/>

## Publications

[1] **Merico, E.**, Gambaro, A., Argiriou, A., Alebic-Juretic, A., Barbaro, E., Cesari, D., Chasapidis, L., Dimopoulos, S., Dinoi, A., Donateo, A., Giannaros, C., Gregoris, E., Karagiannidis, A., Konstandopoulos, A.G., Ivošević, T., Liora, N., Melas, D., Mifka, B., Orlić, I., Poupkou, A., Sarovic, K., Tsakis, A., Giua, R., Pastore, T., Nocioni, A., Contini, D., 2017. Atmospheric impact of ship traffic in four Adriatic-Ionian port-cities: comparison and harmonization of different approaches. *Transport. Res. Part D*. 50, 431-445. <http://dx.doi.org/10.1016/j.trd.2016.11.016>.

[2] **Merico, E.**; Donateo, A., Gambaro, A., Cesari, D., Gregoris, E., Barbaro, E., Dinoi, A., Giovanelli, G., Masieri, S., Contini, D., 2016. Influence of in-port ships emissions to gaseous atmospheric pollutants and to particulate matter of different sizes in a Mediterranean harbour in Italy. *Atmos. Environ.* 139, 1-10. <http://dx.doi.org/10.1016/j.atmosenv.2016.05.024>.

[3] Cesari, D., Donateo, A., Conte, M., **Merico, E.**, Giangreco, A., Giangreco, F., Contini, D., 2016. An inter-comparison of PM<sub>2.5</sub> at urban and urban background sites: Chemical characterization and source apportionment. *Atmos. Res.* 174–175, 106–119 (ISBN: 0169-8095). <http://dx.doi.org/10.1016/j.atmosres.2016.02.004>.

[4] Contini, D., Gambaro, A., Donateo, A., Cescon, P., Cesari, D., **Merico, E.**, Belosi, F., Citron, M., 2015. Inter-annual trend of the primary contribution of ship emissions to PM<sub>2.5</sub> concentrations in Venice (Italy): Efficiency of emissions mitigation strategies. *Atmos. Environ.* 102, 183-190 (ISBN: 1352-2310). <http://dx.doi.org/10.1016/j.atmosenv.2014.11.065>.

[5] Donateo, A., Gregoris, E., Gambaro, A., **Merico, E.**, Giua, R., Nocioni, A., Contini, D., 2014. Contribution of harbour activities and ship traffic to PM<sub>2.5</sub>, particle number concentrations and PAHs in a port city of the Mediterranean Sea (Italy). *Environ. Sci. Pollut. Res.* 21, 9415-9429 (ISBN: 0944-1344). <http://dx.doi.org/10.1007/s11356-014-2849-0>.

Also, during the Ph.D. work 5 proceedings/extended abstracts and 11 contributions at international (1 poster, 2 oral presentations, 6 abstract contributions) and national conferences (1 oral presentation, 1 abstract contribution) were produced.

## **Acknowledgements**

This work was done in the framework of the POSEIDON project (“Pollution Monitoring of ship emissions: an Integrated approach for harbours in the Adriatic basin”), funded by the European Territorial Cooperation MED 2007-2013 (grant 1M-MED14-12). I wish to thank all project partners and Dr. F.M. Grasso (ISAC-CNR, U.O.S. Lecce) for his help in the instrumental setting up and maintenance at the measurement sites. Thanks to the Port Authorities of Brindisi and Venice for providing information regarding local ship traffic.

At the end of this work, I would like to thank my supervisor, Prof. Andrea Gambaro, for his scientific support and for giving me the opportunity to collaborate with him.

I sincerely express my gratitude to Dr. Daniele Contini and to my co-tutor Dr. Antonio Donateo for constantly guiding me in this journey throughout atmospheric sciences research, working together at the Institute of Atmospheric Sciences and Climate in Lecce.

Finally, thanks to my family even if they did not agree with my career choice...and all people who are able to understand the best and the worse aspects of my personality.

*“A ship is always safe at the shore - but that is NOT what it is built for.”*

*(Albert Einstein)*





Università  
Ca' Foscari  
Venezia

## DEPOSITO ELETTRONICO DELLA TESI DI DOTTORATO

### DICHIARAZIONE SOSTITUTIVA DELL'ATTO DI NOTORIETA'

(Art. 47 D.P.R. 445 del 28/12/2000 e relative modifiche)

Io sottoscritto ..... MERICO EVA .....

nat. a ..... SCORRANO ..... (prov. LE ) il 10/03/1984 .....

residente a ..... SUPERSANO (LE) ..... in ..... VIA TRIPOLI ..... n. 19 .....

Matricola (se posseduta) ..... 956093 ..... Autore della tesi di dottorato dal titolo:  
..... ASSESSMENT OF AIR POLLUTANTS CONTRIBUTION OF HARBOUR ACTIVITIES .....

..... IN VENICE AND BRINDISI AREAS .....

.....

Dottorato di ricerca in ..... SCIENZE AMBIENTALI .....

(in cotutela con ..... )

Ciclo ..... XXIX .....

Anno di conseguimento del titolo ..... 2015/2016 .....

### DICHIARO

di essere a conoscenza:

- 1) del fatto che in caso di dichiarazioni mendaci, oltre alle sanzioni previste dal codice penale e dalle Leggi speciali per l'ipotesi di falsità in atti ed uso di atti falsi, decado fin dall'inizio e senza necessità di nessuna formalità dai benefici conseguenti al provvedimento emanato sulla base di tali dichiarazioni;
- 2) dell'obbligo per l'Università di provvedere, per via telematica, al deposito di legge delle tesi di dottorato presso le Biblioteche Nazionali Centrali di Roma e di Firenze al fine di assicurarne la conservazione e la consultabilità da parte di terzi;
- 3) che l'Università si riserva i diritti di riproduzione per scopi didattici, con citazione della fonte;
- 4) del fatto che il testo integrale della tesi di dottorato di cui alla presente dichiarazione viene archiviato e reso consultabile via internet attraverso l'Archivio Istituzionale ad Accesso Aperto dell'Università Ca' Foscari, oltre che attraverso i cataloghi delle Biblioteche Nazionali Centrali di Roma e Firenze;
- 5) del fatto che, ai sensi e per gli effetti di cui al D.Lgs. n. 196/2003, i dati personali raccolti saranno trattati, anche con strumenti informatici, esclusivamente nell'ambito del procedimento per il quale la presentazione viene resa;
- 6) del fatto che la copia della tesi in formato elettronico depositato nell'Archivio Istituzionale ad Accesso Aperto è del tutto corrispondente alla tesi in formato cartaceo, controfirmata dal tutor, consegnata presso la segreteria didattica del dipartimento di riferimento del corso di dottorato ai fini del deposito presso l'Archivio di Ateneo, e che di conseguenza va esclusa qualsiasi responsabilità dell'Ateneo stesso per quanto riguarda eventuali errori, imprecisioni o omissioni nei contenuti della tesi;
- 7) del fatto che la copia consegnata in formato cartaceo, controfirmata dal tutor, depositata nell'Archivio di Ateneo, è l'unica alla quale farà riferimento l'Università per rilasciare, a richiesta, la dichiarazione di conformità di eventuali copie.

Data 06/12/16

Firma Merico Eva

## AUTORIZZO

- l'Università a riprodurre ai fini dell'immissione in rete e a comunicare al pubblico tramite servizio on line entro l'Archivio Istituzionale ad Accesso Aperto il testo integrale della tesi depositata;
- l'Università a consentire:
  - la riproduzione a fini personali e di ricerca, escludendo ogni utilizzo di carattere commerciale;
  - la citazione purché completa di tutti i dati bibliografici (nome e cognome dell'autore, titolo della tesi, relatore e correlatore, l'università, l'anno accademico e il numero delle pagine citate).


## DICHIARO

- 1) che il contenuto e l'organizzazione della tesi è opera originale da me realizzata e non infrange in alcun modo il diritto d'autore né gli obblighi connessi alla salvaguardia di diritti morali od economici di altri autori o di altri aventi diritto, sia per testi, immagini, foto, tabelle, o altre parti di cui la tesi è composta, né compromette in alcun modo i diritti di terzi relativi alla sicurezza dei dati personali;
- 2) che la tesi di dottorato non è il risultato di attività rientranti nella normativa sulla proprietà industriale, non è stata prodotta nell'ambito di progetti finanziati da soggetti pubblici o privati con vincoli alla divulgazione dei risultati, non è oggetto di eventuale registrazione di tipo brevettuale o di tutela;
- 3) che pertanto l'Università è in ogni caso esente da responsabilità di qualsivoglia natura civile, amministrativa o penale e sarà tenuta indenne a qualsiasi richiesta o rivendicazione da parte di terzi.

A tal fine:

- dichiaro di aver autoarchiviato la copia integrale della tesi in formato elettronico nell'Archivio Istituzionale ad Accesso Aperto dell'Università Ca' Foscari;
- consegno la copia integrale della tesi in formato cartaceo presso la segreteria didattica del dipartimento di riferimento del corso di dottorato ai fini del deposito presso l'Archivio di Ateneo.

Data 06/12/16

Firma 

La presente dichiarazione è sottoscritta dall'interessato in presenza del dipendente addetto, ovvero sottoscritta e inviata, unitamente a copia fotostatica non autenticata di un documento di identità del dichiarante, all'ufficio competente via fax, ovvero tramite un incaricato, oppure a mezzo posta

Firma del dipendente addetto .....

Ai sensi dell'art. 13 del D.Lgs. n. 196/03 si informa che il titolare del trattamento dei dati forniti è l'Università Ca' Foscari - Venezia.

I dati sono acquisiti e trattati esclusivamente per l'espletamento delle finalità istituzionali d'Ateneo; l'eventuale rifiuto di fornire i propri dati personali potrebbe comportare il mancato espletamento degli adempimenti necessari e delle procedure amministrative di gestione delle carriere studenti. Sono comunque riconosciuti i diritti di cui all'art. 7 D. Lgs. n. 196/03.

## Estratto per riassunto della tesi di dottorato

L'estratto (max. 1000 battute) deve essere redatto sia in lingua italiana che in lingua inglese e nella lingua straniera eventualmente indicata dal Collegio dei docenti.

L'estratto va firmato e rilegato come ultimo foglio della tesi.

Studente: MERICO EVA

matricola: 956093

Dottorato: Scienze Ambientali – Environmental Sciences

Ciclo: XXIX

Titolo della tesi<sup>1</sup>: Assessment of air pollutants contribution of harbour activities in Venice and Brindisi areas

### Abstract:

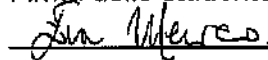
#### Versione Italiana

L'influenza delle emissioni navali in porto alla concentrazione degli inquinanti atmosferici è stata studiata nelle due città portuali di Venezia e Brindisi nel Mare Adriatico, integrando dati sperimentali, modellistica e stime di emissione. A Brindisi è stato stimato il contributo alla concentrazione degli inquinanti gassosi (NO, NO<sub>2</sub>, SO<sub>2</sub> and O<sub>3</sub>) e del particolato (sia in numero che in massa) nell'intervallo dimensionale 0.009-32 µm. L'analisi è stata realizzata separando la fase di stazionamento (incluse le attività di carico/scarico veicolare) e manovra (arrivo/partenza). L'impatto della logistica portuale si è dimostrato rilevante sulle concentrazioni di NO, NO<sub>2</sub> e numero di particelle ed in aumento nel 2014 rispetto al 2012. A Venezia, l'analisi dati inter-annuale ha permesso di valutare l'efficacia della legislazione Europea (2005/33/EC) e delle strategie locali di mitigazione nel ridurre il contributo primario al PM<sub>2.5</sub> nonostante un aumento del traffico navale.

#### English version

The influence of in-port ships emissions to atmospheric pollutants concentration was investigated in the two Adriatic port-cities of Brindisi and Venice, integrating experimental data, modeling and emission inventories. In Brindisi, the contribution to concentration of gaseous pollutants (NO, NO<sub>2</sub>, SO<sub>2</sub> and O<sub>3</sub>) and of particulate matter (in number and mass) of different sizes (range 0.009-32 µm) was estimated differentiating handling (including loading/unloading activities) and manoeuvring (ship arrival/departure) phases. Harbour logistics impact was substantial on concentrations of NO, NO<sub>2</sub> and particles number (increased in 2014 compared to 2012) especially in the ultrafine fraction. In Venice multi-year data allowed evaluate the effectiveness of the European legislation (2005/33/EC) and of local mitigation strategies in lowering the primary contribution to PM<sub>2.5</sub> although an increased ship traffic.

Firma dello studente



<sup>1</sup> Il titolo deve essere quello definitivo, uguale a quello che risulta stampato sulla copertina dell'elaborato consegnato.